Synthesis of Bioresins from Plant Oil Epoxides
By

Vinay Patel

A thesis submitted in partial fulfillment of the requirements for the degree of

Doctor of Philosophy

In

Bioresource Technology

Department of Agricultural, Food and Nutritional Science

University of Alberta

Abstract

The overall objective of this thesis is to develop bioresins from plant oil epoxides for use in biocomposites and other applications. Plant oil-based epoxides show promise as feedstocks to replace non-renewable epoxides used in many applications from biocomposite manufacturing to adhesives and coatings. However, plant oil epoxides are often not directly compatible with many hardeners, requiring a solvent to prepare one phase epoxide-hardener mixtures. The work described in this thesis is aimed at making plant-oil-based bioresins and biocomposites, without the use of solvents and catalysts. In order to achieve a one phase epoxide-curing agent mixture, this thesis explores two possibilities: 1. modification of the plant oil epoxides and 2. modification of the curing agent, specifically in the synthesis of biobased curing agents.

In the first possibility, epoxidised triglycerides are transesterified into epoxidized methyl esters (EMS). These low viscosity EMS were found to act as reactive diluents for the curing agent. However, the curing agent still had limited miscibility in EMS, and so required the use of elevated temperatures to achieve a single phase. As a result, prepolymer mixtures containing EMS have a limited pot life because they start to polymerise, leading to increased viscosity and leads to major difficulties in manufacturing.

In the second possibility, a biobased curing agent (citric acid) was modified into alkyl citrates via solvent- and catalyst-free esterification with the short- to medium-chain alcohols, ethanol, propanol, butanol and hexanol. The synthesized mixtures of, mono-,di-, trialkyl citrate esters and unreacted citric acid (CA-alkyl esters), were found to be fully miscible with plant-oil-epoxides.[1] The resulting homogeneous mixtures of epoxides and curing agents have about 1 hour

---

[1] Jonathan M. Curtis, Vinay Patel, US provisional patent application serial no. 63/075,940, Biobased hardener for epoxy resins

of pot life compared to less than 5 minutes for mixtures produced from epoxidized methyl esters. The optimum molar ratios of epoxy group to carboxylic acid group (Ep/Ac) were identified by the glass transition temperatures (Tg) measurements of bioresins that were prepared by using range of Ep/Ac ratios. Then, properties of the cured resins were measured and characterized. These novel biobased curing agents were found to be reactive at room temperature which could be utilized for certain new applications where low temperature curing is required. Furthermore, the Tg achieved for solvent-free curing of bioresins prepared from CA-alkyl esters were higher than those achieved using citric acid dissolved in solvent, for example 61 °C with epoxidized linseed oil, compared to 38 °C using a citric acid/acetone solution.

Finally, the optimum epoxide-curing agent formulations were used to prepare natural fiber biocomposites without the use of solvents. The Tg of biocomposite prepared by using epoxidized hemp oil and the citric acid/acetone solution was 39 °C. Comparatively, a biocomposite prepared via a solvent-free process using CA-alkyl esters and its Tg of 46 °C was achieved.

Preface

All the research mentioned in this thesis was conducted at University of Alberta in Lipid Chemistry Group (LCG) under the supervision of Drs. Jonathan Curtis and Cagri Ayranci.

Chapter 1 was written for the thesis as "**Patel Vinay**. General Introduction: Epoxy Resins, Plant Oil Based Bioresins And Natural Fiber Biocomposites".

This chapter is a literature review including a background and current scenario of bioresin research. I wrote this manuscript.

Chapter 2 was submitted for publication as "**Patel Vinay**, Omonov Tolibjon, Ayranci Cagri, Curtis Jonathan. Natural Fiber Biocomposites From Epoxidized Plant Oils".

In this chapter, I describe the preparation and analysis of samples in the Drs. Curtis, Ayranci's laboratories. I performed the measurements, analyzed the data, and wrote the manuscript. Dr. Omonov guided me in the sample preparation.

Chapter 3 was published as "Tolibjon S. Omonov, **Vinay Patel**, Jonathan M. Curtis. The development of epoxidized hemp oil prepolymers for the preparation of thermoset networks. Journal of American Oil chemist Society. 2019".

In this chapter, I performed the experiments and analyzed data with the assistance of Dr. Omonov as well as participated in writing the manuscript.

Chapter 4 was published as "Tolibjon S. Omonov, **Vinay Patel**, Jonathan M. Curtis. Biobased Thermosets from Epoxidized Linseed Oil and Its Methyl Esters."

In this chapter, I have designed and performed the experiments. Dr. Omonov assisted me in preparing the samples. I wrote the manuscript and Drs. Omonov and Curtis edited it prior to submission.

Chapter 5 was submitted as a patent application "Curtis, J.M., Patel, **Patel, V.R.**, US patent application serial no. 63/075,940. *Biobased hardener of epoxy resins.*"

In this chapter, Dr. Curtis and I designed the experiments. I have identified and applied some of the critical creative inputs in synthesizing the curing agents, for instance identifying the citric acid particle size has significant impact. I performed the experiments and analyzed the data. I have prepared the draft manuscript/patent under the guidance of Dr. Curtis.

Chapter 6 has been used for a patent application as "Curtis, J.M., Patel, **Patel, V.R.**, US patent application serial no. 63/075,940. *Biobased hardeners of epoxy resins.*"

In this chapter, I have designed and performed the experiments. I have also analyzed the data and laid out the manuscript/patent under the guidance of Dr. Curtis.

Dedication

I would like to thank my wife, Rutvi, for her great support and patience throughout my PhD program. I am also thankful for the support from my parents and friends. Last, I am grateful to create a wonderful memories with my sons, Anay (4 yr.) and Aarush (1 yr.), during my journey.

Acknowledgements

Last but the not least, I am thankful to our Edmonton friends, Tiffany & Sim, Sangeeta & Pritam, Sonal & Rohan for being together and encouraging me.

THANK YOU

VINAY

Table of Contents

List of Tables

List of Figures

List of Abbreviations and Symbols

A&S – Adhesives and sealants

BC – Mixture of citric acid, mono-, di-, and tri-butyl citrate

C16:0 – Palmitic acid

C18:0 – Stearic acid

C18:1 9c – Oleic acid

C18:1 11c – Vaccenic acid

C18:1 9t – Elaidic acid

C18:2 9c,12c - Linoleic acid

C18:3 9c,12c,15c - α-Linolenic acid

C18-3 6c,9c,12c – γ-Linolenic acid

CA – Citric acid (2-hydroxypropane-1,2,3-tricarboxylic acid)

CA-alkyl esters – Mixture of citric acid, mono-, di-, and tri-alkyl esters

CO – Canola Oil

CNSL – Cashew nutshell liquid

DBC – Dibutyl citrate

DGBPA – Diglycidyl bisphenol A

DMA – Dynamic Mechanical Analysis

DSC – Differential scanning calorimetry

ECO – Epoxidized Canola Oil

ELO – Epoxidized Linseed Oil

ELSD – Evaporative light scattering detector

EHO – Epoxidized Hemp Oil

EC – Mixture of citric acid, mono-, di-, and tri-ethyl citrate

ESS – Epoxidized Sucrose Soyate

FAME – Fatty acid methyl ester

FTIR-ATR – Fourier-transform infrared-attenuated total reflection

GC-FID – Gas chromatography-flame ionization detector

GPC – Gel permeation chromatography

HC – Mixture of citric acid, mono-, di-, and tri-hexyl citrate

HO – Hemp Oil

HDPE – High Density PolyEthylene

IB – Internal Bond (Strength)

IV – Iodine Value

LO – Linseed Oil

MBC – MonoButyl Citrate

MOE – Modulus Of Elasticity

MOR – Modulus Of Rupture

MW – Molecular Weight

NFC – Natural Fiber Composite

NMR – Nuclear Magnetic Resonance

OSB – Oriented Strand Board

OOC – Oxirane Oxygen Content

PC – Mixture of citric acid, mono-, di-, and tri-Propyl Citrate

PET – PolyEthylene Terephthalate

PF – Phenol Formaldehyde

TAG – Triacylglycerol, Triglycerides, Triacylglycerides of fatty acids

TBC – TriButyl Citrate

TMA – Trimellitic Anhydride (1,2,4-benzene tricarboxylic anhydride)

TGA – Thermogravimetric Analysis

TOFA – Tall Oil Fatty Acid

T_m – Melting Temperature

T_g – Glass Transition Temperature

G' – Storage Modulus

G'' – Loss Modulus

$tan\ \delta$ – Loss Factor

Chapter 1

General Introduction: Epoxy Resins, Plant Oil Based Bioresins And Natural Fiber Biocomposites

1.1 Resin

A resin is a viscous liquid or noncrystalline material with the potential to form a polymer. Resins can be either of natural origin like a gummy semisolid material from certain tree secretions or synthetically derived substances [1]. Due to the increasing demand for high performance materials, synthetic resins have largely replaced natural resins. Resins are divided into two broad categories: thermoplastic and thermosetting resins. Linearly linked monomers form thermoplastics which can be melted while crosslinked monomers form thermosets which cannot be melted. About 92% of plastics used worldwide are thermoplastics [2]. The words "resin" refers to monomers and sometimes to cured materials, while "plastic" refers to polymers. The 12 major types of resins are being produced commercially worldwide listed in Table 1.1 [3].

Types of Resin	Commercial resin names	Typical Applications
Polyester	a. Polyethylene Terephthalate (PET or PETE) b. Polybutylene Terephthalate (PBT)	Packaging, Textiles • Market size: PET-$43.8 billion (2019)
Unsaturated Polyester	Unsaturated polyester resin	Water tanks, Shower stalls, Boats, Swimming pools
Vinyl ester	Vinyl ester resin	Coating, Printed circuit board, metal foil laminates
Phenolic	Phenol formaldehyde (PF):	

	a. Novolacs b. Resoles	a. Carbon brakes, binder for carbon bonded refractories b. Oriented strand boards (OSB) and Laminated composite lumber (LCL)
Alkyd	Alkyd resins	Paints, varnishes, enamels
Polycarbonate	a. Lexan b. Makrolon	Safety glasses, lenses
Polyamide	a. Nylon b. Kevlar	a. Toothbrush bristles, textile. b. Bulletproof vests.
Polyurethane	Polyurethane resins	Insulations, foam liners for clothing, adhesives, elastomers.
Silicone	Silicone resins	Rubber, laminates, defoamers, water resistant applications
Epoxy	Epoxy resins	Floorings, adhesives, coatings etc.
Polyethylene	a. Low density (LDPE) b. High density (HDPE) c. Ultra-high molecular weight (UHMW-PE)	a. Shopping bags b. Drainpipes, milk-juice container c. Medical devices • Market size: 100 million tons annually.
Acrylic	Acrylic resins	UV resistant properties, Decorative panels, coatings, translucent tiles
Polystyrene	Polystyrene resins	Acid, alkali, salt resistant material, insulation, cooling towers, foams, automotive dashboard, pipes
Polypropylene	Polypropylene resins	Heat resistant so used in medical equipments, electronics, fiber & filament, coatings etc.

Table 1.1 Major commercial resins produced worldwide [3]

Almost all of the above listed resins are synthesized from nonrenewable resources with only a very small proportion derived from renewable feedstocks. Since the beginning of the plastics era,

there has not been enough awareness, research, and effort made to recycle used plastics at the end of their service life. The consequences of not considering the end of service life for these materials is plastic pollution in water, land, and other natural resources. Such plastics may take hundreds of years to degrade in nature. In addition, they can produce microplastics that have the capability of polluting ecosystems and which are difficult to remove. That is why, there is now a demand for new greener products which are biobased, recyclable, and compostable.

There are many biobased feedstocks available which could be transformed into valuable precursors of biobased materials. Specifically, carbohydrates, cellulose, sugars, and lipids are important feedstocks which could be utilized to synthesize biobased resins. Table 1.2 summarizes some commercially available bioresins which are potential replacements for synthetic resins [4].

Name	Type of Bioresin	Raw materials used	Alternate to	Manufacturer
Polyethylene furanoate (PEF)	✓ Partially biobased ✓ Thermoplastic	C_6 sugars	Polyethylene terephthalate (PET)	Avalon, Avantium, Corbion, Synvina
Polylactic acid (PLA)	✓ Fully biobased ✓ Thermoplastic ✓ Biodegradable	Corn starch, Sugarcane	High density polyethylene (HDPE) and others	Corbion, NatureWorks, Futerro, Radici Group SK Chemicals, Synbra
Poly(butylene adipate-co-terephthalate (PBAT)	✓ Thermoplastic ✓ Biodegradable	1,4-butanediol, adipic acid, dimethylterephthalate (DMT)	HDPE, LDPE	BASF, Eastman, Bio-Fed, Jinhui Zhaolong

Biopolyamide OR Polyalkylene sebacamides (PA)		Sebacic acid (castor oil), diamine (C_6, C_{10})	Specific applications	Arkema, Vestamid, DSM
Thermoplastic starch (TPS)	✓ Biodegradable	Biomass	Specific applications and mainly in food packaging	Futerro, Novamont, Biome, Biotec, Biobag, Cardia, Kuraray, PSI, Huhtamaki, Hitachi, NatureWorks
Ethyl cellulose (EC)		Biomass	Limited applications	Ashland, Dow
Methyl cellulose (MC)		Biomass	Water soluble films	Ashland, Dow, Haishen, Tembec, Shin Etsu, Sidley Chemical
Polyhydroxy butyrate (PHB)	✓ Thermoplastic ✓ Biodegradable	Carbohydrates	PE PP	Tianan Biopolymer, BASF, Tepha, Biocycle, Biomer

Cellulose acetate (CA)	✓ Stable cellulose derivative ✓ Thermoplastic	Biomass fermentation	Specified applications	Celanese, Eastman, Nagase, Solvay
Polyhydroxy alkanoates (PHA)	✓ Thermoplastic	Biomass fermentation	Specified applications	Tianan Biopolymer, BASF, Tepha, Biocycle, Biomer
Polyglycolic acid (PGA)	✓ Thermoplastic ✓ Biodegradable			Kureha
Polybutylene succinate (PBS)	✓ Thermoplastic ✓ Biodegradable	Succinic acid & 1,4-butanediol	PLA, PHB	MCPP (Mitsubishi), Succinity, Showa Denko, PTT MCC Biochem, Genomatica (1,4-butanediol), Roquette (succinic acid)

Table 1.2 List of commercial bioresins [4]

Plant oils are versatile feedstocks which can be utilized to manufacture biobased products [5]. All plant oils have a consistent chemical structure, being predominantly triacylglycerides. However, they also contain a variety of fatty acids in different proportions [6]. Having a consistent backbone, but with this variation in functionality, offers many possibilities for synthesizing a wide range of products [7].

1.2 Plant oils as epoxy monomers

Plant oils are extracted from oilseeds via mechanical pressing [8] and solvent extraction [9] processes. Crude plant oils are refined through multiple refining steps include degumming, neutralization, bleaching, deodorization, and fractionation to remove undesirable components which improves oil stability [8]. Refined plant oils are mainly triglyceride of fatty acids where the fatty acids typically include saturated and unsaturated fatty acids (Figure. 1.1). This unsaturation is used to functionalized or to make more reactive monomers via many chemical transformation routes.
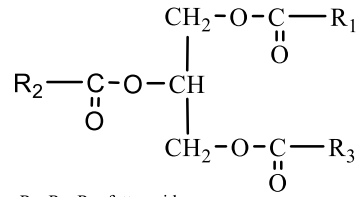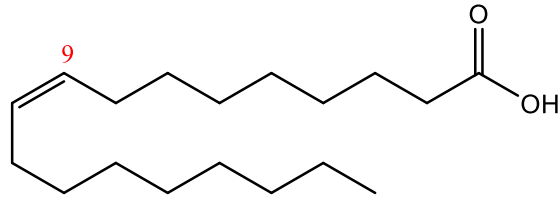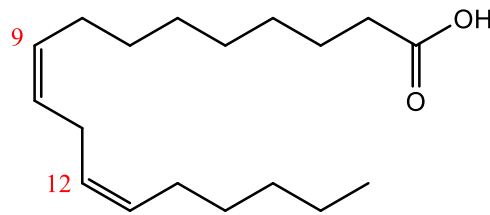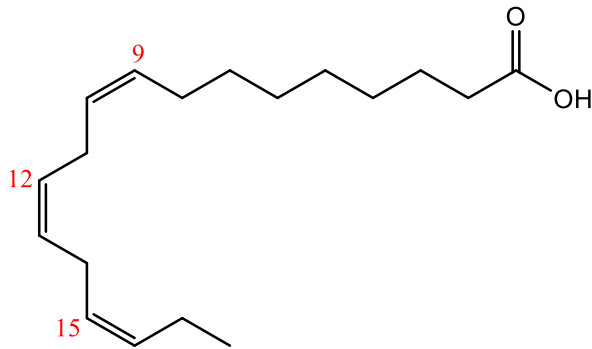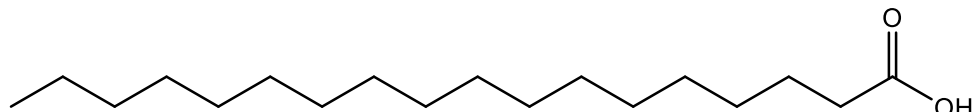
Figure. 1.1 Triglyceride of fatty acids

Oil unsaturation level can be measured by the absorption of iodine or iodine value (IV) and various plant oils have different IV (Table 1.3). The IV of an oil is defined as the number of grams of iodine that is absorbed by 100 g of oil. One of the functionalization routes for triglycerides is

epoxidation, which results in an epoxy ring (Figure. 1.2) at the carbon-carbon double bond position [10]. Hence, the oxirane functionality of the epoxides formed depends on the IV of an oil. The IV of some of the commonly available plant oils are listed in Table 1.3. Additionally, there are some commercially produced genetically modified oilseeds that have very different fatty acid profiles. For instance, high oleic soybean, canola oils. Such oils offer potentially better feedstocks for resin production with more unsaturation or uniform fatty acid profile.

Name of plant oil	Iodine value (gI$_2$/100g)	Reference
Olive	75 - 94	[14]
Peanut	80 - 106	[14]
Karanja (Pongamia)	89	[16]
Rapeseed	94 - 120	[14]
Cottonseed	90 - 140	[14]
Corn	103 - 140	[14]
Sunflower	110 - 143	[14]
Soybean	117 - 143	[14]
Hemp seed	155 - 167	[19]
Linseed	168 - 204	[14]
Camelina	140 - 152	[19]

Table 1.3. Iodine value of plant oils

The mechanism for conversion of a double bond into an epoxy group is described in the following section. The importance of epoxy groups is that they are more reactive or susceptible to be opened by nucleophiles to from an ester linkage than are double bonds.
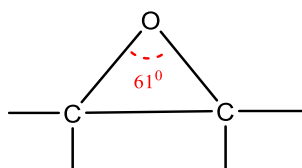
Figure. 1.2 Epoxy ring

C-O-C epoxy bonds are strained due to unusual bond angle of 61° which makes both carbons strong electrophiles. This is because the localized electron cloud stretches towards the oxygen atom making both carbon atoms partial positively charged sites. Such electrophiles can attract an electron pair from nucleophile resulting in opening of an epoxy ring into an ester linkage and a hydroxyl group when the nucleophile contains carboxylic acid [11]. Further detail and significance of nucleophiles are discussed in section 1.3 as they can be used as curing or crosslinking agents or hardeners to make thermoset materials. The properties of such materials are directly associated with the epoxy functionality of the epoxides.

1.2.1 Epoxidation of plant oils

Plant oil epoxidation in the presence of an acidic catalyst and hydrogen peroxide is an efficient and commercially developed reaction to produce epoxy monomers or epoxides [10,12]. Fig 1.3. illustrates the two-step reaction mechanism which occurs during double bond conversion into an epoxy group. The reaction temperature, reaction rate, and type of acid catalyst have direct impact on the conversion of ethylenic double bond into an epoxy group [10,13,15,16]. Omonov et al. studied other side reactions occurring during epoxidation: these include ring opening and oligomerization which should be minimized in this reaction to achieve the maximum oxirane content of epoxides [10]. Since plant oils are composed of a variety of fatty acids, each fatty acid has a different reaction rate in the overall epoxidation process. Scala et al. reported that double bonds of linolenic acid (C18:3) are three times more reactive than the double bonds in oleic (C18:1 9c) and linoleic acids (C18:2 9c,12c) [17].

Step-1: Formation of peroxy-acids

where, R= -H, -CH₃ etc.
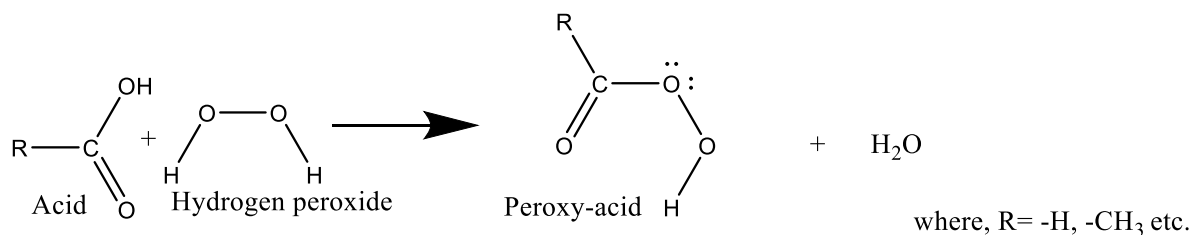
Step-2: Reaction between peroxy-acids and unsaturation
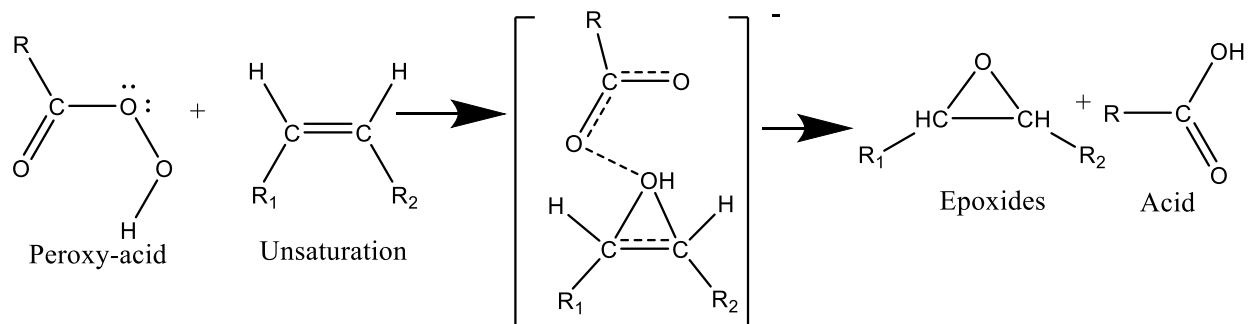
Figure. 1.3 Epoxidation reaction mechanism

The number of epoxy groups in the epoxidized product can be measured by its oxirane oxygen content (%OOC), which has units of grams of oxirane in 100 g of epoxidized product [12]. The significance of %OOC is in calculating the amount of curing agent needed to make a thermoset material or bioresin. Theoretically, higher IV oils could result in epoxides with higher %OOC compared to lower IV oils. For instance, linseed oil (IV=168-204) epoxide has higher amount of %OOC (%OOC=~9.0) compared to soybean oil (IV=117-143) epoxide (%OOC=~7.0) [14]. The higher or lower %OOC which can be achieved for different plant oils has implications for the properties of the thermoset materials. Crosslinking density is one of the important characteristics to determine the property of cured materials. Crosslinking density is the average molecular weight of segments between two crosslinks. Thus, a higher segmental molecular weight material would have a lower crosslinking density than a lower segmental molecular weight material. For instance, material prepared from the linseed oil epoxide is expected to have a higher crosslinking density than a material prepared from soybean oil epoxide. In order to crosslink these epoxy monomers,

10

they are reacted with multifunctional compounds, the structure of which dictates the formation and properties of thermoset materials. Such compounds called hardeners or curing/crosslinking agents.

1.3 Curing agents

The majority of curing agents are short chain and multifunctional compounds derived from nonrenewable sources. They can be categorized by their functional groups: carboxylic acid, amine, amide, anhydride, sulfide; also, by whether their chemical structures include aliphatic or aromatic groups, as summarized in Table 1.2 [18,23].

Type of curing agents	Name of curing agents	Functional group	Reference
Active hydrogen containing compounds	Polybasic acids	-COOH	[18]
	Acid anhydrides	$(CH_3CO)_2O-$	[18]
	Polythiols	-SH	[18]
	Polyamines	$-NH_2-NH-NH_2-$	[18]
	Polyols	-OH	[18]
Anionic and Cationic initiators	Anionic: 1. Alkali metal derivatives 2. Organic compounds (bases)	1. Li, Na, K, Cs 2. Pyridine, Amines etc.	[18]
	Cationic: 1. Complexes of BF_3	NH_3-BF_3	[18]
Reactive cross-linkers	Phenol	C_6H_5-OH	[18]
	Urea (carbamide)	$CO(NH_2)_2$	[18]
	Formaldehyde	-CHO	[18]
	Melamine	$-C_3H_6N_6$	[11]

Table 1.4. Classification of curing agents

Aromatic amines are widely used curing agents which are not only derived from petroleum resources but are also potential human carcinogens [23]. Due to such drawbacks, the possibility of developing biobased curing agents needs to be further explored.

Besides being multifunctional and biobased, the compatibility of curing agents with the intended epoxide is also an important criterion to manufacture a thermoset material with specified properties [20,21,23]. The majority of curing agents require solvent to enhance miscibility with plant oil epoxides [23,24,25]. It is quite difficult to have all the desirable characteristics (fig. 1.4) in a group of curing agents.
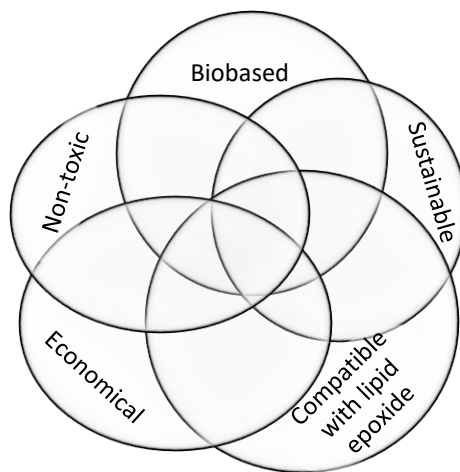
Figure 1.4 Targeted class of curing agent

The focus of this thesis is to utilize the plant-oil-epoxides (section 1.2) so the selection of curing agents could be narrow it down towards the curing agents that are miscible with the plant oil epoxides. Then, the second parameter can be their biobased characteristic, so the biobased

curing agents (section 1.4.2) can be selected from the initial group. Then, the remaining three parameters (Fig 1.4) can be introduced to focus on a group of curing agents that are miscible with the plant oil epoxides, biobased in nature, non-toxic, economical and derived from sustainable sources. There are some non-toxic and biobased food grade carboxylic acids available which could be used as curing agents (Table 1.5). These group of curing agents are not meeting all the requirements depicted in Fig. 1.4, but their derivates could meet all requirements so it was hypothesized (section 1.9.1) and explored in this thesis.

Multifunctional food grade carboxylic acids are listed in Table 1.5 which are commercially available. The cost of these available natural acids and their processing or extraction route and the higher carboxylic acid group functionality of 3 are making only one candidate suitable for a low-cost curing agent application: citric acid. Citric acid (2-hydroxy-propane-1,2,3-tricarboxylic acid) is synthesized from various simple sugars by fermentation with *Aspergillus niger* mycelial fungi [27]. Citric acid is used in many applications, including as a food preservative and antioxidant, as a beverage acidity regulator, in coagulants for many industrial processes to remove metal complexes of iron and aluminum, as a detergent in many cleaning product formulations, as a metal scavenger, in cosmetics, and lately in synthesizing various polymers as a functional compound and plasticizer [27].

Multifunctional carboxylic acids	Molecular formula	Molecular weight (g/mol)	Ref.
Oxalic acid	HOOC-COOH	90.04	[26]
Malonic acid	HOOC-CH$_2$-COOH	104.06	[26]
Succinic acid	HOOC-CH$_2$-CH$_2$-COOH	118.09	[26]
Fumaric acid	HOOC-CH=CH-COOH	116.07	[27]
Malic acid	HOOC-CH$_2$-(CH)OH-COOH	134.09	[26]
Glutaric acid	HOOC-(CH$_2$)$_3$-COOH	132.12	[26]
Itaconic acid	HOOC-CH2-CH$_2$-COOH	130.10	[27]
Tartaric acid	HOOC-(CH)OH-(CH)OH-COOH	150.09	[26]
Citric acid	HOOC-CH$_2$-(HOOC)-C-(OH)-CH$_2$-COOH	192.12	[26]

Table 1.5 Multifunctional biobased carboxylic acids

Aside from being biobased, multifunctional, and an economically viable option, citric acid is hygroscopic and highly water soluble (160.8 g of citric acid/100g H$_2$O at 25 °C for a saturated solution of citric acid in water). However, it has a density of 1.665 g/cm^3 at 25 °C [26] making it incompatible to be use with hydrophobic plant oils. Additionally, such incompatibility between citric acid and plant oils is also due to their polarities, as citric acid is a polar substance while plant oils are non-polar. Songqi et al. prepared fully biobased thermoset materials by utilizing naturally occurring carboxylic acids as crosslinkers with epoxidized sucrose soyate, although these cured resins possess limited chemical resistance [28]. Synthesis of such novel epoxidized sucrose soyate requires multi step chemical process which utilizes organic solvents and catalysts making them less attractive to be used as precursor to make bioresins [29,30].

1.4 Biobased epoxies and curing agents

Due to the environmental concerns, nonrenewable based materials are being replaced with the biobased [31]. About 10% of the total fossil-based feedstock is utilized to make various chemicals and materials [32]. Majority of commercial epoxy resins and curing agents are derived from nonrenewable resource, and studies are showing variety of renewable sources can be utilized to make biobased materials [33,34,35].

1.4.1 Biobased epoxies

There has been variety of biobased feedstocks explored to make biobased epoxy resins as listed below [36]. These building blocks requires derivatization to make epoxides. These derivatization processes are important to determine the commercial viability of epoxy resins. The majority of these extracted materials require derivatization to make epoxy monomers besides epoxidation.

Source(s) of epoxide	Common name of epoxy resin	Advantages/Disadvantages	References
Plant oils	Plant oil-based epoxy resin	Simple epoxidation process to convert plant oils into epoxy monomers	[37,38]
Cashew nutshell liquid (CSNL)	Cardanol-based epoxy resin	Aromatic backbone enhances the thermo-mechanical properties of cured resins	[39,40]
Cellulose and Hemicellulose from agriculture waste	Furan-based epoxy resin	Better mechanical properties of cured resins but relatively difficult/expensive to extract furan derivatives	[41,42]
Tall oil (Pines and Conifers)	Rosin-based epoxy resin	Phenanthrene structure imparts superior mechanical performance of cured resins	[43,44]
Agriculture waste	Lignin-based epoxy resin	Lignin is not stable compound and form a range of derivatives	[45,46]
Agriculture waste (carbohydrates)	Itaconic acid-based epoxy resin	Low cost and high availability	[47,48]

Gallnuts, Tea leaves, Sumac, Oak bark etc.	Gallic acid-based epoxy resin	Very expensive but aromatic backbone provide superior properties of cured resins	[49,50]
Wood	Vanillin-based epoxy resin	Aromatic backbone but complicated extraction/synthesis routes	[51,52]
Sugars and Fruits (Sorbitol derivatives)	Isosorbide-based epoxy resin	Greater progress in synthesizing to make isosorbide but requires elevated curing temperatures to make cured resins	[53,54]
Natural plant extract (cinnamic acid)	Cinnamic acid-based epoxy resin	Not commercially viable to be use as epoxy resins due to expensive extraction/synthesis process	[55,56]
Essential oils (clove, nutmeg, cinnamon, basil, bay leaf)	Eugenol-based epoxy resin	Not commercially viable due to high cost of feedstocks, but comparable mechanical properties of cured resins	[57,58]

Table 1.6 Biobased epoxy resins

Plant oils are versatile feedstock that can be transformed into epoxy monomers via epoxidation reaction as discussed in section 1.2.1. The epoxy groups in the plant oil epoxides are located (Fig 1.3) along with the fatty acid chain that makes them less reactive than the epoxides with the terminal epoxy groups. Additionally, plant oil epoxides are generally nonpolar while many curing agents are polar in nature making them immiscible (detail discussion in chapter 5, section 5.3).

Another commercially available biobased epoxide, with the cardanol backbone, can be derived from the cashew nutshell liquid. One of the significant characteristics of these epoxides is that they possess an aromatic ring with the alkenyl chain, that can make the cured bioresins with the superior thermal and mechanical properties compared to the plant oil based epoxy resins [39,40].

Furan and their derivatives are cyclic compounds that can be used to make epoxides. Furans can be extracted from the cellulose and hemicellulose, but their purification requires additional processing [41,42] and costs.

Tall oil or rosin can be extracted from wood mainly pine and conifer. It is a viscous and dark color oil that contains resin acids including oleic (40-50%) and linoleic (35-45%), sterols, and other compounds. Commercially, rosin is a byproduct of pulp and paper manufacturing operations [43,44]. Commercially, tall oil fatty acids (TOFAs) are converted into dimer acids and they can be used in adhesives, coatings and other applications [44].

Lignin is mixture of aromatic and complex compounds that can be extracted from the biomass, but it is not a stable compound [45,46]. The major monomeric units of aromatic alcohols namely, p-coumaryl, coniferyl, and syringyl, present in lignin that can be used to make epoxides, but to obtain the purified lignin is not a commercially established process [46]. There are some other biobased feedstocks (eugenol, sorbitol, chitosan, gallic acid, itaconic acid, sugars) can be used to make epoxides but in general, the cost of their extraction and conversion to resins make it unlikely that they would be commercially viable [47,48,49,50, 51,52,53,54].

1.4.2 Biobased curing agents

There have been many common sources as indicated in Table 1.6 that are utilized to make biobased curing agents as well [36]. Many studies have shown promising properties of the cured resins prepared by using various biobased curing agents include plant oils, lignin, and rosin derivatives, biobased phenols, acids, and anhydrides [59]. Aliphatic and aromatic amines are widely used commercially as curing agents because of their superior reactivity with the epoxy

monomers and mechanical performance of the cured resins [60,61]. Biobased amines can be synthesized from the renewable sources include carbohydrates, terpenes, and plant oils [62].

1.5 Plant oil based Bioresins

In this thesis, the term "*epoxides*" is used to refer to uncured TAG epoxide monomers while a "*cured resin*" refers to epoxides crosslinked into a rigid thermoset material. A multifunctional compound can crosslink the epoxidised triacylglycerols into a three-dimensional polymer network via oxirane ring opening reactions. The process of crosslinking is referred to as *curing* of the epoxides, to make rigid bioresins or thermoset materials. Plant oils are the most attractive resource and intensively studied for this use, due to their availability and functionality for the synthesis of bioresins [63]. However, sustainable bioresin production without the use of toxic chemicals and solvents is still a challenging task. Omonov et al. reported an aldehyde-free thermoset material from plant oils and other biobased compounds as curing agents which possess adequate thermomechanical properties [64].

The properties of a cured bioresin material depends on the oil epoxide structure, the curing agent and the curing process employed in its to preparation. Li et al. reported that epoxide monomers with higher %OOC produced bioresins which could be cured to a higher crosslinking density, glass transition temperature, tensile strength, and thermal stability. On the other hand, some impact strength is lost compared to cured bioresins produced from lower epoxy monomers [65]. Generally, aliphatic long chain structures of epoxide monomers as well as curing agents afforded flexible bioresins with high impact strength while an aromatic structure imparts rigidity into bioresins [66]. In addition, Jian et al. reported that a longer carbon chain length of the epoxides and curing agents decreases the curing rate as well as producing bioresins that cure to a higher impact strength and heat resistance [67]. Thus, manufacturing of bioresin based materials with

targeted properties can be achieved by selecting appropriate epoxide monomers, curing agents, and curing condition or processes [68]. For instance, material prepared by using the shorter carbon chain length succinic acid (C4) as a curing agent is rigid compared to material prepared by using longer carbon chain length sebacic acid (C10).

Plant oil based bioresins can be used with or without reinforcement material for certain applications due to their high modulus, for instance in a coating application that requires high modulus of elasticity [69]. Additionally, their availability and wide range of thermophysical, mechanical, and superior adhesion characteristics make them one of the ideal candidates to be used as a polymer matrix with natural and synthetic fibers to make biocomposites [70]. Epoxies possess adhesion properties that are superior to other polymer classes, and plant oil epoxies can have good adhesion performance on wood and metal surfaces [99].

1.6 Natural fiber biocomposites

A biocomposite is a material prepared by combining a biobased or non-biobased polymer matrix with natural fibers as reinforcement component. Since two completely different components are involved in forming a biocomposite, its properties are influenced by interfacial adhesion, structure, and their bonding mechanism [71]. Shushanta et al. studied the effects of modified soybean-based resin, epoxidised methyl soyate (EMS), which improved the adhesion between natural fiber and resin matrix resulted in enhanced properties of cured material [72]. EMS was prepared through the base catalyzed transesterification of epoxidised soybean oil. The plant oil chemistry allowing to modify the resin depending on the desired final properties of biocomposites. Additionally, biocomposites properties can be tunable by selecting appropriate bioresin, reinforcement fiber and manufacturing processes. Natural fibers are very diverse materials and their selection has a large impact on biocomposite properties.

1.6.1 Natural fibers

Natural fibers from agriculture waste or byproduct of certain crops are low cost and sustainable materials which could be used to manufacture various products. Only certain natural fibers like flax straw, hemp, coir, and bamboo have the necessary high modulus-to-density and strength-to-density ratios as well as high availabilities, for them to be considered as potential feedstocks to manufacture biobased products, including biocomposites [73]. Although there are challenges to overcome in the utilization of natural fibers, they do have the potential to replace synthetic fibers that are currently used in many composite materials. Such challenges include their typical hydrophilic nature, which makes them incompatible with hydrophobic polymer matrices [74,75]. Due to this drawback, composite materials containing natural fibers may absorb water and eventually degrade more rapidly than composites manufactured from synthetic fibers. Some common synthetic fibers are nylon, polyester, glass fiber, carbon fiber, polyacrylonitrile or rubber, acrylic, rayon, and many more which are mostly derived from fossil-based feedstocks [76].

However, synthetic fibers could be substituted with natural fibers in many cases, and biocomposites are already being used in light weight automobile components, for example [77]. Natural fibers consist of cellulose, hemicellulose, and lignin monomers (Figure 1.5). These monomers are bound together by chemical and hydrogen bonds to form polymer strands which form a bundle and group of these bundles form natural fiber [78]. In addition to this, natural fibers also can contain small percentages of waxes and other higher molecular weight substances which make them an inconsistent feedstock [78]. Natural fibers can be derived or harvested from a wide range of plants including woody species, hemp, flax, banana, coconut, jute, wheat, coir and many more. Some plants are not exclusively used to produce natural fibers, but instead natural fibers are

generated as a by-product. For instance, flax plants can be harvested for oilseed, but flax fibers remain as a valuable by-product [79].

The properties of natural fibers vary based on their chemical composition and structure. A typical composition for natural fibers would be cellulose 60-80%, hemicellulose 5-20%, lignin, and moisture 20% [80], but the ratios may vary depending on the source of fibers. The compositions and origins of some natural fibers are given in Table 1.4. In nature, cellulose and hemicellulose are usually hydrophilic while lignin is hydrophobic [81]. In addition to this, hemicellulose functions as cementing agent in natural fibers; due to its hydrophilic nature, it is responsible for absorption and retention of moisture. Lignins are complex aromatic and aliphatic hydrocarbon compounds which impart rigidity to natural fibers. Since, these complex hydrocarbon compounds absorb UV light, they are susceptible to degrade and lose their rigidity over time [81].
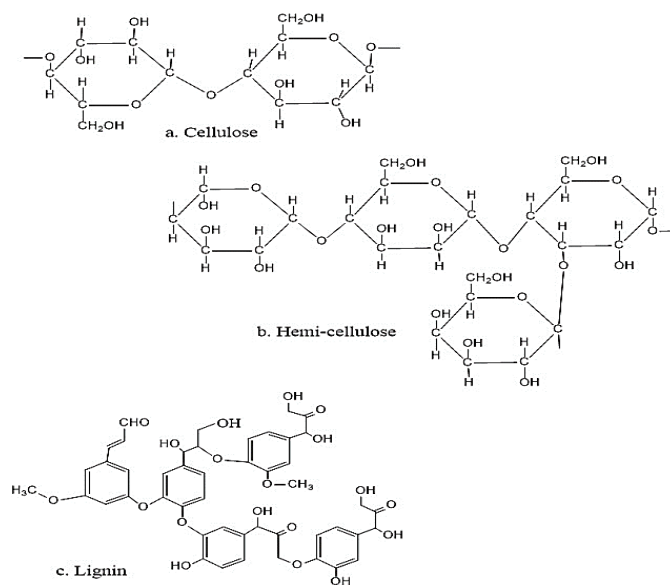
Figure 1.5 Chemical structure of Cellulose, Hemicellulose and Lignin

Utilization of natural fibers as reinforcement in making biocomposites has some disadvantages and some advantages compared with biocomposites reinforced with synthetic fibers. They do not

make perfect reinforcement materials because they are naturally available in a randomly oriented form and usually have less mechanical strength than glass fibers [83]. In addition, they are hydrophilic in nature so tend to absorb or retain moisture. On the other hand, they can form a desirable reinforcement material because of their higher specific modulus, lower processing temperature (costs), low density and carbon footprint [83].

Natural fiber	Type/Origin	Chemical composition		
		Cellulose (%)	Hemicellulose(%)	Lignin (%)
Hemp	bast	68	15	10
Flax	bast	71	18.6-20.6	2.2
Sisal	leaf	65	12	9.9
Coir	fruit/seed	32-43	0.15-0.25	40-45
Ramie	bast	68.6-76.2	13-16	0.6-0.7
Bamboo	grass	26-43	30	21-31
Sugarcane bagasse	stalk residue	55.2	16.8	25.3
Jute	bast	61-71	14-20	12-13
Abaca	leaf	56-63	20-25	7-9
Kenaf	bast	72	20.3	9

Table 1.7 Natural fiber origin, composition, type, characteristics [82]

The chemical composition of natural fibers varies as depicted in Table 1.4. Sushanta et al. showed that the cellulose in natural fiber contributes to tensile strength while lignin provides thermal stability to the natural fibers [72]. Marie et al. revealed that the fiber-matrix adhesion is crucial to make biocomposites [84]. Fiber-matrix interface bonding can be improved by many fiber treatment methods reported in the literature including alkaline, hot water, and salt solutions as well as treatment with silane compounds [82,85]. Surface modified or chemically treated flax fibers tend to establish better fiber-matrix adhesion which results in strong composites [80].

The durability or service life of biocomposites is a crucial factor in their utilization in most applications, including automobile parts, siding panels and many more. The deterioration of biocomposite materials can occur due to factors such as moisture/humidity, temperature, chemical contact, and biological environments that promote mold growth, as well as percentage loading of the cured polymer matrix. Cellulose and hemicellulose can readily uptake and diffuse water inside the fiber microfibrils, which can destabilize the structure. Many material degradation studies have been conducted on various natural fibers and biocomposites. These have demonstrated that the hydrophilic nature of natural fibers is one of the drawbacks to their use as in reinforcement [81]. If the natural fiber is not protected by the polymer matrix, or if there are voids in the biocomposites, water contacts the natural fiber causing swelling. Ultimately the integrity of the biocomposite is compromised. Despite being hydrophilic in nature, natural fibers can be protected from moisture by coating with an appropriate polymer matrix to make biocomposite materials suitable for furniture, light weight interior auto parts, and construction applications [86].

1.7 Applications: Bioresins and Biocomposites

1.7.1 Bioresins

Substantial efforts are being made to discover advanced applications of bioresins from shape memory polymers to thermally stable materials and many more [25,106,107]. In addition, there is a need to replace some existing resins which are nonrenewable and toxic. Epoxy resins make up about 70% of the thermoset resin market, and of this share, about 90% of the resins incorporate the diglycidyl ether of bisphenol A (DGBPA) [87]. This is due to the excellent properties imparted by this structure, including superior adhesion on various substrates, water and thermal resistance, and tunable curing profiles. Hence, DGBPA-based resins can be used in high performance applications including automobile body parts, sports equipment, and siding panels in the construction industry [88]. Considering these attractive properties of epoxy resins, Paramarta et al. reported that bioresins made from soybean oil epoxide with anhydride curing agents have the potential to replace traditional epoxy resins [89]. There are four major applications of epoxy resins: coatings, composite matrices, adhesives, and castings [90]. Out of these, the epoxy adhesives market has grown extensively due to greater demand for low cost and high-performance materials [91].

1.7.1.1 Coatings

The function of a surface coating is to protect the material from corrosion and other environmental impacts, as well as decorative purposes [90]. Coatings can be applied on a variety of surfaces include metal, wood, concrete, and glass. Epoxy resins are versatile materials fulfilling the required characteristics, including bond strength on various substrates, chemical resistance, porosity, and durability [91,92]. Numerous studies shown that vegetable oil-based epoxy coatings, especially with amine hardeners, can replace DGBPA resins [93]. For instance, Patil et. al.

prepared a corrosion-proof coating from epoxidized alkyd resin. This alkyd resin's backbone was modified by amino silane compound in order to enhance the anti-corrosion properties, and the resin was cured by itaconic acid [107]. Many amine hardeners are toxic compounds derived from nonrenewable sources, so there have been many studies to eliminate such compounds from coating formulations to produce environmentally friendly solutions. Kovash Jr. et al. reported a 100% biobased coating formulation from epoxidized sucrose soyate (ESS) and dicarboxylic acids [94]. Despite good compatibility between ESS and dicarboxylic acids, these 100% biobased coatings required a catalyst and still the drying time was not adequate to scale the process for industrial application [94]. There has been a great interest in biobased wood coatings to protect wood from moisture and other environmental factors. Drying oils and other biopolymer-based wood coatings have durability issues like cracking and peeling from the substrate, for instance linseed and tall oils [95]. Such poor performance is caused by poor adhesion to the surface and intramolecular cohesion bonding. between Hence, there is a need to develop a sustainable biobased coating formulation for wood preservation.

1.7.1.2 Adhesives and Sealants

Two surfaces are bonded or sealed through materials called adhesives and sealants (A&S). In particular, adhesives are used for bonding applications while sealants are used for filling or sealing the gap between two surfaces. When the gap between surfaces needs to be filled while bonding them together, sealants are more appropriate than adhesives. The function of these materials is to bond surfaces without compromising properties due to riveting or welding. The sealant materials can also transfer loads throughout a structure making it stronger and eliminating any potential for fracture propagation. With these characteristics, sealants can be used in many industries include aerospace, automobile, construction, packaging, and apparel. There are a wide

range of A&S materials, including epoxies, polyurethanes, and acrylics, that are used depending on the properties required. But epoxy resins are used most widely, across many industries [96]. Epoxies are shown to have a better adhesion and bonding performance than other types, which is why they are widely used in A&S applications [96]. Although the majority of A&S are derived from petroleum sources, there has been extensive research on biobased alternatives, including plant oil biopolymers, starch, lignin, cellulose. These biobased A&S have some disadvantages, including solvent usage in their formulation, and cost-effective synthesis of their monomers, and these issues still need to be explored [97]. For example, Kong et al. prepared canola oil-based polyurethane adhesives, which showed comparable lap shear strength and chemical resistance properties to petroleum derived commercial polyurethane adhesives [98]. Wiebke et al. reported three pressure sensitive adhesive (PSA) formulations prepared from plant oil methyl esters, which have adhesion properties within the range of commercial petroleum derived PSAs [99]. However, this PSA formulation required solvent usage, which can limit its applications in many industries.

1.7.2 Biocomposites

Biocomposites are promising materials due to their properties, for instance low density and biobased feedstocks like natural fibers and bioresins [100]. Traditionally, wood has been a dominate source of fiber for construction but it has certain drawbacks like durability against moisture and fungal degradation, while biocomposites can perform well under a wide range of conditions from dry to humid and from low to high temperatures. A patio deck can be constructed from wood vs. biocomposites prepared from natural fiber and bioresin. The natural fiber of biocomposites can be protected by the polymer that can prevent the natural fiber degradation from water and biological attack from organisms like fungi. Additionally, many research reports indicate that low-cost natural fibers could replace some of the synthetic fibers without

compromising properties, and this allows their applications to be extended as well as replaced [90,91]. For instance, glass fiber could be replaced by natural fiber in making biocomposites for nonstructural applications.

1.7.2.1 Automobile interior parts

Biocomposites prepared from natural and synthetic fibers like carbon fiber have been used to make lightweight automobile components. Compared to traditional metals in automobile construction, light weight automobiles are more fuel efficient [102]. European countries have set a challenging target to reduce CO_2 to of 95 g/km from automobile emission through decreasing vehicle weight [102]. In order to achieve such ambitious goals, biocomposite properties must be acceptable to current standards. Birat et al. made a hybrid composite from sisal and glass fibers and analyzed its mechanical and thermal properties. Their data suggests that such hybrid composites could be used to make numerous interior parts of an automobile [103]. Khalfallah et al. prepared flax laminates from the newly developed resin "ACRODUR" and formed composites for automobile interior applications. Moreover, they have optimized the flax fiber content (at least 40%) with *ACRODUR* resin and processing parameters to make such types of composites [104].

1.7.2.2 Structural and nonstructural construction material

Researchers have also reported utilization of biocomposites for structures such as helmets, electrical cover boards, mailboxes, and mirror covers [105]. Additionally, biocomposites have also been used for making roofs, pedestrian bridges, and beams as load-bearing components in structural applications [105]. Generally, there are 8 major types of material used for building the roof: asphalt shingles, metal, stone-coated steel, rubber slate, clay and concrete slate, and biocomposite materials [109]. In general, the materials used for structural applications require moderate flexural strength, load capacity, and modulus of elasticity. Natural fiber composites are

able to fulfill most of these requirements along with greater renewability. Additionally, biocomposites can be used for nonstructural applications including non-load bearing partitions, cladding systems, and ducting to replace the use of some non-renewable plastics, rubber, and metals.

1.8 Concluding remarks

In spite of some of the current challenges of infusing natural fibers with bioresins to form perfect biocomposites, there is considerable potential for these feedstocks to make competitive materials through further research in this area. Promising biocomposites have been prepared from modified natural fibers by various surface treatment methods of which, some are not sustainable. For example, the alkali treatment of fibers produces hazardous alkali waste as a by-product. The polymer matrix is as important as natural fibers in making biocomposites. Additionally, plant oil epoxides are a promising feedstock to be used as precursor in making the polymer matrix used to manufacture biocomposites. Furthermore, plant oil modifications have not been explored intensively in this context so there are many opportunities to develop novel biobased epoxides. In addition to this, there is a strong opportunity to design novel crosslinking agents for plant oil-based epoxides which can directly affect biocomposite properties.

1.9 Hypothesis, Objective and Thesis organization

There is a need to develop biobased epoxy resins to complement some of the traditional epoxy resins. Additionally, if such bioresins can be synthesized via green chemistry principles then it would not only contribute to the bioeconomy but also minimize the overall carbon footprint of manufacturing.

1.9.1 Objective and Hypothesis

1.9.1.1 Hypothesis

It is hypothesized that;

a. Plant oil epoxides can be cured with a fully biobased curing agent made from citric acid to prepare a high biocontent bioresin, without the use of solvent. This could be achieved by changing or aligning the polarities of either component.

b. Epoxidized fatty acid methyl esters can be synthesized for use as reactive diluents with curing agents such as citric acid and trimellitic anhydride.

c. Citric acid can be partially esterified with short to medium chain length alcohols to create a crosslinking catalyst that is readily soluble in triglyceride epoxides.

The hypotheses were tested as depicted in Figure 1.6.

1.9.1.2 Objective

To develop plant oil based bioresins for biocomposites and other applications:

Approach 1: Produce plant oil epoxides that are miscible with the biobased curing agents.

Approach 2: Produce biobased curing agents that are miscible with plant oil epoxides.

1.9.2 Thesis organization

Plant oil based bioresins

Bioresins & Natural fiber biocomposites

Solvent-free synthesis of bioresins & biocomposites

Chapter 1

General introduction

Chapter 4

Biobased thermosets from epoxidized linseed oil and its methyl esters

Chapter 2

Epoxidized plant oil based natural fiber biocomposites

Chapter 5

Novel biobased curing agents for the plant oil epoxides

Chapter 3

Development of epoxidized hemp oil prepolymers for the preparation of thermoset networks

Chapter 6

Solvent-free manufacturing of high biocontent bioresins and biocomposites

Chapter 7

General conclusion and future work

Figure 1.6 Thesis organization

1.10 References

[1] "Resin | Chemical Compound." *Encyclopedia Britannica*,
https://www.britannica.com/science/resin. Accessed 27 May 2020.

[2] *How Plastics Are Made*. https://plastics.americanchemistry.com/How-Plastics-Are-Made/.
Accessed 27 May 2020.

[3] *Types of Resins and Their Uses and Applications*.
https://www.thomasnet.com/articles/plastics-rubber/types-of-resins. Accessed 27 May 2020.

[4] *Bioresins Suppliers*.
http://polymerdatabase.com/Polymer%20Brands/Bioplastic%20Suppliers.html. Accessed 29
May 2020.

[5] McKeon, Thomas, et al. *Industrial Oil Crops*. Elsevier, 2016.

[6] Zhang, Chaoqun, et al. "Recent Advances in Vegetable Oil-Based Polymers and Their
Composites." *Progress in Polymer Science*, vol. 71, Aug. 2017, pp. 91–143. *ScienceDirect*,
doi:10.1016/j.progpolymsci.2016.12.009.

[7] Miao, Shida, et al. "Vegetable-Oil-Based Polymers as Future Polymeric Biomaterials." *Acta
Biomaterialia*, vol. 10, no. 4, Apr. 2014, pp. 1692–704. *ScienceDirect*,
doi:10.1016/j.actbio.2013.08.040.

[8] Anderson, Dan, et al. "A Primer on Oils Processing Technology." *Bailey's Industrial Oil and
Fat Products*, American Cancer Society, 2020, pp. 1–47. *Wiley Online Library*,
https://onlinelibrary-wiley-
com.login.ezproxy.library.ualberta.ca/doi/abs/10.1002/047167849X.bio077.pub2.

[9] Wan, Peter J., and Phillip J. Wakelyn. *Technology and Solvents for Extracting Oilseeds and
Nonpetroleum Oils*. The American Oil Chemists Society, 1997.

[10] S. Omonov, Tolibjon, et al. "The Epoxidation of Canola Oil and Its Derivatives." *RSC
Advances*, vol. 6, no. 95, 2016, pp. 92874–86. *pubs-rsc-
org.login.ezproxy.library.ualberta.ca*, doi:10.1039/C6RA17732H.

[11] Ellis, B. "Introduction to the Chemistry, Synthesis, Manufacture and Characterization of Epoxy Resins." *Chemistry and Technology of Epoxy Resins*, edited by Bryan Ellis, Springer Netherlands, 1993, pp. 1–36. *Springer Link*, https://doi.org/10.1007/978-94-011-2932-9_1.

[12] Tayde Saurabh, Patnaik M., Bhagt S.L., Renge V.C. "Epoxidation of Vegetable Oils: A Review." *International Journal of Advanced Engineering Technology*, vol. II, no. IV, Dec. 2011, pp. 491–501.

[13] Mungroo, Rubeena, et al. "Epoxidation of Canola Oil with Hydrogen Peroxide Catalyzed by Acidic Ion Exchange Resin." *Journal of the American Oil Chemists' Society*, vol. 85, no. 9, 2008, pp. 887–96. *Wiley Online Library*, doi:10.1007/s11746-008-1277-z.

[14] Roy, Arindam Sinha, et al. "An Overview of Production, Properties, and Uses of Biodiesel from Vegetable Oil." *Green Fuels Technology: Biofuels*, edited by Carlos Ricardo Soccol et al., Springer International Publishing, 2016, pp. 83–105. *Springer Link*, https://doi.org/10.1007/978-3-319-30205-8_4.

[15] Turco, Rosa, et al. "Comparison of Different Possible Technologies for Epoxidation of Cynara Cardunculus Seed Oil." *European Journal of Lipid Science and Technology*, vol. 122, no. 1, 2020, p. 1900100. *Wiley Online Library*, doi:10.1002/ejlt.201900100.

[16] Goud, Vaibhav V., et al. "Epoxidation of Karanja (Pongamia Glabra) Oil Catalysed by Acidic Ion Exchange Resin." *European Journal of Lipid Science and Technology*, vol. 109, no. 6, June 2007, pp. 575–84. *onlinelibrary-wiley-com.login.ezproxy.library.ualberta.ca*, doi:10.1002/ejlt.200600298.

[17] La Scala, John, and Richard P. Wool. "Effect of FA Composition on Epoxidation Kinetics of TAG." *Journal of the American Oil Chemists' Society*, vol. 79, no. 4, Apr. 2002, pp. 373–78. *Springer Link*, doi:10.1007/s11746-002-0491-9.

[18] Ashcroft, W. R. "Curing Agents for Epoxy Resins." *Chemistry and Technology of Epoxy Resins*, edited by Bryan Ellis, Springer Netherlands, 1993, pp. 37–71. *Springer Link*, https://doi.org/10.1007/978-94-011-2932-9_2.

[19] Mikulcová, Veronika, et al. "Formulation, Characterization and Properties of Hemp Seed Oil and Its Emulsions." *Molecules : A Journal of Synthetic Chemistry and Natural Product Chemistry*, vol. 22, no. 5, Apr. 2017. *PubMed Central*, doi:10.3390/molecules22050700.

[20] Frischinger, Isabelle, and Stoil Dirlikov. "Toughening of Epoxy Resins by Epoxidized Soybean Oil." *Toughened Plastics I*, vol. 233, American Chemical Society, 1993, pp. 451–89. *ACS Publications*, https://doi.org/10.1021/ba-1993-0233.ch019.

[21] Niedermann, Péter, et al. "Effect of Epoxidized Soybean Oil on Curing, Rheological, Mechanical and Thermal Properties of Aromatic and Aliphatic Epoxy Resins." *Journal of Polymers and the Environment*, vol. 22, no. 4, Dec. 2014, pp. 525–36. *Springer Link*, doi:10.1007/s10924-014-0673-8.

[22] Kumar, Sudheer, et al. "Toughening of Petroleum Based (DGEBA) Epoxy Resins with Various Renewable Resources Based Flexible Chains for High Performance Applications: A Review." *Industrial & Engineering Chemistry Research*, vol. 57, no. 8, Feb. 2018, pp. 2711–26. *ACS Publications*, doi:10.1021/acs.iecr.7b04495.

[23] Mustapha, Rohani, et al. "Vegetable Oil-Based Epoxy Resins and Their Composites with Bio-Based Hardener: A Short Review." *Polymer-Plastics Technology and Materials*, vol. 58, no. 12, Aug. 2019, pp. 1311–26. *Taylor and Francis+NEJM*, doi:10.1080/25740881.2018.1563119.

[24] Ding, Cheng, and Avtar S. Matharu. "Recent Developments on Biobased Curing Agents: A Review of Their Preparation and Use." *ACS Sustainable Chemistry & Engineering*, vol. 2, no. 10, Oct. 2014, pp. 2217–36. *ACS Publications*, doi:10.1021/sc500478f.

[25] Baroncini, Elyse A., et al. "Recent Advances in Bio-Based Epoxy Resins and Bio-Based Epoxy Curing Agents." *Journal of Applied Polymer Science*, vol. 133, no. 45, 2016. *Wiley Online Library*, doi:10.1002/app.44103.

[26] Peng, Changgeng, et al. "The Hygroscopic Properties of Dicarboxylic and Multifunctional Acids: Measurements and UNIFAC Predictions." *Environmental Science & Technology*, vol. 35, no. 22, Nov. 2001, pp. 4495–501. *ACS Publications*, doi:10.1021/es0107531.

[27] Tsao, G. T., et al. "Production of Multifunctional Organic Acids from Renewable Resources." *Recent Progress in Bioconversion of Lignocellulosics*, edited by G. T. Tsao et al., Springer Berlin Heidelberg, 1999, pp. 243–80. *Springer Link*, https://doi.org/10.1007/3-540-49194-5_10.

[28] Ma, Songqi, and Dean C. Webster. "Naturally Occurring Acids as Cross-Linkers To Yield VOC-Free, High-Performance, Fully Bio-Based, Degradable Thermosets." *Macromolecules*, vol. 48, no. 19, Oct. 2015, pp. 7127–37. *ACS Publications*, doi:10.1021/acs.macromol.5b01923.

[29] Rizzi, George P., and Harry M. Taylor. "A Solvent-Free Synthesis of Sucrose Polyesters." *Journal of the American Oil Chemists' Society*, vol. 55, no. 4, 1978, pp. 398–401. *Wiley Online Library*, doi:10.1007/BF02911900.

[30] Monono, Ewumbua M., et al. "Pilot Scale (10kg) Production and Characterization of Epoxidized Sucrose Soyate." *Industrial Crops and Products*, vol. 74, Nov. 2015, pp. 987–97. *ScienceDirect*, doi:10.1016/j.indcrop.2015.06.035.

[31] Babu, Ramesh P., et al. "Current Progress on Bio-Based Polymers and Their Future Trends." Progress in Biomaterials, vol. 2, no. 1, Mar. 2013, p. 8. Springer Link, https://doi.org/10.1186/2194-0517-2-8.

[32] Stephan Kabasci. Biobased Plastics: Materials and Applications. First edition, vol. 1, John Wiley & Sons, Ltd. Accessed 22 Aug. 2021. http://medien.ubitweb.de/pdfzentrale/978/111/999/Leseprobe_1_9781119994008.pdf

[33] Curran, Mary Ann. "Biobased Materials." Kirk-Othmer Encyclopedia of Chemical Technology, American Cancer Society, 2010, pp. 1–19. Wiley Online Library, https://onlinelibrary-wiley-com.login.ezproxy.library.ualberta.ca/doi/abs/10.1002/0471238961.biobcurr.a01.

[34] Finlay, Mark R. "Old Efforts at New Uses: A Brief History of Chemurgy and the American Search for Biobased Materials." Journal of Industrial Ecology, vol. 7, no. 3–4, 2003, pp. 33–46. Wiley Online Library, https://doi.org/https://doi.org/10.1162/108819803323059389.

[35] Biswas, E., et al. "Recent Advances and Technologies of Biobased Composites." Biobased Composites, John Wiley & Sons, Ltd, 2021, pp. 107–21. Wiley Online Library, https://onlinelibrary-wiley-com.login.ezproxy.library.ualberta.ca/doi/abs/10.1002/9781119641803.ch8.

[36] Kumar, Sudheer, et al. "Recent Development of Biobased Epoxy Resins: A Review." Polymer-Plastics Technology and Engineering, vol. 57, no. 3, Feb. 2018, pp. 133–55. Taylor and Francis+NEJM, https://doi.org/10.1080/03602559.2016.1253742.

[37] La Scala, John, and Richard P. Wool. "Effect of FA Composition on Epoxidation Kinetics of TAG." Journal of the American Oil Chemists' Society, vol. 79, no. 4, Apr. 2002, pp. 373–78. Springer Link, https://doi.org/10.1007/s11746-002-0491-9.

[38] Kim, Joo Ran, and Suraj Sharma. "The Development and Comparison of Bio-Thermoset Plastics from Epoxidized Plant Oils." Industrial Crops and Products, vol. 36, no. 1, Mar. 2012, pp. 485–99. ScienceDirect, https://doi.org/10.1016/j.indcrop.2011.10.036.

[39] Unnikrishnan, K. P., and Eby Thomas Thachil. "Synthesis and Characterization of Cardanol-Based Epoxy Systems." Designed Monomers and Polymers, vol. 11, no. 6, Jan. 2008, pp. 593–607. Taylor and Francis+NEJM, https://doi.org/10.1163/156855508X363870.

[40] Kanehashi, Shinji, et al. "Preparation and Characterization of Cardanol-Based Epoxy Resin for Coating at Room Temperature Curing." Journal of Applied Polymer Science, vol. 130, no. 4, 2013, pp. 2468–78. Wiley Online Library, https://doi.org/https://doi.org/10.1002/app.39382.

[41] Hu, Fengshuo, et al. "Preparation and Characterization of Fully Furan-Based Renewable Thermosetting Epoxy-Amine Systems." Macromolecular Chemistry and Physics, vol. 216, no. 13, 2015, pp. 1441–46. Wiley Online Library, https://doi.org/https://doi.org/10.1002/macp.201500142.

[42] Eid, Nadim, et al. "Synthesis and Properties of Furan Derivatives for Epoxy Resins." ACS Sustainable Chemistry & Engineering, vol. 9, no. 24, June 2021, pp. 8018–31. ACS Publications, https://doi.org/10.1021/acssuschemeng.0c09313.

[43] Zhang, Haibo, et al. "Synthesis and Characterization of Bio-Based Epoxy Thermosets Using Rosin-Based Epoxy Monomer." Iranian Polymer Journal, vol. 30, no. 7, July 2021, pp. 643–54. Springer Link, https://doi.org/10.1007/s13726-021-00918-9.

[44] Vevere, Laima, et al. "A Review of Wood Biomass-Based Fatty Acids and Rosin Acids Use in Polymeric Materials." Polymers, vol. 12, no. 11, Nov. 2020, p. 2706. www.mdpi.com, https://doi.org/10.3390/polym12112706.

[45] Xu, Chunbao, and Fatemeh Ferdosian. "Lignin-Based Epoxy Resins." Conversion of Lignin into Bio-Based Chemicals and Materials, edited by Chunbao Xu and Fatemeh Ferdosian, Springer Berlin Heidelberg, 2017, pp. 111–31. Springer Link, https://doi.org/10.1007/978-3-662-54959-9_7.

[46] Lu, Xinyu, et al. "Pyrolysis Mechanism and Kinetics of High-Performance Modified Lignin-Based Epoxy Resins." Journal of Analytical and Applied Pyrolysis, vol. 154, Mar. 2021, p. 105013. ScienceDirect, https://doi.org/10.1016/j.jaap.2020.105013.

[47] Jahandideh, Arash, et al. "Synthesis and Characterization of Novel Star-Shaped Itaconic Acid Based Thermosetting Resins." Journal of Polymers and the Environment, vol. 26, no. 5, May 2018, pp. 2072–85. Springer Link, https://doi.org/10.1007/s10924-017-1112-4.

[48] Li, Peng, et al. "Itaconic Acid as a Green Alternative to Acrylic Acid for Producing a Soybean Oil-Based Thermoset: Synthesis and Properties." ACS Sustainable Chemistry & Engineering, vol. 5, no. 1, Jan. 2017, pp. 1228–36. ACS Publications, https://doi.org/10.1021/acssuschemeng.6b02654.

[49] Patil, Deepak M., et al. "Synthesis of Bio-Based Epoxy Resin from Gallic Acid with Various Epoxy Equivalent Weights and Its Effects on Coating Properties." Journal of Coatings Technology and Research, vol. 14, no. 2, Mar. 2017, pp. 355–65. Springer Link, https://doi.org/10.1007/s11998-016-9853-x.

[50] Tarzia, Antonella, et al. "Synthesis, Curing, and Properties of an Epoxy Resin Derived from Gallic Acid." BioResources, vol. 13, no. 1, 2018, pp. 632–45.

[51] Yuan, Wangchao, et al. Research Progress on Vanillin-Based Thermosets. 2018, https://www-ingentaconnect-com.login.ezproxy.library.ualberta.ca/contentone/ben/cgc/2018/00000005/00000003/art00004.

[52] Mogheiseh, Mohsen, et al. "Vanillin-Derived Epoxy Monomer for Synthesis of Bio-Based Epoxy Thermosets: Effect of Functionality on Thermal, Mechanical, Chemical and Structural Properties." Chemical Papers, vol. 74, no. 10, Oct. 2020, pp. 3347–58. Springer Link, https://doi.org/10.1007/s11696-020-01164-8.

[53] Saxon, Derek J., et al. "Next-Generation Polymers: Isosorbide as a Renewable Alternative." Progress in Polymer Science, vol. 101, Feb. 2020, p. 101196. ScienceDirect, https://doi.org/10.1016/j.progpolymsci.2019.101196.

[54] Yum, Sugil, et al. "Synthesis and Characterization of Isosorbide Based Polycarbonates." Polymer, vol. 179, Sept. 2019, p. 121685. ScienceDirect, https://doi.org/10.1016/j.polymer.2019.121685.

[55] Bang, Hyun Bae, et al. "High-Level Production of Trans-Cinnamic Acid by Fed-Batch Cultivation of Escherichia Coli." Process Biochemistry, vol. 68, May 2018, pp. 30–36. ScienceDirect, https://doi.org/10.1016/j.procbio.2018.01.026.

[56] Xin, Junna, et al. "Study of Green Epoxy Resins Derived from Renewable Cinnamic Acid and Dipentene: Synthesis, Curing and Properties." RSC Advances, vol. 4, no. 17, 2014, pp. 8525–32. pubs-rsc-org.login.ezproxy.library.ualberta.ca, https://doi.org/10.1039/C3RA47927G.

[57] Caillol, Sylvain, et al. "Eugenol, a Developing Asset in Biobased Epoxy Resins." Polymer, vol. 223, May 2021, p. 123663. ScienceDirect, https://doi.org/10.1016/j.polymer.2021.123663.

[58] Chen, Chien-Han, et al. "A Facile Strategy to Achieve Fully Bio-Based Epoxy Thermosets from Eugenol." Green Chemistry, vol. 21, no. 16, 2019, pp. 4475–88. pubs-rsc-org.login.ezproxy.library.ualberta.ca, https://doi.org/10.1039/C9GC01184F.

[59] Ding, Cheng, and Avtar S. Matharu. "Recent Developments on Biobased Curing Agents: A Review of Their Preparation and Use." ACS Sustainable Chemistry & Engineering, vol. 2, no. 10, Oct. 2014, pp. 2217–36. ACS Publications, https://doi.org/10.1021/sc500478f.

[60] de Nograro, F.Fdez, et al. "Dynamic and Mechanical Properties of Epoxy Networks Obtained with PPO Based amines/mPDA Mixed Curing Agents." Polymer, vol. 37, no. 9, Apr. 1996, pp. 1589–600. ScienceDirect, https://doi.org/10.1016/0032-3861(96)83707-4.

[61] Maity, T., et al. "Curing Study of Epoxy Resin by New Aromatic Amine Functional Curing Agents along with Mechanical and Thermal Evaluation." Materials Science and Engineering: A, vol. 464, no. 1, Aug. 2007, pp. 38–46. ScienceDirect, https://doi.org/10.1016/j.msea.2007.01.128.

[62] Froidevaux, Vincent, et al. "Biobased Amines: From Synthesis to Polymers; Present and Future." Chemical Reviews, vol. 116, no. 22, Nov. 2016, pp. 14181–224. ACS Publications, https://doi.org/10.1021/acs.chemrev.6b00486.

[63] *Sustainable Synthetic Approaches for the Preparation of Plant Oil-Based Thermosets | SpringerLink*. https://link-springer-com.login.ezproxy.library.ualberta.ca/article/10.1007/s11746-016-2932-4. Accessed 15 May 2020.

[64] Omonov, Tolibjon, and Jonathan Curtis. *Aldehyde Free Thermoset Bioresins and Biocomposites*. US20160215088A1, 28 July 2016, https://patents.google.com/patent/US20160215088A1/en.

[65] Li, Yantao, et al. "Synthesis and Characterization of Cast Resin Based on Different Saturation Epoxidized Soybean Oil." *European Journal of Lipid Science and Technology*, vol. 112, no. 4, Apr. 2010, pp. 511–16. *onlinelibrary-wiley-com.login.ezproxy.library.ualberta.ca*, doi:10.1002/ejlt.200900191.

[66] Fache, Maxence, et al. "Biobased Epoxy Thermosets from Vanillin-Derived Oligomers." *European Polymer Journal*, vol. 68, July 2015, pp. 526–35. *ScienceDirect*, doi:10.1016/j.eurpolymj.2015.03.048.

[67] Jian, Xin-Yi, et al. "All Plant Oil Derived Epoxy Thermosets with Excellent Comprehensive Properties." *Macromolecules*, vol. 50, no. 15, Aug. 2017, pp. 5729–38. *ACS Publications*, doi:10.1021/acs.macromol.7b01068.

[68] Pascault, Jean-Pierre, and Roberto J. J. Williams. *Epoxy Polymers: New Materials and Innovations*. John Wiley & Sons, 2009 pp. 215-230.

[69] Wool, Richard, et al. *High Modulus Polymers and Composites from Plant Oils*. US6121398A, 19 Sept. 2000, https://patents.google.com/patent/US6121398A/en.

[70] Lu, Yongshang, and Richard C. Larock. "Novel Polymeric Materials from Vegetable Oils and Vinyl Monomers: Preparation, Properties, and Applications." *ChemSusChem*, vol. 2, no. 2, Feb. 2009, pp. 136–47. *chemistry-europe-onlinelibrary-wiley-com.login.ezproxy.library.ualberta.ca (Atypon)*, doi:10.1002/cssc.200800241.

[71] Zhou, Yonghui, et al. "Interface and Bonding Mechanisms of Plant Fibre Composites: An Overview." *Composites Part B: Engineering*, vol. 101, Sept. 2016, pp. 31–45. *Crossref*, doi:10.1016/j.compositesb.2016.06.055.

[72] Sushanta K. Sahoo, Smita Mohanty, Sanjay K. Nayak. (2015). "Effect of lignocellulosic fibers on mechanical, thermomechanical and hydrophilic studies of epoxy modified with novel bioresin epoxy methyl ester derived from soybean oil." *Polymers Advanced Technologies*, 2015, 26 1619-1626.

[73] Rudi Dungani, Myrtha Karina, Subyakto, A. Sulaeman, Dede Hermawan and A. Hadiyane. "Agricultural Waste Fibers Towards Sustainability and Advanced Utilization: A Review." *Asian Journal of Plant Sciences*, vol. 15, no. 1–2, 2016, pp. 42–55.

[74] John, Maya Jacob, and Rajesh D. Anandjiwala. "Recent Developments in Chemical Modification and Characterization of Natural Fiber-Reinforced Composites." *Polymer Composites*, vol. 29, no. 2, 2008, pp. 187–207. *Wiley Online Library*, doi:10.1002/pc.20461.

[75] Célino, Amandine, et al. "Characterization and Modeling of the Moisture Diffusion Behavior of Natural Fibers." *Journal of Applied Polymer Science*, vol. 130, no. 1, 2013, pp. 297–306. *Wiley Online Library*, doi:10.1002/app.39148.

[76] Council, National Research, et al. *High Performance Synthetic Fibers for Composites*. National Academies Press, 1992.

[77] Monteiro, Sergio Neves, et al. "Natural-Fiber Polymer-Matrix Composites: Cheaper, Tougher, and Environmentally Friendly." *JOM*, vol. 61, no. 1, Jan. 2009, pp. 17–22. *Springer Link*, doi:10.1007/s11837-009-0004-z.

[78] Chen, Hongzhang. "Chemical Composition and Structure of Natural Lignocellulose." *Biotechnology of Lignocellulose: Theory and Practice*, edited by Hongzhang Chen, Springer Netherlands, 2014, pp. 25–71. *Springer Link*, https://doi.org/10.1007/978-94-007-6898-7_2.

[79] Fuqua, Michael A., et al. "Natural Fiber Reinforced Composites." *Polymer Reviews*, vol. 52, no. 3, July 2012, pp. 259–320. *Taylor and Francis+NEJM*, doi:10.1080/15583724.2012.705409.

[80] Savita Dixit, Ritesh Goel, Akash Dubey, Price Raj Shivhare, Tanmay Bhalavi. (2017). "Natural fiber reinforced polymer composite materials - A review" *Polymers from renewable resources*, Vol 8, No. 2, January 2017: 71-77.

[81] Maya Jacob John, Sabu Thomas. (2007)."Review: Biofibres and biocomposites" *Carbohydrate Polymers* 71 (2008) 343-364.

[82] A. Ticoalu, T. Aravinthan, F. Cardona. (2010). "A review of current development in natural fiber composites for structural and infrastructure applications." *Southern Region Engineering Conference*, 11-12 November 2010, Toowoomba, Australia.

[83] Alejandrina Campanella, Mingjiang Zhan, Paula Watt, Alexander T. Grous, Connie Shen, Richard P. Wool. (2015). "Triglyceride-based thermosetting resins with different reactive diluents and fiber reinforced composite applications." *Composites: Part A*, 72 (2015) 192-199.

[84] Marie-Alix Berthet, Claire Mayer-Laigle, Xavier Rouau, Nathalie Gontard, Helene Angellier-Coussy. 2017. "Sorting natural fibers: A way to better understand the role of fiber size polydispersity on the mechanical properties of biocomposites." *Composites Part A: Applied Science and Manufacturing*, 95 (2017): 12-21.

[85] George, Jayamol, et al. "A Review on Interface Modification and Characterization of Natural Fiber Reinforced Plastic Composites." *Polymer Engineering & Science*, vol. 41, no. 9, 2001, pp. 1471–85. *Wiley Online Library*, doi:10.1002/pen.10846.

[86] Wu, Yingji, et al. "Water-Resistant Hemp Fiber-Reinforced Composites: In-Situ Surface Protection by Polyethylene Film." *Industrial Crops and Products*, vol. 112, Feb. 2018, pp. 210–16. *ScienceDirect*, doi:10.1016/j.indcrop.2017.12.014.

[87] Ma, Songqi, et al. "Research Progress on Bio-Based Thermosetting Resins." *Polymer International*, vol. 65, no. 2, 2016, pp. 164–73. *Wiley Online Library*, doi:10.1002/pi.5027.

[88] Jin, Fan-Long, et al. "Synthesis and Application of Epoxy Resins: A Review." *Journal of Industrial and Engineering Chemistry*, vol. 29, Sept. 2015, pp. 1–11. *ScienceDirect*, doi:10.1016/j.jiec.2015.03.026.

[89] Paramarta, Adlina, and Dean C. Webster. "Bio-Based High Performance Epoxy-Anhydride Thermosets for Structural Composites: The Effect of Composition Variables." *Reactive and Functional Polymers*, vol. 105, Aug. 2016, pp. 140–49. *ScienceDirect*, doi:10.1016/j.reactfunctpolym.2016.06.008.

[90] Chen, X. M., and B. Ellis. "Coatings and Other Applications of Epoxy Resins." *Chemistry and Technology of Epoxy Resins*, edited by Bryan Ellis, Springer Netherlands, 1993, pp. 303–25. *Springer Link*, https://doi.org/10.1007/978-94-011-2932-9_9.

[91] Shaw, S. J. "Epoxy Resin Adhesives." *Chemistry and Technology of Epoxy Resins*, edited by Bryan Ellis, Springer Netherlands, 1993, pp. 206–55. *Springer Link*, https://doi.org/10.1007/978-94-011-2932-9_7.

[92] *What Is Epoxy Paint? - Bright Hub Engineering*. https://www.brighthubengineering.com/building-construction-design/63632-characteristics-of-epoxy-paint-and-thinner/. Accessed 21 May 2020.

[93] Atul Tiwari, Anthony Galanis, and Mark D. Soucek. *Biobased and Environmental Benign Coatings*. 1st ed., John Wiley & Sons, Ltd, 2016. *Wiley Online Library*,

https://onlinelibrary-wiley-com.login.ezproxy.library.ualberta.ca/doi/10.1002/9781119185055. pp 121-140.

[94] Kovash Jr., Curtiss S., et al. "Thermoset Coatings from Epoxidized Sucrose Soyate and Blocked, Bio-Based Dicarboxylic Acids." *ChemSusChem*, vol. 7, no. 8, Aug. 2014, pp. 2289–94. *chemistry-europe-onlinelibrary-wiley-com.login.ezproxy.library.ualberta.ca (Atypon)*, doi:10.1002/cssc.201402091.

[95] Teaca, Carmen, Dan Roşu, Fănică Mustaţă, Teodora Rusu, Liliana Roşu, Irina Roşca, & Cristian-Dragoş Varganici. "Natural Bio-Based Products for Wood Coating and Protection against Degradation: A Review." *BioResources* [Online], 14.2 (2019): 4873-4901. Web. 22 May. 2020

[96] Edward M. Petrie. Handbook of Adhesives and Sealants, Second Edition. AN OVERVIEW OF ADHESIVES AND SEALANTS, Chapter (The McGraw-Hill Companies, Inc., 2007). https://www-accessengineeringlibrary-com.login.ezproxy.library.ualberta.ca/content/book/9780071479165/chapter/chapter1

[97] Magalhães, Solange, et al. "Brief Overview on Bio-Based Adhesives and Sealants." *Polymers*, vol. 11, no. 10, Oct. 2019, p. 1685. *www.mdpi.com*, doi:10.3390/polym11101685.

[98] Kong, Xiaohua, et al. "Characterization of Canola Oil Based Polyurethane Wood Adhesives." *International Journal of Adhesion and Adhesives*, vol. 31, no. 6, Sept. 2011, pp. 559–64. *ScienceDirect*, doi:10.1016/j.ijadhadh.2011.05.004.

[99] Maassen, Wiebke, et al. "Unique Adhesive Properties of Pressure Sensitive Adhesives from Plant Oils." *International Journal of Adhesion and Adhesives*, vol. 64, Jan. 2016, pp. 65–71. *ScienceDirect*, doi:10.1016/j.ijadhadh.2015.10.004.

[100] Panthapulakkal, Suhara, and Mohini Sain. "Agro-Residue Reinforced High-Density Polyethylene Composites: Fiber Characterization and Analysis of Composite Properties." *Composites Part A: Applied Science and Manufacturing*, vol. 38, no. 6, June 2007, pp. 1445–54. *ScienceDirect*, doi:10.1016/j.compositesa.2007.01.015.

[101] Rouison, David, et al. "Resin Transfer Molding of Hemp Fiber Composites: Optimization of the Process and Mechanical Properties of the Materials." *Composites Science and Technology*, vol. 66, no. 7, June 2006, pp. 895–906. *ScienceDirect*, doi:10.1016/j.compscitech.2005.07.040.

[102] Akampumuza, Obed, et al. "Review of the Applications of Biocomposites in the Automotive Industry." *Polymer Composites*, vol. 38, no. 11, 2017, pp. 2553–69. *Wiley Online Library*, doi:https://doi.org/10.1002/pc.23847.

[103] Birat, K. C., et al. "Hybrid Biocomposites with Enhanced Thermal and Mechanical Properties for Structural Applications." *Journal of Applied Polymer Science*, vol. 132, no. 34, 2015. *Wiley Online Library*, doi:https://doi.org/10.1002/app.42452.

[104] Khalfallah, M., et al. "Innovative Flax Tapes Reinforced Acrodur Biocomposites: A New Alternative for Automotive Applications." *Materials & Design*, vol. 64, Dec. 2014, pp. 116–26. *ScienceDirect*, doi:10.1016/j.matdes.2014.07.029.

[105] Ticoalu, A., et al. "A Review of Current Development in Natural Fiber Composites for Structural and Infrastructure Applications." *Proceedings of the Southern Region Engineering Conference (SREC 2010)*, edited by Steven C. Goh and Hao Wang, Engineers Australia, 2010, pp. 113–17. *eprints.usq.edu.au*, http://www.usq.edu.au/engsummit.

[106] Feng, Yechang, et al. "Biobased Thiol-Epoxy Shape Memory Networks from Gallic Acid and Vegetable Oils." *European Polymer Journal*, vol. 112, Mar. 2019, pp. 619–28. *ScienceDirect*, doi:10.1016/j.eurpolymj.2018.10.025.

[107] Baroncini, Elyse A., et al. "Recent Advances in Bio-Based Epoxy Resins and Bio-Based Epoxy Curing Agents." *Journal of Applied Polymer Science*, vol. 133, no. 45, 2016. *Wiley Online Library*, doi:https://doi.org/10.1002/app.44103.

[108] Patil, Deepak M., et al. "Design and Synthesis of Bio-Based Epoxidized Alkyd Resin for Anti-Corrosive Coating Application." *Iranian Polymer Journal*, vol. 27, no. 10, Oct. 2018, pp. 709–19. *Springer Link*, doi:10.1007/s13726-018-0646-1.

[109] *Types of Roofing Materials - Nationwide*.
https://www.nationwide.com/lc/resources/home/articles/types-of-roofing. Accessed 21 May
2021.

[110] "12 Principles of Green Chemistry." *American Chemical Society*,
https://www.acs.org/content/acs/en/greenchemistry/principles/12-principles-of-green-
chemistry.html. Accessed 21 May 2021.

Chapter 2

Epoxidized plant oil based natural fiber composites

2.1 Introduction

Fiber reinforced composite materials can have excellent elastic and mechanical properties, such as high modulus and strength, as well as toughness while maintaining a low density compared to engineering materials, such as metals, alloys and ceramics. These properties can also be tailored via ratios of constituents and their arrangement in the composites. Consequently, they are used widely in many applications including in the aerospace, automotive, construction, marine, oil and gas industries [1]. The mechanical properties of a composite depend, to a large extent, on the properties of the reinforcing fibers. However, the polymer/resin component forms a matrix that binds fibers together, and distributes applied load to the reinforcing fibrous component. At the same time, it protects the stiff but brittle fibers, and gives the fiber preforms a structural shape that is otherwise not possible to maintain [2]. In doing so, the matrix must be chosen such that it has the necessary mechanical properties to transfer mechanical load to the fibers without failure [3]. In addition, a resin should provide a high enough glass transition temperature (T_g) since this determines the useful operating temperature range of the composite material: the higher the T_g of the resin component, the broader the range of applications for the material [4].[2]

Composite materials have often been made using conventional petrochemical polymers such polyolefins, polyesters, polyethers or epoxy resins and incorporating glass, carbon, aramid or other fibers [5]. While synthetic fibers such glass or carbon fibers provide excellent mechanical performance and are not greatly affected by moisture, solvents, acids and bases [2], some drawbacks of these fibers can include their cost, their relatively high densities and their abrasive behaviors, which may be detrimental to the processing equipment [6, 7].

Such factors, along with an increasing environmental awareness which favors materials with a lower carbon footprint, have stimulated the development of natural fiber composites (NFC) from renewable resources. NFC have the potential to be biodegradable, require lower amounts of fossil fuels for their manufacture, and can still be manufactured at a reasonable cost. Typically, NFC are made from fibers derived from agriculture or forestry along with a petrochemical thermoset, or thermoplastic, binding adhesive polymer [1, 8-10]. There are many successful examples of petrochemical polymer-based NFC in the literature that have been made using hemp, flax, kenaf, cellulose, jute, straw, bamboo, wood and other fibers [8-15]. However, most of these NFC are described as non-biodegradable and/or non-recyclable. Moreover, it has been reported that poor interfacial adhesion between the polar-hydrophilic fibers and the predominantly non-polar-hydrophobic polymeric matrix, can result in matrix-fiber incompatibilities [16].

There have also been reports on making fully biobased composite materials, such as from lignocellulosic fibers bound in plant oil derived epoxy or acrylated epoxy resins [1, 5, 9, 16-19] . Also, biodegradable plastic materials originating from either renewable or petrochemical sources, have been used in composites [9, 16, 18]. However, a major drawback limiting the wider use of natural fibers in biocomposite applications is the hydrophilic nature of the fibers, which makes them incompatible with the hydrophobic polymer matrix [16]. Modification of fiber to improve

surface "wettability" is often required to overcome poor fiber/matrix interfacial adhesion [16, 20-22]. Examples of such surface modifications for natural fibers include the use of isocyanates, enzymes, ozone, peroxide treatments, silylation, acetylation, benzoylation and polymer grafting [20-22]. Surface modification has the disadvantage of adding cost and requires the appropriate handling and disposal of significant quantities of hazardous chemicals [16].

Epoxidized plant oils, along with suitable curing agents, could be used in place of other resins and thermoplastic polymers that are currently used to make NFC. This requires identifying appropriate reaction conditions, including temperature, an appropriate catalyst, and the possible use of a solvent medium to facilitate reactions and proper impregnation of natural fibers by monomers or oligomers of the binding resin. In addition, in spite of the hydrophobic nature of epoxidized plant oils, their epoxy groups can also react with hydroxyl moieties of lignocellulosic fibers to form ether linkages.

This study reports on the properties of fully biobased composites (also referred as green composites) made using hemp/wood fibermats bound with biobased resins containing three different epoxidized plant oils (ECO - epoxidized canola oil, EHO – epoxidized hemp oil and ELO – epoxidized linseed oil), and cured with either an aliphatic or an aromatic curing agent.

2.2 Materials and methods

In addition to the Materials and Methods given here, a description of the bioresin synthesis and composite material preparation is given in Sections 3.2 and 3.3 below.

2.2.1   Materials

Canola oil was purchased in bulk (20 L) from the local supermarket (Loblaws, Inc., Canada), hempseed oil was purchased in bulk (20 L) from Rocky Mountain Grain Products (Lethbridge,

AB, Canada) and linseed oil was purchased in bulk (20 L) from the Shape Foods Inc. (Brandon, MB, Canada). All oils were used as supplied to produce epoxidized derivatives. Formic acid (85%) and aqueous hydrogen peroxide (H_2O_2, 35%) were purchased from Univar Canada (Richmond, BC, Canada) and used in epoxidation process. Hydrogen bromide (HBr), 33 wt% solution in glacial acetic acid (Fisher Scientific Canada) and glacial acetic acid (99.7%, Caledon Laboratory Chemicals, Georgetown, ON, Canada) were used in oxirane oxygen content titration of epoxides. ACS grade (≥99.5%) acetone was purchased from Fisher Scientific Canada and used as a solvent medium to prepare epoxy prepolymers. Trimellitic anhydride (1,2,4-benzene tricarboxylic anhydride, MW=192 g/mol; T_m=156 °C) was purchased from Sigma-Aldrich Canada and citric acid (2-hydroxypropane-1,2,3-tricarboxylic acid, MW=192 g/mol; T_m=165 °C) were purchased from Jungbunzlauer Canada Inc. Both TMA and CA were used as curing agents for epoxidized oils to produce bioresins. Hemp/wood-based nonwoven, randomly oriented fibermats (40/60 w/w) with specific density of 2.5 kg/m^2 were provided by BioComposites Group (Drayton Valley, AB, Canada) and used in making biocomposites with epoxidized oil-based resins.

2.2.2 Methods

2.2.2.1 Internal bond strength (IB)

Internal bond strength is defined as a cohesive strength of the material determined through the tensile measurement conducted perpendicular to the test specimen surface [23]. Test samples from each biocomposite formulation were cut with dimensions of 50 mm × 50 mm, and internal bond strength was tested according to ASTM standard ASTM-D1037-12 [23] using an Instron 4204 with a 10 kN load cell and Instron 4482 with 50 kN load cell (Norwood, MA, USA). Test specimens surfaces were bonded to aluminum alloy end-tab fixtures for the test. The loading of the test specimens was conducted by separating the loading fixtures until failure at a crosshead

speed of 3.80 mm/min ± 0.60 mm/min. Internal bonding of the samples were calculated using the equation (1) [23]:

$$Internal\ Bond\ Strength = \frac{Failing\ load}{Length \times Width}; \left[\frac{N}{mm^2}\right] \qquad (1)$$

Five test specimens were used for each biocomposites and results of the measurements were averaged.

2.2.2.2 Static 3-point bending test

Static bending test samples from each biocomposite formulations were cut with dimensions of 75 mm × 150 mm (width × length) and tests were conducted to measure the flexural properties including the modulus of rupture and flexural modulus of elasticity. Tests were then performed in a three-point bend jig, using an Instron 3369 (Norwood, MA, USA) with 30 kN load cell. Tensile loading was applied at a crosshead speed of 8.55 mm/min for 3.90 mm nominal thickness (speed = 0.02*span² /6*nominal thickness) to obtain a load/deflection curve of the test process. Modulus of elasticity (MOE) and modulus of rupture (MOR) were calculated according to the ASTM standard ASTM-D1037-12 [23] using the maximum load at the linear range of the curve and the complete failure curve, respectively as shown in equations (2) and (3):

$$MOR = \frac{3P_{max}L}{2bd^2} \qquad (2)$$

$$MOE = \frac{L^3}{4bd^3} \times \left(\frac{\Delta P}{\Delta y}\right) \qquad (3)$$

where P_{max} is the maximum failure load [N], L is the distance between support centers [mm], b is the test specimen width [mm], and d is the average test specimen thickness [mm]. ΔP is the

increment in load (N) on the straight-line portion of the load/deflection curve, and Δy represents the increment in deflection at mid-span (mm) corresponding to the P increment in load.

2.2.2.3 Dynamic Mechanical Analysis (DMA)

Dynamic mechanical properties of biocomposites such storage modulus (G'), loss modulus (G''), and loss factor (*tan δ*) were measured with a TA Instruments' DMA Q800 (New Castle, DE, USA) equipped with a liquid nitrogen cooling system. Measurements were performed according to ASTM standard method [24] at a fixed frequency of 1 Hz in the dual cantilever bending mode, at a constant heating rate of 2 °C/min from -50 to 180 °C. Similar sized specimens prepared by cutting of the bulk thermoset resin sheet, and results of the measured Tg values were averaged. TA Universal Analysis (version 4.7A) software was used to analyze the experimental data.

2.2.3 Preparation of plant oil epoxides

Epoxidation of plant oils was conducted using *in-situ* generated performic acid as described elsewhere [25, 26] using 20 kg of each oil in 100 L glass reactor (Across International, NJ, USA) equipped with a bottom drain, a water jacket and attached to a recirculating liquid cooler/heater unit. The molar ratio of formic acid: H_2O_2 used was 0.25: 1.5 per double bonds of the oils and the epoxidation process was conducted at 60 °C, for up to 48 hours. The extent of epoxide formation was followed by measuring the OOC of the epoxidized products according to the ASTM standard titrimetric method "Standard Test Method for Epoxy Content of Epoxy Resins" [27], as described elsewhere [25, 26].

2.3   Results and discussion

2.3.1   Characterization of plant oils and their epoxides

Canola (CO), hempseed (HO) and linseed oils (LO) were used to produce epoxidized oils. The fatty acid profiles of these oils before epoxidation reactions were measured by GC-FID according to the method described in [25] and are given in Table 2.1. In addition, Table 2.1 also lists some properties of the oil and the fully epoxidized oil, that were calculated based on these experimentally derived fatty acid profiles.

Fatty acids	Canola [%]	Hempseed [%]	Linseed [%]
C16:0	5.0	7.0	4.9
C16:1	0.3	-	-
C18:0	1.8	3.0	3.0
C18:1 n9	64.1	14.7	17.5
C18:2 n6	18.9	56.0	14.3
C18:3 n3	7.3	17.9	60.3
C20:0	0.6	0.7	-
C20:1	1.6	0.4	-
C22:0	0.4	0.3	-
Total monounsaturated [%]	66.0	15.1	17.5
Total polyunsaturated [%]	26.2	73.9	74.6
Total saturated [%]	7.8	11.0	7.9
Properties (calculated)	**Canola**	**Hempseed**	**Linseed**
Average number of double bonds/mol [-]	3.8	5.5	6.8
Average MW of oil [g/mol]	882	876	874
Average MW of epoxide [g/mol]	944	965	985
Maximum OOC of epoxide [%][†]	6.3/6.1	9.0/8.3	11.0/9.8

[†] Both respective theoretical/experimental OOC values are given

Table 2.1 Fatty acid profiles of canola, hempseed, and linseed oils, along with some important calculated properties of their epoxidized derivatives.

It can be seen from the Table 2.1 that all three oils consist mainly of 18 fatty acids with a high content (~90%) of unsaturated fatty acids. The saturated fatty acid content of these oils (mainly C16:0 and C18:0) varies between 8-11% whereas the abundances of major unsaturated fatty acids oleic acid (C18:1n9), linoleic acid (C18:2n6), and linolenic acid (C18:3n3), differ substantially.

The major fatty acid for CO is C18:1 9c (64%), for HO is C18:2 (56%) and for LO is C18:3 (60%). As a result, CO has a lower number of double bonds (3.8) per triacylglycerol (TAG), HO has a moderate number of double bonds (5.5/TAG) and LO has the highest double bond content (6.8/TAG). Hence, when near complete epoxidation of all double bonds is achieved, these oils significantly differ in their epoxy content. The calculated and experimentally measured OOC of the epoxidized oils used in this study are shown in Table 1. The slightly smaller values of OOC actually achieved compared to the theoretical maximum values, can be explained by both incomplete epoxidation and by epoxide ring-opening side reactions, as we have reported previously [25]. These epoxidized oils were used in preparing biobased resins and composites as described below.

2.3.2 Prepolymer solution preparation

Two types of curing agents - citric acid (CA) and trimellitic anhydride (TMA) - were selected as model curing agents to produce bioresin solutions with epoxidized oils. These curing agents have molecular formulae of $C_6H_8O_7$ and $C_9H_4O_5$ respectively, and hence they have the same nominal molecular weights (MW) of 192.1 g/mol. They also have similar melting points at 165°C (CA) and 156°C (TMA). Despite these similarities, CA and TMA are structurally quite different. CA is an alpha hydroxy tri-carboxylic acid and both hydroxyl and acid functional groups can participate in epoxy ring opening reactions, resulting in multiple curing mechanisms. TMA is an aromatic carboxylic acid anhydride which is readily hydrolyzed to trimellitic acid (benzene-1,2,4-tricarboxylic acid). Both are solid curing agents with very limited solubility at room temperature in EHO, which is viscous and low polarity. Acetone was chosen as the reaction medium, since it can effectively dissolve both curing agents and epoxidized oils while at the same time it is an aprotic solvent and will not participate in reactions with epoxides. In addition, the presence of

solvent will assist in prepolymers penetration into the fibermats, which is otherwise difficult to achieve. Acetone also has a low boiling point so is easily distilled from the impregnated fibermat and then reusable. Resins were prepared from ECO, EHO and ELO using CA and TMA curing agents at stoichiometric ratios 1:1 of epoxy moieties of epoxidized oils to acid moieties of CA or TMA (see Table 2.2).

Resin Composition	Ratio ^{a} [mol/mol]	MOR ^{b} [MPa]	MOE ^{b} [MPa]	IB ^{b} [MPa]	T_g ^{b} [°C]
ECO/CA	1.0/1.27	15.4 ± 1.6	2531 ± 387	0.2 ± 0.0	25.7 ± 1.7
EHO/CA	1.0/1.80	23.9 ± 0.8	2843 ± 319	0.8 ± 0.1	39.1 ± 1.4
ELO/CA	1.0/2.27	38.2 ± 5.2	3982 ± 356	3.0 ± 0.2	52.7 ± 1.5
ECO/TMA	1.0/1.27	28.6 ± 3.0	2891 ± 75	1.8 ± 0.2	38.0 ± 1.7
EHO/TMA	1.0/1.80	45.0 ± 4.7	4190 ± 494	3.8 ± 0.3	85.5 ± 1.4
ELO/TMA	1.0/2.27	40.1 ± 1.7	4352 ± 292	3.4 ± 0.3	83.1 ± 1.5

† In all biocomposites, the hemp/wood 40/60 w/w fibermats were used.

^{a} At these ratio of components the stoichiometric ratio of epoxy to acid groups are equal to one.

^{b} Values are means ± standard deviation of 3 to 5 samples for each group

Table 2.2 The thermal-mechanical properties of biocomposites produced using resin made from various combinations of epoxidised oils with CA or TMA curing agents †

In calculating the stoichiometric ratios of reactive moieties, TMA contributes three carboxylic acid groups (similar to trimellitic acid) since TMA has one free acid group and upon hydrolysis, the anhydride group will potentially yield two more acid groups. It should be noted that due to considerable differences of the epoxy functionality between different epoxidized oils, the molar ratios of curing agents differs significantly. For example, one mole of ECO requires about 1.27 moles of either CA or TMA curing agent for complete curing, while ELO requires 2.27 moles of curing agent (Table 2.2) to react with all epoxide sites.

Using the above information, prepolymer resin solutions were prepared by stirring the required weight of the curing agent (CA or TMA) into the same weight of acetone at a temperature of 50±1°C, until solid particles were dissolved. The appropriate amount of epoxidized oil (Table 2.2) was then mixed into this solution to constitute the resin solutions.

2.3.3   Biocomposite preparation via hot compression moulding

The homogenous (prepolymer) solutions of bioresins produced from different epoxidized oils and curing agents were then used to make biocomposites with hemp/wood fibermats. Hemp/wood based nonwoven, randomly oriented fibermats 15mm × 15mm were soaked in prepolymer solution for about 2 minutes and excess solution was removed by rolling the saturated fibermats through a roller. The space between two rollers was controlled to extrude any excess solution through multiple passes without damaging integrity.

Resin saturated fibermats were placed between two aluminum foil covered steel plates at room temperature and were transferred to the electrically heated platens (150mm × 150mm) of a benchtop Carver press. (Model 3851 Carver Inc., Wabash, IN, USA). Pressure (14000 kPa) was applied and the molding/curing process of biocomposites was achieved by heating to 200 °C for about 5 minutes to allow for heat transfer into the core of the biocomposite. Under these conditions, excess resin was squeezed from the fibermats. The final molded hemp/wood biocomposites were close to 3 mm thick and had a resin content of 30 ± 2 wt%, as measured by the weight differences between each cured biocomposite material and the dry fibermat used to make it. Full removal of the solvent was ensured by post-curing storage in an oven at 200 °C until a constant weight was determined and subsequent cooling to room temperature at 0.5 °C/min.

2.3.4 Mechanical performance of ECO, EHO and ELO based biocomposites

By starting with natural oils covering the range of 3.8-6.8 double bonds per mole of triacylglyceride, resins possessing a corresponding range of OOC were produced (Table 2.1). These resins were used to study the effects of oil composition and epoxide content on NFC material properties. The mechanical properties of these biocomposites were evaluated using flexure, internal bonding, and dynamic mechanical thermal analysis tests.

Table 2.2 and Figure 2.1 demonstrates the MOR and MOE (from the SB test); IB strength (from IB test); and T_g (from DMA test) of the biocomposites produced using two different curing agents.
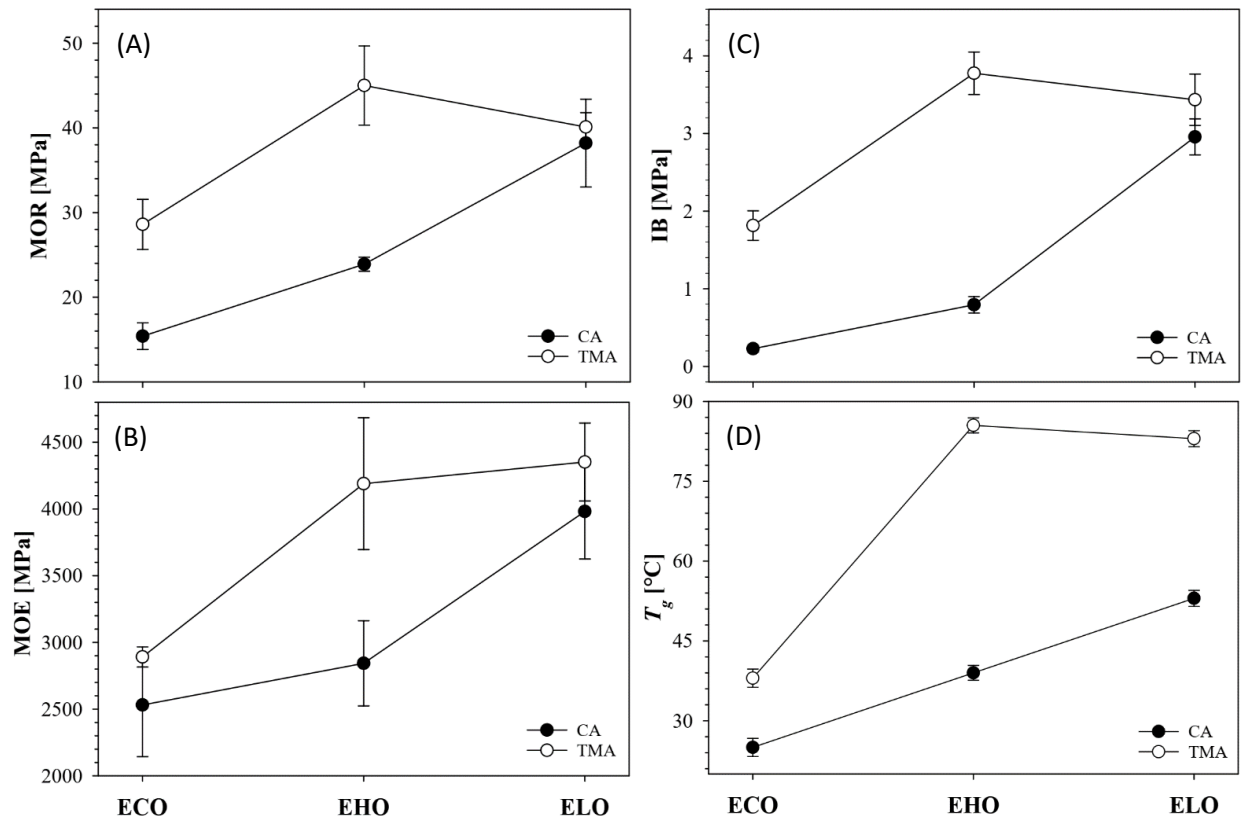
Figure 2.1 The MOR (A), MOE (B), IB (C) and T_g (D) (standard deviation ±3 SD) of biocomposites produced using different epoxidized oils and curing agents. The solid lines are

connecting the experimental values of biocomposites with the same curing agents and drawn as guide for the eye.

2.3.4.1 Modulus of Rupture (MOR)

Figure 2.1(A) shows the measured MOR for biocomposites made using a range of resins. As expected, the MOR varies with the OOC of epoxidized oils. Thus, biocomposites made using ECO resins, which have the lowest OOC, have lower MOR values than those made with ECO or EHO regardless of curing agent. In addition, the MOR values for biocomposites prepared with ECO/TMA resin are nearly two times higher than MOR values for biocomposites prepared with ECO/CA resin. Since the MOR is a material's ultimate bending strength, larger values of MOR reflect a higher resistance to failure, as seen for biocomposites made using the TMA curing agent. This can be explained in a general way by the molecular rigidity imparted by incorporating an aromatic crosslinking agent [28]. In addition, the anhydride ring of TMA may react with the surface hydroxyl groups of the reinforcing fibers to form ester bonds, which would enhance the resin's adhesive strength [29, 30]. At the same time, the acid moiety formed by anhydride ring opening can further participate in epoxy resin curing reactions.

The MOR of biocomposites made with medium and high OOC epoxides (EHO and ELO) are significantly higher than for the ECO resin based biocomposite (Fig. 2.1A), due to the higher crosslinking density in these resins. In all resin systems, the biocomposites prepared with the aromatic curing agent demonstrated significantly higher MOR values. Surprisingly, the ELO/TMA resin based biocomposites showed somewhat lower MOR values compared to EHO/TMA. It is believed that this unexpected behavior is directly related to another outcome of using a very high OOC epoxy resin. The reaction rate of ELO with the curing agents to form esters, and further to form oligomers, is significantly higher compared to that for epoxides with lower OOC. As a result,

56

oligomers (prepolymers) generated during curing reactions quickly form thermoset resin coagulates. This was visually observed as the formation of white powder precipitates in the solution. These local thermoset network chains remain unbound, or weakly bound, even after compression molding of the biocomposites. This in turn, significantly reduces the adhesive and cohesive strength of the resin. Moreover, the presence of such resin aggregates creates structural defects, or high stress concentration points, in the bulk volume, which lead to premature mechanical failure of biocomposites at relatively low degrees of deformation and/or loads.

This behavior is most pronounced in biocomposites made using ELO/TMA resin formulations where the reaction rate between ELO and TMA, and consequently the formation of such local resin coagulates, are highest. In the ELO/CA curing system the reaction rate is moderate, and the formation of such thermoset coagulates is negligible, so that the biocomposites made with this resin ultimately demonstrate a mechanical performance that is comparable to the ELO/TMA system. To summarize, the observed MOR results reflect the competing processes of desired network crosslinking that occurs during compression molding, and, possibly, the undesired, premature formation of coagulates in the resin prior to this time.

2.3.4.2 Modulus of Elasticity (MOE)

In contrast to the MOR, the MOE is a measure of material' flexural stiffness, defined as the material's resistance to elastic deformation (non-permanently) under an applied external bending load [23]. Therefore, composites which have a larger MOE have greater flexural stiffness. This is particularly important in stiffness critical design applications when the criteria of low deflection is imposed, for example in medical, aerospace, and automotive applications [31]. Figure 2.1 (B) illustrates the MOE values for all three groups of biocomposites studied. Overall, the MOE values of the biocomposites follow a similar trend to MOR, increasing with increasing epoxy content in

the resin systems (Fig 2.1 B). In addition, the MOE values are higher for biocomposites made using the aromatic curing agent TMA compared to those containing the aliphatic curing agent, CA. In this case, despite showing the somewhat early rupturing failure during the bending test, the average MOE for biocomposites made with ELO/TMA shows no statistically significant difference to that using the EHO/TMA resin (Figure 2.1(B)).

2.3.4.3 Internal bond strength (IB)

The internal bond measurement provides information regarding the tensile strength of the material as determined by applying tension perpendicular to the plane surface of the material. The procedure is detailed in Sections 11 and 28 of the ASTM standard D-1037-12 [23]. Failures of internal bonds in natural fiber composites are often due to failure of adhesion and/or the lignocellulose component [32]. Figure 2.1 (C) shows the internal bonding strength values for the biocomposites made using different epoxidized oils cured with two different curing agents. As with MOR and MOE, the biocomposite made using ECO/CA (low OOC) resin system had weaker IB, while the IB values were much higher for biocomposites produced with medium and high OOC epoxides (Fig. 2.1 C).

Overall, TMA based resin formulations produced biocomposites with stronger internal bonding compared to their CA based counterparts, and IB values depends on the epoxy functionality of epoxidized oils. The one exception, however, is that IB failure occurred earlier than expected for biocomposites made with the ELO/TMA resin. As described earlier, this behavior can be explained with an inhomogeneous resin matrix that caused defects in the integrity of biocomposites. The IB depends on the stress distribution and stress allocation in the test specimen [33], and in an ideal scenario, applied stress is distributed evenly throughout the sample. Upon increase of applied stress to the biocomposite, re-allocation and re-distribution of the stress

occurs at the defective sections. Further increase of the applied stress leads to further de-bonding at the defective area, and finally to biocomposite failure.

2.3.4.4 Dynamic Mechanical Analysis (DMA)

DMA was used to determine the glass transition temperature, T_g, of the specimens. The T_g values for the biocomposites were found using the peak point of the *tan δ* (Fig. 2.1D). The trend in T_g values for the biocomposites shows nearly identical behavior to that observed in MOR and IB test results. As expected, the T_g values for biocomposites proportionally depends on the epoxy content in the epoxidized oils, so that higher the epoxy number, the higher the T_g. Although both curing agents have nearly identical molecular weights of 192 g/mol and bear similar reactive acid moieties (3 acid groups/mol In addition, Figure 2.1(D) demonstrates the influence of the type and molecular architecture of the curing agents to the dynamic mechanical properties of biocomposites,). The aromatic curing agent TMA produces more rigid biocomposites with higher T_g values compared to those made using the aliphatic curing agent. Epoxy resins cured with aromatic amine curing agents had T_g values nearly 50 °C higher than those of resins cured with aliphatic curing agents having similar functionalities [28]. In addition, the storage moduli are also higher for biocomposites prepared with plant oil epoxides of high epoxy content (not shown here). For example, the ECO resin based biocomposites has a low storage modulus due to its low epoxy content and low crosslinking density. On the other hand, the structure of the main fatty acid of canola oil, oleic acid (~65%), possesses a nine carbon highly mobile chain end with no double bonds. this flexible structure contributes to the lower storage modulus and the T_g [35] of ECO. For fatty acids with double bonds closer to the omega carbon than oleic acid the molecular motions are reduced. Also, in the fatty acids of oils with more double bonds there are more epoxy groups prior to polymerization and this results in greater crosslinking density in their biocomposites.

2.3.5 Mechanical performance of ECO/ELO mixture based biocomposites

The previous section demonstrates the production of biocomposites using variety of epoxidized oils differing in epoxy content. It was shown that the mechanical performance of these biocomposites proportionally depends on the OOC content of the uncured resin. However, it was also shown that high epoxy content was not always beneficial and led to the fast and uncontrolled reaction conditions, especially when it is cured with the more reactive aromatic TMA. In addition, the availability of highly unsaturated oils such hemp and flax oils are limited, and the price of these oils relatively high compared to canola oil. To illustrate this point, canola/rapeseed oil is the third most widely produced plant oil worldwide (28.8 Mt in 2017) while the production of flaxseed (0.75 Mt in 2017) [36] and hemp oils are produced in much lower amounts. Therefore, it is rational to use the mixture of cheaper and readily available canola oil with flaxseed oil (relatively expensive and has a limited availability) in producing bioresins and biocomposites. This could include inedible industrial rapeseed oil and off-specification canola oil that is not suitable for food use. Here, we test the hypothesis that ECO/ELO blends can be used to produce biocomposite materials with mechanical performance that is "tunable" by varying the ECO/ELO ratio.

Bioresin solutions from ECO/ELO mixtures varying in ratios from 0% ECO (*w/w*) to 100% ECO (*w/w)* were prepared. Table 3 lists the resin compositions and thermal-mechanical properties of the biocomposites made using hemp/wood (40/60 *w/w*) fibermats and various resin compositions.

Resin Composition	Ratio [a] [mol/mol]	MOR [b] [MPa]	MOE [b] [MPa]	IB [b] [MPa]	T_g [b] [°C]
(ECO/ELO 100/0)/CA	1.0/1.27	15.4 ± 1.6	2531 ± 387	0.2 ± 0.0	25.7 ± 1.7
(ECO/ELO 80/20)/CA	1.0/1.47	26.2 ± 3.5	4042 ± 665	0.7 ± 0.1	26.2 ± 1.2
(ECO/ELO 60/40)/CA	1.0/1.67	27.4 ± 1.6	3807 ± 321	1.4 ± 0.2	29.6 ± 1.4
(ECO/ELO 40/60)/CA	1.0/1.87	31.1 ± 1.8	4303 ± 465	2.3 ± 0.4	33.3 ± 1.4
(ECO/ELO 20/80)/CA	1.0/2.07	32.1 ± 2.2	4283 ± 147	3.4 ± 0.3	46.5 ± 1.5
(ECO/ELO 0/100)/CA	1.0/2.27	35.3 ± 1.4	3982 ± 356	3.0 ± 0.2	52.7 ± 1.5
(ECO/ELO 100/0)/TMA	1.0/1.27	28.6 ± 3.0	2891 ± 750	1.8 ± 0.2	38.0 ± 1.7
(ECO/ELO 80/20)/TMA	1.0/1.47	39.0 ± 0.2	3684 ± 114	3.5 ± 0.6	43.4 ± 1.2
(ECO/ELO 60/40)/TMA	1.0/1.67	48.0 ± 0.5	4801 ± 311	3.9 ± 0.3	57.3 ± 1.5
(ECO/ELO 40/60)/TMA	1.0/1.87	48.0 ± 3.4	5196 ± 680	3.9 ± 0.1	61.6 ± 1.4
(ECO/ELO 20/80)/TMA	1.0/2.07	46.4 ± 1.9	4913 ± 358	4.0 ± 0.2	74.3 ± 1.5
(ECO/ELO 0/100)/TMA	1.0/2.27	40.1 ± 1.7	4352 ± 292	3.4 ± 0.3	83.1 ± 1.5

[†] In all biocomposites, the hemp/wood 40/60 *w/w* fibermats were used.

[a] At these ratio of components the stoichiometric ratio of epoxy to acid groups are equal to one.

[b] Values are means ± standard deviation of 3 to 5 samples for each group

Table 2.3 The thermal-mechanical properties of biocomposites produced using resin made from various ratios of ECO/ELO, with CA or TMA curing agents[†]

The molar amount of curing agent needed was calculated using the following equation:

$$MR_C = \left\{ \frac{\left(x F_{ECO} + y F_{ELO} \right)}{F_C} \right\} \frac{C}{100} MR_E \qquad (4)$$

where MR_C is the number of moles of curing agent required for curing of the epoxidized oil blends; MR_E is the number of moles of epoxidized oil; x and y are the weight percentages of the epoxidized oils in the mixture; F_{ECO} and F_{ELO} are the epoxy functionalities of ECO and ELO, respectively; F_C is the acid functionality of the curing agent; C is the selected molar ratio of epoxy groups to carboxylic acid moieties in the curing agent. In this work, we aim for an equal number

of epoxide and carboxylic acid groups to achieve complete ring opening, i.e. C=1 in the calculation used for Table 3. The functionalities are listed in Table 1, and F_C=3 for both CA and TMA, as discussed earlier. Table 3 indicates how the required amount of curing agent changes with the ECO/ELO ratio in order to achieve C=1.

The measured mechanical performances of all composites are tabulated in Table 3 and plotted in Figure 2.2. The average densities of these biocomposites were between 840-860 kg/m^3 and their resin content was between 27-29%.
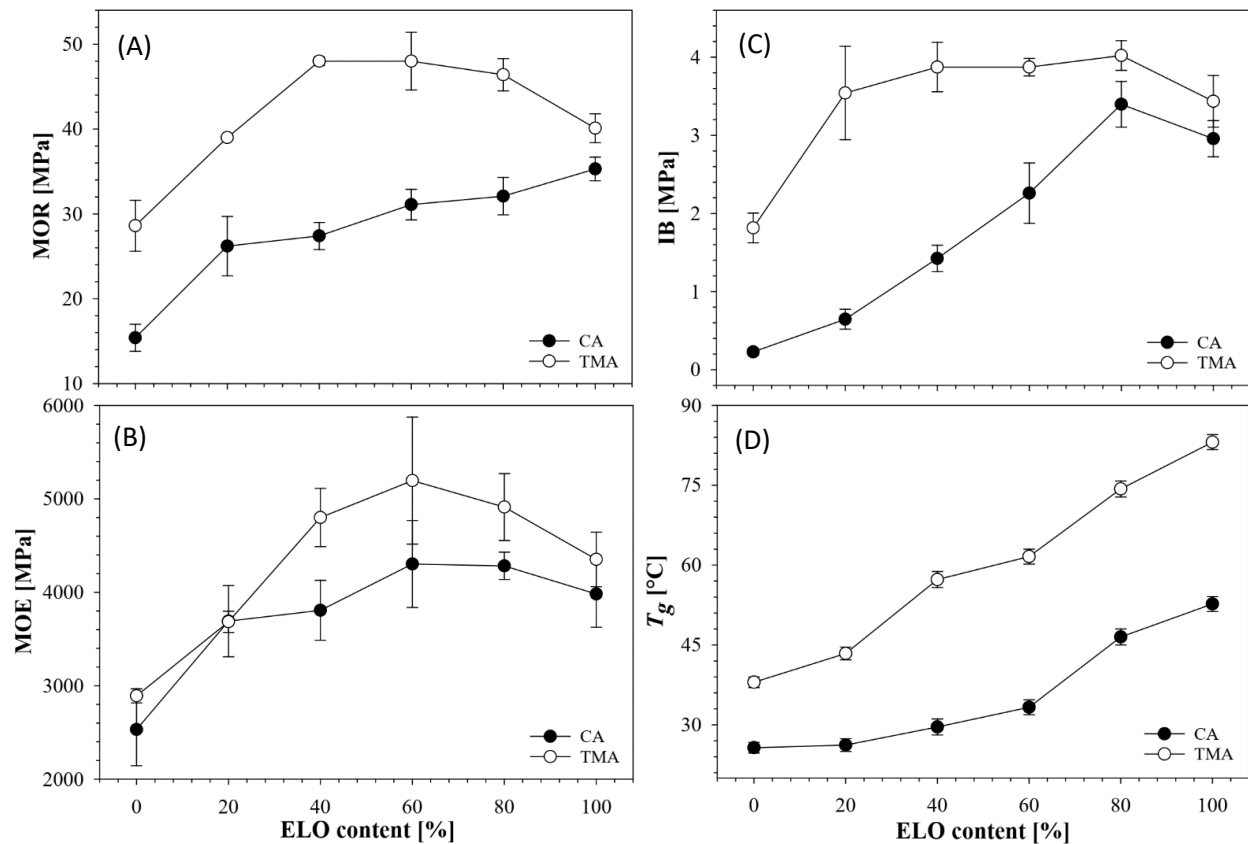
Figure 2.2 The MOR (A), MOE (B), IB (C) and T_g (D) (standard deviation ±3) of biocomposites produced using different mixtures of ECO/ELO and curing agents. The solid lines are connecting

the experimental values of biocomposites with the same curing agents and drawn as guide for the eye.

It can be seen from Table 2.3 and Figure 2.2 that the mechanical performance of biocomposites made using ECO/ELO mixtures follow the general trends seen in Figure 1, i.e. increasing with increasing OOC, as the percentage of ELO increases. For instance, increasing values of MOR of biocomposite materials were observed (Figure 2(A)) with increasing ELO content, when both aliphatic and aromatic curing agents were used, but with TMA curing agent giving higher MOR values. For the TMA based resin system, at ECO/ELO ratios of between 60/40 and 20/80 *w/w*, the biocomposites have achieved the maximum values of MOR of 48.0 to 46.4 MPa, respectively. These values actually exceed the MOR value of biocomposites produced with ELO alone (40.1 MPa). This modest improvement in mechanical performance is associated with better optimized reaction conditions, since the presence of the lower OOC ECO reduces the reaction rate and results in curing conditions for the resin where premature agglomeration is minimized.

In contrast, the reduced MOR, MOE and IB values observed for biocomposites with >60% ELO (most pronounced when TMA was used) are associated with the formation of local resin agglomerates within the bulk resulting from premature curing. These agglomerates can create defects that lead to failure of biocomposites at low mechanical loads.

The glass transition temperatures of the biocomposites, estimated using DMA (Table 3, Figure 2(D)), show that for all of the ECO/ELO composition range the T_g of the biocomposites varies in proportion to the epoxy content of the resin. It should be noted that the biocomposites prepared using CA as curing agent have multiple transitional peaks in storage modulus (especially at high ECO content) indicating likely inhomogeneity in the cured structures. In contrast, the storage modulus of the TMA based biocomposites show a single transition, which suggests more

homogenous structures for these biocomposites. As discussed above, TMA based biocomposites show higher T_g compared to their CA based counterparts, which is associated with enhanced crosslinking density in these resins.

These results demonstrate the possibility of the producing bioresins, and biocomposites using blends made of epoxidized oils having low and high epoxy group content, using the example of canola and linseed. An illustration of this is that the mechanical performances of most of the biocomposites produced meet the ANSI requirements for Medium Density Fiberboards (A208.2-2016) and siding panels (ANSI A135.6-2012). Hence, these bioresins/biocomposites can be made without compromising their mechanical properties while reducing the overall costs of manufacturing by maximizing the incorporation of the lower cost monounsaturated oils. It should be noted that these results apply to oils that are low in saturated fatty acids (less than 8% for canola and linseed) so only contain a small percentage of fatty acyl groups that are not epoxidized and so are not able to participate in crosslinking reactions.

2.4   Conclusions

Natural fiber composites were prepared from hemp/wood fibermats and resins made from 3 different epoxidized plant oils. Both aliphatic and aromatic curing agents of similar molecular weight were used in these resins. It was shown that the mechanical performance of the biocomposites varies in proportion to the epoxy content of the resin. Thus, for the local plant oil feedstocks investigated, the mechanical performances of the biocomposites produced, measured via MOR, MOE, IB and T_g, followed the trend ECO < EHO < ELO. It was also demonstrated that the aromatic curing agent, TMA, produces biocomposites with improved MOR, MOE, IB and T_g compared to CA.

In a series of experiments, blends of ECO with ELO were used in resins for compression moulding of biocomposite materials. Such an approach allows the use of more widely available and lower cost plant oils for epoxidation and so may reduce the cost of manufacturing biocomposites without compromising their mechanical performance, if the optimum ratios of components are selected. The trend in the mechanical performance of biocomposites produced with ECO/ELO mixtures were similar to those observed for individual epoxidized oils in that upon increase in the ELO content (and hence OOC) the MOR, MOE, IB or T_g become greater, and this behavior is more pronounced in TMA based biocomposites. However, for ELO contents of >60-80% a decrease in MOR, MOE and IB values was observed due to the formation of localized resin agglomerates prior to bulk curing (compression moulding). These results demonstrate the feasibility of producing fully- or high- biocontent resins using unsaturated plant oils blended to achieve the optimum mechanical properties in composite materials, whilst minimizing the content of the more expensive and less abundant component.

2.5   References

[1] R.P. Wool, X.S. Sun, *Bio-Based Polymers and Composites*, Elsevier Academic Press, Burlington, MA, (2005).

[2] W.D. Callister Jr., D.G. Rethwisch, *Materials Science and Engineering: An Introduction*, 9 ed., Wiley, Danvers, MA, (2014).

[3] K.L. Pickering, M.G.A. Efendy, T.M. Le, *Compos Part a-Appl S* **83** 98 (2016).

[4] L.W. McKeen, *Effect of Temperature and other Factors on Plastics and Elastomers*, William Andrew Inc., NY, USA, (2008).

[5] A. O'Donnell, M.A. Dweib, R.P. Wool, *Compos Sci Technol* **64**(9), 1135 (2004).

[6] D. Romanzini, A. Lavoratti, H.L. Ornaghi, S.C. Amico, A.J. Zattera, *Mater Design* **47** 9 (2013).

[7] L. Granda, Q. Tarres, F.X. Espinach, F. Julian, J.A. Mendez, M. Delgado-Aguilar, P. Mutje, *Cell Chem Technol* **50**(3-4), 417 (2016).

[8] M.S. Salit, M. Jawaid, N.B. Yusoff, M.E. Hoque, *Manufacturing of Natural Fibre Reinforced Polymer Composites*, Springer, Cham, Switzerland (2015).

[9] A.K. Mohanty, M. Misra, L.T. Drzal, *Natural Fibers, Biopolymers, and Biocomposites*, CRC Press Boca Raton. USA, (2005).

[10] K.O. Niska, M. Sain, *Wood-Polymer Composites*, Woodhead Publishing, Boca Raton, FL, (2008).

[11] R.D.S.G. Campilho, *Natural Fiber Composites*, CRC Press, Boca Raton, FL, (2016).

[12] A. Hodzic, R. Shanks, *Natural Fibre Composites. Materials, Processes and Properties*, Woodhead Publishing, Cambridge, UK, (2014).

[13] K.L. Pickering, *Properties and Performance of Natural-Fibre Composites*, Woodhead Publishing, Cambridge, UK, (2008).

[14] D.D. Stokke, Q. Wu, G. Han, *Introduction to Wood and Natural Fiber Composites*, John Wiley & Sons, West Sussex, UK, (2014).

[15] M.O. Seydibeyoglu, A.K. Mohanty, M. Misra, *Fiber Technology for Fiber-Reinforced Composites*, Woodhead Publishing, Cambridge, UK, (2017).

[16] S. Kalia, *Biodegradable Green Composites*, John Wiley & Sons, Hoboken, NJ, (2016).

[17] A. Rana, R.W. Evitts, *J Appl Polym Sci* **132**(15), 41807 (2015).

[18] A.K.-t. Lau, A.P.-Y. Hung, *Natural Fiber-Reinforced Biodegradable and Bioresorbable Polymer Composites*, Woodhead Publishing, Duxford, UK, (2017).

[19] T.S. Omonov, J.M. Curtis. *Aldehyde Free Thermoset Bioresins and Biocomposites*. (2016).

[20] A.K. Mohanty, M. Misra, L.T. Drzal, *Compos Interface* **8**(5), 313 (2001).

[21] M.R. Rahman, M.N. Islam, M.M. Huque, *J Polym Environ* **18**(3), 443 (2010).

[22] A. Ali, K. Shaker, Y. Nawab, M. Jabbar, T. Hussain, J. Militky, V. Baheti, *Journal of Industrial Textiles* **47**(8), 2153 (2018).

[23] ASTM-D1037-12, Standard Test Methods for Evaluating Properties of Wood-Base Fiber and Particle Panel Materials, ASTM, PA, USA, p. 32 (2012).

[24] ASTM-E1640-18, Standard Test Method for Assignment of the Glass Transition Temperature by Dynamic Mechanical Analysis, ASTM, PA, USA, p. 6 (2018).

[25] T.S. Omonov, E. Kharraz, J.M. Curtis, *Rsc Adv* **6**(95), 92874 (2016).

[26] T.S. Omonov, E. Kharraz, J.M. Curtis, *Ind Crop Prod* **107** 378 (2017).

[27] ASTM-D1652-11E1, Standard Test Method for Epoxy Content of Epoxy Resins, ASTM, PA, USA, p. 4 (2011).

[28] E. Crawford, A.J. Lesser, *J Polym Sci Pol Phys* **36**(8), 1371 (1998).

[29] J.M. Felix, P. Gatenholm, *J Appl Polym Sci* **42**(3), 609 (1991).

[30] R.X. Ou, Q.W. Wang, F.P. Yuan, B.Y. Liu, W.J. Yang, *Adv Mater Res-Switz* **221** 27 (2011).

[31] C. Ayranci, J. Carey, *Compos Struct* **85**(1), 43 (2008).

[32] M. Jawaid, M. Thariq, N. Saba, *Failure Analysis in Biocomposites, Fibre-Reinforced Composites and Hybrid Composites*, Woodhead Publishing, Duxford, UK, (2019).

[33] C.P. Dai, C.M. Yu, J.W. Jin, *Wood Fiber Sci* **40**(2), 146 (2008).

[34] N. Saba, M. Jawaid, O.Y. Alothman, M.T. Paridah, *Constr Build Mater* **106** 149 (2016).

[35] N. Boquillon, C. Fringant, *Polymer* **41**(24), 8603 (2000).

[36] Production of major vegetable oils worldwide, https://www.statista.com (Accessed March 1, 2019).

Chapter 3

The development of epoxidized hemp oil prepolymers for the preparation of thermoset networks

3.1 INTRODUCTION

Epoxy thermosets have been used in many composite applications because of their outstanding adhesion, high strengths, and superior fatigue strength [1,6,53]. Currently, the major components used in most epoxy-based thermoset polymer formulations originate from petroleum-based derivatives. Biobased thermosets only represent a very small percentage of the entire polymers market, despite the trend towards their use in increasingly diverse areas due to the potential life cycle greenhouse gas reductions and decreased reliance on fossil fuel resources [2].

A recent review paper [3] outlines the current state and future prospects of the biobased thermosetting epoxides with description of some important chemical reactions and formulations of biobased epoxy polymers. Epoxidized plant oils could be used as versatile alternative to petrochemical epoxides [4]. By manipulating the unsaturation level of the input oil, and by controlling epoxidation conditions, epoxidized plant oils with a wide range of epoxy content can be produced [5]. Hemp is an industrial oil crop with high content of unsaturated fatty acids that makes it an excellent feedstock for producing epoxidized derivatives.[3]

---

[3] A version of this chapter has been published, "Omonov, Tolibjon & Patel, Vinay & Curtis, Jonathan. (2019). The Development of Epoxidized Hemp Oil Prepolymers for the Preparation of Thermoset Networks. Journal of the American Oil Chemists' Society. 96. 10.1002/aocs.12290."

Approximately 90% of the fatty acids in hempseed oil are unsaturated (Table 3.1) which make this oil well suitable for chemical modification to produce epoxidized derivatives. Currently, more than 30 countries are cultivating industrial hemp as an agricultural commodity as a source of fiber for textile, construction, and composites industries, while hempseed oil has a great potential to be utilized as a feedstock for producing oleochemicals. Moreover, in Canada the cultivation of industrial hemp is increasing rapidly, from about 3,260 hectares in 2008 to 31,540 hectares in 2018 [6]. Therefore, the industrial hemp oil is becoming readily available for the use as a component in the burgeoning biobased economy.

Modification of the double bonds of the unsaturated oils to produce epoxidized derivatives is well known process [7,8]; and these epoxidized oil monomers can further be cured into thermoset epoxy networks, in similar ways as used for their petroleum-based counterparts. The possible reaction pathways and cure mechanisms between epoxy and acid moieties [9,10], and between epoxy and amine or anhydride groups [11] have been well described in the literature. The use of an aqueous citric acid solution as a curing agent for epoxidized soybean oil is reported to produce self-healable polymer network [1] and biodegradable coating for mulch [12]. Although, use of an aqueous citric acid solution in making epoxy networks provides "greener" route, the presence of water might be disadvantageous as water might act as a nucleophile to open epoxy rings forming hydroxyl moieties [13,14]. This in turn, reduces the number of epoxy groups available for the intended reactions.

Recently, an attempt has been made to examine all possible epoxy-acid reaction pathways using the density functional theory and simplified physical molecular models to demonstrate comprehensive epoxy cure mechanism [15]. Most of these studies are carried out during the curing of epoxides in bulk, in the absence of solvent. However, when making biocomposites with fibrous

materials, the components of the epoxy based bonding adhesives are usually dissolved, mixed or pre-polymerized in solvents to allow homogenous impregnation of the fibers. In such systems, the cure behavior of the epoxides may differ from the bulk, due to dilution effects. In addition, a great number of curing agents or hardeners are incompatible with, or insoluble in, epoxidized plant oils. In order to reveal the full potential of a curing agent, proper homogenization/mixing of such incompatible curing agents in the epoxy monomer is necessary. This can positively affect the cure kinetics, speed up gelation and lead to improvements to the final properties of the resulting epoxy network.

Therefore, the main aim of this work is to study and compare the cure behavior of epoxidized hemp oil (EHO) with the 2 otherwise incompatible curing agents trimellitic anhydride (an aromatic petrochemical compound) and citric acid (a non-aromatic, fully biobased compound), *in the presence of a solvent*. A comparison between the thermomechanical properties of the resulting partly or fully biobased thermoset polymers, can then be made.

3.2 EXPERIMENTAL SECTION

3.2.1 Materials.

Hemp oil was purchased in bulk (20 L) from Rocky Mountain Grain Products (AB, Canada) and was used as supplied. Formic acid (85%) and aqueous hydrogen peroxide (H_2O_2, 35%) were purchased from Univar Canada (Richmond, BC, Canada) and used in epoxidation process. Trimellitic anhydride (1,2,4-benzenetricarboxylic anhydride) was purchased from Sigma-Aldrich Canada and used as curing agent for epoxidized hemp oil. Food grade citric acid (2-hydroxypropane-1,2,3-tricarboxylic acid) was purchased from Jungbunzlauer Canada Inc. (ON, Canada) and used as a curing agent. ACS grade ($\geq$99.5%) acetone was purchased from Fisher Scientific Company (Ottawa, ON, Canada) and used as a solvent for curing reactions. Hydrogen

bromide (HBr), 33 wt% solution in glacial acetic acid (Fisher Scientific Company) and glacial

acetic acid (99.7%, Caledon Laboratory Chemicals, Georgetown, ON, Canada) were used in the

oxirane oxygen content titration of epoxides. The lipid standard methyl-9,10-dihydroxystearate of

molecular weight (MW) 330.51 g/mol was purchased from Frinton Laboratories (Hainesport, NJ,

USA); 1,2-distearin (MW of 625.03 g/mol) and trieicosapentaenoin (MW of 945.42 g/mol) were

purchased from Nu-Chek Prep, Inc. (Elysian, MN, USA). These standards were used in gel

permeation chromatography analysis of the products.

3.2.2 Characterization of hemp oil and preparation of epoxidized hemp oil.

The fatty acid profile of hemp oil as measured by the GC-FID, along with some important

calculated parameters of its derivatives are given in the Table 3.1.

Fatty acids	[%]
C16:0	7.0
C18:0	3.0
C18:1 9c, 11c	14.7
C18:2 n6	56.0
C18:3 n3	17.9
C20:0	0.7
C20:1 11C	0.4
C22:0	0.3
Total monounsaturated [%]	15.1
Total polyunsaturated [%]	73.9
Total saturated [%]	11.0
Properties (calculated)	
Average number of double bonds/mol [-]	5.42
Average MW of oil [g/mol]	876
Average MW of epoxide [g/mol]	965
Maximum OOC of epoxide [%]	9.0

Table 3.1 Fatty acid profile of hemp oil, along with some important calculated parameters of

its derivatives

It can be seen from the Table 3.1 that hemp oil mainly consists of 18 carbon fatty acids, with an average MW of 876 g/mol. The majority of fatty acids of the hemp oil are polyunsaturated fatty acids including 56% of linoleic acid and about 18% linolenic acid. As a result, hemp oil has an average of 5.4 double bonds per triacylglycerol (TAG) molecule. If epoxidation of hemp oil proceeds to completion at all of its double bonds, it would produce epoxidized hemp oil (EHO) with an average MW of 965 g/mol and an oxirane oxygen content (OOC) of 9.0%. This OOC value is high compared to the calculated OOC values of, for example, epoxidized canola oil (6.34 %, [8]) or soybean oil (7.79%, [16]). This makes industrially grown hempseed oil an attractive option as a feedstock for the manufacture of epoxidized oil derivatives.

In this work, epoxidation of hemp oil was carried out using performic acid generated *in-situ* from formic acid and H_2O_2. Although, the efficiency of the different types of carboxylic acids in epoxidation of vegetable oils is still the subject of debate, the order of formic acid reactivity is described to be greater compared to benzoic or acetic acids [17]. The molar ratio of hemp oil: formic acid : H_2O_2 used was 1.0 : 1.36 : 8.13, respectively. This means that for every mole of double bonds in hemp oil there will be ~0.25 moles of formic acid and 1.5 moles of H_2O_2. Under such ratios of reactive components, epoxides with high yields can be produced with negligible loss of formed epoxy groups during epoxidation [8]. The epoxidation reactions were carried out using 3 kg of hemp oil in 22 L glass reactor (Chemglass Life Sciences), as described previously [5,7]. The epoxidation of hemp oil was carried out for up to 48 hours to establish the optimum conditions

to produce EHO with the highest epoxy content within the shortest reaction time. Figure 3.1 shows

the kinetics of hemp oil epoxidation carried out at 60 °C.
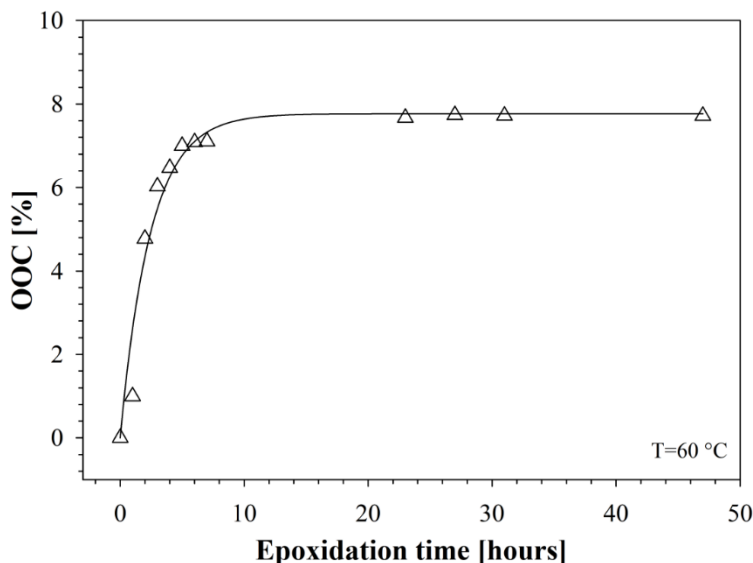
Figure 3.1 Epoxidation kinetics (OOC vs epoxidation time) for the hemp oil using *in-situ* generated performic acid, at 60 °

It can be seen that the OOC reached a plateau region within 24 hours, after which the change

in OOC is negligible for the rest of the 48 hours reaction time. The final experimental OOC of

EHO that was achieved (~8%) was a little lower than the calculated maximum value, likely due to

competing ring opening reactions, as has been described [8]. Hence, all EHO samples necessary

for this study were prepared within 24 hours, and used for the following studies of epoxy curing

behavior.

3.2.3 Thermoset polymer preparation

The biobased thermosets of EHO were prepared using CA and TMA as curing agents, under

similar conditions. The study of EHO curing process was carried out in 2-stages. The first was to

study the curing behavior between EHO and its immiscible curing agents at the initial stages of

the low temperature prepolymerization reaction, in the presence of a solvent. The second stage

was to measure the thermomechanical properties of the thermoset networks that were produced by subjecting the prepolymers to full curing at high temperatures, after removal of the solvent.

The EHO/CA aliphatic network was prepared at a molar ratio of 1.0 : 1.8. This ratio was chosen because each CA molecule has 3 carboxylic acid groups which could potentially react with the epoxy groups of EHO [18]. At the same time, each molecule of EHO has 5.4 epoxide groups on average. Hence, the expected stoichiometric ratio of the reactive moieties of these components was close to 1:1 at a molar ratio of EHO to CA of 1.0 : 1.8 [19].

The EHO/TMA aromatic network was prepared in similar manner to EHO/CA, at molar ratio of EHO to TMA of 1.0 : 1.8. In doing so, the carboxylic acids reactive groups for TMA was taken as 3, taking into consideration TMA has one acid group plus the anhydride group which will yield two more acid groups after hydrolysis. Coincidentally, both CA and TMA have similar MW, so the weight amounts of these curing agents to be added into EHO are identical.

The required amount of curing agent, CA or TMA, was dissolved in acetone in a 500 ml glass flask that was placed in oil-bath at a temperature of 50±1 °C. Continuous mixing with a magnetic stirrer at 500±10 rpm was used until complete disappearance of all solid particles occurred. The amount of acetone used was approximately equal to the weight of EHO plus curing agent, which is sufficient to dissolve both curing agents. Although the TMA is readily soluble in acetone (49.6 g/100 g @25 °C), CA has a more limited solubility in acetone (18g/100 g @20 °C, [20]) so requires a longer stirring at 50 °C. Then, after complete dissolution of the curing agents in acetone the required amount of EHO was added into the solution to produce thermoset network solutions.

3.2.4 Characterization methods

3.2.4.1 Oxirane Oxygen Content (OOC)

The OOC of an epoxidized hemp oil was measured according to the ASTM standard titrimetric method [21], as described elsewhere [22]. For these purposes, the aliquots (~15 ml) of epoxidized products were taken and diluted with an equal amount of ethyl acetate and washed with an equal amount of saturated NaCl solution at least three times (or until pH≈6) to remove the formic acid and unreacted H_2O_2. Then, the epoxide solution in ethyl acetate was dried with anhydrous Na_2SO_4, and finally concentrated from ethyl acetate using rotary evaporator at low pressure (20 mbar and 60 °C).

3.2.4.2 Attenuated Total Reflectance Fourier Transform Infrared (ATR-FTIR) spectroscopy

The analysis of EHO and product formation during the prepolymerization processes, were carried out using a Bruker Alpha FTIR spectrometer equipped with an ATR accessory. IR spectra (4000-650 cm^{-1}, 32 scans, 4 cm^{-1} resolution) of the products were obtained by placing ca. 10 μl of the epoxidized product onto the ATR crystal. FTIR data analysis was carried out using Bruker's OPUS spectroscopy software package.

3.2.4.3 Gas chromatography (GC)

A Perkin Elmer (Waltham, MA, USA) Clarus 500 Gas Chromatograph equipped with a Flame Ionization Detector (GC-FID) was used for the fatty acid analysis of hemp oil FAME. Details of the GC-FID measurements were described earlier [22]. A 100 m ×0.25 mm SP-2560 Supelco capillary column with film thickness of 0.20 μm was utilized. The oven temperature was maintained at 45 °C for 4 min, increased to 175 °C at a rate of 13 °C/min, maintained at 175 °C for 27 min then increased to 215 °C at a rate of 4 °C/min, and finally held at 215 °C for 35 min. The injector and detector temperatures were 240 and 280 °C, respectively. Hydrogen was used as

carrier gas at 1.3 mL/min and the injection port was in split mode of 20:1. 1.0 μL of sample was injected into the GC. The individual FAMES are identified by their retention times and the relative percentage (area %) of the fatty acids using a reference standard mixture of methyl esters of fatty acids. This reference standard mixture was GLC-463, from Nu-Chek Prep, Inc. The analysis of the products was carried out at least in duplicates.

3.2.4.4 Gel permeation chromatography (GPC)

A 1200 series High Performance Liquid Chromatograph (HPLC) from Agilent Technologies Inc (Santa Clara, CA, USA) equipped with an Agilent 1200 evaporating light scattering detector (ELSD) was used for all GPC experiments to measure MW distributions of the products during prepolymerization, as described elsewhere [22]. A Styragel HR 4E THF column (with the size of 4.6 × 300 mm) from Waters Corporation (Milford, MA, USA) was used along with tetrahydrofuran (THF) as mobile phase and at a flow rate 0.5 mL/min. For every run, the eluent was the same as the sample buffer. The random run-to-run difference in retention times for system was <0.1%. The SEC calibration curve for the column was carried out using the lipid standards, described in Materials section. All data were processed using the Agilent's ChemStation for LC 3D Systems (Rev. B.03.01).

3.2.4.5 Dynamic Mechanical Analysis (DMA)

The dynamic mechanical properties of the thermosets were measured with a TA Instrument DMA Q800 (New Castle, DE, USA) equipped with a liquid nitrogen cooling system. The DMA experiments were carried out according to ASTM E 1640-09 in the dual cantilever bending mode at a fixed frequency of 1 Hz, strain 0.04% and constant heating rate of 2 °C/min from -50 to 175 °C, as described elsewhere [19]. At least two similar sized specimens with approximate dimensions of 60 mm ×12 mm×4 mm were prepared by the cutting of the bulk thermosets and the results of

the measured glass transition temperatures were averaged. TA Universal Analysis (version 4.7A) software was used to analyze the experimental data.

3.2.4.6 Thermogravimetric analysis (TGA)

The thermogravimetric analysis of the neat components and their polymers was performed using a TA Instruments' TGA Q50 Thermogravimetric Analyzer (New Castle, DE, USA) under a nitrogen atmosphere at a flow rate of 40 mL/min. About 10 mg of material in a ceramic pan was used in the thermogravimetric analysis. The sample was heated from ambient temperature to 600 °C at a constant heating rate of 10 °C/min and the weight loss was recorded as a function of temperature. The TA Universal Analysis (version 4.7A) software was used to analyze the experimental data.

3.3 RESULTS AND DISCUSSION

3.3.1 Prepolymerization reactions of EHO in solvent

Although the curing mechanisms of epoxides [9,10,18,23] and plant oil epoxides [18,23] without solvents are well described in the literature, the (pre)polymerization reactions of epoxides in solvents have not been extensively reported.

Epoxidized hemp oil (conceptual structure of EHO is shown in Figure 3.2) is a clear, light yellow, viscous liquid at room temperature. The two curing agents selected to study the curing behavior of EHO (Table 3.2) have nearly identical molecular weights, and comparable melting points, and densities.

Curing agent	Structure	MW [g/mol]	T_m [°C]	Density [g/cm^3]
Citric acid (CA)		192.03	156	1.66
Trimellitic anhydride (TMA)		192.13	165	1.54
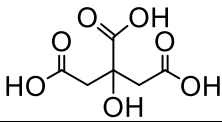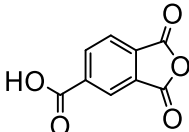
Table 3.2 Structure and some properties of the citric acid and trimellitic anhydride

They are widely used and inexpensive chemicals that are readily available at an industrial scale. However, despite their similarities, CA and TMA are structurally and chemically very different. CA, 2-hydroxypropane-1,2,3-tricarboxylic acid, is an alpha-hydroxy carboxylic acid containing 3 carboxylic acid groups and 1 hydroxyl group. Both of these functional groups can participate in epoxy curing reactions. TMA, 1,2,4- benzenetricarboxylic anhydride, contains 1 carboxylic acid group and 1 anhydride group on the aromatic ring. TMA is commercially available as solid white flakes, which readily hydrolyze to form trimellitic acid, while citric acid is a colorless translucent crystalline compound. Both curing agents are in solid form at room temperature and have very limited solubility in the viscous, nonpolar EHO. Acetone was selected as the solvent for the curing reaction, since it can effectively dissolve both curing agents and EHO.

3.3.2 Chemistry of curing reaction

The reactions of epoxy groups with curing agents are complex, and with multiple competing reactions, such as the formation of ethers or esters, occurring [17,18]. Figure 3.2 shows some of the reaction pathways that could occur during the early stages of the curing of EHO with CA (Figure 3.2, Path **I**) and with TMA (Figure 3.2, Path **II**).
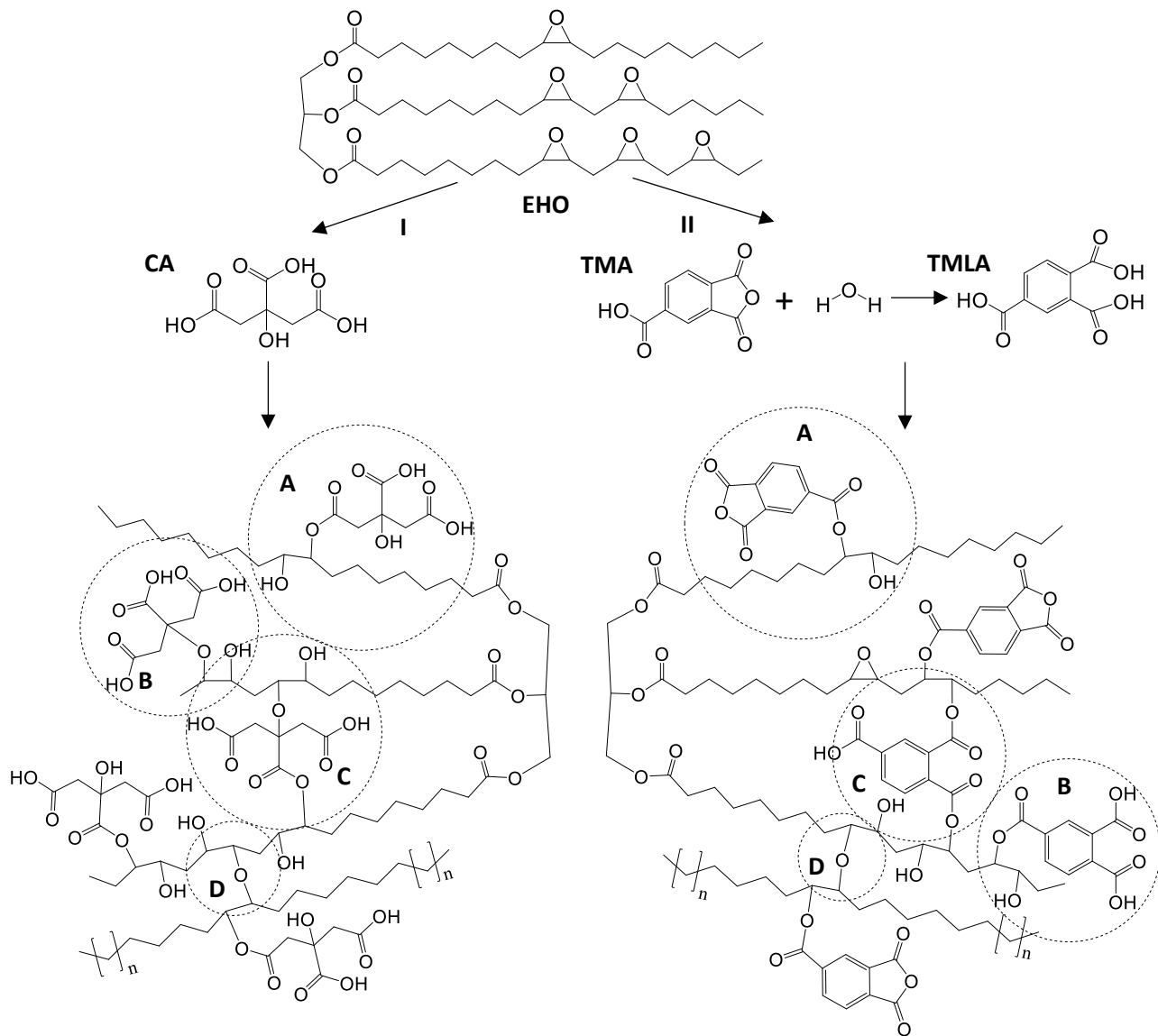
Figure 3.2 The possible curing reaction paths between EHO with CA (Path **I**) and with TMA

(Path **II**).

The acid groups of CA may react with an epoxy group of EHO to produce both an ester linkage and a hydroxyl group (Path **I-A**). Moreover, the presence of the hydroxyl group makes CA potential nucleophile to react with epoxy ring, although requires strong acidic catalytic conditions [7,9]. Nevertheless, it is reasonable to expect that some amount of CA may also react with an epoxide to produce ether linkage [18] and another secondary hydroxyl group (Path **I-B**). Thus, hydroxyl groups participating in further reactions with oxiranes may also originate from the products of esterification and etherification reactions of CA with epoxides (reaction Path **I-A** or **I-B**). Furthermore, these esterified and etherified monomeric units having acid and hydroxyl groups (or both) will react both with other epoxy moieties on unreacted EHO and through inter- or intra-molecular reactions of partially reacted EHO (such as the example in Figure 3.2) to give rise to the oligomeric structures. As an example, Figure 3.2 **I-C** represents the intramolecular reaction of epoxidized TAG due to an esterification and etherification reaction with CA. Similarly, Scheme 1 **I-D** represents an example of the dimerized EHO formed from an intermolecular etherification reaction.

The curing reactions for TMA are different due to the presence of the reactive cyclic anhydride, which does not react directly with the epoxy group [24,25]. Instead, to initiate uncatalyzed curing with TMA the anhydride ring is first opened by a hydroxyl group to form carboxylic acids which then react with epoxy groups [19,25,26]. Scheme 1, Path **II** shows possible anhydride ring opening via hydrolysis of TMA to form trimellitic acid (TMLA) due to residual water present [27] in the EHO or acetone. Later in the process, the anhydride ring opening can also occur with any available hydroxyl group, resulting in ester formation. For example, Figure 3.2 **II-A** and **II-B** shows EHO esterified with TMA and TMLA, respectively, resulting in the formation of an additional hydroxyl group. This hydroxyl group may then take part in a further anhydride ring opening reaction. In

addition, the carboxylic acid groups of TMLA can participate in epoxy ring opening as shown in Figure 3.2 **II-C**, resulting in dimerization. Further curing reactions occur, resulting in oligomeric structures such as the example in Figure 3.2 **I-D**. It has been reported that hydrolysis of the anhydride group to form acid groups is rapidly followed by their subsequent reaction with epoxides at relatively low temperatures [18,23]. Higher temperature and strong catalytic conditions are necessary for the reaction between hydroxyl groups and epoxy groups [28].

The progress of prepolymerization reactions were studied via measurement of some physical and chemical properties of samples during the initial stages of reaction. Monitoring the decrease in the OOC of EHO provides direct information on the extent of the esterification and other reactions of the system. To measure these OOC changes, samples (15 ml) were taken from the curing medium periodically, without significant disturbance of the reaction conditions. Each sample was washed with saturated NaCl solution to remove the unreacted CA or TMA, and the resulting product was extracted into ethyl acetate, dried (anhydrous sodium sulfate), filtered and the ethyl acetate was removed using a rotary evaporator (at 25 ºC).

Figure 3.3 shows the change of the OOC of the EHO upon reaction with CA (A) and with TMA (B). It is clear that the reaction of the EHO with CA occurs at significantly lower rates compared to the reaction with TMA. For the EHO/CA system, the OOC decreases from its initial value of 7.8% down to about 4% after 6 hours of reaction. In contrast, the reaction of EHO with TMA occurs very rapidly, and reaches a similar OOC of about 4% within 30 min. Hence, the

reactivity of TMA is much higher than that of CA, even though both curing agents can provide 3 carboxylic acid groups for reaction.
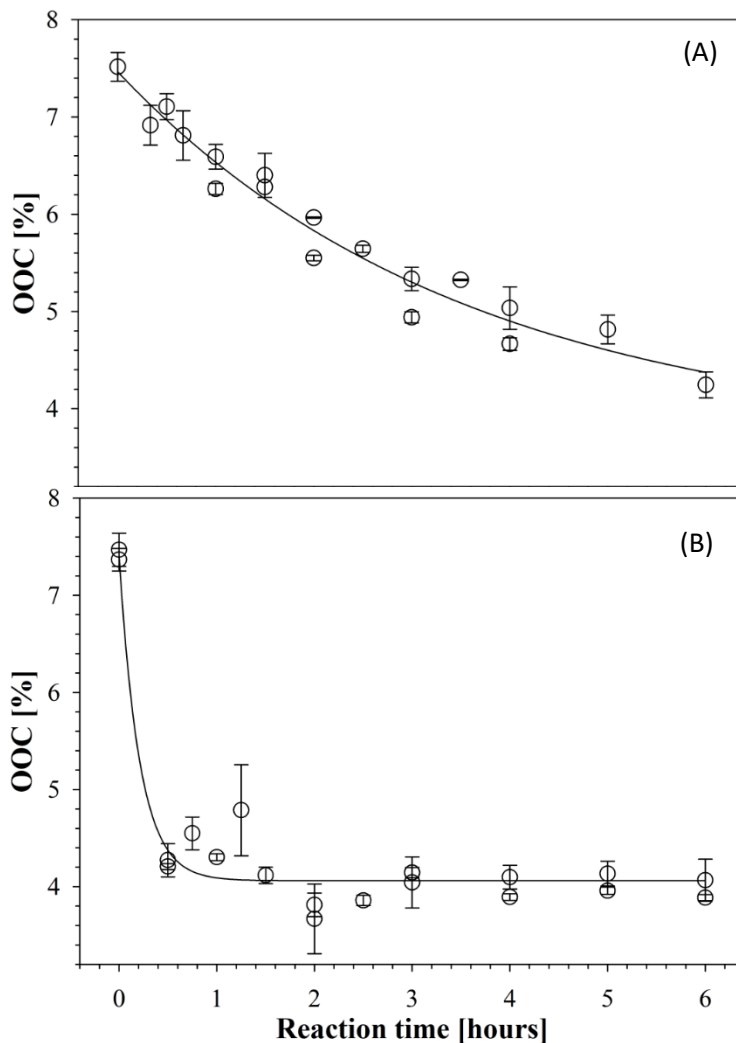
Figure 3.3 The change of OOC of EHO upon curing reaction with CA (A) and TMA (B), in acetone, at 50 °C. Note that the line is showing a cumulative fitting of the two sets of experiments

The epoxide group is a 3-membered cyclic ether, almost in the shape of equilateral triangle. It has been reported [29] that the oxirane molecule has C–O bond lengths of 1.428 Å, a C–C bond length of 1.467 Å, and a C–O–C bond angle of 61.62°. This shape results in ring strain with a strain enthalpy of 27 kcal/mol; as a result, the epoxide is highly reactive. The opening of the epoxy

ring is generally described as occurring in two steps: a) the epoxide is protonated; b) a nucleophile attacks at the most substituted position. Protonation can occur either when an epoxy reacts with an acidic compound which itself opens the ring, or when there is a separate proton source and nucleophile [10,15]. In the present case, where low temperature conditions are used, epoxy ring opening with TMA and CA is expected to occur via such reactions with the formation of ester linkages (Figure 3.2 **I-A** and **II-A**) and a secondary hydroxyl group.

The greater reactivity of TMA towards EHO compared to CA (see Figure 3.3) comes about both as a result of the anhydride functionality and as a consequence of resonance stabilization of carboxylate anions due to their substitution on an aromatic ring. The greater acidity of TMLA as compared to CA is indicated by its 3 pK_a values (pK_1=2.40, pK_2=3.71 and pK_3=5.01) which are all lower than those of CA (pK_1=2.87, pK_2=4.35 and pK_3=5.69) [30]. In an anhydride, both carbonyl groups are effectively competing for the same oxygen electron pair, [31] and therefore the carbonyl groups of anhydrides are less stabilized, and are reactive towards nucleophiles such as water or hydroxyl groups. Hence, TMA can react with epoxides either through reactions involving the anhydride group or the acid group, or both [32]. For these reasons, it is not surprising to observe that TMA or TMLA are more reactive towards epoxides than citric acid.

However, it is interesting to note that the OOC of EHO reaches a similar minimum in the case of low temperature prepolymerization with both CA and TMA, indicating a similar ultimate level of ester formation giving rise to products similar to those shown in Figure 3.2 **I-A** and **I-B** and Figure 3.3 **II-A** and **II-B**, respectively. Negligible changes in OOC were observed for extended reaction times beyond those shown in Figure 3.3, indicating that no further esterification reactions occur under these low temperature conditions and in the presence of solvent (see GPC results

below). Further curing reactions forming higher oligomeric structures and polymers require the elimination of solvent, high temperatures and/or catalytic curing conditions.

3.3.3 ATR-FTIR

It is clear from the above discussion there is a significant difference between the curing of EHO with CA compared to the curing behavior of EHO with TMA. However, although TMA appears to be much more reactive as a curing agent than CA, after 6 hours of reaction, the OOC of both systems had decreased by about 40%. The structural changes which occurred during this curing period were studied using ATR-FTIR spectroscopy. Detailed interpretations of the FTIR spectra of plant oils and their derivatives can be found in the literature; [32,33,34,35,36,37] therefore here we focus on describing those regions of the FTIR spectra that are most relevant in the present context of curing reactions. Figure 3.4 (A) and (B) compares fingerprint region of ATR-FTIR spectra for EHO/CA and EHO/TMA curing system respectively, at times of 0, 0.5, 1.5, 3.0 and 6.0 hours of curing.
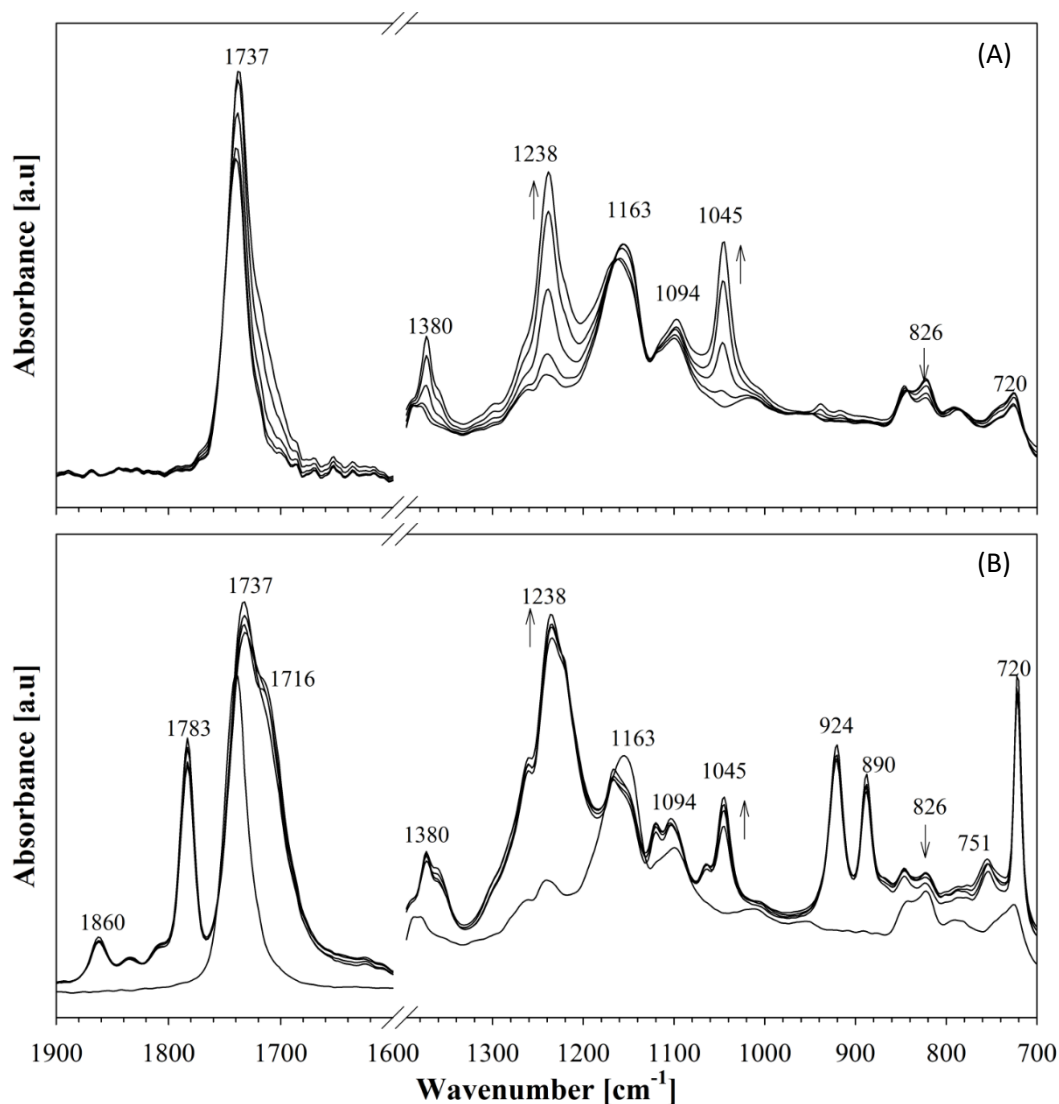
Figure 3.4 Stacked ATR-FTIR plots showing (A) EHO/CA, and (B) EHO/TMA curing systems over curing time (0, 0.5, 1.5, 3.0 and 6.0 hours). The arrows indicate the direction in which curing times increase from 0 to 6 hours, for each feature. Samples were prepared at 50 °C, in acetone

It is evident that the change in the FTIR spectra occurs much faster when TMA is used as a curing agent (almost complete esterification reaction at 0.5 h) when compared to using CA, indicating the much greater reactivity of TMA over CA. Consistent with OOC data shown in Figure 3.3, the primary indication of the occurrence and progress of the esterification reaction is a

reduction in absorbance in regions of the spectra that arise due to oxirane groups. For example, in Figure 3.4 the peak at 826 cm^{-1} corresponding to C–O–C stretching from an oxirane vibration [8,35,38,39] gradually decreases over reaction time for the EHO/CA based system (Figure 3.4 (A)), although this is only a weak absorbance. A much clearer change is the increase in a strong peak at 1238cm^{-1}, which is due to an ester C–O–C stretching vibration [8,33,36,40]. This appears due to the ester formation that accompanies oxirane ring opening, as discussed above. The stretching vibrations of ether linkages - for example, for aliphatic ethers - should appears at 1075 cm^{-1}, However, the lack of such absorbances witnesses the absence of etherification reactions.

It can be seen from Figure 3.4 (B) that the TMA esterification reaction occurs at much faster rates compared to CA (for example compare the absorbances at 1238cm^{-1}), and that the decrease in the intensity of the epoxy moieties beyond 1 hour of reaction is negligible. Note that the arrows indicate the direction in which curing times increase for each main feature; however, the oxirane peak for EHO prior to curing (Figure 3.4(B), time 0hr) appears anomalous because of the absence of underlying absorbances associated with TMA. Overall, it can be concluded that in both curing systems, the trend in the oxirane group consumption is similar to the direct measurements of OOC shown in Figure 3.1, and that TMA reacts faster than CA. Similarly, a moderately strong absorbance band is seen at 1045 cm^{-1} due to O–C stretching vibrations, in carboxylic acids and their derivatives [40]. Less readily explained is the increase in absorbance at 1380 cm^{-1} seen for both curing systems. A possible interpretation is a –CH$_3$ aliphatic bending vibration [35,36], but this remains ambiguous.

There are a few distinctive peaks only seen in the EHO/TMA system. The sharp peak at 720 cm^{-1} is attributed to aromatic C–H out of plane bending [43] of esterified TMA. This peak is overlapped by the weak peaks due to −CH$_2$ rocking vibrations and to the stretching vibrations of

cis-olefins, which is typical for lipids [8,36]. The C=O in-plane bending vibration of the anhydride group [41] is observed at 751 cm^{-1}. The peak at 890 cm^{-1} is assigned to the out of plane bending of O−H in TMA, while the symmetric stretching vibration of C−O−C anhydride functional group [41] is observed at 924 cm^{-1}. The peak around 1860 cm^{-1} and 1716 cm^{-1} (appears as a shoulder) is assigned to the asymmetric stretching of C=O groups of the anhydride while strong resolved peak at 1783 cm^{-1} is assigned to the symmetric stretching of C=O groups of the anhydride [41,42]. The expected strong peak at 1743 cm^{-1} from the C=O stretching modes of the triglycerides [19,34,36] is overlapping a strong peak at around 1737 cm^{-1} that is assigned to the stretching vibration of the ester groups, which are formed during the reaction [42].

Thus, it is apparent that the initial stages of the cure reaction of EHO with CA and TMA occur at different rates, mostly resulting in ester formation through reactions between EHO and either CA or TMA. Further prepolymerization reactions between these CA or TMA esters with the remaining EHO would be expected to form higher molecular weight, oligomeric structures, so this possibility was investigated using gel permeation chromatography.

3.3.4 Gel Permeation Chromatography

Figure 3.5 (A) and (B) shows the GPC chromatograms for the products of EHO cured with CA and TMA, at different reaction times.
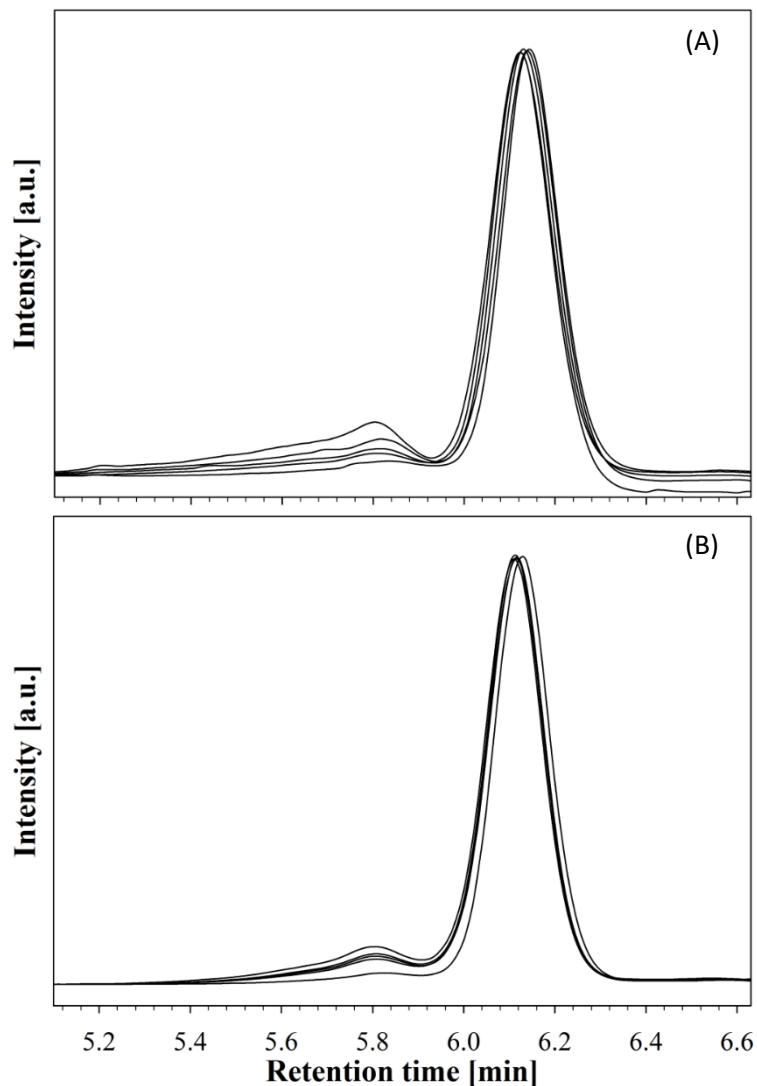
Figure 3.5 Normalized (to the monomer intensity) GPC chromatograms of (A) EHO/CA and (B) EHO/TMA systems over curing time (0, 0.5, 1.5, 3.0 and 6.0 hours). The arrows indicate the direction in which curing times increase from 0 to 6 hours. Samples were prepared at 50 °C, in acetone

These show primarily a monomer peak due to molecules with similar molecular weight (MW) to EHO. In addition, an earlier eluting peak is seen due to the presence of dimeric species. These are present at low abundance but increase in abundance with the reaction time. The formation of

esters of CA and TMA leads to an increase of the average molecular weight, which in turn is reflected by the observed small shift in retention times to the lower values. It can be seen that under the reaction conditions used (60 °C in acetone, 6h reaction time) the majority of products remain in a monomeric state. It can also be seen from Figure 3.5 (A) that whilst the esterification of CA with EHO occurs gradually over the reaction period, the reaction of TMA with EHO (Figure 3.5 (B)) occurs rapidly, as seen by the jump in the retention time of the monomer peak to a lower value and the appearance of the dimer peak, at between 0 h and 0.5 h.

The increase in intensity at low retention times seen in Figure 3.5(A) shows that the CA containing system forms more trimers and higher oligomers with longer reaction times. Overall, the trends observed by GPC during the curing of EHO with CA or with TMA, are consistent with the changes in OOC discussed above.

3.3.5 Structural changes upon prepolymerization

In order to relate the changes in OOC that occurred during curing reactions to structural changes, two main factors must be considered. Firstly, there is decrease in OOC due to oxirane ring opening by the curing agent. Secondly, there is a decrease in OOC due to an increase in the average MW, since OOC is defined as the grams of oxirane oxygen in 100 g of product. Fully epoxidized hemp oil has an average of 5.4 epoxy groups per epoxidized TAG molecule (equivalent to OOC=9.0%; see Table 3.1). Hence, each mole of EHO could react with up to 5.4 moles of carboxylic acid groups from the curing agent, to form esters of CA or TMA. The curing agent (either CA or TMA) was added such that there are 1.0 moles of epoxy groups from EHO to every 1.0 moles of acid groups from the curing agent. This is achieved by using a molar ratio of 1.0 : 1.8 for both EHO/CA and EHO/TMA systems (assuming that 1 mole of TMA yields 3 moles of acid groups).

Hypothetically, if only one carboxylic acid group from each molecule of curing agent (CA or TMA) reacts with one epoxy group of EHO, then the number of moles of oxirane groups on the esterified product should decrease to 3.6 (=5.4-1.80). As a result, the average molecular weight of the esterified product is expected to be around 1310 g/mol. Then, using the equation

$OOC = \dfrac{\# \, of \, epoxy \, groups \times 16}{MW_{epoxide}} \times 100\%$, the OOC of the esterified product is expected to be about

4.4%. This number is only slightly higher than the experimental result of 4.2% for the EHO/CA system and 4.0% for the EHO/TMA system, after 6 hours of reaction. The small deviation of OOC from the calculated values could be associated with lower OOC value of the starting EHO compared to theoretical values and with a small loss of epoxides due to the formation of oligomeric compounds [7].

The reaction between epoxide and carboxylic acid is described in the literature using the model reaction systems of phenylglycidyl ether/caproic acid [43] and diglycidyl ether of 2,2-di-*p*-hydroxyphenyl propane/caproic acid [10]. These authors found that at the initial stages, the reaction of epoxide with carboxylic acid resulted in fast monoester formation. Further reaction of these formed monoesters with residual epoxides (etherification) and carboxylic acids (condensation esterification) led to the branching and crosslinking.

As confirmed in Figure 3.5, the majority of products formed during the prepolymerization reaction in acetone are monomeric compounds. The small difference in the final prepolymerization OOC value for the EHO/CA system after 6 h of reaction maybe partly a result of the slower transesterification reaction (see Figure 3.3), and partly due to the competing reactions which form oligomers, with a somewhat higher oligomer content observed for the EHO/CA system at 6h compared to EHO/TMA (Figure 3.5).

3.3.6 Fully cured EHO based thermosets and their properties

Ultimately, our aim is to use solutions of the EHO/CA or EHO/TMA prepolymers as binding adhesives in biocomposite materials. To this end, we have evaluated and compared the thermo-mechanical properties of these thermosetting networks in their fully cured state. Determination of the thermo-mechanical properties of the thermosets, helps to define the operating temperature range over which the material can be used [44]. Therefore, thermosets made from EHO with CA or TMA were prepared in acetone solution according to the procedure described above. After prepolymerization for 3 hours (this time was chosen to achieve adequate prepolymerization without immediate curing upon removal of solvent), the acetone was removed using a rotary evaporator at room temperature. After acetone evaporation, formed prepolymer is homogenous and has honey-like consistency. The prepolymer was then transferred into a Teflon mold and subsequently was placed into an oven, cured at 170 °C for 4 hours, then cooled down to room temperature at a rate of 0.5 °C/min. The resulting resin samples were believed to be fully cured, as indicated by the complete disappearance of the of the epoxy peak at 826 cm^{-1} in the ATR-FTIR spectrum.

3.3.7 Dynamic Mechanical Analysis (DMA)

The resulting fully cured thermoset samples (100 ×100 × 4 mm^3) were used for DMA analysis to determine their dynamic mechanical behaviors. Figures 3.6 (A) and (B) demonstrates the storage modulus (G`) and loss factor (tan δ) for the EHO/CA and EHO/TMA thermoset systems, as a function of temperature.
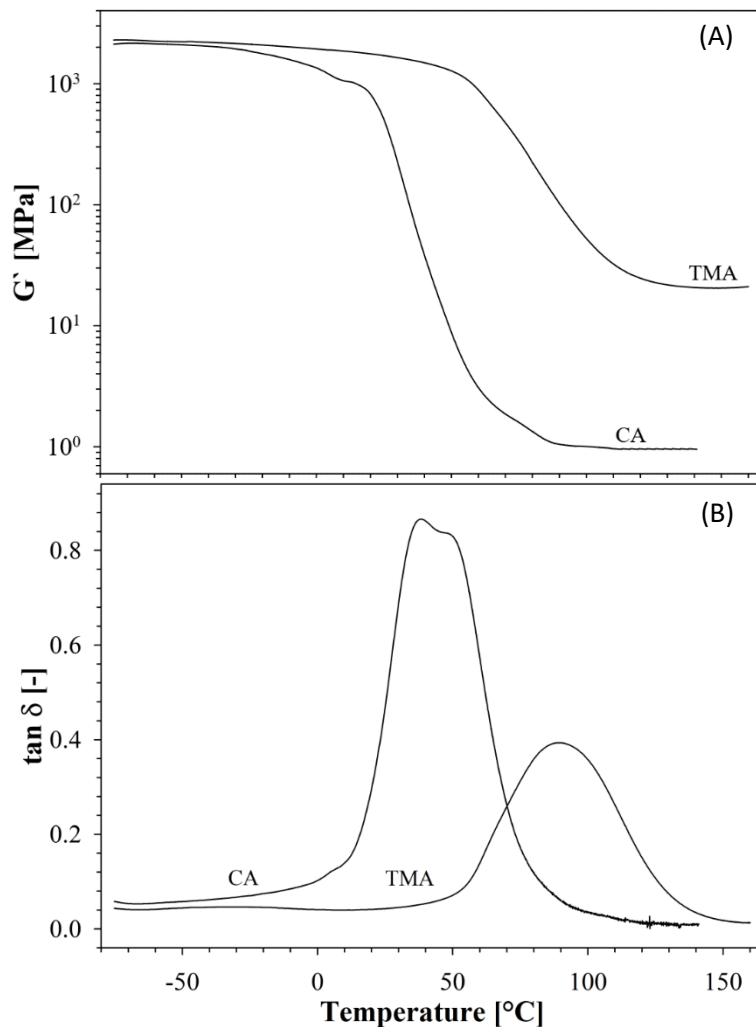
Figure 3.6 Storage moduli, $G^{`}$, (A) and loss factor, *tan δ*, (B) as functions of the temperature for the EHO/CA and EHO/TMA resin systems, cured at 170 °C

Overall, the trend in dynamic mechanical behavior of these thermosets is similar. EHO/TMA network has a higher storage modulus compared to the EHO/CA system (Figure 3.6 (A)), over the whole temperature range of the experiments. The alpha relaxation temperatures ($T_α$), which is associated with the glass transition temperatures of the networks were determined from the peak of the dynamic transition temperature of tan δ. It is seen from the Figure 3.6 (B) that the $T_α$ of the EHO/CA aliphatic network is 38 °C, which is significantly lower than the EHO/TMA aromatic network system (89 °C). This could be due to a lower crosslinking density and to the presence of

low molecular weight, unreacted CA esters of EHO (monomeric compounds) in the EHO/CA system. It can be seen from Figure 3.6(B) that the tan δ < 1, which suggests that the networks are gelled at this point. Moreover, the temperature dependence of tan δ curves that EHO/CA network represents two overlapping but distinguishable relaxations. These could be attributed to the relaxation of segregated networks that are yet not part of the integrated network. The presence of such segregated formations can be seen in TGA thermograms, where their decompositions occur at different temperatures (see Section 3.2.2 below).

Crosslinking density can be defined as the number of moles of elastically effective network chains per cubic centimeter of polymer (mol/cm^3), as described in the literature [45]. In calculations of crosslinking density, it is assumed that all functional groups of the same type are equally reactive, they can react independently, and no intramolecular reactions occur [46]. With these assumptions, the networks have an ideal network, all chains are elastically effective and the storage modulus is not dependent on the frequency at the rubbery plateau [45,47]. The crosslinking density, v_e, can then be estimated using the following equation: $v_e = \dfrac{G'}{RT} = \dfrac{E'}{3RT}$, where G' (shear storage modulus) or E' (tensile storage modulus) are obtained in the rubber plateau of the storage modulus; T is temperature corresponding to the storage modulus value (in °K) and R is the gas constant. While v_e is appropriate to characterize networks, it was also described [45] for the easy visualization of the "tightness" of a polymer network through "number average molecular weight of the effective network chains" using the following equation: $M_c = \dfrac{\rho}{v_e}$, where M_c [g/mol] is weight of sample in grams that contains one mole of elastically effective chains, and ρ is bulk density of material. M_c is often called molecular weight between crosslinks.

The crosslinking density of the epoxy networks was estimated from the storage modulus (at 1Hz) of the samples in the rubbery plateau, about 50 °C above T_α of the respective samples. These storage moduli were found to be 1.07 MPa at 88 °C for the CA based networks and 20.72 MPa at 139 °C for the TMA based system. The bulk densities of epoxy networks were measured to be 1.16 g/cm^3 for EHO/CA system and 1.09 g/cm^3 for EHO/TMA based thermoset. Using these values in the equation, we obtain the crosslinking density of EHO/CA epoxy network to be 0.36×10^{-3} mol/cm^3 while EHO/TMA system has a crosslinking density of about 6.05×10^{-3} mol/cm^3. This gives rise to a number average MW of "effective network chains"[46], M_c, of 3260 g/mol and 180 g/mol for EHO/CA and EHO/TMA networks, respectively. These values are in the range of previously reported soybean oil based epoxy resins cured with variety of different anhydride and amine based curing agents [48]. For example, epoxidized soybean oil (ESO) cured with succinic anhydride and triethylamine (TEA) showed M_c=3277 g/mol, while ESO cured with phthalic anhydride and TEA showed M_c=352 g/mol. A high value of M_c corresponds to a "loose" network and a low value to a "tight" network. Most importantly, the present results differ considerably between EHO/TMA and EHO/CA. The "loose" network for the EHO/CA system may be explained by the presence of unreacted, and partially reacted, curing agent, resulting dangling chain ends which do not count as elastically effective chains but contribute to the volume of the sample [45]. In this case, the resulting unreacted epoxy groups lead to mobile pendant chain ends, which also account for the decrease in T_g [48]. It is important to note that the *tan δ* peak intensity for the EHO/TMA aromatic network is significantly lower that the peak intensity of EHO/CA system (see Figure 3.6). This is understandable since the EHO/TMA system has a higher crosslinking density and so chain mobility is suppressed by the bonding. In addition, it was previously reported [49] that the network architecture of an epoxy network has significant effect

on the glass transition temperature. For example, it has been shown [49] that epoxy networks cured with aromatic trifuctional and tetrafunctional amine curing agents demonstrated T_g that were nearly 50 °C higher than T_g with aliphatic curing agents having similar functionalities. Therefore, the contribution of the aromatic structure of TMA curing agent is consistent with the observed 51 °C increase in T_α between the EHO/CA and EHO/TMA epoxy networks.

A further indication of the differences in between EHO/TMA and EHO/CA network structures was seen by an experiment in which cured samples of each (0.4 cm^3) were immersed in acetone. After 5h the EHO/TMA sample had swollen by <10% by weight; subsequent drying of this sample in a vacuum oven at 110 °C showed that there was no loss of weight, i.e. the insoluble fraction of the resin is ~100%. In contrast, the EHO/CA resin sample swelled by about 50% on soaking in acetone for 5 h, and started to crack. On drying, it was found that the insoluble fraction was 91.4%, again suggesting a less tightly crosslinked material compared to EHO/TMA resin.

3.3.8 Thermogravimetric Analysis (TGA)

Thermogravimetric analysis, which measures weight change in materials as its temperature is increased, provides a way to determine the presence of unreacted components in the resin. The presence of these unreacted or unbound components should give rise to a mass change that is over a temperature range that is characteristic of their decomposition. In this study, TGA experiments were carried out on samples of about 10 mg in a ceramic crucible, with a constant heating rate of 10 °C/min from 25 °C to 600 °C, and under a nitrogen flow of 60 mL/min. Figure 3.7 contains the TGA thermograms (weight loss (A) and derivative weight (B) as a function of temperature) for the EHO/CA and EHO/TMA epoxy networks.
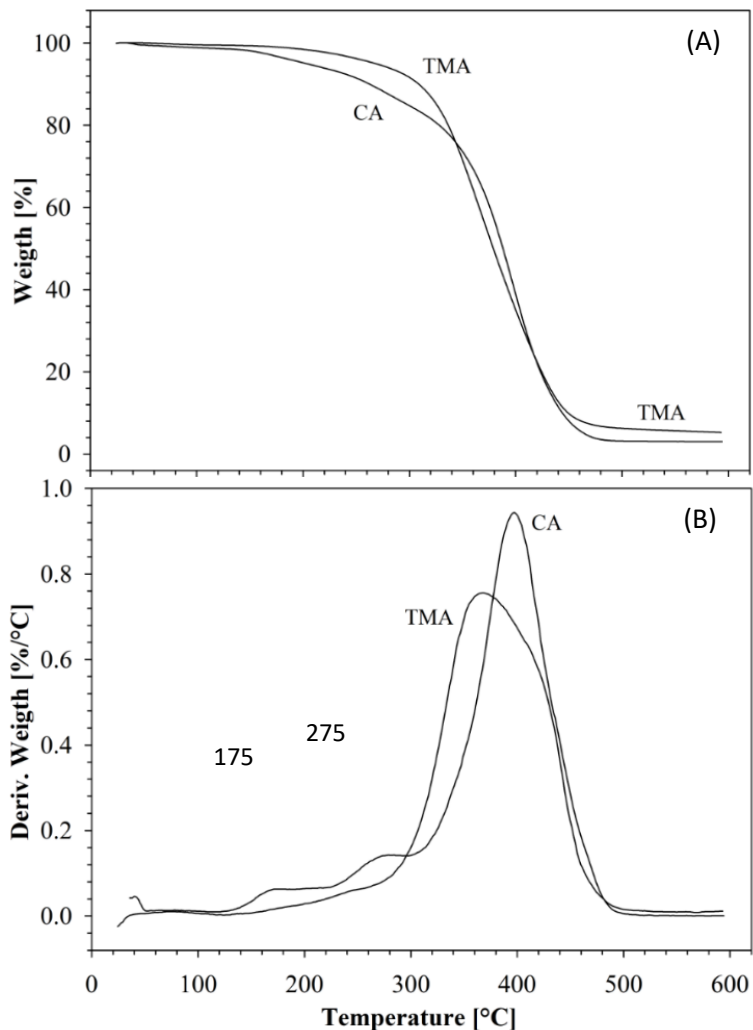
Figure 3.7 Weight loss (A) and weight loss derivative (B) curves for fully cured EHO/CA and EHO/TMA resin systems. Horizontal dashed line refers to the 5% weight loss, while inserted numbers above the arrows refers to the temperature positions of the respective transitions

The initial decomposition temperature of the resins, taken as the temperature for 5% weight loss, occurred at 204 °C for the EHO/CA system and at 269 °C for the EHO/TMA system. This demonstrates the higher thermal stability for the EHO/TMA system (Figure 3.7 (A)). In addition, the decomposition behavior of the epoxy networks also differs, i.e. EHO/TMA is a single-step decomposition, whereas the EHO/CA system appears as a multi-step decomposition (Figure 3.7 (B)), which is evidence for the heterogeneous structure of this epoxy network.

The thermal decomposition of citric acid is a complex process proceeding via dehydration and decarboxylation reactions to various intermediate products [50,51,52]. It was reported that citric acid undergoes a single step decomposition with a maximum weight loss temperature of between 198-205 °C, at a heating rate of 10 °C/min [50,51]. The first stage of decomposition observed at about 175 °C in EHO/CA system (see Fig 3.7(B)) can be attributed to the decomposition of unbound citric acid species. Such decomposition is reported to occur at temperatures about 175 °C by dehydration of citric acid to form *cis-* or *trans-* aconitic acid, and further to form *cis-* or *trans-* aconitic anhydride due to loss of water molecule [50,52]. The second stage of decomposition observed at about 275 °C may correspond to the reported further decomposition of *cis-* or *trans-* aconitic acids [52]. Alternatively, this might be attributed to the decomposition of CA esterified to EHO. In either case, the decomposition products result from the presence of CA that is not fully crosslinked into the polymer.

The decomposition of the remaining products occurs between 300-480 °C, which is typical for plant oil epoxide based networks, and is similar for both EHO/CA and EHO/TMA systems. It has been reported that the decomposition temperature range of plant oil epoxy networks depends on their content of epoxy groups. For example, the decomposition temperatures of soybean oil based epoxy networks are between 300-420 °C [48], whilst this range is higher (400-560 °C) for epoxy networks made with more highly unsaturated oils such as for fish oil [53] or tung oil [54]. It can be concluded that the EHO/TMA network represents a more homogenous structure compared to the EHO/CA system, as indicated by the lower temperature decompositions of citric acid derivatives.

3.4 CONCLUSIONS

The formation of prepolymers by the reaction of EHO with aliphatic (CA) and aromatic (TMA) curing agents in a solvent medium at 50 °C, was studied. Significant differences were found between the prepolymerization rates for these two curing agents with EHO in acetone, and between the thermo-mechanical properties of the fully cured biobased epoxy networks. The prepolymerization of EHO with CA resulted in the formation of citric acid esters of EHO, along with simultaneous formation of dimers and higher oligomeric compounds. The reduced reaction rate after 3 h of mixing appears to indicate the point at which most of the CA species are attached to epoxidized fatty acids. Beyond this, further stirred reaction leads to enhanced oligomerization of the citric acid esters.

When TMA is used as the curing agent with EHO, TMA esters (or possibly TMLA esters) form at rapidly but subsequent oligomerization of the TMA esters of EHO proceeds slowly compared to the CA based system. This maybe because TMA has less ability to self-catalyze the curing reaction since an additional step of hydrolysis of the anhydride group to form acid moieties is required.

The ultimate goal of this work was to explore the use of EHO/CA and EHO/TMA epoxy network prepolymer solutions as binding adhesives in biocomposite materials. Therefore, we compared the thermo-mechanical properties of both epoxy networks in their fully cured state (cured at ~170 °C, after removal of the solvent). This showed that the EHO/TMA based network is rigid and has a high T_g of 89 °C, while the EHO/CA based system is somewhat flexible with a T_g of 40 °C.

These findings have several practical implications. Firstly, the use of a solvent overcomes the barrier to using a curing agent that is immiscible with EHO or other epoxide, allowing for the

production of a homogeneous phase containing prepolymers of the epoxy networks. Secondly, the prepolymer solution in solvent has a very low viscosity, so is able to impregnate fibers in the manufacturing of (bio)composites much more readily than can a more viscous mixture of an epoxidized plant oil based network alone. These advantages become apparent by separating the epoxy monomer curing into the two stages of prepolymerization and final curing, as described in this work.

The use of such biobased epoxy networks has been successfully demonstrated in manufacturing natural fibre biocomposites, as will be reported separately.

3.5 REFERENCES

[1] Altuna, F. I., Pettarin, V., & Williams, R. J. J. (2013). Self-healable polymer networks based on the cross-linking of epoxidised soybean oil by an aqueous citric acid solution, *Green Chemistry*, **15**: 3360-66. https://doi.org/10.1039/c3gc41384e.

[2] Omonov, T. S., Kharraz, E., & Curtis, J. M. (2016). The epoxidation of canola oil and its derivatives, *RSC Advances*, **6**: 92874-86. https://doi.org/10.1039/c6ra17732h.

[3] Auvergne, R., Caillol, S., David, G., Boutevin, B., & Pascault, J. P. (2014). Biobased Thermosetting Epoxy: Present and Future, *Chemical Reviews*, **114**: 1082-115. https://doi.org/10.1021/cr3001274.

[4] Llevot, A. (2017). Sustainable Synthetic Approaches for the Preparation of Plant Oil-Based Thermosets, *Journal of the American Oil Chemists Society*, **94**: 169-86. https://doi.org/10.1007/s11746-016-2932-4.

[5] Omonov, T. S., Kharraz, E., & Curtis, J. M. (2017). Camelina (Camelina Sativa) oil polyols as an alternative to Castor oil, *Industrial Crops and Products*, **107**: 378-85. https://doi.org/10.1016/j.indcrop.2017.05.041.

[6] HealthCanada. (July 03, 2019). Statistics, Reports and Fact Sheets on Hemp, HealthCanada, https://www.canada.ca/en/health-canada/services/health-concerns/controlled-substances-precursor-chemicals/industrial-hemp/about-hemp-canada-hemp-industry/statistics-reports-fact-sheets-hemp.html.

[7] Omonov, T. S., & Curtis, J. M. (2016). 'Chapter 7. Plant Oil-Based Epoxy Intermediates for Polymers.' in Madbouly, S. A., Zhang, C. & Kessler, M. R. (eds.), *Bio-Based Plant Oil Polymers and Composites* (Elsevier Inc.: Oxford, UK). https://doi.org/10.1016/B978-0-323-35833-0.00007-4.

[8] Bai, J. (2013). *Advanced Fibre-Reinforced Polymer (FRP) Composites for Structural Applications* (Woodhead Publishing: Cambridge, UK). https://doi.org/10.1533/9780857098641.

[9] Madec, P. J., & Marechal, E. (1985). Kinetics and Mechanisms of Polyesterifications. 2. Reactions of Diacids with Diepoxides, *Advances in Polymer Science*, **71**: 153-228. https://doi.org/10.1007/3-540-15482-5_9.

[10] Shechter, L., & Wynstra, J. (1956). Glycidyl Ether Reactions with Alcohols, Phenols, Carboxylic Acids, and Acid Anhydrides, *Industrial and Engineering Chemistry*, **48**: 86-93. https://doi.org/10.1021/ie50553a028.

[11] Wang, R., & Schuman, T. (2015). 'Towards Green: A Review of Recent Developments in Bio-renewable Epoxy Resins from Vegetable Oils.' in Liu, Z. & Kraus, G. (eds.), *Green Materials from Plant Oils* (RSC: Cambridge, UK). https://doi.org/10.1039/9781782621850-00202.

[12] Shogren, R. L. (1999). Preparation and characterization of a biodegradable mulch: Paper coated with polymerized vegetable oils, *Journal of Applied Polymer Science*, **73**: 2159-67. https://doi.org/10.1002/(Sici)1097-4628(19990912)73:11<2159::Aid-App12>3.0.Co;2-Q.

[13] Coates, J. (2011). 'Interpretation of Infrared Spectra, A Practical Approach.' in Meyers, R. A. (ed.), *Encyclopedia of Analytical Chemistry* (John Wiley & Sons: Chichester, UK). https://doi.org/10.1002/9780470027318.a5606.

[14] Wang, Z., Cui, Y. T., Xu, Z. B., & Qu, J. (2008). Hot water-promoted ring-opening of epoxides and aziridines by water and other nucleopliles, *Journal of Organic Chemistry*, **73**: 2270-74. https://doi.org/10.1021/jo702401t.

[15] Ly, U. Q., Pham, M. P., Marks, M. J., & Truong, T. N. (2017). Density functional theory study of mechanism of epoxy-carboxylic acid curing reaction, *J Comput Chem*, **38**: 1093-102. https://doi.org/10.1002/jcc.24779.

[16] Sun, S. D., Li, P., Bi, Y. L., & Xiao, F. G. (2014). Enzymatic Epoxidation of Soybean Oil Using Ionic Liquid as Reaction Media, *Journal of Oleo Science*, **63**: 383-90. https://doi.org/10.5650/jos.ess13197.

[17] Johnson, D. S. (1983). Accelerator for anhydride-cured epoxy resins, U.S. Patent 4398013. Karak, N. (2012). *Vegetable oil-based polymers. Properties, processing and applications.* (Woodhead Publishing: Cambridge, UK). https://doi.org/10.1533/9780857097149.

[18] Petrie, E. M. (2006). *Epoxy adhesive formulations* (McGraw-Hill: New York, USA). https://doi.org/10.1036/0071455442.

[19] Omonov, T. S., & Curtis, J. M. (2014). Biobased Epoxy Resin from Canola Oil, *Journal of Applied Polymer Science*, **131**. https://doi.org/10.1002/app.40142.

[20] Shishikura, A., Takahashi, H., Hirohama, S., & Arai, K. (1992). Citric-Acid Purification Process Using Compressed Carbon-Dioxide, *Journal of Supercritical Fluids*, **5**: 303-12. https://doi.org/10.1016/0896-8446(92)90022-C.

[21] ASTM®. (American Society for Testing and Materials). (2019) ASTM D1652-11E1. Standard Test Method for Epoxy Content of Epoxy Resins, 4. https://doi.org/10.1520/D1652-11R19.

[22] Li, F. K., & Larock, R. C. (2000). Thermosetting polymers from cationic copolymerization of tung oil: Synthesis and characterization, *Journal of Applied Polymer Science*, **78**: 1044-56. https://doi.org/10.1002/1097-4628(20001031)78:5<1044::Aid-App130>3.0.Co;2-A.

[23] Pascault, J.-P., & Williams, R. J. J. (2010). *Epoxy Polymers: New Materials and Innovations* (Wiley-VCH: Germany). https://doi.org/10.1002/9783527628704.

[24] Fisch, W., Hofmann, W., & Koskikallio, J. (1956). The Curing Mechanism of Epoxy Resins, *Chemistry & Industry*: 756-57. https://doi.org/10.1002/jctb.5010061005.

[25] Steinmann, B. (1989). Investigations on the Curing of Epoxy-Resins with Hexahydrophthalic Anhydride, *Journal of Applied Polymer Science*, **37**: 1753-76. https://doi.org/10.1002/app.1989.070370702.

[26] Kolar, F., & Svitilova, J. (2007). Kinetics and mechanism of curing epoxy/anhydride systems, *Acta Geodynamica Et Geomaterialia*, **4**: 85-92.

[27] Barabanova, A. I., Lokshin, B. V., Kharitonova, E. P., Karandi, I. V., Afanasyev, E. S., Askadskii, A. A., & Philippova, O. E. (2019). Cycloaliphatic epoxy resin cured with anhydride in the absence of catalyst, *Colloid and Polymer Science*, **297**: 409-16. https://doi.org/10.1007/s00396-018-4430-8.

[28] Curtis, J. M., Liu, G., Omonov, T. S., & Kharraz, E. (2015). Polyol Synthesis from Fatty Acids and Oils., U.S. Patent 9,216,940 B2.

[29] Alvarez-Builla, J., Vaquero, J. J., & Barluenga, J. (2011). *Modern Heterocyclic Chemistry* (Wiley-VCH Verlag: Weinheim, Germany). https://doi.org/10.1002/9783527637737.

[30] Bhattacharyya, L., & Rohrer, J. S. (2012). *Applications of Ion Chromatography for Pharmaceutical and Biological Products* (Wiley: New Jersey, USA). https://doi.org/10.1002/9781118147009.

[31] Carey, F. A., & Giuliano, R. M. (2017). 'Carboxylic Acid Derivatives: Nucleophilic Acyl Substitution.' in Carey, F. A. & Giuliano, R. M. (eds.), *Organic Chemistry* (McGraw-Hill: Boston, USA).

[32] Chen, M., Ding, W., Kong, Y., & Diao, G. (2008). Conversion of the surface property of oleic acid stabilized silver nanoparticles from hydrophobic to hydrophilic based on host-guest binding interaction, *Langmuir*, **24**: 3471-78. https://doi.org/10.1021/La704020j.

[33] Miller, D. R., & Macosko, C. W. (1988). Network Parameters for Crosslinking of Chains with Length and Site Distribution, *Journal of Polymer Science Part B-Polymer Physics*, **26**: 1-54. https://doi.org/10.1002/polb.1988.090260101.

[34] Lee, D. H., & Condrate, R. A. (1999). FTIR spectral characterization of thin film coatings of oleic acid on glasses: I. Coatings on glasses from ethyl alcohol, *Journal of Materials Science*, 34: 139-46. https://doi.org/10.1023/A:1004494331895.

[35] Mahendran, A. R., Aust, N., Wuzella, G., & Kandelbauer, A. (2012). Synthesis and Characterization of a Bio-Based Resin from Linseed Oil, *Macromolecular Symposia*, **311**: 18-27. https://doi.org/10.1002/masy.201000134.

[36] Vlachos, N., Skopelitis, Y., Psaroudaki, M., Konstantinidou, V., Chatzilazarou, A., & Tegou, E. (2006). Applications of Fourier transform-infrared spectroscopy to edible oils, *Analytica Chimica Acta*, **573**: 459-65. https://doi.org/10.1016/j.aca.2006.05.034.

[37] Wu, N. Q., Fu, L., Su, M., Aslam, M., Wong, K. C., & Dravid, V. P. (2004). Interaction of fatty acid monolayers with cobalt nanoparticles, *Nano Letters*, **4**: 383-86. https://doi.org/10.1021/Nl1035139x.

[38] Park, C.-M., & Sheehan, R. J. (2000). 'Phthalic acids and other benzenepolycarboxylic acids.' in Kroschwitz, J. I. & Howe-Grant, M. (eds.), *Kirk-Othmer Encyclopedia of Chemical Technology* (Wiley-Interscience: New Jersey, USA). https://doi.org/10.1002/0471238961.1608200816011811.a01.

[38] Theophanides, T. (2012). *Infrared Spectroscopy. Materials Science, Engineering and Technology* (InTech Open: Rijeka, Croatia). https://doi.org/10.5772/2055.

[39] Vlcek, T., & Petrovic, Z. S. (2006). Optimization of the Chemoenzymatic Epoxidation of Soybean Oil, *Journal of the American Oil Chemists Society*, **73**: 247-52. https://doi.org/10.1007/s11746-006-1200-4.

[40] Vo-Dinh, T. (2015). *Biomedical Photonics Handbook. Volume 1. Fundamentals, Devices, and Techniques* (CRC Press: Boca Raton,FL). https://doi.org/10.1201/b17290.

[41] Arjunan, V., Raj, A., Subramanian, S., & Mohan, S. (2013). Vibrational, electronic and quantum chemical studies of 1,2,4-benzenetricarboxylic-1,2-anhydride, *Spectrochimica Acta Part A - Molecular and Biomolecular Spectroscopy*, **110**: 141-50. https://doi.org/10.1016/j.saa.2013.02.031.

[42] Matejka, L., Pokorny, S., & Dusek, K. (1982). Network Formation Involving Epoxide and Carboxyl Groups - Course of the Model Reaction Monoepoxide-Monocarbonic Acid, *Polymer Bulletin*, **7**: 123-28. https://doi.org/10.1007/BF00265462.

[42] Zhou, Y., Chen, G. F., Wang, W., Wei, L. H., Zhang, Q. J., Song, L. P., & Fang, X. Z. (2015). Synthesis and characterization of transparent polyimides derived from ester-containing dianhydrides with different electron affinities, *Rsc Advances*, **5**: 79207-15.

[43] Campanella, A., & Baltanas, M. A. (2006). Degradation of the oxirane ring of epoxidized vegetable oils in liquid-liquid heterogeneous reaction systems, *Chemical Engineering Journal*, **118**: 141-52. https://doi.org/10.1016/j.cej.2006.01.010.

[44] Menard, K. P., & Menard, N. R. (2014). 'Dynamic Mechanical Analysis in the Analysis of Polymers and Rubbers.' in Mark, H. F. (ed.), *Encyclopedia of Polymer Science and Technology* (John Wiley & Sons: Hoboken, NJ). https://doi.org/10.1002/0471440264.pst102.pub2.

[45] Hill, L. W. (1997). Calculation of crosslink density in short chain networks, *Progress in Organic Coatings*, **31**: 235-43. https://doi.org/10.1016/S0300-9440(97)00081-7.

[46] Last, D. J., Najera, J. J., Percival, C. J., & Horn, A. B. (2009). A comparison of infrared spectroscopic methods for the study of heterogeneous reactions occurring on atmospheric aerosol proxies, *Physical Chemistry Chemical Physics*, **11**: 8214-25. https://doi.org/10.1039/B901815h.

[47] Hill, L. W. (2012). 'Dynamic Mechanical and Tensile Properties.' in Koleske, J. V. (ed.), *Paint and Coating Testing Manual: 15th. Edition of the Gardner-Sward Handbook* (ASTM International: West Conshohocken, PA, USA). https://doi.org/10.1520/MNL12229M.

[48] Gerbase, A. E., Petzhold, C. L., & Costa, A. P. O. (2002). Dynamic mechanical and thermal behavior of epoxy resins based on soybean oil, *Journal of the American Oil Chemists Society*, **79**: 797-802. https://doi.org/10.1007/s11746-002-0561-z.

[49] Crawford, E., & Lesser, A. J. (1998). The effect of network architecture on the thermal and mechanical behavior of epoxy resins, *Journal of Polymer Science Part B-Polymer Physics*, **36**: 1371-82. https://doi.org/10.1002/(SICI)1099-0488(199806)36:8<1371::AID-POLB11>3.0.CO;2-4.

[50] Barbooti, M. M., & Alsammerrai, D. A. (1986). Thermal-Decomposition of Citric-Acid, *Thermochimica Acta*, **98**: 119-26. https://doi.org/10.1016/0040-6031(86)87081-2.

[51] Umemura, K., Ueda, T., & Kawai, S. (2012). Characterization of wood-based molding bonded with citric acid, *Journal of Wood Science*, **58**: 38-45. https://doi.org/10.1007/s10086-011-1214-x.

[52] Wyrzykowski, D., Hebanowska, E., Nowak-Wiczk, G., Makowski, M., & Chmurzynski, L. (2011). Thermal behaviour of citric acid and isomeric aconitic acids, *Journal of Thermal Analysis and Calorimetry*, **104**: 731-35. https://doi.org/10.1007/s10973-010-1015-2.

[53] Li, F., Marks, D. W., Larock, R. C., & Otaigbe, J. U. (2000). Fish oil thermosetting polymers: synthesis, structure, properties and their relationships, *Polymer*, **41**: 7925-39. https://doi.org/10.1016/S0032-3861(00)00030-6.

[54] Wool, R., & Sun, X. S. (2005). *Bio-Based Polymers and Composites* (Elsevier Academic Press: Waltham, MA, USA). https://doi.org/10.1016/B978-0-12-763952-9.X5000-X.

Chapter 4

Biobased thermosets from epoxidized linseed oil and its methyl esters

4.1 Introduction

Recently, many scientific publications and patents have described the rational use of renewable resources to produce monomers, polymers and other reactive intermediates, as alternatives to petrochemicals [1]. Several reviews and books have been published describing the current achievements, as well as the outstanding issues for manufacturing biobased monomers, polymers and composites [2,3,4,5,6];(lubricants and greases [7]; surfactants and detergents [8]; and biocomposites for many high performance applications[6,9,10,11]. The opportunities and challenges encountered while manufacturing and commercializing the biobased products are well described in a recently published comprehensive review[12], which also outlines environmental-economic benefits and the technology and market risks.

Plant oil derivatives, such epoxides[13,14,15], polyols [16,17,18] or acrylates [9,19] are being used extensively as reactive intermediates or monomers. The uses for epoxidized plant oils are to some extend governed by the number of epoxy groups per mole of triacylglycerides (TAG).[4]

---

[4] A version of this chapter has been submitted as a journal manuscript, "Tolibjon Omonov, Vinay Patel, Jonathan M. Curtis, Biobased thermosets from epoxidized linseed oil and its methyl esters."

Epoxidized plant oils with lower epoxy numbers, such epoxidized palm olein [20] or canola oil [21] tend to crystallize at room temperature, which may limit their use in some applications. Moreover, upon curing they produce flexible thermosets while epoxidized plant oils with high epoxy content produce rigid thermoset with enhanced mechanical performances[22]. Unlike petroleum-based epoxides, such bisphenol A diglycidyl ether (DGEBA) that has a terminal oxirane group, plant oil epoxides produced *via* epoxidation of their double bonds have internal epoxy groups along the fatty acid chains. These epoxy moieties have significantly lower reactivity compared with terminal epoxy groups[23]. As a result of this, and the presence of unreactive saturated fatty acids, plant oil based epoxy networks normally have a lower crosslinking density [23] and exhibit a self-plasticizing effect, resulting in poorer thermal-mechanical properties.

Clearly, the properties of these thermosets also depend on the curing agents' reactive functionality (amine, acid, anhydride etc) and molecular architecture (molecular weight (MW), chain length, aromatic *vs.* aliphatic, linear *vs.* branched etc)[21,24,25]. For example, epoxidized oils cured with aliphatic curing agents usually produce flexible networks while aromatic curing agents are more likely to produce semi-flexible to rigid thermosets[26]. There are many curing agents/hardening compounds in liquid, powder or solid forms that can be used in making plant oil based epoxy polymers[24,25]. As with the epoxidized oils, curing agents or hardeners that are in the liquid form are often easier to use in epoxy network applications at relatively low temperatures. However, in practice many curing agents are in solid form, which likely require the use of solvents or high temperatures to dissolve them in the epoxidized oil, and which is not always a controllable process. In this study, we specifically attempt to overcome the incompatibility between an epoxidized plant oil and a solid curing agent by developing novel epoxy monomers that both have low viscosity and can effectively dissolve the curing agent.

Converting plant oils into epoxidized fatty acid alkyl esters (eFAAE) is an efficient way to prepare such low viscosity derivatives. These eFAAE can be produced either by epoxidation of the fatty acid alkyl esters (FAAE) produced by transesterification of plant oils by alcohols, or by transesterification of the epoxidized plant oils (triacylglycerides, TAG) by alcohols, usually methanol or ethanol. It has been shown that transesterification of epoxidized plant oils by methanol produces low viscosity eFAME while the epoxy functionality of the resulting product remains unaffected[27,28].

When the goal of producing eFAAE is to use them in biobased thermoset applications, then eFAAE should have at least two epoxy groups per molecule to allow the polymer chain to grow. Therefore, not all epoxidized plant oil derivatives are suitable for thermoset applications. For example, epoxidized FAME from canola oil has about 1.3 epoxy group/mol[21], which apparently not ideal to produce epoxy networks. In contrast, a more suitable plant oil for producing the eFAAE is linseed oil (LO), which has around 6.8 double bonds per mole. Consequently, epoxidized FAME from LO should have on average 2.3 epoxy groups/mol which is well suited for use in thermoset applications.

This work explores the possibility of producing low viscosity epoxidized LO fatty acid methyl esters (denoted further as ELOME) that can effectively dissolve the curing agent (trimellitic anhydride) flakes at a relatively low temperature *without use of solvent*, to produce thermoset resins. The thermo-mechanical performance of the resulting thermosets are also evaluated.

4.2   Material and methods

4.2.1   Materials

Linseed oil was purchased in bulk (20 L) from the Shape Foods Inc. (Brandon, MB, Canada) and was used as supplied. In order to avoid any differences in fatty acid profiles, the epoxidized linseed oil (ELO) and ELOME were prepared from the same batch of oil. Formic acid (85%) and aqueous hydrogen peroxide (H_2O_2, 35%) were purchased from Univar Canada (Richmond, BC, Canada) and used in epoxidation process. ACS grade (≥99.5%) ethyl acetate purchased from Fisher Scientific Canada (Ottawa, ON, Canada) was used in work-up process of epoxidized derivatives. Sodium chloride (NaCl) was a food grade and was purchased from Univar Canada, and used in work-up processes. Anhydrous sodium sulfate (Na_2SO_4) was technical grade and also was purchased from Univar Canada and used as drying agent. Hydrogen bromide (HBr), 33 wt % solution in glacial acetic acid (Fisher Scientific) and glacial acetic acid (99.7%, Caledon Laboratory Chemicals, Georgetown, ON, Canada) were used in oxirane oxygen content titration of epoxides.

Anhydrous methanol (99.8%) and reagent grade sodium methoxide powder (CH_3ONa, 95%) were purchased from Sigma-Aldrich Canada (Oakville, ON, Canada) and used for transesterification reactions to produce ELOME. Reagent grade hydrochloric acid (HCl, 37%) was purchased from Caledon Laboratory Chemicals and used in work-up process of ELOME. Trimellitic anhydride (1,2,4-benzenetricarboxylic anhydride, TMA) was purchased from Sigma-Aldrich Canada and used as a curing agent for epoxidized derivatives of linseed oil. The gas-liquid chromatography reference standard GLC-463 was purchased from Nu-Chek Prep, Inc. (Elysian Township, MN, USA) and used gas chromatography analysis. The lipid standard methyl-9,10-dihydroxystearate of molecular weight (MW) 330.51 g/mol was purchased from Frinton

Laboratories (Hainesport, NJ, USA); 1,2-distearin (MW of 625.03 g/mol) and trieicosapentaenoin (MW of 945.42 g/mol) were purchased from Nu-Chek Prep, Inc. (Elysian, MN, USA). These standards were used in gel permeation chromatography analysis of the products.

4.2.2 Methods

4.2.2.1 Oxirane Oxygen Content (OOC)

The OOC of an ELO and ELOME were measured according to the ASTM standard titrimetric method "Standard Test Method for Epoxy Content of Epoxy Resins"[29], as described elsewhere[30].

4.2.2.2 Attenuated Total Reflectance Fourier Transform Infrared (ATR-FTIR) spectroscopy

The analysis of the LO and its epoxidized derivatives were carried out using a Bruker Alpha FTIR spectrometer equipped with an ATR accessory. IR spectra (4000-650 cm^{-1}, 32 scans, 4 cm^{-1} resolution) of the products were obtained by placing ca. 10 µl of the product onto the ATR crystal. FTIR data analysis was carried out using Bruker's OPUS spectroscopy software package.

4.2.2.3 Gel permeation chromatography (GPC)

An Agilent 1200 series High Performance Liquid Chromatograph (HPLC) (Santa Clara, CA, USA) equipped with an Agilent 1200 evaporating light scattering detector (ELSD) was used for all GPC experiments to measure MW distributions of the LO and its epoxidized derivatives. A Styragel HR 4E THF column (with the size of 4.6 x 300 mm) from Waters Corporation (Milford, MA, USA) was used, and the details of the GPC measurements were described elsewhere[30].

4.2.2.4 Proton Nuclear Magnetic Resonance (^{1}H-NMR) Spectroscopy

The structure of LO, ELO and ELOME were qualitatively examined and compared using A 400 MHz Varian Inova 400-MR NMR spectrometer. The samples for ^{1}H-NMR spectroscopy were

prepared by dissolving 10 mg of LO and its epoxidized derivatives in deuterated (D6) acetone (0.7 mL) and the spectra were obtained at room temperature.

4.2.2.5 Dynamic Mechanical Analysis (DMA)

The dynamic mechanical properties of the produced thermosets were measured with a TA Instruments DMA Q800 (New Castle, DE, USA) equipped with a liquid nitrogen cooling system. The measurements were performed according to ASTM standard method (ASTM E1640-18, 2018) at a fixed frequency of 1 Hz in the single cantilever bending mode, at a constant heating rate of 2 °C/min from -50 to 180 °C, as described elsewhere[31].

4.2.2.6 Thermogravimetric analysis (TGA)

The thermogravimetric analysis was performed using a TA Instruments TGA Q50 Thermogravimetric Analyzer (New Castle, DE, USA) on 10 mg thermoset samples in a ceramic crucible, at a constant heating rate of 10 °C/min under a nitrogen flow (balance purge 40 mL/min and sample purge 60 mL/min) from 25 °C to 600 °C. The TA Universal Analysis software (version 4.7A) was used to analyze the experimental results.

4.3 Procedures

4.3.1 Epoxidation of linseed oil.

The epoxidation of LO (~3000 g) was performed as described previously [30] using a molar ratio of LO/ formic acid/ H_2O_2 of 1.0:1.7:10.2, which translates into the ratio of 1.0:0.25:1.5 double bond/ formic acid/ H_2O_2, respectively. Such conditions are the optimal ratios to yield epoxides with high oxirane content and negligible loss of epoxy groups (Omonov et al., 2016; Curtis et al., 2019). The extent of epoxide formation was followed by periodically measuring the OOC of aliquots (~15 mL) of the epoxidized products. Using the above epoxidation conditions, the process is typically completed within 24 hours.

4.3.2 Transesterification of epoxidized linseed oil.

ELO (3000 g) was loaded into a 22 L glass reactor at 60 °C under reflux (condenser temperature at 5 °C) and with continuous mixing (350±10 rpm). Separately, about 30 g (1% to the total weight of ELO) of NaOCH$_3$ was dissolved in anhydrous methanol (682 g) at room temperature under continuous mixing, taking care because of the resulting release of heat. The methanolic NaOCH$_3$ solution was then transferred into the reactor with the ELO, resulting in a molar ratio of ELO to methanol of 1 : 7, as described elsewhere (Rashid and Anwar, 2008). The extent of ELO transesterification was monitored by GPC through the disappearance of the ELO peak as ELOME forms. The Figure 4.1 compares the GPC chromatograms of LO, ELO and ELOME.
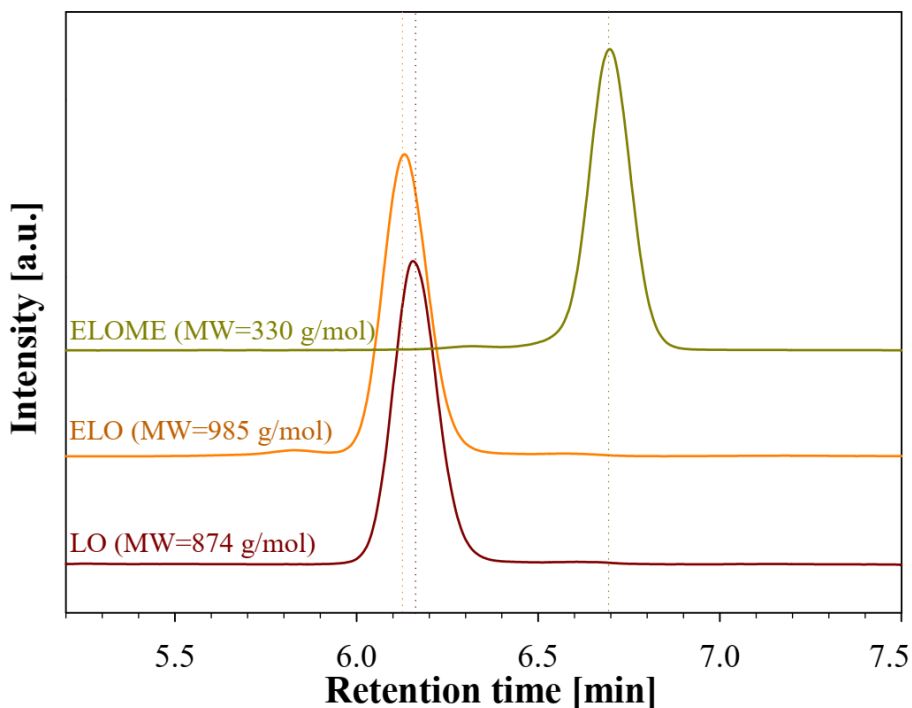
Figure 4.1 GPC chromatograms of LO, ELO and ELOME. Average molecular weights of products are inserted next to their respective chromatograms. Vertical dashed lined to demonstrate the peak positions of the respective products.

After 2 hours of reaction, GPC chromatograms showed that no ELO remained, and negligible formation of oligomeric structures occurred. The mixture was allowed to cool down to room temperature to allow separation of the liberated glycerol and $NaOCH_3$, after which, the remaining product was washed at least 3 times with equal volumes of saturated aqueous NaCl solution to remove excess methanol and the traces of catalyst. During the first wash, the product was neutralized with 1N HCl aqueous solution to adjust the pH of the system to 5-6. The final product, ELOME, was dried over anhydrous Na_2SO_4 and filtered.

The ^{1}H NMR spectroscopy is used to get insights into fatty acid composition of the LO and its epoxidized derivatives, while the structural changes that occurred during epoxidation and transesterification processes were monitored by ATR-FTIR.

4.3.3 Sample preparation to study the pot-life of ELOME based prepolymers.

The ELOME based prepolymer sample for the evaluation of the pot-life was prepared using TMA as curing agent, at the molar ratio of acid groups of the TMA and the epoxy groups of the ELOME (Ac/Ep) of 0.68 at 60 °C. The desired amount of ELOME and TMA was loaded into the glass flask with magnetic stirrer and placed into oil bath at a temperature of at 60 °C with continuous mixing at 500 RPM. Agitation of the reactive components continued until complete dissolution of TMA. After this, the reactive mixture is cooled down to room temperature. The stability of the prepared prepolymer is estimated through evaluating the structural changes of the product over the storage time at room temperature (~25±2 °C), using the rheometer, FTIR and GPC.

4.4 Results and discussion

4.4.1 Linseed oil and its epoxidized derivatives

The average MW of LO is about 874 g/mol as measured by GPC (Figure 4.1). Also, as measured by GC-FID, LO consists mainly of linolenic acid (C18:3, 60%) along with oleic acid (C18:1, 18%) and linoleic acid (C18:2, 14%), and has a total saturated fatty acid content of about 8%. The high double bond content of LO (an average of 6.8 double bonds per triacylglycerol molecule) compared with other commodity plant oils makes it an attractive feedstock for manufacturing reactive derivatives, such epoxides. The epoxidation process is a common route to functionalize plant oils for further use in variety of applications[13,32]. The epoxidation of linseed oil using *in situ* generated performic acid is schematically illustrated in Figure 4.4. As mentioned above the products from epoxidation and transesterification processes were analyzed by ^{1}H NMR and ATR-FTIR spectroscopy.

The ^{1}H chemical shifts of the oils and main FFA identified by the ^{1}H NMR can be found in many literatures and NMR spectrum of vegetable oils and its derivatives have relatively small number of characteristic peaks. Figure 4.2 demonstrates and compares the ^{1}H NMR spectrum of the LO, ELO and ELOME.
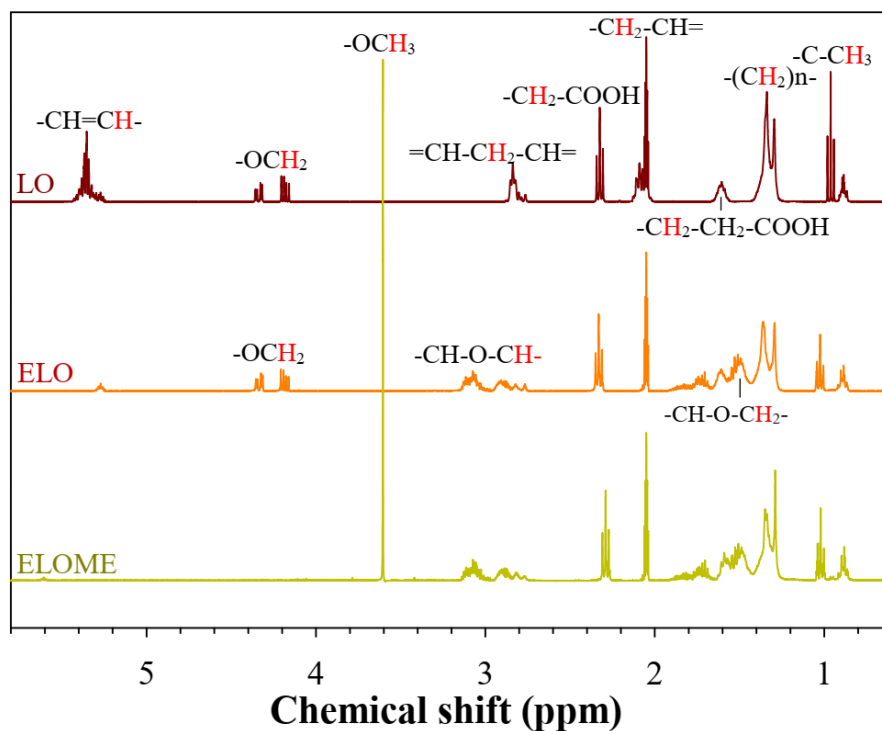
Figure 4.2 ^{1}H-NMR spectra of LO, ELO and ELOME at room temperature (solvent D6 acetone).

The chemical shift values for the olefinic protons (-CH=CH-) and bis-allylic protons (=CH-CH$_2$-CH=) can be seen for the LO at 5.36 and 2.80 ppm. Triacylglyceride structure of the LO can be evidenced by the presence of signals from the glycerol protons at 4.18 and 4.33 ppm. After epoxidation these peaks responsible for the unsaturated fatty acids disappears and new peaks will appear in the epoxidized oils with the chemical shift values at 3.06 and 1.50 ppm which represents signals from oxirane protons (-CH-O-CH) and -CH$_2$ neighboring oxirane protons (-CH-O-CH$_2$-)[33]. The small peak of the olefinic protons in the ELO indicates to the traces of the remaining unsaturates of the LO. Transesterification of the ELO with methanol leads to the formation of epoxidized linseed oil fatty acid methyl esters (ELOME). This can be evidenced by the absence of the signals from the glycerol protons in the ELOME spectra, in which the liberated glycerol is removed during the workup process. And finally, the strong peak with the chemical shift with the value of 3.60 ppm represents the signal from the methoxy protons (-OCH$_3$) of the ELOME[34].

Moreover, the signals from the oxirane protons remains unaltered in the ELOME which indicates the stability of the epoxy groups during transesterification process.

Similar trend in structural changes which occurred during epoxidation and transesterification processes were observed on the FTIR measurements of the ELO and its derivatives. Figure 4.3 compares the ATR-FTIR spectra for LO, ELO and ELOME. Detailed descriptions of the FTIR spectra of plant oils and oil derivatives can be found in the literature[13,27].
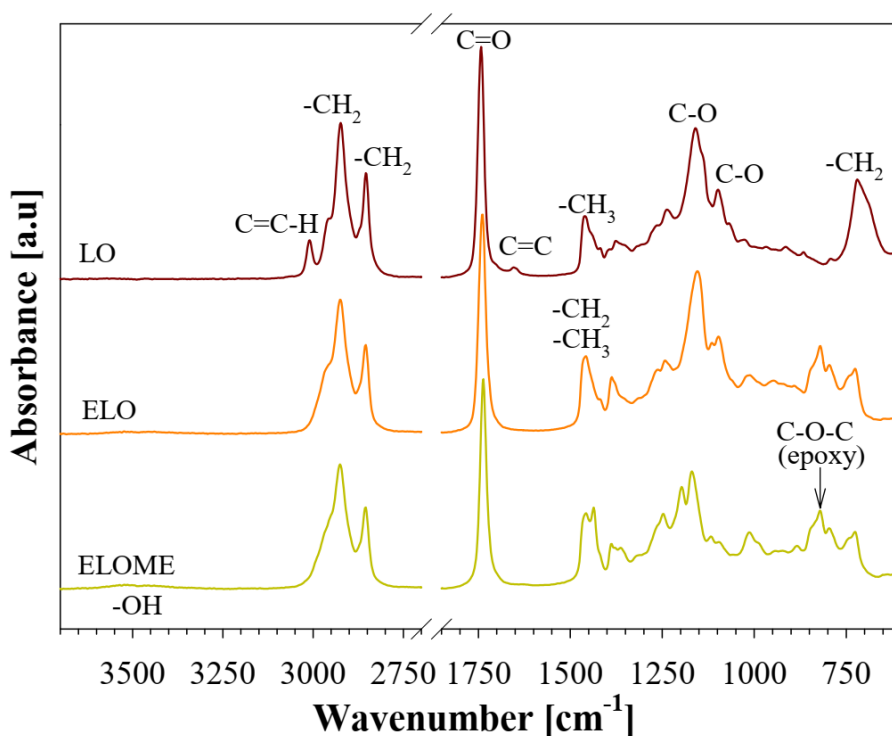
Figure 4.3 ATR-FTIR spectra of LO, ELO and ELOME.

Figure 4.3 shows the linseed oils C=C–H double bonds stretching at 3006 cm^{-1} and C=C vibrations at 1655 cm^{-1}, which disappears in the epoxidized oils derivatives. The transformation of double bonds into epoxy groups is confirmed by the appearance of the new band at 826 cm^{-1}, which corresponds to the C–O–C stretching from the oxirane vibration. There is nearly no change in the oxirane peak in the FTIR spectra of the ELO and ELOME, which indicates the stability of

the epoxy moieties. Small deviation of the baseline between 3100-3650 is due to the hydroxyl group stretching vibration which evidences a negligible loss of oxirane during epoxidation and transesterification processes, to form O–H groups.

Thus, both $_1$H NMR and FTIR spectrum evidences the complete conversion of the unsaturates of the LO into epoxides in ELO spectra, and a successful transformation the ELO in to ELOME upon transesterification with methanol.

Ideally, completely epoxidized LO should produce ELO with an oxirane oxygen content (OOC) of 11%. However, a typical final OOC of ELO is slightly lower at about 9.4%, as shown in Table 4.1.

Product	Density @25 °C [g/cm^3]	Viscosity @25 °C [Pa.s]	MW [g/mol]	OOC* [%]	# Epoxy** 1/mol
LO	0.924	0.051	874	-	-
ELO	1.032	1.076	985	11.1/9.4	6.8/5.8
ELOME	0.994	0.045	330	11.0/9.5	2.3/2.0

*
  OOC values calculated using fatty acid profile and experimentally measured
**
  Number of epoxy groups calculated using fatty acid profile and estimated from the OOC

Table 4.1 Physical-chemical and structural properties of the LO and of its epoxidized derivatives.

Note that while it is possible to increase the OOC beyond this point by extended epoxidation, at the same time some degradation of oxirane may take place, due to epoxy ring reactions (Omonov et al., 2016). Moreover, the small gain in OOC does not usually justify the extra time and energy required.

Hence, here ELO of OOC ~9.4% was used for transesterification to ELOME as described above. The OOC of the resulting ELOME was 9.5 %, with the small increase in OOC likely due to the loss of saturated fatty acid methyl esters (methyl stearate or methyl palmitate) which are solid at room temperature and easily filtered out during the work-up process. Example structures of ELOME resulting from the transesterification reaction are illustrated in ESI (Figure 3.1). These

components - methyl oleate, methyl linoleate and methyl linolenate - are the main constituents of the resulting product.

4.4.2 Comparative analysis of LO and its epoxidized derivatives

The main aim of this study was to produce low viscosity reactive derivatives of LO that could also be used as a diluent for the curing agent used in making biobased thermosets. To this end, it was necessary to compare the physical properties and structures of LO and its epoxidized derivatives. Hence, the densities of the LO, ELO and ELOME were measured according to an ASTM method[36]; their viscosities as a function of temperature were measured using a rheometer; and their molecular weight distributions were determined by GPC (Figure 4.1). Table 4.1 above compares the measured densities, viscosities, calculated average molecular weights for LO, ELO and ELOME and the OOC and epoxy content per moles of epoxidized derivatives of ELO and ELOME.

As can be seen from the Table 4.1, the unsaturated LO has a density of 0.924 g/cm^3 and a low viscosity of 0.051 Pa.s. ELO has a significantly higher density (1.032 g/cm^3), a more than two-fold increase in viscosity (1.076 Pa.s) compared with LO, and an increased average MW due to the addition of oxiranes. Fully epoxidized linseed oil has an OOC of 11% (calculated), which translates into 6.8 epoxy groups per moles of the epoxidized TAG. Transesterification of ELO by methanol leads to a slight decrease in density for the resulting ELOME to 0.994 g/cm^3, along with a large decrease in viscosity to 0.045 Pa.s, which is even lower than the viscosity of the starting LO. Note that the OOC of ELOME remains similar to ELO despite the decrease in molecular weight from 985 g/mol to 330 g/mol (Figure 4.1), since 100 g of either still contains a comparable percentage of oxirane oxygen. The low viscosity of ELOME makes it useful to consider as a

reactive diluent compound for many curing agents, while the number of epoxy groups per mole of ELOME is still sufficient (≥ 2) to grow the polymer chain upon curing.

4.4.3 Biobased thermosets from ELOME and ELOME/ELO mixtures

A series of ELOME based epoxy thermosets at different concentrations of TMA curing agent were prepared. In calculating the required amount of TMA, it was assumed that anhydride ring opening via hydrolysis results in formation of two acid groups (Omonov and Curtis, 2014; Omonov and Curtis, 2016) so that there were effectively 3 acid groups per mole of TMA. In this way, the molar ratio of carboxylic acid groups on TMA to epoxy groups on ELOME (2.3 epoxy groups/mole) was varied from 0.68 to 1.32. Under the experimental conditions used, it was shown that within this range it is possible to dissolve TMA in ELOME without extensive polymerization occurring (see below). In contrast, at higher concentrations of TMA solvation in ELOME and polymer network growth occur simultaneously, so that the curing process initiates before complete solvation of TMA.

In these studies, the selected amounts of ELOME and TMA were loaded into a glass flask with a overhead stirrer, and placed into oil bath at a temperature of at 100 ± 2 °C, mixing at 500 ± 10 RPM. The prepolymers can also be prepared at 60 °C although this then requires 45-60 min (depending on Ac/Ep ratio) to completely dissolve the curing agent, whereas successful dissolution of TMA was achieved within 7-15 min at 100 °C, without polymerization. Mixing of the reactive components continued until the complete disappearance of TMA. Then, the reactive mixture was transferred into preheated (170 °C) Teflon mold (100 x 100 mm^2) and placed in an oven (170 °C) for 4 hours of curing. Five different ELOME based thermoset compositions were prepared by varying the concentration of the TMA curing agent. Two further thermosets were prepared in which 1/3 and 1/2 of the ELOME in the thermoset formulation was replaced by ELO. To prepare

these epoxy networks, first the TMA was dissolved in the ELOME, then subsequently ELO was added to this mixture. In these cases, the molar abundance of epoxy groups was calculated considering both ELOME and ELO; the thermosets were then made such that the molar ratio of acid to epoxide groups (Ac/Ep) was kept constant at 0.68 (Table 4.2). The Ac/Ep ratio of 0.68 was found to be the maximum proportion of TMA can be dissolved in ELOME without extensive polymerization occurring prior to adding ELO. It was hypothesized that due to the TAG structure, the ELO containing networks will exhibit different mechanical performance compared with thermosets made from ELOME alone.

Figure 4.4 illustrates some of the possible curing reaction pathways between epoxidized methyl linoleate and TMA. The curing process starts with the reaction of an acid group from TMA with an epoxy group from ELOME to produce both an ester linkage and a hydroxyl group, as shown in the structure in Figure 4.4 (circled area **A)**. For the sake of clarity, the background network is grayed out, while the examples of the areas of the network under discussion, are circled.
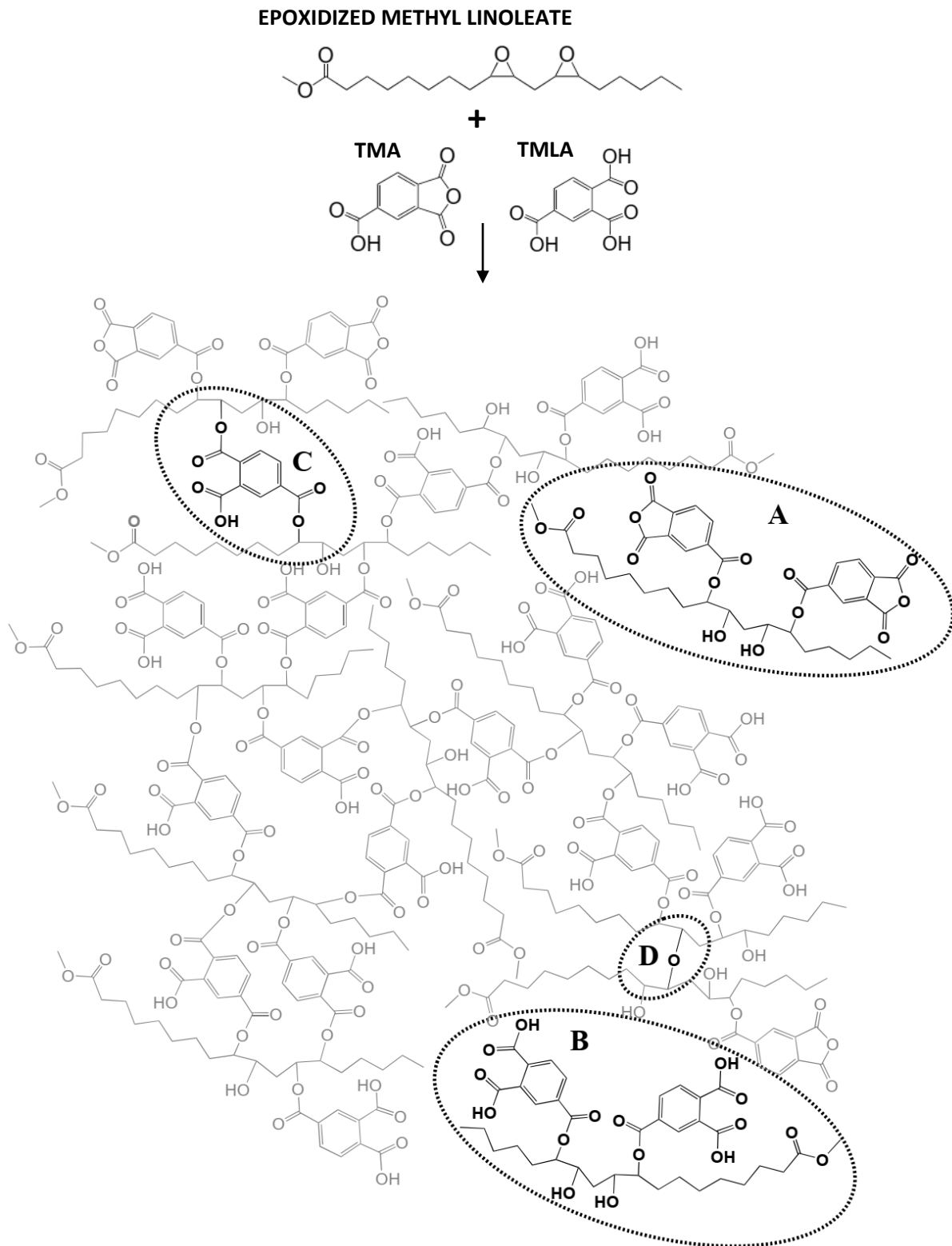
Figure 4.4 ELOME (epoxidized methyl linoleate, as example) curing pathway with TMA (and TMLA) and, the schematic illustration of the resulting epoxy resin network.

It is known that the cyclic anhydride group does not react directly with the epoxy group; the anhydride ring is first opened by a hydroxyl group to form a carboxylic acid, which then reacts with an epoxy groups [35]. Anhydride ring opening may occur either through reaction with residual water present in the epoxide to form trimellitic acid (TMLA), or by reaction with hydroxyl groups formed from epoxide rings-opening reactions. Following TMLA formation, opening of epoxide rings results in the formation of esters, as shown in Figure 4.4 (circled area **B)**. This in turn results in hydroxyl moieties which participate in further anhydride ring opening to produce an additional ester linkage plus a carboxylic acid group that can further participate in polymer chain growth (Figure 4.4, circled area **C**). In addition, epoxide ring opening by hydroxyl moieties can take place, which allows the network to grow via the formation of ether linkages (Figure 4.4, circled area **D**). Thus, thermoset network formation may occur due to the formation of both ester (acid-epoxy and/or hydroxyl-anhydride reactions) and ether (hydroxyl-epoxy reactions) linkages.

Stability (pot-life) of the thermoset. The ability to manufacture low-viscosity, high-biocontent thermosets at relatively low temperatures, without the need for solvents, has some practical implications. Such low-viscosity prepolymers with stable and controllable pot-lives can further be used to impregnate natural, mineral or synthetic fibers to produce biocomposite materials. Obviously, the main indicator of the prepolymer stability is the viscosity, which determines the dispensability of the prepolymer into fibers or fibermats.

As can be seen from Figure 4.1 that the viscosity of the ELOME is 0.05 Pa.s. The viscosity of ELOME mixture with its curing agent increases to 0.83 Pa.s after dissolving/reacting for about 40 min.
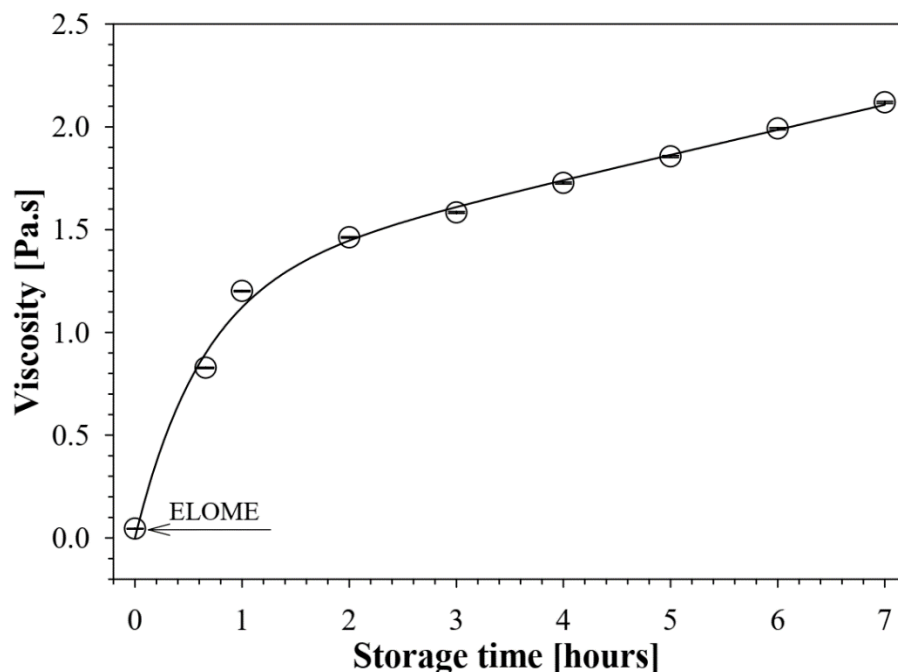
Figure 4.5 The viscosity of the ELOME/TMA based prepolymer over storage period at room temperature. The prepolymer is prepared at 60 °C for 40 min under continuous mixing.

Further storage of this mixture for 7 hours at room temperature increases its viscosity slightly, up to 2.2 Pa.s. However, this viscosity of the mixture is still low enough and is suitable spray impregnation of the solution into fibermats.

The GPC chromatograms (Figure 4.1) show a corresponding increase in the dimeric and trimeric compounds over storage time that accounts for this increase in viscosity. A similar trend can also be seen in the FTIR spectra (Figure 4.3) of the bioresin over the storage period. A small reduction in the absorbance corresponding to the presence of epoxy groups over the storage period was observed (the peak at 826 cm^{-1} corresponding to C–O–C oxirane stretching vibration). There is also an increase in the strong peak at 1238 cm^{-1}, corresponding to a C–O–C ester stretching vibration. This arises since the ester group formation accompanies epoxy ring opening to form oligomeric epoxy network. From the stability of the product, it can be concluded that the

composition with the molar ratio of components giving Ac/Ep =0.68 and a temperature of 60 °C could be used to produce a prepolymers which is suitable for manufacturing biocomposites, having a useful pot life of at least few hours.

4.4.4 Dynamic mechanical analysis

A determination of the thermo-mechanical properties of the thermosets, such as their glass transition temperatures, helps to define the operating temperature range over which the material can be used[37]. DMA test specimens were machined from cured thermosets with approximate dimensions of 35 mm×12 mm×4 mm. The single cantilever-bending mode of DMA was used, with a temperature range from -50 °C to 180 °C, and at a constant frequency of 1 Hz. Figures 4.6 (A) and (B) demonstrate the storage modulus (E') and loss factor (*tan δ*) as a function of temperature, for the ELOME thermoset networks cured with different concentrations of TMA.
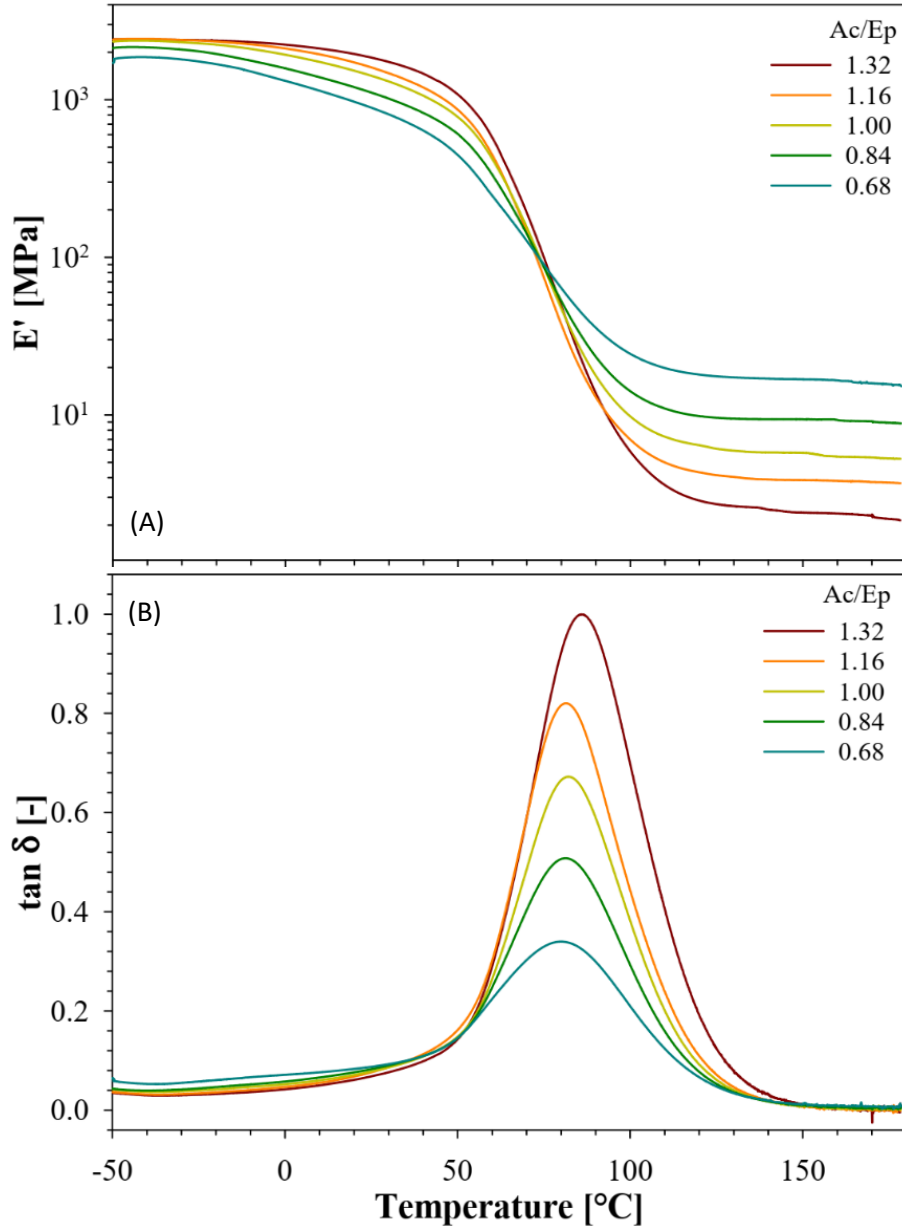
Figure 4.6 Storage modulus, E′, (A) and loss factor, tan δ, (B) for the ELOME based resin cured with different concentration of the TMA. The ratio of the epoxy to acid groups resin components are shown in the inserted legends for the respective curves

It can be seen in Figure 4.6(A) that the trends in the dynamic mechanical behavior of all thermosets are similar, but differences between the behaviors of these samples in the glassy state and rubbery state are apparent. Specifically, in the low temperature region, the network with the

lowest Ac/Ep ratio of 0.68 has the lowest E' (1.8 GPa), most likely due to correspondingly low crosslinking density (Sindt et al., 1996) resulting from insufficient curing agent. In addition, the unbound long aliphatic chains of ELOME have a plasticizing effect in the network (Roudsari et al., 2017), which results in the formation of relatively flexible network. It has been reported [38] that either decreased cross-link density or increased flexibility have a similar effect to decrease the glassy modulus of the polymer.

In the thermoset with an equimolar Ac/Ep ratio, the glassy storage modulus increases up to 2.3 GPa, which indicates the formation of tighter network structure and a stiffer polymer. Only a minimal increase of the glassy storage moduli is observed by further increasing the Ac/Ep ratio up to 1.32 (Figure 4.6(A)). The observation of these fairly consistent values of the glassy storage modulus (2.3-2.4 GPa) with above equimolar Ac/Ep ratios (in the range of 1.0-1.3) suggests that within this range, all ELOME chains are integrated into the thermoset polymer network. In addition to these differences in E', significant changes in the glass transition region of the thermosets are also apparent. In the thermoset compositions with higher Ac/Ep ratios, the samples exhibit an extended glassy state, the glass to rubber transition zone is noticeably narrow, and the transition slope is relatively steeper (Figure 4.6(A)). This can be seen, for example, in the E' values of the thermosets at room temperature (25 °C). At this temperature, the E' value for the network with lowest Ac/Ep ratio of 0.68 is about 0.9 GPa, and this value increases with increasing Ac/Ep ratio up to values of 1.9 GPa for the thermoset prepared at an Ac/Ep ratio of 1.32 (see Figure S4).

Based on the trend of the E' observed on the glassy state of the thermosets we could expect similar behavior in the rubbery state. However, in the rubbery plateau region the storage modulus demonstrates invert tendency and the samples with the lower Ac/Ep ratio that exhibit the highest value of E'. This indicates to the two concurrent reaction, TMA ester formation (circled area A and

B) and integration of the formed TMA (or TMLA) ester into the thermoset network (circled are C and D) that occurs during the thermoset preparation, as shown in the Scheme 1. This is explained in detail below with the temperature dependence of the loss factor for the all resin f studied. The intensities of the loss factor (*tan δ)* peaks in Figure 4.5(B) reflect the degree of mobility of polymer chain segments in cured ELOME thermosets made using various Ac/Ep ratios, at this temperature. Figure 4.5(B) shows that the *tan δ* peak intensity increases with the Ac/Ep ratio. This indicates that the network demonstrates enhanced viscous behavior at higher Ac/Ep ratios, as the energy dissipated by the network become larger. In contrast, one might expect reduced *tan δ* peak intensities with increasing Ac/Ep ratios due to increased crosslinking densities that restrict segmental mobility of polymer chains in the network (Perera, 2001). This unusual increase in the *tan δ* peak intensity with increasing Ac/Ep ratios could be explained by the excess of curing agent used, which forms high amounts of monomeric TMA (or TMLA) esterified fatty acids (see isolated structures **A** and **B** in Figure 4.4). At a high Ac/Ep ratio, not all of the TMA esterified fatty acids are incorporated into the polymer network, and these unbound compounds demonstrate their mobility within the network. This is also consistent with the width of the glass transition region of *tan δ*, which is seen to be much broader for the thermoset prepared with an Ac/Ep ratio of 1.32 (Figure 4.5(B)), indicating greater structural heterogeneity (Menard, 2008). On the other hand, in another elastomeric polymer system it was reported [39] that an increase in the crosslink density resulted in a broadening of the *tan δ* peak caused by more densely located structures on the chains arising from reaction with the curative and dependent on its structure. In addition, these authors proposed an increased number and size of "heterogenic microregions", that relaxed over a broader range of temperatures.

It can be concluded that the increased structural inhomogeneities of the networks that occur in thermosets made when the Ac/Ep ratio is increased are related to the both the high molecular weight heterogenic local areas that are the result of the higher curing agent concentration, and an excess of monomeric esterified components in the system, and which are not integrated to the polymer network.

Nonetheless, it was expected that a rise in the Ac/Ep ratio should increase the crosslinking density, at least up to the expected stoichiometric ratio. This would be reflected in increased glass transition temperatures[40]. The glass transition temperatures, T_g, of the biobased thermosets were determined from the respective peaks of the dynamic transition temperature of *tan δ* (Figure 4.5(B)). The T_g of the thermoset with the lowest Ac/Ep ratio (0.68) is 79.8 °C and T_g values were found to slightly increase up to 85.9 °C for the network with highest Ac/Ep ratio (see Table 2).

ELOME/ELO PROPERTIES	100/0	100/0	100/0	100/0	100/0	66/34	50/50
Ac/Ep ratio [-]	0.68	0.84	1.00	1.16	1.32	0.68	0.68
ρ_{exp} [g/cm^3]	1.148	1.162	1.168	1.181	1.182	1.140	1.144
E' @25 °C [MPa]	887	1107	1416	1599	1848	1144	1359
E' @T_g+50°C [MPa]	17.3	9.4	5.9	4.0	2.6	38.6	66.6
T_g [°C, DMA]	79.8	81.4	82.2	82.6	85.9	96.2	101.7
v_e ($\times$ 10^{-3}) [mol/cm^3]	0.52	0.28	0.17	0.12	0.08	1.11	1.89
M_c ($\times$ 10^3) [g/mol]	2.22	4.14	6.70	10.01	15.52	1.03	0.61
10% weight loss [°C, TGA]	304	300	287	282	264	309	319
T_{onset} [°C, TGA]	320	313	304	300	291	315	320

Table 4.2 Properties of bioresins prepared from EMOME/ELO mixtures

Thus, there are two simultaneous processes which vary with the Ac/Ep ratio and which determine the mechanical performance of the thermosets: enhanced crosslinking which increases the T_g, and suppression of the polymer network formation due to the excess formation of TMA

esters, which consume epoxy moieties. The crosslinking densities of the networks are further discussed in Section 3.5.

The above discussion refers to thermoset networks made using only epoxides in the methyl ester form (ELOME). In order to test the possibility that better mechanical performance of the network could be achieved by incorporating the intact triacylglycerol structure of ELO, in a series of experiments, 34% and 50% of the ELOME was replaced by ELO whilst keeping the Ac/Ep ratio of the reactive components constant at 0.68. DMA plots, such temperature dependence of E' and $tan\ \delta$, of the networks prepared with the mixtures of ELOME and ELO are shown in Figures 4.6(A) and 4.6(B).
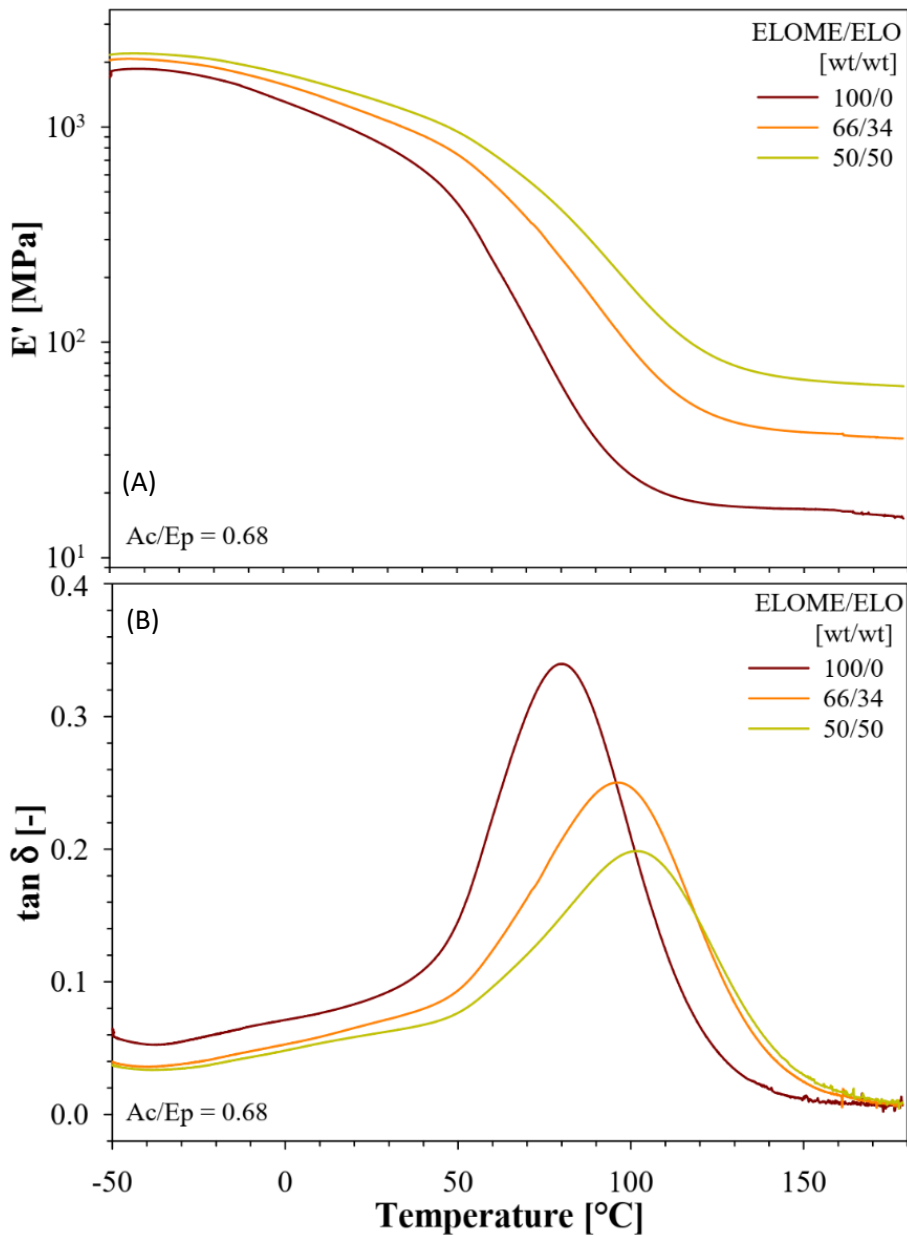
Figure 4.7 Storage modulus, E', (A) and loss factor, tan δ, (B) for the resins made at different ratios of ELOME and ELO. Ac/Ep ratio is 0.68 in all resin systems. ELOME/ELO ratios are shown in the inserted legends for the respective curves.

Whilst the trends in E' plots for all network compositions are similar, replacing a portion of ELOME with ELO results in a proportional increase in E' values. For example, the E' for the ELOME network at Ac/Ep ratio of 0.68 is about 0.9 GPa at 25 °C, but this increases to 1.4 GPa for the thermoset where 50% of the ELOME replaced by ELO, consistent with the triacylglycerol

structure of ELO contributing to the crosslinking density of the network. This is expected because in ELO the 3 epoxidized fatty acids already have junction points (ester linkages to glycerol) prior to curing, which increases the probability that all epoxides become be part of polymer network on curing. In contrast, the small amount of saturated FAME (5% methyl palmitate and 3% methyl stearate) in ELOME can dissolve TMA but will never become part of thermoset network, since they lack the reactive groups necessary to participate in the curing reaction. However, all of the saturated fatty acids present in ELO are already incorporated into the triacylglycerol structure, and hence still become part of the crosslinked structure and contribute to the performance of the thermoset. It is interesting to note that the crosslinking densities of the thermosets made from ELOME/ELO mixtures noticeably differ from the ones that are prepared from pure ELOME, as discussed in Section 3.5.

Figure 4.7(B) shows the *tan δ* as a function of temperature for the ELOME/ELO based thermosets at different ratios of components. Clearly, the intensity of the *tan δ* peak decreases with increasing ELO content, due to the higher crosslinking densities which restrict the segmental mobility of polymer network. The observed glass transition temperature of the thermosets increased from 79.8 °C for 100% ELOFAME (Table 4.2) to 96.2 °C and 101.7 °C when 34% and 50% of the ELOFAME was replaced by ELO. The estimation of T_g values by modulated DSC measurements also demonstrated a similar trend (see Figure 4.5).

4.4.5 Cross-linking density of epoxy networks

The crosslinking density, v_e, is a well described concept in the literature that has been calculated using the modulus at the rubbery plateau of polymer networks[41,42]. By making the simplifying assumptions that all functional groups are equally reactive and that no intramolecular reactions occur[43]; that the resins have an ideal network [44] and all chains are elastically

131

effective; and that the storage modulus is not dependent on the frequency at rubbery plateau[41,45]; the values of v_e can then be calculated using the equation: $v_e = E'/RT$. In this equation, the E' value is obtained from the rubbery plateau of the storage modulus; T is temperature corresponding to the E' value (in °K) and R is the gas constant. In addition, an estimation of the degree of "tightness" of a polymer network can be obtained [41] from the "average molecular weight of the effective network chains" using the following equation: $M_c = \rho/v_e$, where M_c [g/mol] is weight of sample in grams that contains one mole of elastically effective chains and ρ is the bulk density of material.

Using these concepts, crosslinking densities for the various biobased thermosets were estimated using E' values from the rubbery plateau (50 °C above T_g) resulting in the values for v_e and M_c that are given in Table 4.2. It was observed that the v_e value for the cured thermoset made using an Ac/Ep ratio of 0.68 is 0.52×10^{-3} mol/cm³. Increases to the Ac/Ep ratio resulted in a decrease in v_e such that with an Ac/Ep ratio of 1.32, the v_e value is only 0.08×10^{-3} mol/cm³. The decrease in v_e and corresponding increase in M_c with increasing Ac/Ep ratio (Table 2), is believed to be a result of the increasing concentration of TMA esters that are not incorporated into the polymer network, and which oppose an increase in v_e. An illustration of the cured ELOME/TMA epoxy network is shown in Figure 4.5, using an epoxidized methyl linoleate as an example. As described above, the reaction of the TMA (or/and TMLA) with ELOME starts with the esterification reaction as shown in the Figure 4.5 (circles **A** and **B)** and each carboxylic acid group consumes one epoxy moiety. The esters so formed then react with remaining epoxy groups to allow the polymer chain growth, until all of the epoxy groups of ELOME is consumed. At high concentrations of TMA (Ac/Ep>1.00), the esterification process consumes a significant portion of

the available epoxy moieties, and fewer reactive groups might be available to grow the polymer chain. In addition, any excess amounts of TMA esters will not be integrated into the polymer network but rather will create the defects and free volumes that allow for chain mobility (**A** and **B** in Scheme 1). It should be mentioned that there is not a significant amount of unreacted TMA left in the cured network, as confirmed by DSC measurements which did not show any melting points (at 166 °C) which belong to pure TMA. Hence, any contribution of unreacted TMA to the crosslinking behavior is negligible.

Thus, it can be concluded that an increase in the Ac/Ep ratio (and consequently the TMA content) in the thermosets slightly increases their crosslinking density, as demonstrated indirectly by increased E' and T_g values. However, the calculations of v_e suggest that crosslinking density was inhibited by an excess formation of TMA esters that in turn reduces the availability of epoxy groups for polymer chain growth. Partly as a result of this heterogeneity in the epoxy network, *i.e.* the separation of polymer and unreacted ester monomers, a basic assumption used in estimating v_e from an *ideal network*, does not apply.

In contrast, the estimated v_e values of the ELOME/ELO epoxy networks with a fixed Ac/Ep ratio of 0.68 increased with their increasing ELO content (Table 4.2). This increase in v_e values, and the consequent decrease in M_c values, could be explained by the increased number of junction points and enhanced physical entanglement of the polymer chains in the network[41], which incorporates the triacylglycerol structure of ELO.

4.4.6   Thermogravimetric analysis (TGA)

In TGA analysis, is expected that unreacted or unbound components, if present, should demonstrate individual decomposition transitions over the experiment. Here, TGA experiments were carried out on 10 mg samples in a ceramic crucible, at a constant heating rate of 10 °C/min

from 25 °C to 600 °C, and under a flow of nitrogen. TGA thermograms (weight loss as a function of temperature) for the ELOME based epoxy network made using a range of Ac/Ep ratios are shown in Figure 4.8(A), and those for the cured thermoset systems prepared using different ELOME/ELO ratios but a fixed Ac/Ep ratio are shown in Figure 4.8(B).
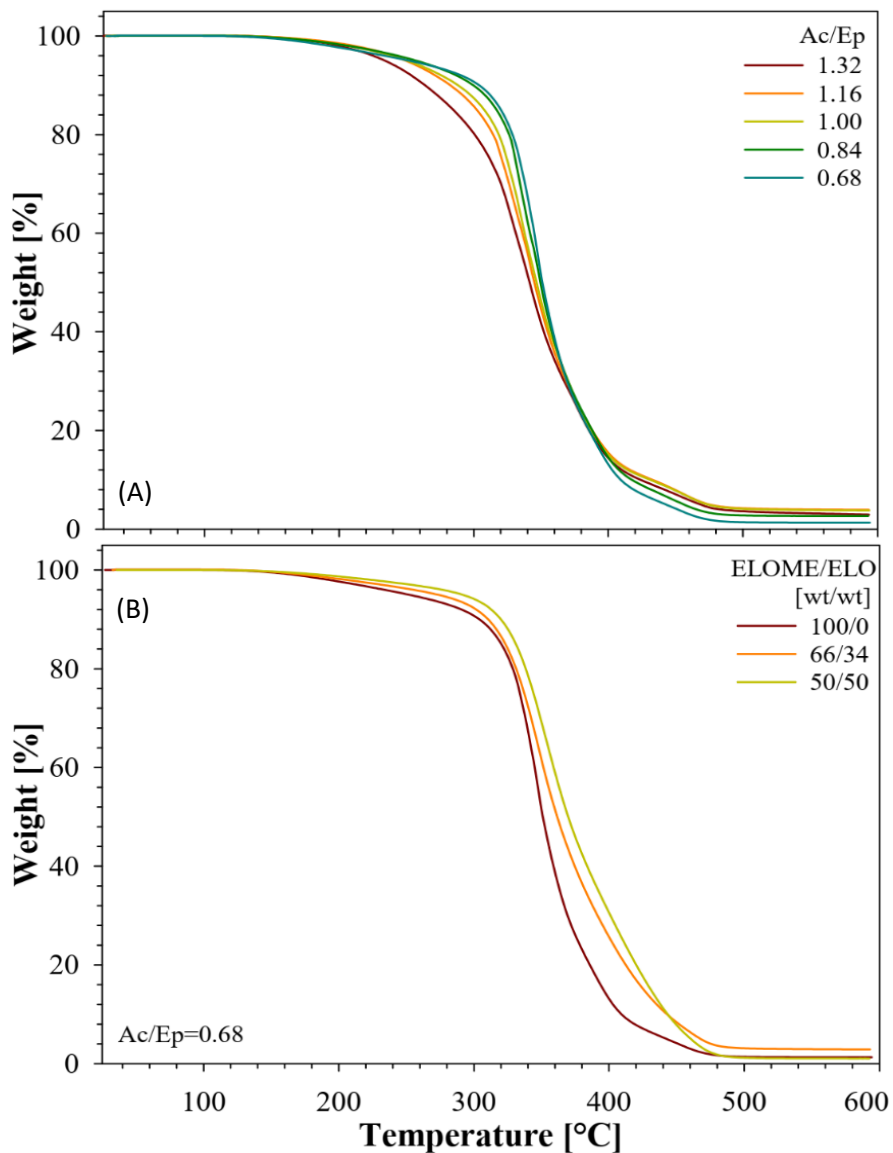
Figure 4.8 TGA thermograms (weight loss as a function of temperature) for the ELOME resin systems cured at different Ac/Ep ratio (A) and for the resins made at different ELOME/ELO ratios cured with the fixed amount of Ac/Ep=0.68 (B).

All thermosets demonstrate similar single-step decompositions that is consistent with a relatively uniform network structure, despite the presence of some inhomogeneities, as discussed earlier. The initial decomposition temperatures of the thermosets (defined as the temperature for 10% weight loss) are given in the Table 4.2. These decrease with increasing Ac/Ep ratio, so the epoxy network produced using Ac/Ep =0.68 shows higher thermal stability with 10% weight loss occurring at 304 °C, compared with 264 °C for the network with Ac/Ep=1.32 (Figure 4.8(A), Table 2). Thus, there is a greater proportion of compounds with low decomposition temperatures, in the thermoset with higher TMA content. The decomposition of the major part of the network occurs between 300 °C and 480 °C, which is typical for plant oil epoxide based thermosets. For example, the decomposition range for soybean oil based epoxy thermosets was reported to be between 300-420 °C [46] while fish oil [47] or tung oil [48] based thermoset networks show higher temperature decomposition ranges of 400-560 °C. In the latter cases, the higher decomposition temperatures are related to the epoxy content of the monomers in the thermoset formulation. The temperatures for the onset of the main network decomposition, T_{onset}, are listed in the Table 2, and also show a decreasing trend with increasing Ac/Ep ratios in the thermosets. This indicates that at low Ac/Ep ratio the majority of the TMA esters are integrated into the network, while the amount of unbound compounds rises with increasing the Ac/Ep ratio. Note that the values of T_{onset} for the neat ELOME, TMA and ELO are 217 °C, 231°C and 380 °C respectively, as measured by TGA (Figure 4.8). This data is consistent with the trend of a decrease in the calculated values of the crosslinking density with an increase of the Ac/Ep ratio (TMA content). At the same time, the contrasting enhancement in the crosslinking density that was suggested by the DMA results most likely occurs due to the formation of highly crosslinked local domains, whereas its extrapolation to the whole network is constrained by the negative influence of the excessive TMA esters.

The ELOME/ELO epoxy network demonstrate higher thermal stability compared with ELOME based network formulations, and this varies with the ELO content (Figure 4.8(B), Table 4.2). The relatively high decomposition temperatures (at 10% weight loss) for these systems are most likely related to the higher decomposition temperatures of ELO, as well as to the enhanced crosslinking densities within such networks, as discussed earlier. Note that the temperatures for 10% weight loss measured for neat ELOME, TMA and ELO are 200 °C, 211°C and 374 °C, respectively (Figure 4.8).

4.5 Conclusion

In this work, an ELOME preparation procedure giving a high epoxy content has been described. ELOME was then used in studies of the curing behavior of ELOME and ELOME/ELO mixtures with an aromatic curing agent to produce a thermoset material.   These thermosets contain high percentages of LO and hence have a high biocontent. Unlike ELO, ELOME acts more like a solvent to efficiently dissolve a curing agent such as TMA, at a moderate temperature. It was demonstrated that an increase in the curing agent concentration (Ac/Ep) results in an increase in the storage modulus and the glass transition temperature of the resulting thermoset materials. This was attributed to the formation of highly crosslinked local domains within the network. However, the calculations of the crosslinking densities using DMA results showed a decrease in v_e values upon increasing the Ac/Ep ratio. This was interpreted as being due to the resulting restraints to crosslinked network formation due to an excessive amount of TMA ester formation. These also consume epoxy moieties, hence reducing their availability further polymer chain growth.

In thermoset systems prepared with ELOME/ELO mixtures, an improvement to the thermomechanical properties was observed. The increase in v_e values, consequently decreased M_c values for these series of samples was explained by the increased junction points and enhanced

physical entanglement of the polymer chains in the network, originating from the branched structure of ELO.

The ability to manufacture high-biocontent thermosets, without the need for solvents, has some practical implications. Specifically, the method allows the production of low-viscosity, solvent-free epoxy prepolymers at relatively low temperatures, that can further be used to impregnate fibers to produce biocomposite materials. These prepolymers can achieve pot lives which are practical for industrial use. As an example, a solvent-free ELOME based prepolymer prepared at 60 °C was still useable with a viscosity of ~2 Pa.s after 6 hours of storage at room temperature (see Figure 4). Furthermore, there is considerable scope for optimization of conditions and curing agents, which will likely result in further improvements.

4.6 **References**

[1] Belgacem, M.N., & Gandini, A., 2008. Monomers, Polymers and Composites from Renewable Resources, Elsevier: Oxford, UK. https://doi.org/10.1016/B978-0-08-045316-3.X0001-4.

[2] Smith, P.B., & Gross, R.A., 2012. Biobased Monomers, Polymers, and Materials, American Chemical Society: Washington, USA. https://doi.org/10.1021/bk-2012-1105.

[3] Thakur, V.K., Thakur, M.K., & Kessler, M.R., 2017. Soy-based Bioplastics, Smithers Rapra: Shawbury, UK.

[4] Kabasci, S., 2014. Bio-based plastics. Materials and Applications, John Wiley & Sons: Chichester, UK. https://doi.org/10.1002/9781118676646.

[5] Mohanty, A.K., Misra, M., & Drzal, L.T., 2005. Natural Fibers, Biopolymers, and Biocomposites, CRC Press Boca Raton. USA. https://doi.org/10.1201/9780203508206.

[6] Madbouly, S., Zhang, C., & Kessler, M.R., 2016. Bio-Based Plant Oil Polymers and Composites, Elsevier: Oxford, UK. https://doi.org/10.1016/C2014-0-02157-0.

[7] Honary, L.A.T., & Richter, E., 2011. Biobased Lubricants and Greases. Technology and Products, John Wiley & Sons: Chichester, UK. https://doi.org/10.1002/9780470971956.

[8] Hayes, D.G., Kitamoto, D., Solaiman, D.K.Y., & Ashby, R.D., 2009. Biobased Surfactants and Detergents. Synthesis, Properties, and Applications, AOCS Press: Urbana, USA.

[9] Wool, R., & Sun, X.S., 2005. Bio-Based Polymers and Composites, Elsevier: Burlington, USA. https://doi.org/10.1016/B978-0-12-763952-9.X5000-X.

[10] Ray, D., 2017. Biocomposites for High-Performance Applications. Current Barriers and Future Needs Towards Industrial Development, Woodhead Publishing: Duxford, UK. https://doi.org/10.1016/C2015-0-04020-5.

[11] Smitthipong, W., Chollakup, R., & Nardin, M., 2014. Bio-Based Composites for High-Performance Materials: From Strategy to Industrial Application, CRC Press: Boca Raton, USA. https://doi.org/10.1201/b17601.

[12] Snyder, S.W., 2016. Commercializing Biobased Products. Opportunities, Challenges, Benefits, and Risks, Royal Society of Chemistry: Cambridge, UK. https://doi.org/10.1039/9781782622444.

[13] Omonov, T.S., & Curtis, J.M., 2016. Plant Oil-Based Epoxy Intermediates for Polymers, in: Madbouly, S.A., Zhang, C. & Kessler, M.R. (Eds.), Bio-Based Plant Oil Polymers and

Composites, Elsevier: Oxford, UK, pp. 99-125. https://doi.org/10.1016/B978-0-323-35833-0.00007-4.

[14] Huang, X.J., Yang, X.X., Liu, H., Shang, S.B., Cai, Z.S., & Wu, K., 2019. Bio-based thermosetting epoxy foams from epoxidized soybean oil and rosin with enhanced properties, Ind Crop Prod, 139: 111540. https://doi.org/10.1016/j.indcrop.2019.111540.

[15] Khundamri, N., Aouf, C., Fulcrand, H., Dubreucq, E., & Tanrattanakul, V., 2019. Bio-based flexible epoxy foam synthesized from epoxidized soybean oil and epoxidized mangosteen tannin, Ind Crop Prod, 128: 556-565. https://doi.org/10.1016/j.indcrop.2018.11.062.

[16] Li, Y., Luo, X., & Hu, S., 2015. Bio-based Polyols and Polyurethanes, Springer: London, UK. https://doi.org/10.1007/978-3-319-21539-6.

[17] Borugadda, V.B., & Goud, V.V., 2019. Hydroxylation and hexanoylation of epoxidized waste cooking oil and epoxidized waste cooking oil methyl esters: Process optimization and physico-chemical characterization, Ind Crop Prod, 133: 151-159. https://doi.org/10.1016/j.indcrop.2019.01.069.

[18] Kirpluks, M., Kalnbunde, D., Benes, H., & Cabulis, U., 2018. Natural oil based highly functional polyols as feedstock for rigid polyurethane foam thermal insulation, Ind Crop Prod, 122: 627-636. https://doi.org/10.1016/j.indcrop.2018.06.040.

[19] Liang, B., Zhao, J., Li, G., Huang, Y.K., Yang, Z.H., & Yuan, T., 2019. Facile synthesis and characterization of novel multi-functional bio-based acrylate prepolymers derived from tung oil and its application in UV-curable coatings, Ind Crop Prod, 138: 111585. https://doi.org/10.1016/j.indcrop.2019.111585.

[20] Lee, C.S., Ooi, T.L., Chuah, C.H., & Ahmad, S., 2007. Synthesis of palm oil-based diethanolamides, J Am Oil Chem Soc, 84: 945-952. https://doi.org/10.1007/s11746-007-1123-8.

[21] Omonov, T.S., Kharraz, E., & Curtis, J.M., 2016. The epoxidation of canola oil and its derivatives, RSC Adv, 6: 92874-92886. https://doi.org/10.1039/c6ra17732h.

[22] Kim, J.R., & Sharma, S., 2012. The development and comparison of bio-thermoset plastics from epoxidized plant oils, Ind Crop Prod, 36: 485-499. https://doi.org/10.1016/j.indcrop.2011.10.036.

[23] Wang, R., & Schuman, T.P., 2013. Vegetable oil-derived epoxy monomers and polymer blends: A comparative study with review, Express Polym Lett, 7: 272-292. https://doi.org/10.3144/expresspolymlett.2013.25.

[24] Espinoza-Perez, J.D., Nerenz, B.A., Haagenson, D.M., Chen, Z.G., Ulven, C.A., & Wiesenborn, D.P., 2011. Comparison of Curing Agents for Epoxidized Vegetable Oils Applied to Composites, Polym Composite, 32: 1806-1816. https://doi.org/10.1002/pc.21213.

[25] Dotan, A., 2014. Biobased Thermosets, in: Dodiuk, H. & Goodman, S. (Eds.), Handbook of Thermoset Plastics, Elsevier: Amsterdam, pp. 577-622. https://doi.org/10.1016/B978-1-4557-3107-7.00015-4.

[26] Omonov, T.S., Patel, V.R., & Curtis, J.M., 2018. "Epoxidized Hemp Oil: Synthesis, Cure Kinetics and Properties of Polymers." In *15th International Symposium on Bioplastics, Biocomposites and Biorefining*. Guelph, ON, Canada

[27] Curtis, J.M., Omonov, T.S., Kharraz, E., Kong, X., & Tavassoli-Kafrani, M.H., 2019. Method for Polyol Synthesis from Triacylglyceride Oils, U.S. Patent 10,189,761 B2.

[28] Holser, R.A., 2008. Transesterification of epoxidized soybean oil to prepare epoxy methyl esters, Ind Crop Prod, 27: 130-132. https://doi.org/10.1016/j.indcrop.2007.06.001.

[29] ASTM D1652-11. (Reapproved 2019). Standard Test Method for Epoxy Content of Epoxy Resins. https://doi.org/10.1520/D1652-11R19.

[30] Omonov, T.S., Kharraz, E., & Curtis, J.M., 2017. Camelina (Camelina Sativa) oil polyols as an alternative to Castor oil, Ind Crop Prod, 107: 378-385. https://doi.org/10.1016/j.indcrop.2017.05.041.

[31] Omonov, T.S., & Curtis, J.M., 2014. Biobased Epoxy Resin from Canola Oil, J Appl Polym Sci, 131: 40142. https://doi.org/10.1002/app.40142.

[32] Pascault, J.-P., & Williams, R.J.J., 2010. Epoxy Polymers: New Materials and Innovations, Wiley-VCH: Germany. https://doi.org/10.1002/9783527628704.

[33] Di Pietro, M.E., Mannu, A., & Mele, A., 2020. NMR Determination of Free Fatty Acids in Vegetable Oils, Processes, 8: 410-425. https://doi.org/10.3390/pr8040410.

[34] Moawia, R.M., Nasef, M.M., Mohamed, N.H., Ripin, A., & Farag, H., 2019. Production of Biodiesel from Cottonseed Oil over Aminated Flax Fibres Catalyst: Kinetic and Thermodynamic Behaviour and Biodiesel Properties, Advances in Chemical Engineering and Science, 9: 281-298. https://doi.org/10.4236/aces.2019.94021.

[35] Steinmann, B., 1989. Investigations on the Curing of Epoxy-Resins with Hexahydrophthalic Anhydride, J Appl Polym Sci, 37: 1753-1776. https://doi.org/10.1002/app.1989.070370702.

[36] ASTM D1475-13. Standard Test Method for Density of Liquid Coatings, Inks, and Related Products. https://doi.org/10.1520/D1475-13.

[37] Menard, K.P., & Menard, N.R., 2014. Dynamic Mechanical Analysis in the Analysis of Polymers and Rubbers, in: Mark, H.F. (Ed.), Encyclopedia of Polymer Science and Technology, John Wiley & Sons: USA, pp. 12344 https://doi.org/10.1002/0471440264.pst102.pub2.

[38] Sindt, O., Perez, J., & Gerard, J.F., 1996. Molecular architecture mechanical behaviour relationships in epoxy networks, Polymer, 37: 2989-2997. https://doi.org/10.1016/0032-3861(96)89396-7.

[39] Bandzierz, K., Reuvekamp, L., Dryzek, J., Dierkes, W., Blume, A., & Bielinski, D., 2016. Influence of Network Structure on Glass Transition Temperature of Elastomers, Materials, 9: 607. https://doi.org/10.3390/ma9070607.

[40] McKenna, G.B., 1989. Glass Formation and Glassy Behavior, in: Allen, G. & Bevington, J.C. (Eds.), Comprehensive Polymer Science and Supplements, Pergamon Press: UK, pp. 311-362. https://doi.org/10.1016/B978-0-08-096701-1.00047-1.

[41] Hill, L.W., 1997. Calculation of crosslink density in short chain networks, Prog Org Coat, 31: 235-243. https://doi.org/10.1016/S0300-9440(97)00081-7.

[42] Shaw, M.T., & MacKnight, W.J., 2005. Introduction to Polymer Viscoelasticity, John Wiley & Sons: New Jersey. https://doi.org/10.1002/0471741833.

[43] Miller, D.R., & Macosko, C.W., 1988. Network Parameters for Crosslinking of Chains with Length and Site Distribution, J Polym Sci Pol Phys, 26: 1-54. https://doi.org/10.1002/polb.1988.090260101.

[44] Hild, G., 1998. Model networks based on 'endlinking' processes: Synthesis, structure and properties, Prog Polym Sci, 23: 1019-1149. https://doi.org/10.1016/S0079-6700(97)00055-5.

[45] Hill, L.W., 2012. Dynamic Mechanical and Tensile Properties, in: Koleske, J.V. (Ed.), Paint and Coating Testing Manual, ASTM International, pp. 624. https://doi.org/10.1520/MNL12229M.

[46] Gerbase, A.E., Petzhold, C.L., & Costa, A.P.O., 2002. Dynamic mechanical and thermal behavior of epoxy resins based on soybean oil, J Am Oil Chem Soc, 79: 797-802. https://doi.org/10.1007/s11746-002-0561-z.

[47] Li, F., Marks, D.W., Larock, R.C., & Otaigbe, J.U., 2000. Fish oil thermosetting polymers: synthesis, structure, properties and their relationships, Polymer, 41: 7925-7939. https://doi.org/10.1016/S0032-3861(00)00030-6.

[48] Li, F.K., & Larock, R.C., 2000. Thermosetting polymers from cationic copolymerization of tung oil: Synthesis and characterization, J Appl Polym Sci, 78: 1044-1056. https://doi.org/10.1002/1097-4628(20001031)78:5<1044::Aid-App130>3.0.Co;2-A.

[49] ASTM E1640-18. Standard Test Method for Assignment of the Glass Transition Temperature by Dynamic Mechanical Analysis. https://doi.org/10.1520/E1640-18.

[50] Menard, K.P., 2008. Dynamic Mechanical Analysis: A Practical Introduction, CRC Press: Boca Raton, FL. https://doi.org/10.1201/9781420053135.

[51] Omonov, T.S., Patel, V., & Curtis, J.M., 2019. The Development of Epoxidized Hemp Oil Prepolymers for the Preparation of Thermoset Networks, J Am Oil Chem Soc, 96: 1389-1403. https://doi.org/10.1002/aocs.12290.

[52] Perera, M.C.S., 2001. Development of formulations based on acrylate monomers for optical cable applications, J Appl Polym Sci, 82: 3001-3012. https://doi.org/10.1002/app.2155.abs.

[53] Rashid, U., & Anwar, F., 2008. Production of biodiesel through base-catalyzed transesterification of safflower oil using an optimized protocol, Energ Fuel, 22: 1306-1312. https://doi.org/10.1021/ef700548s.

[54] Roudsari, G.M., Misra, M., & Mohanty, A.K., 2017. A study of mechanical properties of biobased epoxy network: Effect of addition of epoxidized soybean oil and poly(furfuryl alcohol), J Appl Polym Sci, 134: 44352. https://doi.org/10.1002/app.44352.

[55] Zheng, S., Patel, P.G., Vedage, G.A., Tijsma, E.J., & Lal, G.S., 2018. Epoxy liquid curing agent compositions, U.S. Patent US 9,862,798 B2.

Chapter 5

Novel biobased curing agents for plant oil epoxides: Synthesis of alkyl citrates via solvent- and catalyst-free esterification of citric acid with the short to medium chain length alcohols

5.1 Introduction

Epoxy monomers are vital building blocks for making thermoset polymers, which are derived mainly from petroleum-based feedstocks. For instance, diglycidyl ether of bisphenol A (DGEBA) is a widely used epoxy monomer. However, there are also some natural or biobased feedstocks available to be converted into biobased epoxy monomers, for instance plant oils and cashew nut shell liquid (CNSL) which is composed of phenolic compounds with a fatty acid chain, cardanol, cardol, anacardic acid and 6-methyl cardol. The double bonds of the plant oils are converted into epoxy group via epoxidation reaction [1,2]. The detail description about the types of plant oils, their functionality, and other chemical characteristics described in the section 1.2. They are unique compared to other natural feedstocks in terms of their composition as they are more than 99% triacylglycerides (TAG). However, the types of fatty acids and their positions within TAG structures are diverse. One of the focuses of this research is functionalizing the double bonds of the fatty acids (-C=C-) into epoxy groups (-C-O-C-).[5]

---

[5] A version of this chapter has been submitted as a patent, "Jonathan M. Curtis, Vinay Patel, US provisional patent application serial no. 63/075,940, Biobased hardener for epoxy resins."

A discussion of the process parameters for the epoxidation and the reaction mechanism is given in the Section 1.2.1.

The reason for forming -C-O-C- epoxy rings is because of their enhanced reactivity. The ideal tetrahedral geometry has bond angle of 109.5° but oxirane (-C-O-C-) has a bond angle of 60° which make them less stable or strained due to the bond angle. Hence, they are susceptible to be opened by nucleophiles by accepting an electron pair to form a hydroxyl group, as depicted in Section 1.3. In order to form a crosslinked polymer network via epoxy ring opening reactions, multifunctional nucleophiles or crosslinking/curing agents are required [2]. The strained epoxy ring can be protonated by suitable active hydrogen, oxygen or nitrogen containing groups like carboxylic acid (-COOH), amine (-NH$_2$), anhydride (-CO-O-CO-) and others [3] (Section 1.3). One of the important properties of such curing agents is their miscibility in epoxy monomers. Since plant oils are hydrophobic, most of these curing agents are not miscible with plant oil epoxide, which leads resin formulators to the use of polar aprotic solvents like acetone. These facilitate the preparation of one phase epoxide-curing agent mixtures [4,5]. Any toxicity of the curing agent is also an important factor because it not only makes the bioresin synthesis process unattractive but also poses a threat to the final consumers [6] if any level of these toxic compounds leach from the product into human contact, for instance plastic toys prepared from bisphenol A (BPA) resin.

In this work, a solvent-free synthetic route for making bioresins has been explored. Citric acid is a fully biobased, multifunctional, and nontoxic compound, so it was used in this study. It is also available in abundant quantity as their synthesis route is very well explored at a commercial scale [8]. According to the BCC research, a market research organization, about 2.39 million tons of citric acid produced in 2020 globally and it was sold for about $1.5 per kilogram [10]. There are other food grade carboxylic acids available, as depicted in Table 1.5, but their price, availabilities

and lower functionality make them less attractive to be use as curing agent as citric acid has functionality of 3 while these carboxylic acids have only functionality of 2. Despite citric acid's unique features, it is not suitable to be used with the plant oil epoxides because it is immiscible with them. That is why, it was hypothesized that if citric acid's polarity was modified by incorporating short to medium carbon hydrocarbons which would make it less polar, then such derivatives could be miscible with the plant oil epoxides. Such hydrocarbon chains can be introduced through the esterification reaction between carboxylic acid group of citric acid and an alcohol. For a substance or mixture to be used as the multifunctional curing agent, it must have at least two functional groups so that it can incorporate two epoxy groups and the polymerization reaction grows to form polymer network. Since, citric acid contains three carboxylic acid groups, monoesterification is required to preserve two carboxylic acid groups. There have been multiple studies on citric acid esterification, although most of them are focused on forming trialkyl citrates [11,12,13,14]. Formation of trialkyl citrate with higher yield is difficult so these studies explored strategies to maximize the yield of trialkyl citrate while minimizing inputs. For instance, use an excess amount of alcohol, catalyze the reaction, and perform a multistep reaction to remove byproduct water from the system, which moves the reaction forward with higher yield of trialkyl citrate. Grigoryan et al. synthesized and reported properties of long chain esters of citric acid [16]. They have used 6, 8, 9, 10, 12, and 15 carbon chain alcohols and used 120 to 180 °C reaction temperature range and formed milky white to thick brown mass which has softening points around 50 °C. As these studies were focused on producing trialkyl citrate under various reaction conditions, and their applications does not require high functionality such as food preservatives, cosmetics ingredient, and as plasticizers. The dialkyl citrate has only one carboxylic acid which make it insignificant to be use for curing agent application. The monoalkyl citrate has two

functional groups so it could be utilized for crosslinking applications. Kotick et al. synthesized monoalkyl citric acid ester for surfactant application by a complex regioselective multistep synthesis procedure [15]. First, they synthesized anhydro-methylene citric acid, a citric acid derivative with anhydride group derived by utilizing a hydroxyl and a secondary position carboxylic acid groups of citric acid, by using paraformaldehyde. In a second step, they have used long chain alcohols from C7 to C19 to react with the product formed in step 1 to synthesize 2-mono ester of alcohol with 90% purity. The overall process parameters of this pathway are lengthy, 2 hrs. at 145 °C and 45 hrs. at 60 °C. In addition, the second reaction step involves chloroform followed by multistep purification steps. In contrast, this work illustrates the greener and economical way of synthesizing mixture of alkyl citrate which could be used as curing agent for plant oil epoxide.

5.2 Materials and methodologies

5.2.1 Materials

Citric acid (2-hydroxypropane-1,2,3-tricarboxylic acid, MW=192 g/mol) was purchased from Jungbunzlauer Canada Inc. and ground it into a fine powder by Fitz Das06 hammer mill and passed through 0.25 mm sieve. Synthesis grades of ethanol, n-propanol, n-butanol, and n-hexanol were purchased from Sigma. Analytical ACS grade deionized water, acetonitrile, formic acid, and methanol were purchased and used in HPLC/ELSD.

5.2.2 Methodologies

5.2.2.1 Synthesis of alkyl citrates

All of the following alkyl citrates were synthesized via a solvent- and catalyst-free esterification of citric acid with four different alcohols: ethanol, n-propanol, n-butanol and n-hexanol. The esterification reaction was performed under reflux condition which not only keeps

the reactant alcohol and byproduct water in the reaction mixture, but it also could restrict the formation of trialkyl citrates or hinder the esterification reaction [9] which is significant for it to be used as curing agent. Removal of byproduct, water, from the esterification reaction enhances the reaction rate towards formation of the thermodynamically possible products. However, if the water byproduct stays in the reaction mixture, this restricts the reaction between the remaining carboxylic acids and alcohols to form an ester bonds. For a curing agent application, the product must have to have at least two functional groups which could react with epoxy group to form a crosslinked network. Thus, if all or two carboxylic groups from the three available in the citric acid structure participate in the esterification reaction, then the resulting di- and trialkyl citrates cannot serve the purpose of a crosslinking or curing agent. That is why, intermediate samples were analyzed to determine the citric acid conversion and mono, di and trialkyl esters formation.

Figure 5.1 illustrates the structures of three citrate esters formed during this reaction, although there are possibilities of forming other isomers of mono- and dialkyl citrates in the mixture. However, in this study such isomers are not separated. Since the goal of synthesizing these citrates is for them to be used as curing agents, so they should be multifunctional and miscible with the plant oil epoxides. To synthesize the suitable alkyl citrate mixture, the process should form the maximum amount of monoalkyl ester component, ideally with no formation of di- and trialkyl ester components. The reaction temperature was selected based on the boiling point of the alcohol used in the reaction. As described below, the reaction temperature selected was about 10 °C above the alcohol's boiling point which facilitates better mixing. The reaction mixtures are milky at the beginning of the reaction, because of the natural white color of the citric acid and its limited solubility in alcohols. However, it was found that after a specific reaction time they become fully transparent. This reaction time is dependent on the concentration of the citric acid in

the alcohol. As the objective is to synthesize the maximum amount of monoalkyl citrate and minimum or no formation of di- and trialkyl citrates, the alcohol amount used in the reaction is crucial as excess alcohol leads formation of di- and trialkyl citrates. For this reason, various amounts of alcohols were tested in order to synthesize the suitable alkyl citrate formulation which should ultimately have maximum amount monoalkyl and no formation of di- and trialkyl esters, as explained above.
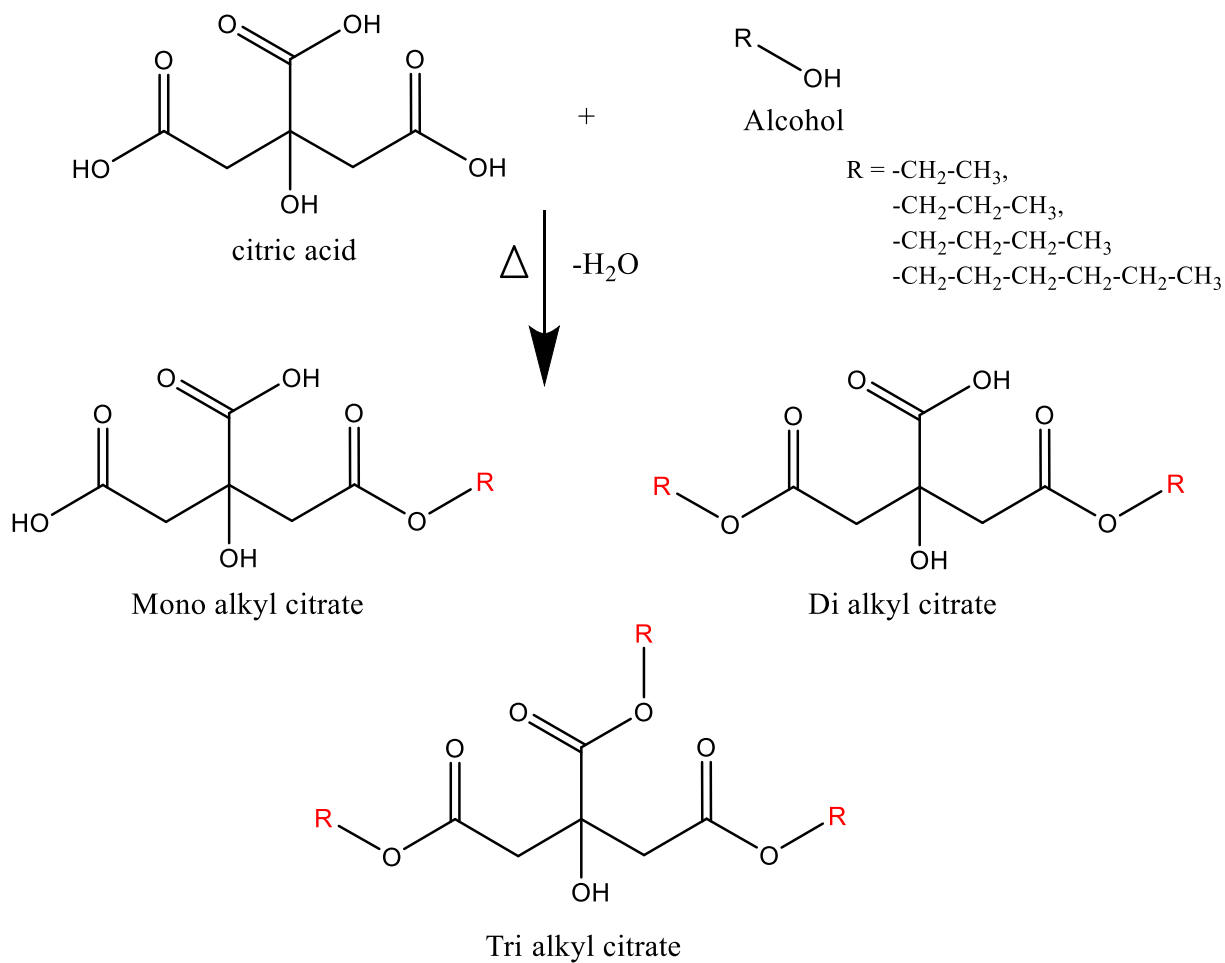
Figure 5.1 Citric acid esterification

5.2.2.2 Synthesis parameters

For studying the reaction progress at various citric acid to alcohol mole ratios, 200 grams of citric acid was used, and intermediate samples were collected and analyzed. These studies illustrated (Figures 5.6 and 5.7) that the citric acid consumption and the monoalkyl citrate formation continue up to certain point then their consumption/synthesis progress become constant. Additionally, it was also discovered that the highest functionality can be achieved at the minimum reaction time at which the reaction mixture becomes transparent. By discovering these reaction behaviors, the remaining two alkyl citrates, ethyl and hexyl, were synthesized and studied by taking 20 grams of citric acid with various amounts of alcohols. Citric acid esterification was performed under reflux condition at 90 °C with ethanol which has a boiling point is 78 °C. The reaction temperature was determined by considering two factors: the boiling point of the alcohol and the decomposition temperature of citric acid, which occurs above 130 °C. Therefore, the reaction temperatures for all four alcohols used in this study were less than 130 °C. Lower reaction temperatures may be possible, but they are avoided due to the limited solubility of citric acid in alcohols at lower temperatures, which leads to higher reaction times. Simultaneously, the reaction time should be minimized because with longer reaction times, the di- and trialkyl citrate compounds formation occurred as illustrated in the results and discussions section.

Citric acid esterification was performed at 110 °C with n-propanol which has a boiling point of 97 °C and under reflux condition. The boiling point of n-butanol is 117 °C so a 130 °C reaction temperature was selected. Despite the boiling point of hexanol being 157 °C, reaction temperatures of 120 °C and 130 °C were tested to avoid citric acid decomposition. All the intermediate and final alkyl citrate samples were evaporated at 100 °C under vacuum pressure in

a rotary evaporator to remove byproduct water and unreacted alcohols. The residual alcohol content in these samples were below 0.3%.

5.2.2.3 Quantification of alkyl citrates by HPLC-ELSD

Suaza et al. synthesized, separated, quantified, and measured some physical properties of dibutyl citrate [7]. They separated dibutyl citrate from citric acid, mono- and tributyl citrate mixtures through a reversed phase C18 column while using a UV detector operating at 210 nm wavelength. In this work, they assumed that the response factor of dibutyl citrate is same as the citric acid which is commercially available with high purity of 99.9%. In this work, the ELSD detector was used and followed the following procedure to establish the analytical method. First, the ELSD detector parameters, tube temperature and nitrogen gas flow rate, were optimized. It was found that the tube temperature of 30 °C and nitrogen gas flow rate of 1.5 L/min were optimum to obtain the highest peak area of citric acid, di- and trialkyl citrates. The detector gain factor of 16 used and impactor set at OFF position. Second, the calibration range was determined by considering the estimated composition of the citrate mixtures fall within these concentrations as long as the data are linear. All these calibration data of citric acid and various alkyl citrates are presented in the Figures 5.2 and 5.3. A butyl citrate mixture separation is depicted in Figure 5.4.
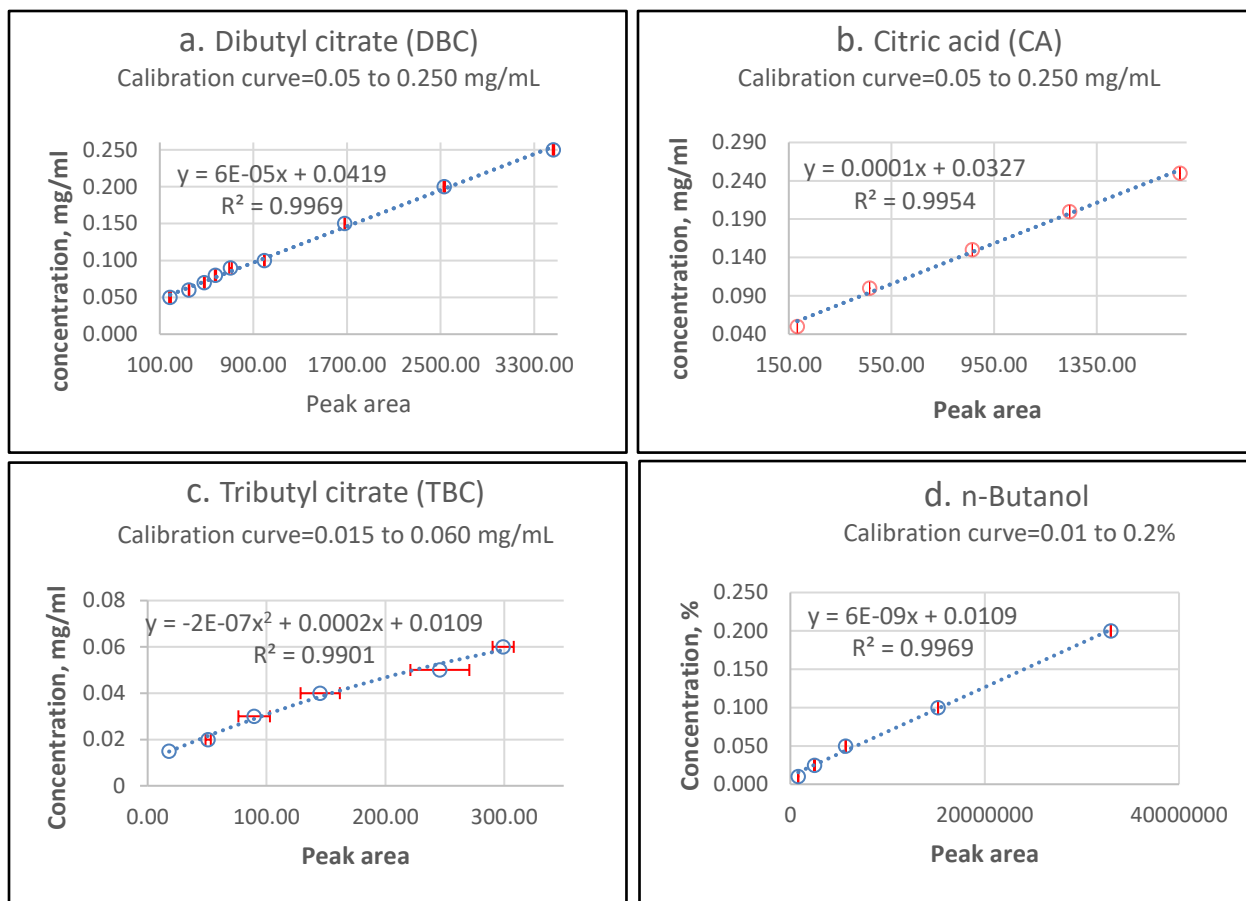
Figure 5.2. Calibration curves for citric acid, mono-, di- and tributyl citrates

In order to prepare a dibutyl citrate standard for quantification purposes, butyl citrate was separated from the citric acid, mono-, and tributyl citrates by liquid-liquid extraction procedure by using diethyl ether as solvent at various pH levels [7]. First, the mixture dissolved in a diethyl ether and the solution pH increased to 8.0 and separated aqueous phase from the organic phase which contains tributyl citrate. The pH of the organic phase decreased to 5.0 and separated the aqueous phase which contains dibutyl citrate. Finally, the solution pH further decreased to 2.0 and removed the aqueous phase containing monobutyl citrate. Tributyl citrate was commercially available with greater than 99% purity so it was purchased and used to obtain a calibration curve. Linear calibration curves were obtained as depicted in Figure 5.2 for citric acid, di-, and tributyl citrates.

The monobutyl citrate amount was quantified by subtracting the sum of the quantified amounts of

citric acid, di- and tributyl citrates.
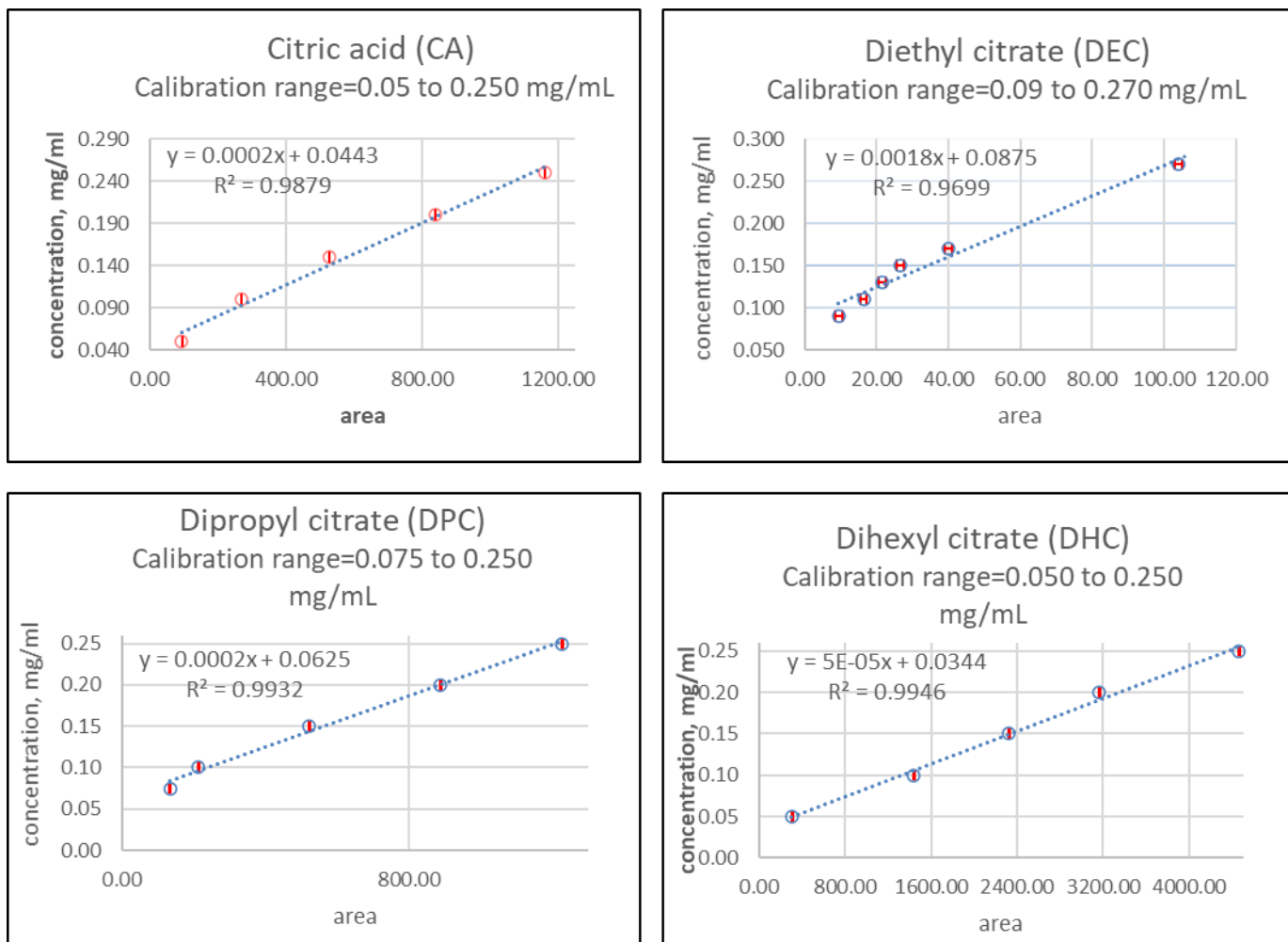
Figure 5.3. Calibration curve for citric acid, diethyl, dipropyl and dihexyl citrates
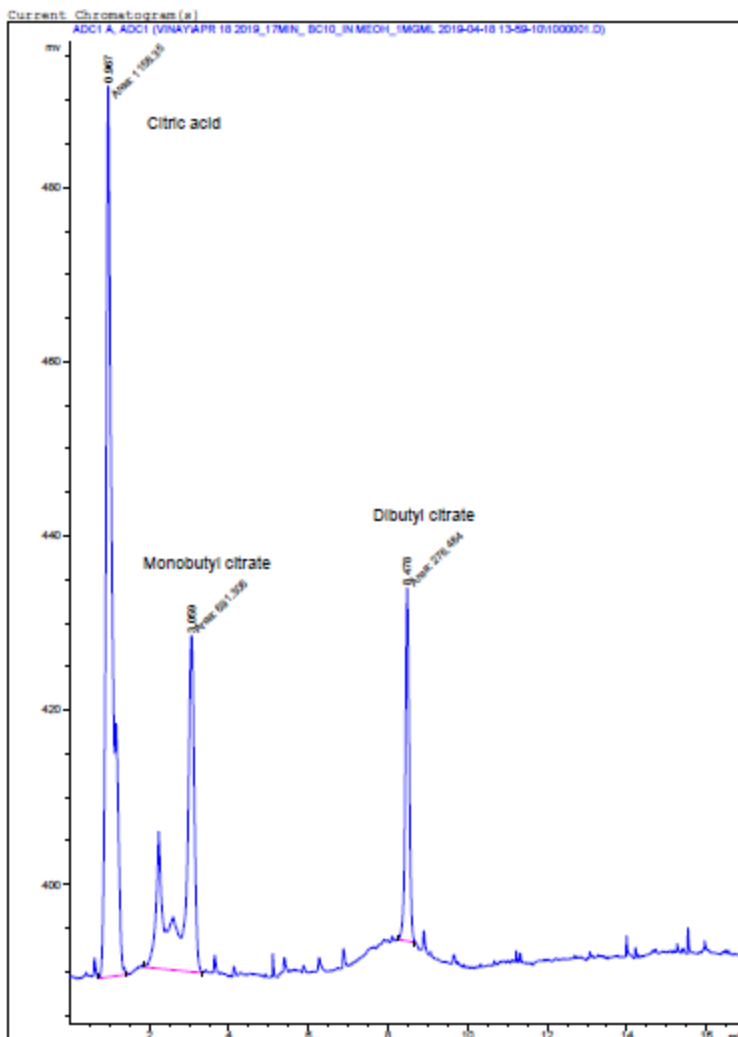
Figure 5.4 A butyl citrate mixture separation

Diethyl citrate was purified by liquid-liquid extraction [7] and used to obtain the calibration curve as depicted in Figure 5.3. Since the formation of trialkyl citrates are not useful or have negative implications for bioresin synthesis application, so one of the objectives was not to synthesize any di- and trialkyl citrates. That is why, di-, and triethyl citrates were not quantified and aim for no peak of these compound in the ethyl citrate mixtures.

Since the various chain length alcohols were used to synthesized alkyl citrates, each alkyl citrate was separated in a C18 column by slight modification of the mobile phase gradient, as illustrated in Figure 5.5. Water and acetonitrile buffers were used as mobile phase solvents.
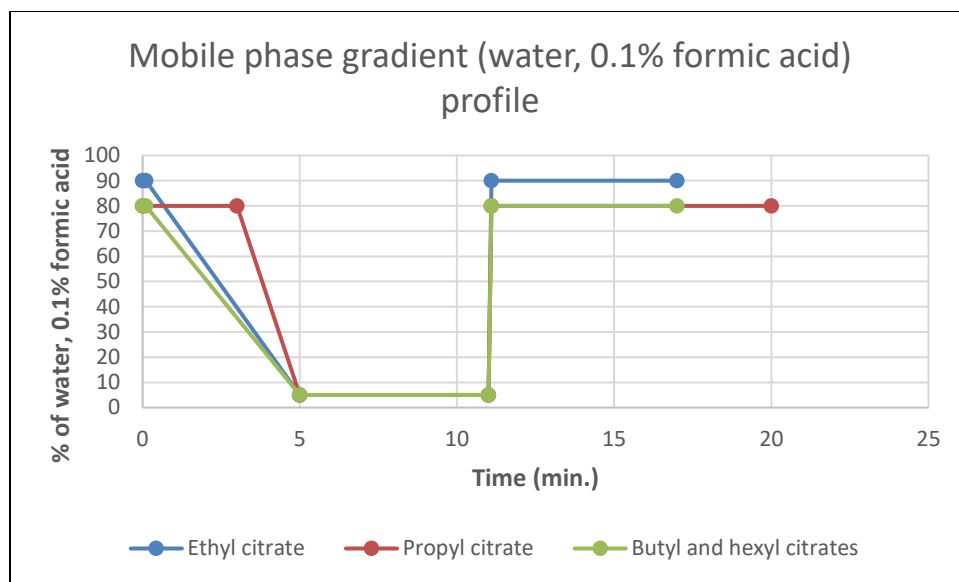
Figure 5.5 Gradient profile of mobile phase for separation of citric acid, mono-, di- and trialkyl citrates mixtures: ethyl, propyl, butyl and hexyl citrates

5.3 Results and discussions

These synthesized half esters of citric acid are mixtures of free or unreacted citric acid, mono, di and trialkyl citrates.

5.3.1 Ethyl citrate

First, the realistic citric acid to ethanol ratio was identified by considering the reaction time not exceeding 5 hours because at a greater reaction time, di- and trialkyl citrates started to form. To keep the reaction time minimum, higher amount of alcohol can be used but at too excess amount of alcohol contribute to formation of di- and trialkyl citrates. That is why, realistic ratio needs to be identified then further other parameters, mainly reaction time, can be implemented to have an optimum synthesis condition. A citric acid to ethanol equimolar ratio, 1:1, was not suitable because the citric acid was not fully dissolved at 90 °C, and the mixture did not become one phase after 6 hours of reaction.

154

Citric acid to ethanol (mol:mol)	Reaction time (min.)	Reaction temperature (°C)	Free citric acid (%)	Monoethyl citrate (%)	Diethyl citrate (%)	Triethyl citrate (%)	Average carboxylic acid functionality
1 : 1	360	90	Reactants did not become homogeneous				n/a
1 : 2	77*		34.3	65.7	0.0	0.0	2.3
1 : 2	120		17.2	82.8	0.0	0.0	2.2
1 : 2	180		8.9	73.6	17.5	0.0	1.9

The reaction time at which mixture become transparent

Table 5.1. Ethyl citrate formation under various ethanol mole ratios

Then, a citric acid to ethanol mole ratio of 1:2 was used, and the mixture become one phase and transparent after 77 minutes of reaction. Finally, with the citric acid to ethanol molar ratio fixed at 1:2, the reaction time was increased in order to investigate the reaction behavior in terms of formation of mono-, di-, and trialkyl esters formation. The results clearly indicate that when the mixture become transparent, the free citric acid amount was 34.3% and over time it gets consumed in the reaction to 17.2% at 2 hours and 8.9% at 3 hours of reaction. Additionally, it was found that at 3 hours of reaction, formation of diethyl citrate (17.5%) occurred, and the carboxylic acid functionality was reduced from 2.3 to 1.9.

5.3.2 Propyl citrate

The three different mole ratios of citric acid to n-propanol that are depicted in Fig. 5.6 resulted in the formation of dipropyl citrate from the beginning or the reaction. The percentage of dipropyl citrate increased over reaction time, which correspondingly decreased the average carboxylic acid group functionality of the mixture.
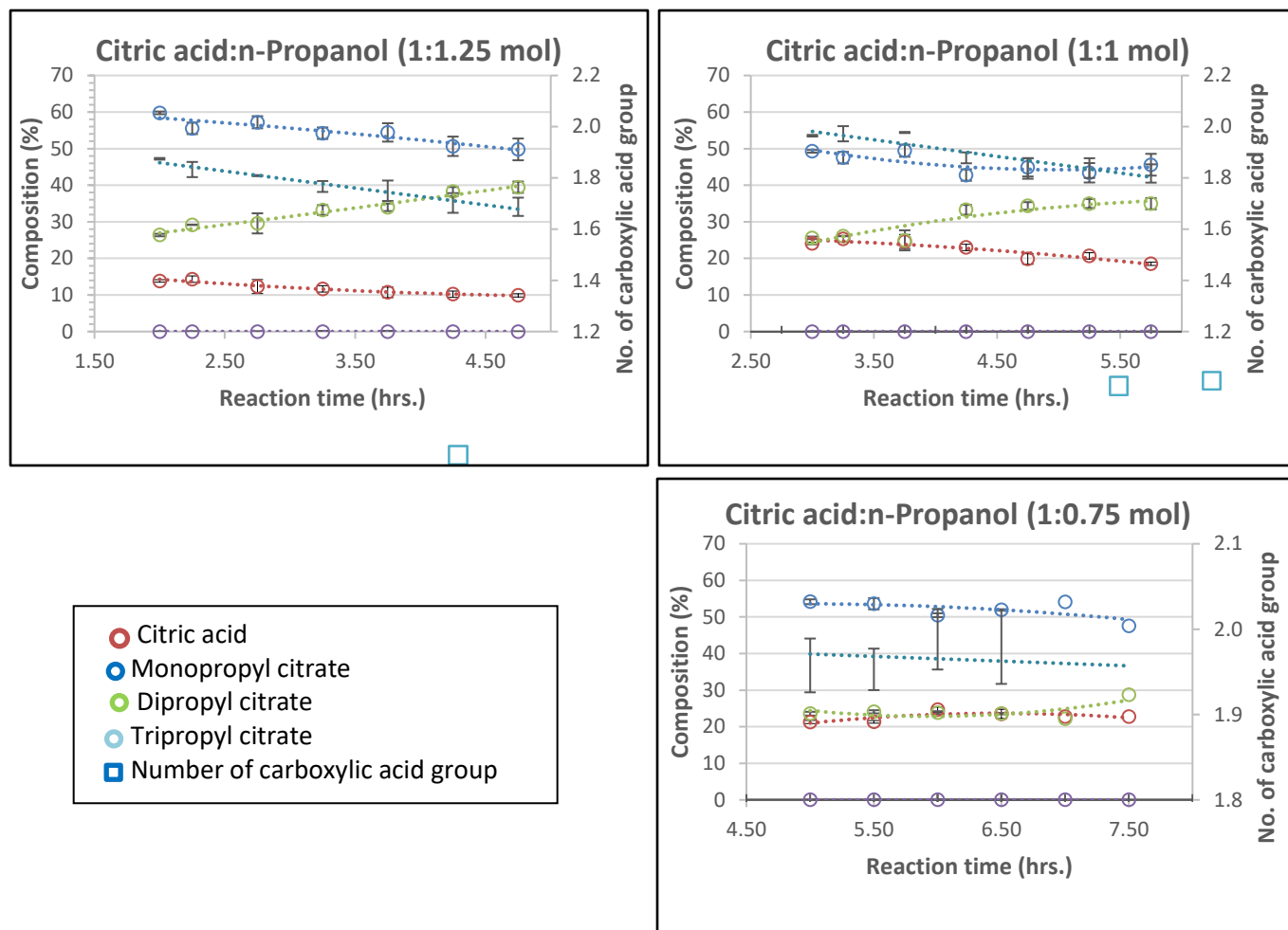
Figure 5.6 Citric acid conversion into their propyl esters at various mole ratios of n-

propanol

For crosslinking applications, the presence of di- and trialkyl citrate is not suitable because they inhibit the polymer chain growth. Therefore, additional propyl citrate formulations were prepared to avoid formation of di- and tripropyl citrates as depicted in Table 5.2.

Citric acid to n-propanol (mol:mol)	Reaction time* (min.)	Reaction temperature (°C)	Free citric acid (%)	Monopropyl citrate (%)	Dipropyl citrate (%)	Tripropyl citrate (%)	Average carboxylic acid functionality
1 : 1.50	77	110	24.7	57.6	16.7	0.0	2.1
1 : 1.75	50		21.5	60.3	17.2	0.0	2.0
1 : 2.00	50		29.1	69.9	0.0	0.0	2.3
1 : 2.50	35		20.2	61.3	17.5	0.0	2.0

The reaction time at which mixture become transparent

Table 5.2. n-propyl citrate formation under various n-propanol mol ratios

Dipropyl citrate was not formed when citric acid to n-propanol ratio of 1:2 used and an average carboxylic acid functionality of 2.3 was achieved as indicated in Table 5.2. The dipropyl citrate amount is increasing as the alcohol amount increases, and it becomes 0 at the citric acid to propanol ratio of 1:2. Then, at the 1:2.5 mol ratio, it increased again to 17.5% as it is not only dependent on alcohol amount but also the reaction time. It also can be concluded that higher amount of alcohol is decreasing the reaction time, although at the same time after certain level of alcohol, the dipropyl citrate starts to form.

5.3.3 Butyl citrate

Four different citric acid to n-butanol mol ratios were used and the reaction progress was monitored as depicted in Figure 5.7. Tributyl citrate was not formed when limiting amounts of n-butanol was used for the reaction, as seen with 0.50 and 0.75 moles of butanol per mole of citric acid. At these citric acid-to-n-butanol mole ratios, dibutyl citrate formation of between 10 and 15 occurred %. For all four different mole ratios, the monobutyl citrate content is comparatively similar (between 50 to 55%) and as the reaction progresses monobutyl citrate amounts stabilized

which indicated that the reaction establishes to its equilibrium. The citric acid conversion also reaches an equilibrium state for all mole ratios except for the case of mole ratio of 1:4, where excess n-butanol is available to be used in the reaction, and free citric acid continues to be consumed.
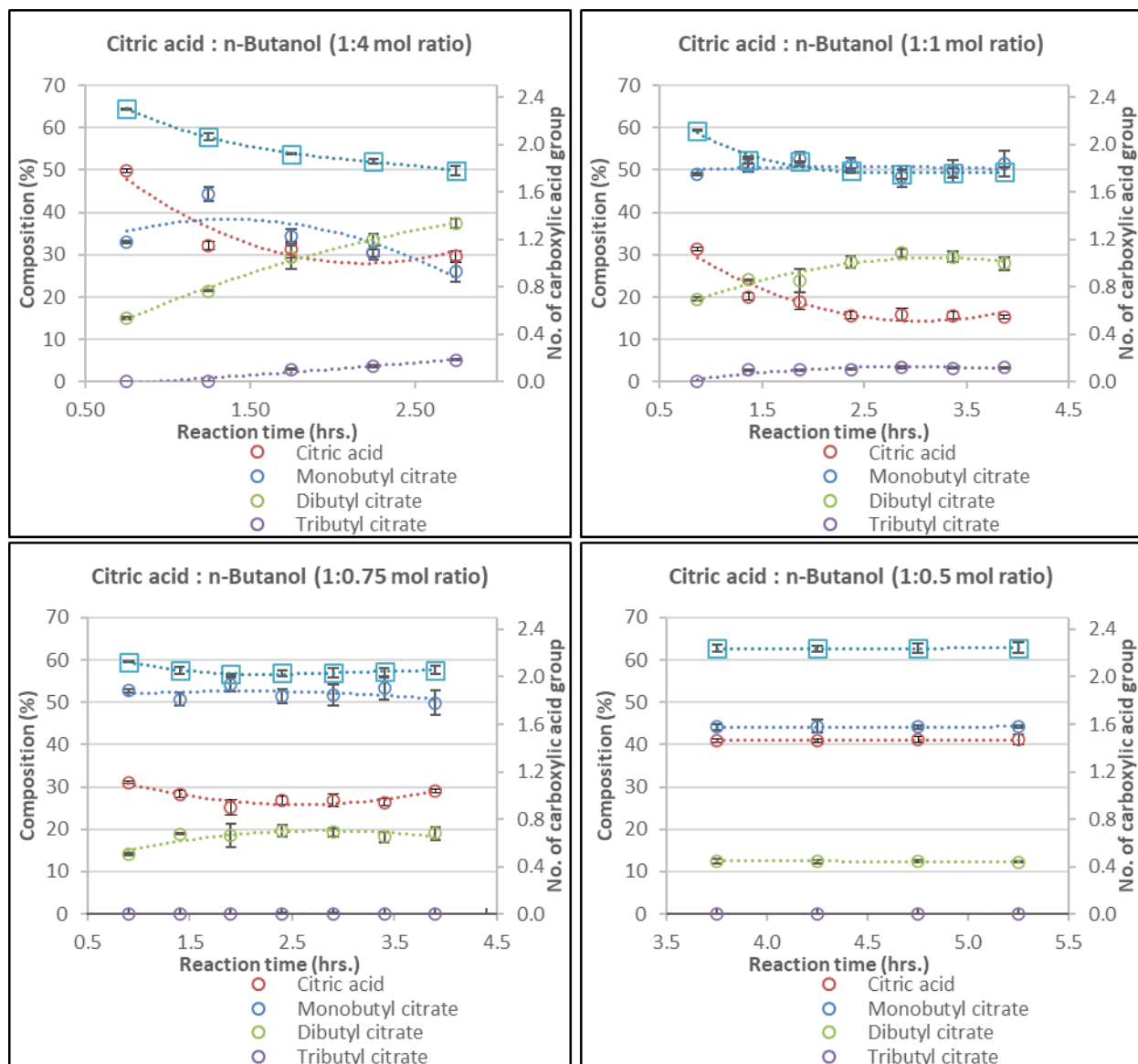
Figure 5.7 Citric acid conversion into butyl esters at various mol ratios of citric acid : n-butanol

It can be concluded that the n-butanol amount and the reaction time affect the carboxylic acid functionality of the citrate mixture and can be tunable to achieve desired functionality. After

studying the effects of esterification reaction parameters onto the citric acid conversion and mono-, di-, and tributyl citrates formation, five additional butyl citrate formulations were prepared to determine their viscosities and how they are corelated with the composition of the mixture as depicted in the Table 5.3.

	CA	MBC	DBC	TBC	Viscosity (Pa.S)					
	(%)				25 °C	30 °C	35 °C	40 °C	45 °C	50 °C
BC-1	17.3	49.4	29.0	3.4	3264	1887	1463	1403	1391	1402
BC-2	28.7	51.0	19.3	0.0	10825	6956	4439	2073	1562	1481
BC-3	22.0	63.1	13.8	0.0	3224	1207	488	209	97	48
BC-4	42.0	44.4	12.4	0.0	23929	18336	13970	11523	9266	5017
BC-5	37.9	47.3	13.6	0.0	17159	5665	2069	820	349	157

Table 5.3 Viscosities of butyl citrate formulations

Since each compound affects the overall viscosity of the formulation would have multiple effects as one compound increasing while other is decreasing, for instance, trialkyl citrates are low viscosity compounds while citric acid is a solid substance. It cannot be concluded the precise effect of individual compound's viscosity on the overall viscosity of the formulation. The viscosities are drastically reduced at 50 °C, specifically for formulation no. 3, which could be highest amount of monobutyl citrate and lower amount of free citric acid present compared to formulation no. 4. Additionally, such a high viscosity formulation is not suitable for plant oil epoxide as they are not miscible at room temperature.

5.3.4 Hexyl citrate

Two reaction temperatures were used and various citric acid to n-hexanol mol ratios were used to synthesize hexyl citrate mixtures as depicted in Table 6. It was found that dihexyl citrate was formed at both temperatures that is why the average carboxylic acid group functionality was less

than 2.0 for all formulations. Since the curing agent must have at least two functional groups in order to form infinite crosslinks, those formulations with less than 2 functionalities are not suitable.

Citric acid to n-hexanol (mol:mol)	Reaction time (min.)	Reaction temperature (°C)	Free citric acid (%)	Monohexyl citrate (%)	Dihexyl citrate (%)	Trihexyl citrate (%)	Average carboxylic acid functionality
1 : 1	282	120	14.7	52.8	27.2	5.4	1.8
1 : 1.25	210		10.3	47.5	36.1	6.0	1.6
1 : 0.75	96	130	20.7	56.1	20.1	3.0	1.9
1 : 1	120		17.2	54.2	24.9	3.7	1.9
1 : 1.25	60		16.1	58.9	22.2	2.8	1.9

Table 5.4 n-hexyl citrate formation under various n-hexanol mol ratios

5.3.5 Bioresins

The objective of synthesizing these partial esters of citric acid was to prepare a plant oil epoxide miscible curing agent. This miscible curing agent then make possible to prepare fully biobased epoxy resins without the use of solvent. These citrates were miscible with the plant oil epoxides as depicted in the Figure 5.8. Then, this mixture was kept at room temperature and it become a tack-free solid cured mass within 48 hours as depicted in Figure 5.9.
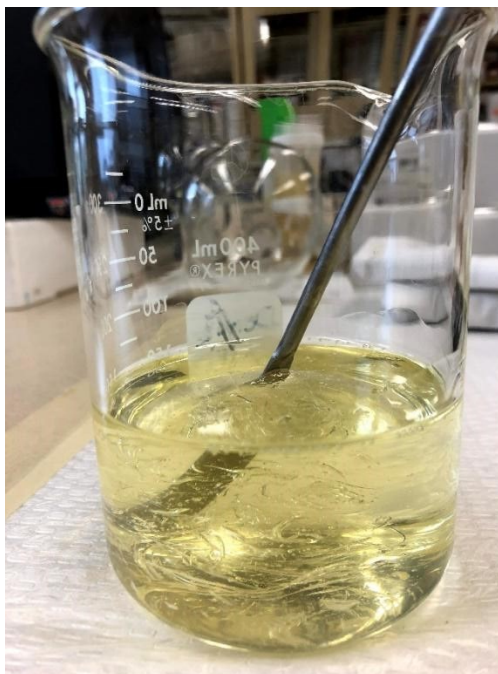
Fig 5.8. Miscibility between alkyl citrate and epoxidized plant oil
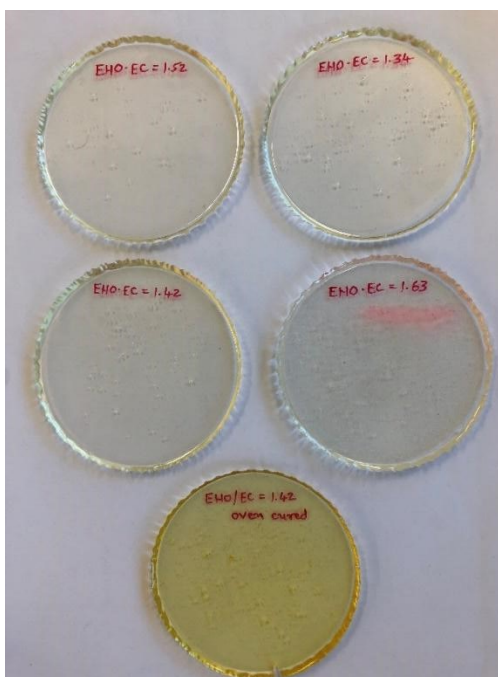
Fig 5.9. Room and elevated temperatures cured plant oil epoxide with the alkyl citrate

Name of the curing agent	Composition of the curing agent				Miscible with the plant oil epoxide* at 50 °C
	Free citric acid (%)	Monoalkyl citrate (%)	Dialkyl citrate (%)	Trialkyl citrate (%)	
Ethyl citrate-1	36.8	63.2	0.0	0.0	No
Ethyl citrate-2	17.2	82.8	0.0	0.0	Yes
Propyl citrate-1	22.0	60.0	18.0	0.0	Yes
Propyl citrate-2	29.1	69.9	0.0	0.0	Yes
Butyl citrate-1	22.0	63.1	13.8	0.0	Yes
Butyl citrate-2	41.3	44.7	12.9	0.0	No
Hexyl citrate-1	20.7	56.1	20.1	3.0	Yes
Hexyl citrate-2	10.3	47.5	36.1	6.0	Yes

Epoxides to curing agent ratio1:0.4 w/w

Table 5.5 Miscibility of novel biobased curing agents with the plant oil epoxides

These biobased curing agent mixtures were miscible with the plant oil epoxides at 50 °C, when the free citric acid content was less than 30% in the mixture.

5.4 Conclusions

Biobased, multifunctional, and compatible curing agents were synthesized for use with the plant oil epoxides. The partial esters of citric acid were synthesized by using short to medium chain

length alcohols, ethanol, propanol, butanol and hexanol via green chemistry route. An HPLC-ELSD analytical method was established to quantify these synthesized alkyl esters of citric acid. It was found that the composition of these alkyl citrate formulations depends on the citric acid to alcohol mole ratio, reaction time and temperature. Then, these synthesis parameters were used to prepare alkyl citrate with the highest carboxylic acid functionalities. The di- and trialkyl citrates have carboxylic acid functionality of 1 and 0, respectively which cannot contribute to crosslinking, so they are avoided in the formulations. By utilizing the synthesis parameters described, it was possible to synthesize ethyl and propyl citrate mixtures without the formation of di- and trialkyl citrates. However, this was not possible for the butyl and hexyl citrates. Finally, it was also found that these biobased curing agents are reactive at room temperature, 25 °C with the plant oil epoxides and formed tack-free and light colored cured resins within 48 hours. It was also found that the room temperature cure sample's Tg is keep increasing up 4 weeks and matching with the sample which is cured at elevated temperature. Although, Fig 5.9 clearly indicating that the pale yellowish color bioresin formed when it cured at elevated temperatures while room temperature cured samples remain light colored.

5.5 References

[1] S. Omonov, Tolibjon, et al. "The Epoxidation of Canola Oil and Its Derivatives." RSC Advances, vol. 6, no. 95, 2016, pp. 92874–86.

[2] Omonov, Tolibjon S., et al. "The Development of Epoxidized Hemp Oil Prepolymers for the Preparation of Thermoset Networks." *Journal of the American Oil Chemists' Society*, vol. 96, no. 12, 2019, pp. 1389–403.

[3] Ashcroft, W. R. "Curing Agents for Epoxy Resins." *Chemistry and Technology of Epoxy Resins*, edited by Bryan Ellis, Springer Netherlands, 1993, pp. 37–71

[4] Tan, S. G., and W. S. Chow. "Biobased Epoxidized Vegetable Oils and Its Greener Epoxy Blends: A Review." *Polymer-Plastics Technology and Engineering*, vol. 49, no. 15, Nov. 2010, pp. 1581–90.

[5] Sahoo, Sushanta K., et al. "Development of Toughened Bio-Based Epoxy with Epoxidized Linseed Oil as Reactive Diluent and Cured with Bio-Renewable Crosslinker." *Polymers for Advanced Technologies*, vol. 29, no. 1, 2018, pp. 565–74.

[6] Bourne, L. B., et al. "Health Problems of Epoxy Resins and Amine-Curing Agents." *Occupational and Environmental Medicine*, vol. 16, no. 2, Apr. 1959, pp. 81–97.

[7] Suaza, Andrea, et al. "Dibutyl Citrate Synthesis, Physicochemical Characterization, and Px Data in Mixtures with Butanol." *Journal of Chemical & Engineering Data*, vol. 63, no. 6, June 2018, pp. 1946–54. *ACS Publications*, doi:10.1021/acs.jced.7b01064.

[8] Wang, Junqi, et al. "Techno-Economic Analysis and Environmental Impact Assessment of Citric Acid Production through Different Recovery Methods." *Journal of Cleaner Production*, vol. 249, Mar. 2020, p. 119315. *ScienceDirect*, doi:10.1016/j.jclepro.2019.119315.

[9] Kakasaheb Y. Nandiwale, Vijay V. Bokade. "Sustainable Catalytic Process for Synthesis of Triethyl Citrate Plasticizer over Phosphonated USY Zeolite." *Bulletin of Chemical Reaction Engineering and Catalysis*, vol. 11, no. 3, 2016, pp. 292–98.

[10] BCC market report. *BCC Library - Report View - CHM088A*. https://academic-bccresearch-com.login.ezproxy.library.ualberta.ca/market-research/chemicals/carboxylic-acids-applications-and-global-markets.html. Accessed 10 Apr. 2021.

[11] Hongqin Yang, Haiyan Song, Han Zhang, Ping Chen, Zhixi Zhao. "Esterification of Citric Acid with N-Butanol over Zirconium Sulfate Supported on Molecular Sieves." *Journal of Molecular Catalysis A: Chemical*, vol. 381, 2014, pp. 54–60.

[12] X.U. Junming, Jiang Jianchun, Zuo Zhiyue, Li Jing. "Synthesis of Tributyl Citrate Using Acid Ionic Liquid as Catalyst." *Process Safety and Environmental Protection*, vol. 88, 2010, pp. 28–30.

[13] Pratibha Singh, Sanjay P. Kable, Prakash V. Chavan. "Kinetics of Esterification of Citric Acid with Butanol Using Sulphuric Acid." *Int. J. Chem. Sci.*, vol. 12, no. 3, 2014, pp. 915–20.

[14] Yun Lu, Shengxian Xu, and Feng Zhao. "Synthesis of Tributyl Citrate Using Preyssler Acid as Catalyst." *AIP Conference Proceedings*, 2017, https://aip.scitation.org/doi/abs/10.1063/1.4971953.

[15] Michael P. Kotick, Elkhart, Ind. *Regioselective Synthesis of Mono-Alkyl Citric Acid Esters*. 5,049,699.

[16] G.S. Grigoryan, Z.G. Grigoryan, A.Ts. Malkhasyan. *Obtaining Esters of Citric Acid with High Aliphatic Alcohols*. Proceedings of the Yerevan State University, Chemistry and Biology, 51(2), p. 88-91 2017.

Chapter 6

Solvent-free manufacturing of high biocontent bioresins and biocomposites

6.1 Introduction

Greenhouse gas emissions are rapidly increasing which causes devastating global climate change effects. One of the major sources of greenhouse gas emissions is from nonrenewable feedstocks. Hence, there is a need to diversify our dependence towards alternate or biobased resources [1] that have low carbon footprints. Large amounts of polymeric based materials are manufactured from petroleum-based feedstock. Epoxy resin is a class of thermoset material which makes up about 10% of the overall plastics or polymer based materials market [2]. Out of this, more than 90% of the epoxy resins are formulated from petroleum-based feedstocks such as bisphenol A [2]. The abundant usage of this class of resin is due to its versatility - the phenolic ring and a 3-dimensional polymer network contributes for its toughness and rigidity, the ether linkage imparts chemical resistance, and the hydroxyl group can contribute towards adhesion properties [3]. These BPA based thermoset materials are being used in electronics, as coatings, polymer matrices for natural fiber composites, and many other applications [4].[6]

---

[6] A version of this chapter has been submitted as a patent, "Jonathan M. Curtis, Vinay Patel, US provisional patent application serial no. 63/075,940, Biobased hardener for epoxy resins."

In spite of having such a versatile material, studies have shown that BPA is a potential human hormone disruptor and could be responsible for many diseases include hypertension, peripheral artery disease, and atherosclerosis [5]. Additionally, the majority of this BPA is produced via the condensation reaction between phenol and acetone, and these are derived from petroleum sources. As such, there is a need to find an alternate source of resin which could be biobased and not have any adverse human health effects.

There has been a growing research trend towards biobased materials from plant or animal sources [6]. For instance, lactic acid is being produced commercially by fermentation of starch and sugars that is one of the biobased monomers to produce polylactic acid (PLA), a thermoplastic resin [7]. There are a few biobased thermoset resins that are commercially produced, for instance, polyhydroxyalkanoates (PHA) is a polyester. The PHA monomers can be produced via fermentation of sugars and lipids, and they can be mixed and extruded to form a rigid material [8]. Despite being produced from biobased feedstocks, these bioresins have limitations in terms of efficient synthesis route as well as the overall cost of the final product [9].

Plant oils are another biobased resource which could be utilized to replace some of the petroleum-based resins. These are desirable because they naturally contain almost entirely triacylglycerides, and have wide availability (a detailed description can be found in Section 1.2). They can be functionalized into reactive monomers, which could be used for many applications from coatings to biocomposites.

This work utilizes epoxidized oils: namely, hemp and linseed, because they contain higher amounts of polyunsaturated fatty acids, linoleic and linolenic and least amounts of saturated and oleic acid. The three novel biobased curing agents, propyl-, ethyl-, and butyl-citrates (*CA-alkyl*

esters), are used with these two epoxidized oils to make fully biobased thermoset materials without the use of a solvent. Many biobased curing agents are not compatible with the plant oil epoxides and the ones that are miscible have limitations include availability and costs [10]. So, one of the obstacles of using epoxidized plant oils in making fully biobased materials is that it requires a solvent to make a homogeneous mixture of epoxide and biobased curing agent. The previous chapter described a novel process to make these *CA-alkyl esters* which are miscible with the plant oil epoxides. It was discovered that the mixture of citric acid and their partial alkyl esters are readily miscible with the plant oil epoxides that can crosslink epoxy monomers to form a rigid thermoset material.

This chapter first describes an optimisation of the epoxy to curing agent ratios. This was achieved through differential scanning calorimetry (DSC) measurements on epoxide-curing agent mixtures and cured resins. Then, utilizing these optimum ratios, bioresins and natural fiber biocomposites were prepared, and their mechanical and thermomechanical properties measured using flexure tests and dynamic mechanical analysis (DMA). One of the objectives was to prepare a miscible plant-oil-epoxide-curing agent mixture that can impregnate the natural fiber without the use of solvent. Ultimately, the purpose of the testing was to determine the comparative mechanical and thermomechanical performances of the newly synthesized bioresins for biocomposite applications.

6.2 Materials and methodologies

6.2.1 Materials

The nonwoven natural fibermat with 60% wood, 40% hemp fiber content and density of 2.5 kg/m^3 was generously provided by the Biocomposites Group, Drayton Valley, Alberta. The epoxidized hemp and linseed oils were prepared in the lab using hydrogen peroxide and formic

acid as catalyst [10]. The double bonds present in the oils were transformed into oxiranes via peroxyacids (R-COO-O-H) formation from formic acid and hydrogen peroxide. The detailed synthesis process to make biobased curing agents was described in the previous chapter, and compositions of the CA-alkyl esters used in this study are depicted in Table 6.1. These curing agent formulations were chosen because they are miscible with the plant oil epoxides at 50 °C and has pot life of about 1 hour.

Composition of CA-alkyl citrates					
Propyl citrate (PC)	Citric acid (%)	Monopropyl citrate (%)	Dipropyl citrate (%)	Tripropyl citrate (%)	Average carboxylic acid functionality/mole
	29.1	69.9	0	0	2.3
Ethyl citrate (EC)	Citric acid (%)	Monoethyl citrate (%)	Diethyl citrate (%)	Triethyl citrate (%)	
	17.2	82.8	0	0	2.2
Butyl citrate (BC)	Citric acid (%)	Monobutyl citrate (%)	Dibutyl citrate (%)	Tributyl citrate (%)	
	22.0	63.1	13.8	0	2.1

Table 6.1 Compositions of the CA-alkyl citrates

6.2.2 Methodologies

The first portion of this work uses pure resin without any reinforcement material to determine the optimum epoxy to carboxylic acid groups ratios for all epoxide-curing agents formulations. Then, biocomposites were prepared from this resin by utilizing natural fiber as the reinforcement material. The mechanical and thermomechanical properties were compared to determine the effect of each curing agent on the biocomposites' properties. These properties are correlated with

characteristics including the %OOC of the epoxides, the curing agent's functionality, and the amount of plasticizing compounds present in the curing agent.

6.2.2.1 Bioresin preparation

To study the curing behavior through DSC, the epoxide and curing agent were separately heated to 50 °C and then mixed for about 10 minutes to achieve a homogeneous mixture. Then, the mixture was placed in vacuum (25 mmHg) to remove any trapped air bubbles from the bulk liquid at room temperature for about 10 minutes. It was then transferred to an aluminum pan and kept at 25 °C over the next 22 days. Previously, it was observed that such epoxide-curing agent mixtures were cured to become tack-free rigid material withing 48 hours (at 25 °C) so every 10 days the curing progress was measured. Figure 6.1 illustrate bioresin samples prepared from epoxidized linseed oil and propyl citrate.

Figure 6.1 Bioresins prepared from epoxidized linseed oil and propyl citrate at 25 °C

Additionally, bioresin samples were cured at elevated temperature. The epoxide and curing agent mixture was prepared as described above until degassing under vacuum. Then, the liquid mass was transferred into an aluminum pan, and it was placed in an oven which was set at 25 °C. Then the oven temperature increased to 140 °C at a rate of about 2 °C/min. The oven temperature was kept isothermal at 140 °C for 1 hour then cooled down to 25 °C.

6.2.2.2 Biocomposites preparation

The resin was prepared using the aforementioned procedure and used to impregnate the fiber mat at room temperature by hand lay-up. Particular attention was paid to ensure homogeneous impregnation of the fibermat with the resin system. Consolidation of the constituents of the biocomposite was done by placing the impregnated fiber mat between two steel plates and placing this onto a hot press which was preset at 140 °C. About 2 ton pressure applied onto the 6"X6" area and maintained for 20 minutes. Then, it was removed and cooled down to room temperature for further measurements and analysis. Figure 6.2 illustrates a biocomposite and a bioresin mixture prepared using this manufacturing method.

Figure 6.2 A biocomposite and a bioresin mixture samples

6.2.2.3 Sample preparation for flexure (3-point bend) test

As indicated above, 6"X6" biocomposite plates were prepared for each epoxide-curing agent combination. Then, five samples were cut with dimensions of 96 mm length, 13 mm width, and 5 mm thickness. A Bose Electroforce 3200 series III universal testing machine was used for the flexure tests. The unit was equipped with a 450 N maximum capacity load cell and a 3-point bending fixture. The span length was set to 80 mm. The rate of the crosshead movement was 1.0 mm/min as per the ASTM D7274/D7274M-15 standard method used for flexural test. All tests were conducted after 4 weeks of sample preparation and the time for all samples was constant. These tests performed at room temperature of 25 °C.

6.2.2.4 Sample preparation for DMA

DMA model Q800 (TA instruments, USA) was used for these measurements. Optimum epoxy to carboxylic acid groups ratios was used to prepared bioresin samples. The homogeneously mixed epoxide-curing agent mixture was poured into a Teflon mold with dimension: 95mm length, 15mm width, and 4mm thickness. It was cured at 140 °C for 1 hour and cooled down to room temperature. All samples were polished by a sandpaper size P600 in order to have precise dimension. A dual cantilever clamp used for the test and a fixed 1 Hz frequency was set for temperature scan to measure the viscoelastic properties of the samples. There was no load applied during the temperature scan. The temperature scan range was -70 to 100 °C.

6.3 Results and discussions

Differential scanning calorimetry is one of the tools used to determine the optimum ratio of epoxide and curing agents by measuring their glass transition temperatures. At the optimum epoxy to carboxylic acid groups ratio, the crosslinking density would be highest and there would remain the lowest number of unreacted components, the epoxy monomers and curing agent. As a result of these two effects, at the optimum epoxy to carboxylic acid groups ratio, where there would be highest crosslinking density, the highest glass transition temperature amongst samples prepared by using different epoxy to carboxylic acid groups ratios would be observed.

6.3.1 Determine the optimum epoxy to carboxylic acid molar ratios

Since the curing agents used in this study were synthesized and used with the plant oil epoxides for the first time, the optimum epoxide to curing agent ratio needs to be determined. The epoxide-curing agent mixture was prepared as described in section 6.2.2.1 and allowed to cure at 25 °C over the next 22 days. The Tg was measured at days 0, 12 and 22. The Tg at day 0 was determined

by taking the bulk liquid sample and cured in the DSC as follows. The sample mixture was heated to 160 °C at 2 °C/min then held isothermal for 10 min. It was cooled down to -90 °C and the temperature was raised to 160 °C within ±1 °C/min. using the modulated mode. At days 12 and 22, samples were taken from the bulk bioresin for measurement of their Tg. The material with the highest crosslinking density would have a higher glass transition temperature (Tg) than the material with a lower crosslinking density. Additionally, the highest Tg can also indicate the lowest amount of unreacted monomer present in the cured sample compared to the material with the lower Tg. Such an unreacted monomers have plasticizing effect which is responsible for the low Tg of the material. By considering these parameters, it can be hypothesized that if the maximum number of epoxy groups are crosslinked via reaction with carboxylic acid groups, then in this case there should be least amount of unreacted monomers/curing agents present in the cured sample.

Epoxidized linseed oil/Butyl citrate				
Epoxy/Acid (Ep/Ac) groups molar ratio	Day 0	Day 12	Day 22	Cured @ 140 °C, 1 hrs.
	Cured at room temperature			
	Tg0 (°C)	Tg12 (°C)	Tg22 (°C)	Tg (°C)
1.00	18.8	23.0	21.7	
1.52	26.0	33.2	34.4	
1.61	29.7	32.6	36.2	
1.71	31.3	37.0	43.6	37.6
1.82	28.1	38.7	38.9	
1.95	28.4	28.5	33.4	

Table 6.2 Optimum Ep/Ac groups molar ratio for the epoxidized linseed oil and butyl citrate mixture

This material should have the highest Tg compared to one which has an unbalanced number of epoxy to carboxylic acid groups in the reaction mixture. In the case of the butyl citrate curing agent with epoxidized linseed oil, the epoxide to carboxylic acid group molar ratio of 1.7 is optimum as it has the highest Tg among all other ratios. The highest Tg was also observed at this molar ratio as curing progresses for the day 12 and 22 samples (Table 6.2).

The same epoxy to carboxylic acid groups molar ratio, 1.7, was used to prepare a bioresin at an elevated curing temperature of 140 °C, and this sample has Tg of 37.64 °C which was about 6 °C less than the sample cured at 25 °C for 22 days. This could be due to differences between the curing profiles at room temperature vs 140 °C as the reactive compounds in the bulk mixture have more time to react at room temperature. In contrast, with the higher temperature curing, these reactive components are crosslinked quicker and hence the remaining unreacted monomers do not get enough time to become part of overall crosslinking network.

When the epoxidized hempseed oil was used with the butyl citrate as curing agent (Table 6.3), the optimum epoxy to carboxylic acid groups molar ratio was determined as 1.5. Thus, the ratio of 1.7 was optimum for the epoxidized linseed oil but 1.5 for epoxidized hempseed oil, which means that the later formulation is less epoxy rich. This could be due to the differences between the curing kinetics of these two epoxidized oils, as it was proven that epoxides with higher %OOC have higher reactivities than those with lower %OOC [11].

Epoxidized hempseed oil/Butyl citrate				
Epoxy/Acid (Ep/Ac) groups molar ratio	Day 0	Day 12	Day 22	Cured @ 140 °C, 1 hrs.
	Cured at room temperature			
	Tg0 (°C)	Tg12 (°C)	Tg22 (°C)	Tg (°C)
1.00	8.9	11.8	12.5	
1.40	10.0	17.5	18.3	
1.49	14.3	19.8	23.0	16.6
1.59	10.3	16.4	21.1	
1.70	11.9	20.6	21.6	
1.84	9.4	12.7	14.6	

Table 6.3 Optimum Ep/Ac groups molar ratio for the epoxidized hempseed oil and butyl citrate mixture

The difference between bioresin's Tg prepared from epoxidized linseed and hempseed oil with the butyl citrate was about 21 °C due to the differences in their %OOC, as 8.3% and 9.8% OOC of EHO and ELO, respectively.

The optimum Ep/Ac ratio of 1.7 was determined for the epoxidized linseed oil and propyl citrate since this ratio results in the maximum Tg for day 0, 12 and 22 (Table 6.4). The Tg of bioresin prepared by using this ratio of 1.7 and cured at elevated temperature was about 3 °C higher than the sample cured at 25 °C for 22 days.

Epoxidized linseed oil/Propyl citrate				
Epoxy/Acid (Ep/Ac) groups molar ratio	Day 0	Day 12	Day 22	Cured @ 140 °C, 1 hr
	Cured at room temperature			
	Tg0 (°C)	Tg12 (°C)	Tg22 (°C)	Tg (°C)
1.91	41.3	40.0	48.7	
1.79	39.8	44.6	42.0	
1.69	42.3	46.3	49.0	52.9
1.59	36.2	43.0	35.0	

Table 6.4 Optimum Ep/Ac groups molar ratio for the epoxidized linseed oil and propyl citrate mixture

When the epoxidized linseed oil replaced with the epoxidized hempseed oil, the optimum epoxy to carboxylic acid groups ratio was decreased from 1.7 to 1.6 (Table 6.5). This small difference could be due to their unique reactivities. Since the epoxidized linseed oil curing rate is faster than epoxidized hempseed oil [11], the mixture of epoxidized linseed oil and propyl citrate form a crosslinked network faster, which does not allow all of the epoxy groups to become part of the network, and this could the reason that the optimum Ep/Ac molar ratio is greater than 1 requiring higher amount of epoxy groups than equimolar amount.

Epoxidized hempseed oil/Propyl citrate				
Epoxy/Acid (Ep/Ac) groups molar ratio	Day 0	Day 12	Day 22	Cured @ 140 °C, 1 hr
	Cured at room temperature			
	Tg0 (°C)	Tg12 (°C)	Tg22 (°C)	Tg (°C)
1.67	20.4	27.9	28.4	
1.57	21.8	29.2	31.3	29.2
1.47	21.6	24.6	24.5	

Table 6.5 Optimum Ep/Ac groups molar ratio for the epoxidized hempseed oil and propyl citrate mixture

The optimum epoxy to carboxylic acid groups ratio of 1.7 was determined for epoxidized linseed oil with the ethyl citrate (Table 6.6). Interestingly, the sample cured at 25 °C over time appears to be maximally cured in 12 days as the 22 day sample does not show any further increase in Tg. However, the bioresin prepared at elevated temperature has about 5 °C higher Tg than the sample cured at 25 °C.

Epoxidized linseed oil/Ethyl citrate				
Epoxy/Acid (Ep/Ac) groups molar ratio	Day 0	Day 12	Day 22	Cured @ 140 °C, 1 hr
	Tg0 (°C)	Tg12 (°C)	Tg22 (°C)	Tg (°C)
1.86	35.4	43.8	44.3	
1.74	38.7	40.3	40.1	45.1
1.63	33.4	39.4	37.1	

Table 6.6 Optimum Ep/Ac groups molar ratio for the epoxidized linseed oil and ethyl citrate mixture

The optimum epoxy to carboxylic acid groups ratio was decreased from 1.7 to 1.4 when the epoxidized linseed oil replaced with the epoxidized hempseed oil with the ethyl citrate curing agent

(Table 6.7). Additionally, a similar 25 °C curing rate phenomenon was observed so that most of the curing occurred within 12 days and there was no further significant change in Tg, when bioresin cured for longer. For this epoxidized hempseed oil/ethyl citrate case it was also observed that there was no significant difference in Tg between bioresins prepared at elevated temperature vs. cured at 25°C. Hence, it can be concluded that such bioresin mixture can maximally cured at 25 °C within 12 days.

Epoxidized hempseed oil/Ethyl citrate				
Day 0		**Day 12**	**Day 22**	
Epoxy/Acid groups ratio	Tg0 (°C)	Tg12 (°C)	Tg22 (°C)	Tg (Cured in oven @ 140 °C, 1 hrs.)
1.63	20.2	22.2	24.8	
1.52	23.0	26.2	25.1	
1.42	23.8	23.4	23.0	24.1
1.34	20.2	23.1	26.4	

Table 6.7 Optimum Ep/Ac groups molar ratio for the epoxidized hempseed oil and ethyl citrate mixture

6.3.2 Flexural properties of biocomposites

Five specimens for each test were used for repeatability. A representative stress (N) versus deflection (mm) graph is shown in Figure 6.3.
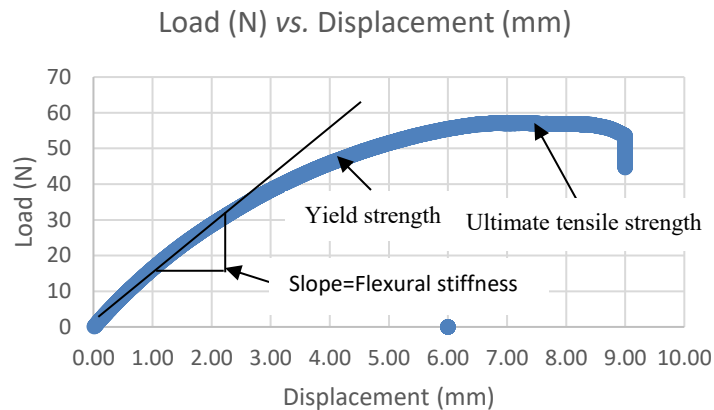
Fig 6.3 A representative load (N) *vs.* Deflection (mm) graph for biocomposite specimen

The initial linear portion of the curve was used to calculate the flexural stiffness of the specimens. The maximum load was considered as the ultimate tensile strength. These points are also shown in fig. 6.3. The averages of the flexural stiffness and the ultimate tensile strength for the specimens tested for each case is presented in Tables 6.8, 6.9, and 6.10.

The ultimate tensile strength and flexural stiffness were higher for the biocomposites that were prepared from epoxidized linseed oil compared to the biocomposites prepared from the epoxidized hempseed oil (Table 6.8). These higher mechanical properties of epoxidized linseed oil based biocomposites are due to higher %OOC of the epoxidized linseed oil.

Curing agent	Propyl citrate	
Epoxidized oil	Hempseed	Linseed
Ultimate tensile strength (N/mm^2)	33.4 ± 2.8	58.2 ± 2.1
Flexural stiffness (N/mm^2)	7.6 ± 0.9	10.6 ± 1.8
Resin content (%)	48.9	50.6
Density (g/cm^3)	1.0	1.1

Table 6.8 Flexural stiffness of biocomposite prepared by using epoxidized hempseed-linseed oils with propyl citrate curing agent

Similar superior mechanical properties were recorded for the biocomposites that were prepared by using ethyl and butyl citrates with epoxidized linseed oil vs hempseed oil. The biocomposites prepared from ethyl and propyl citrates were found to have better mechanical performance than the biocomposite prepared from butyl citrate. This could be due to the 14% of the plasticizing compound, dibutyl citrate, present in butyl citrate curing agent, and there were no such compounds present in other two CA-alkyl esters. This data is also in agreement with the Tg data from the DSC (Tables 6.5, 6.6 and 6.7). Despite having slightly different composition between ethyl and propyl citrates (Table 6.1), the ultimate tensile strength and flexural stiffness differences between these two biocomposites were within standard deviation. Such negligible difference could be because of a small carboxylic acid functionality difference between ethyl citrate (2.2) and propyl citrate (2.3).

Curing agent	Ethyl citrate	
Epoxidized oil	Hempseed	Linseed
Ultimate tensile strength (N/mm^2)	33.6 ± 1.6	60.9 ± 3.9
Flexural stiffness (N/mm^2)	7.6 ± 1.1	11.4 ± 1.5
Resin content (%)	42.4	49.0
Density (g/cm^3)	1.0	1.1

Table 6.9 Flexural stiffness of biocomposite prepared by using epoxidized hempseed/linseed oils with ethyl citrate curing agent

In spite of differences in the resin amounts, 6.4% for hempseed and 1.6% for linseed, the mechanical stiffnesses of the biocomposites were negligible (Table 6.8 and 6.9). Similarly, there were not significant density differences between biocomposites.

Curing agent	Butyl citrate	
Epoxidized oil	**Hempseed**	**Linseed**
Ultimate tensile strength (N/mm^2)	15.9 ± 0.8	37.67 ± 5.7
Flexural stiffness (N/mm^2)	5.4 ± 1.1	6.8 ± 1.3
Resin content (%)	45.4	44.9
Density (g/cm^3)	1.0	1.2

Table 6.10 Flexural stiffness of biocomposite prepared by using epoxidized hempseed/linseed oils with butyl citrate curing agent

The ultimate tensile strength of the biocomposites prepared from butyl citrate was the lowest among the 3 types of curing agents because of its composition (Table 6.1), which includes dibutyl citrate resulting in the lowest functionality. The density of biocomposites prepared from butyl citrate and hempseed epoxides was also the lowest at 0.98 g/cm^3 result in low crosslinking density polymer network, although this could also be possibly a result of sample preparation.

6.3.3 Dynamic mechanical analysis (DMA)

Figure 6.4 Test set up for DMA

Figure 6.4 illustrates the test set up for the DMA measurements. Fully biobased bioresins and biocomposites were prepared without the use of solvent. Once these objective, fully biobased and solvent-free process, had been achieved then systematically viscoelastic properties of these bioresins and biocomposites were measured by dynamic mechanical analyzer (Table 6.11). Each bioresin and biocomposite sample was prepared in duplicate and their properties were measured to investigate the effect of the biobased curing agent on the properties of the final cured samples. Since the butyl citrate curing agent has substantial amount of dibutyl citrate which act as a plasticizer [12], it was of interest to see what effect this has on the cured sample compared to cured materials prepared using ethyl and propyl citrates.

Curing agent	Tg (°C)					
	EC		PC		BC	
Epoxide	Hempseed	Linseed	Hempseed	Linseed	Hempseed	Linseed
Bioresins	41.9 ± 1.1	56.0 ± 0.5	45.7 ± 0.2	60.8 ± 0.5	39.7 ± 0.2	54.7 ± 0.6
Biocomposites	27.1 ± 0.6	41.0 ± 0.3	30.4 ± 0.2	44.2 ± 2.0	23.8 ± 1.1	37.5 ± 1.4

Table 6.11 Glass transition temperatures (Tg) of bioresins and biocomposites

The impacts of three different biobased curing agents on the final properties of the bioresins and biocomposites were significant. The curing agents used in this study was a mixture of two or more compounds as depicted in Table 6.1. First, the effect of the curing agent's composition was evaluated. One common compound present in these three curing agents was citric acid, although its amount in each curing agent was different. For instance, citric acid in ethyl citrate was 17.2%, propyl citrate 29.2%, and butyl citrate 22.0%. Therefore, theoretically, the higher citric acid content curing agent have higher functionality so it could produce material with highest Tg. At the same time, it is better to consider the overall functionality of the curing agent (Table 6.1) to make the predictions about the material properties. Using this assumption, the bioresin and biocomposite prepared by using propyl citrate should have the highest Tg, which is what was found in this study,

where the bioresin and biocomposite prepared from propyl citrate had a Tg of 60.8 and 44.2 °C, respectively when epoxidized linseed oil used. Similarly, when the epoxidized hempseed oil was used, the highest Tg for both bioresin and biocomposite were observed with propyl citrate, at 45.7 and 30.4 °C respectively. Thus, even though there are only small differences in carboxylic acid functionalities between 3 curing agents, the Tg and storage modulus of bioresins and biocomposites have significant differences. Such differences in mechanical properties could be partly due to the plasticizing effects from the non-reactive compounds present in the curing agents. Tri- and dialkyl citrates have functionality of 0 and 1, respectively, they are considered as plasticizer and contribute to lowering the Tg and storage modulus of the material. Since the butyl citrate contains the highest amount of these di- and tributyl citrates, material prepared from this curing agent possess the weaker mechanical performance than the other two material samples.
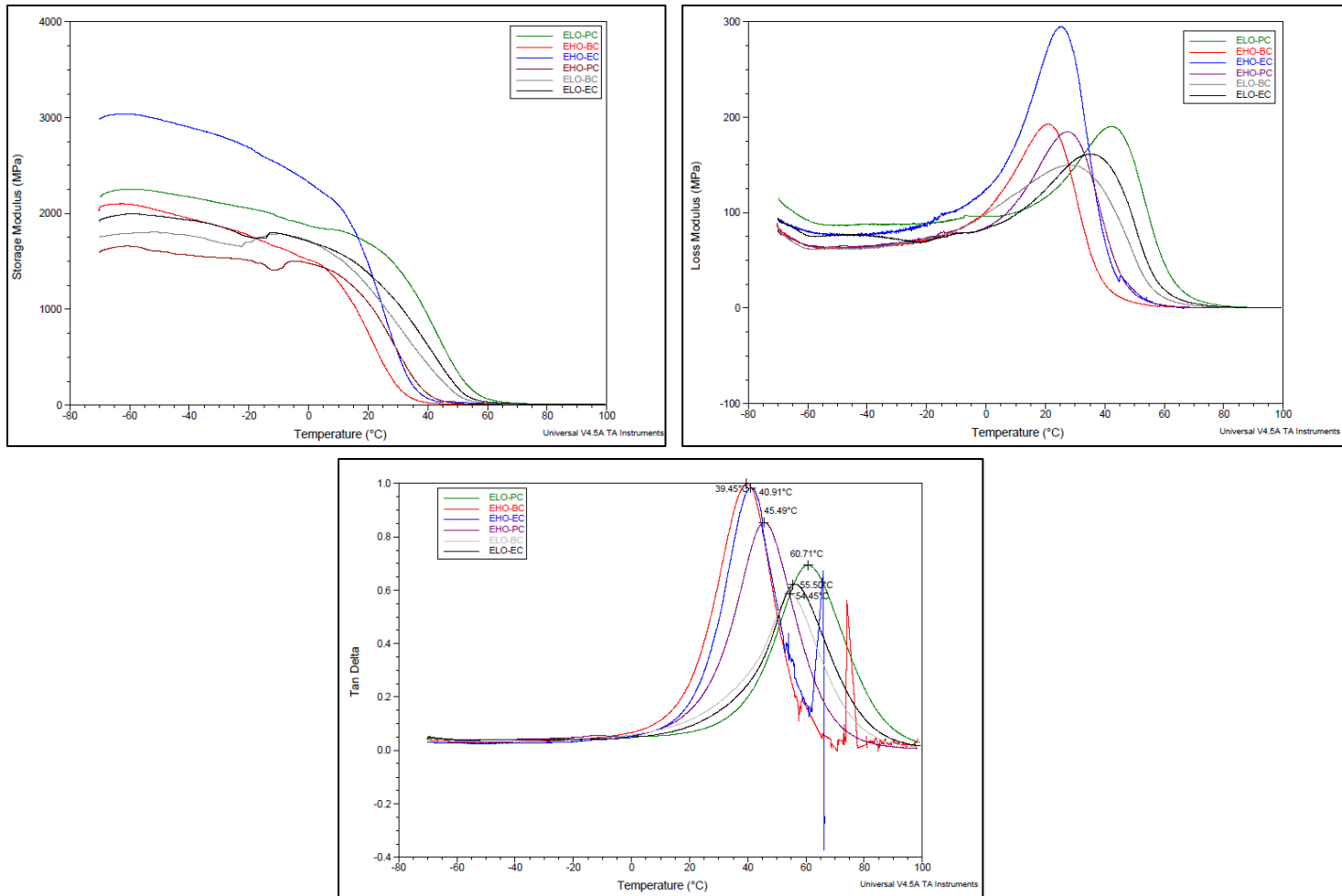
Figure 6.5 Bioresins - Storage (G') , loss (G") modulus, and Tan δ

Another possible justification for having the lower Tg and mechanical strengths of the materials prepared by using butyl citrate compared to ethyl- and propyl-citrates due to the difference is the carbon chain length. Butyl citrate contains 4 carbon compared to 2 and 3 for the ethyl- and propyl-citrates, respectively.
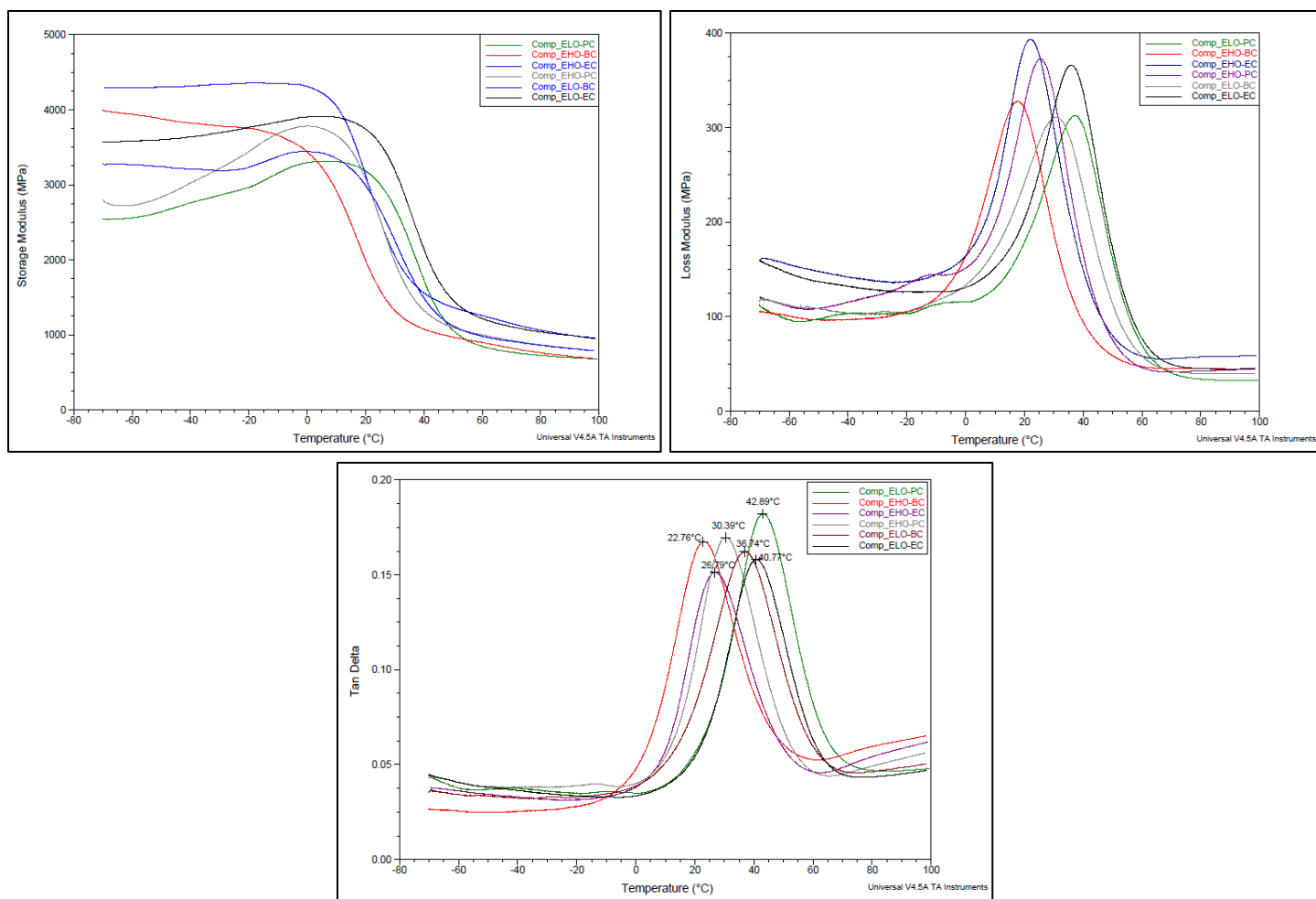
Figure 6.6 Biocomposites – Storage (G'), loss (G") modulus, and Tan δ

The viscoelastic behaviors of the bioresins are illustrated in Figure 6.5 with their storage and loss modulus, and tan delta curves. The bioresin's storage modulus from 20 to 40 °C was highest (~1800 MPa) for the epoxidized linseed oil with the ethyl and propyl citrates because of superior functionality as well as no plasticizing compound in both curing agents. In contrast, the storage modulus of the biocomposite (~500 MPa) prepared from butyl citrate and hempseed oil epoxide was the lowest (Figure 6.5). Similar effects were observed from the tan delta curves, and in addition the biocomposites prepared from linseed oil epoxide and ethyl and propyl citrates had the highest Tg (55.5 and 60.7 °C).

Similar viscoelastic behaviors were observed for the biocomposites such as the maximum storage modulus ~2800 MPa was recorded between 20 to 30 °C for the linseed epoxide with the ethyl and propyl citrates (Fig 6.6). Additionally, the viscoelastic properties and Tg values of bioresin and biocomposites were also in agreement.

Overall, these fully biobased resins possess properties that match with commercial resin products that are partially biobased. The *Super Sap resin* brand offers a range of epoxy resins and hardeners, and it is commercially produced by Entropy Resins [13], and all of their resins contain 21-30% biocontent by mass [14]. The properties of five commercial epoxy resins produced by entropy resins were reported [14], and some of the properties are comparable with the fully biobased resins prepared in this work. Super Sap resin's cure cycle at 25 °C is from 3 days to 10 days with a post cure recommended, while fully biobased resins cure between 2 (tack-free state) to 15 (fully cured) days. The cured Super Sap resin's Tg (DSC) are between 63 °C and 115 °C [13,14], while the fully biobased resin's (ELO/PC) Tg is 52 °C is achieved in this work.

A resole prepolymer was synthesized from cardanol (a phenolic by-product of cashew nut industry) and diglycidyl ether of bisphenol A (DGEBA) to prepare a thermoset resin, and such resin used to prepare biocomposites [15]. These resin contains 40% biobased cardanol, and their Tg (DMA) was in a range of 42-56 °C while using silane compound as curing agent in presence of amine catalyst [15]. In contrast, the Tg (DMA) in a range of 39 to 60 °C of fully biobased resins prepared from epoxidized plant oils and CA-alkyl esters curing agents. Additionally, the tensile strength of biocomposites prepared from 40% biobased phenolic resin was in a range of 9 to 20 MPa [15], and the biocomposites prepared from fully biobased resin possess tensile strength in a range of 15 to 60 MPa (Tables 6.8,6.9,6.10).

6.4 Conclusion

Novel biobased curing agents were developed and used to prepare bioresins and biocomposites without the use of solvent. Differential scanning calorimetry (DSC) data was used to determine the optimum epoxy to carboxyl acid groups ratios. It was found that epoxy group to carboxylic acid groups ratios between 1.40 to 1.80 or about epoxide to curing agents 1:0.4 (w/w) for all formulations. It was also concluded that these formulations are curing at room temperature (25 °C) and reach to the level of curing where samples cured at elevated temperatures in about 2 weeks. Additionally, the glass transition temperature was highest for the formulations which has higher amount of free citric acid and minimum amounts of di-and tri-alkyl citrates. The bioresins and biocomposites viscoelastic properties and 3-point bend test data are also in the agreement with the DSC data.

The fully biobased bioresins and biocomposites possess properties that are comparable to some of the commercial partially biobased resins, for instance the Super Sap brand resin from Entropy Resins. Additionally, these commercial resins contain 28% biocontent and their retail price is about $30/kg [13]. In contrast, these fully biobased resins can be produced for a predicted price of under $15/kg. Moreover, there are some other biobased resins synthesized from natural phenolic feedstock, cardanol, to prepared biocomposites. The properties, Tg and tensile strength, of fully biobased biocomposites were higher than the one prepared by using natural phenolic resins. These fully biobased bioresins prepared from novel hardeners and epoxidized plant oils could replace some of the commercial resins and partially biobased resins.

6.5 References

[1] Kuhns, Roger James, and George H. Shaw. "Peak Oil and Petroleum Energy Resources." *Navigating the Energy Maze: The Transition to a Sustainable Future*, edited by Roger James Kuhns and George H. Shaw, Springer International Publishing, 2018, pp. 53–63. *Springer Link*, https://doi.org/10.1007/978-3-319-22783-2_7.

[2] Yildizhan, Fatih Selim. "A Technical and Industrial Analysis of Global Plastics Market, Trade, Financing, and Operations." *ScienceOpen Preprints*, Jan. 2021. *www.scienceopen.com*, doi:10.14293/S2199-1006.1.SOR-.PPDUNRN.v1.

[3] Pham, Ha Q., and Maurice J. Marks. "Epoxy Resins." *Ullmann's Encyclopedia of Industrial Chemistry*, American Cancer Society, 2005. *Wiley Online Library*, https://onlinelibrary-wiley-com.login.ezproxy.library.ualberta.ca/doi/abs/10.1002/14356007.a09_547.pub2.

[4] Jin, Fan-Long, et al. "Synthesis and Application of Epoxy Resins: A Review." *Journal of Industrial and Engineering Chemistry*, vol. 29, Sept. 2015, pp. 1–11. *ScienceDirect*, doi:10.1016/j.jiec.2015.03.026.

[5] Vom Saal, Frederick S., and Laura N. Vandenberg. "Update on the Health Effects of Bisphenol A: Overwhelming Evidence of Harm." *Endocrinology*, vol. 162, no. 3, Mar. 2021. *academic.oup.com*, doi:10.1210/endocr/bqaa171.

[6] Galankis, Charis M. *Biobased Products and Industries*. Elsevier, 2020. University of Alberta Internet Internet Access, *EBSCOhost*, https://login.ezproxy.library.ualberta.ca/login?url=https://search.ebscohost.com/login.aspx?direct=true&db=cat03710a&AN=alb.8927031&site=eds-live&scope=site.

[7] Reddy, Gopal, et al. "Amylolytic Bacterial Lactic Acid Fermentation — A Review." *Biotechnology Advances*, vol. 26, no. 1, Jan. 2008, pp. 22–34. *ScienceDirect*, doi:10.1016/j.biotechadv.2007.07.004.

[8] Babu, Ramesh P., et al. "Current Progress on Bio-Based Polymers and Their Future Trends." *Progress in Biomaterials*, vol. 2, no. 1, Mar. 2013, p. 8. *Springer Link*, doi:10.1186/2194-0517-2-8.

[9] S. Omonov, Tolibjon, et al. "The Epoxidation of Canola Oil and Its Derivatives." *RSC Advances*, vol. 6, no. 95, 2016, pp. 92874–86. *pubs-rsc-org.login.ezproxy.library.ualberta.ca*, doi:10.1039/C6RA17732H.

[10] Baroncini, Elyse A., et al. "Recent Advances in Bio-Based Epoxy Resins and Bio-Based Epoxy Curing Agents." *Journal of Applied Polymer Science*, vol. 133, no. 45, 2016. *Wiley Online Library*, doi:https://doi.org/10.1002/app.44103.

[11] Omonov, Tolibjon S., et al. "The Development of Epoxidized Hemp Oil Prepolymers for the Preparation of Thermoset Networks." *Journal of the American Oil Chemists' Society*, vol. 96, no. 12, 2019, pp. 1389–403. *Wiley Online Library*, doi:https://doi.org/10.1002/aocs.12290.

[12] Ljungberg, Nadia, and Bengt Wesslén. "Tributyl Citrate Oligomers as Plasticizers for Poly (Lactic Acid): Thermo-Mechanical Film Properties and Aging." *Polymer*, vol. 44, no. 25, Dec. 2003, pp. 7679–88. *ScienceDirect*, doi:10.1016/j.polymer.2003.09.055.

[13] "Entropy Resins | Biobased Epoxy Resins | Learn More." *Entropy Resins*, https://entropyresins.com/. Accessed 31 May 2021.

[14] D. Ray, S. Sain. "Thermosetting Bioresins as Matrix for Biocomposites." *Biocomposites for High-Performance Applications*, Jan. 2017, pp. 57–80. *www-sciencedirect-com.login.ezproxy.library.ualberta.ca*, doi:10.1016/B978-0-08-100793-8.00003-X.

[15] Maffezzoli, Alfonso, et al. "Cardanol Based Matrix Biocomposites Reinforced with Natural Fibres." *Composites Science and Technology*, vol. 64, no. 6, May 2004, pp. 839–45. *ScienceDirect*, doi:10.1016/j.compscitech.2003.09.010.

Chapter 7

General Conclusion and Future Work

7.1 General conclusion

The high biocontent bioresins could replace some of the existing synthetic resins as well as they could be used for new applications like wood and other coatings. These biobased materials could accelerate the transition to meet the sustainability goals by fulfilling the circular economy concept.

In this thesis, fully biobased plant oil epoxides and citric acid were used to prepare high biocontent bioresins and biocomposites via a solvent-free manufacturing process. To achieve these criteria, two approaches were adopted: 1. modification of plant oil epoxide and 2. modification of citric acid. The mechanical and thermomechanical performances of bioresins and biocomposites prepared from various plant oil epoxides (canola, hemp, and linseed) were tested (Chapter 2 & 4). As expected, the bioresins made using higher %OOC epoxides (hemp and linseed) have better mechanical performance than bioresins prepared from lower %OOC epoxides (canola), as indicated by their modulus of rupture and elasticity, and their Tg values. Additionally, it was confirmed that the high %OOC epoxide (linseed) are more reactive than the low %OOC epoxides (hemp) (Chapter 3). Since the linseed oil epoxide was reactive, the mechanical and thermomechanical performances of bioresins and biocomposites were not maximum compared to hemp oil epoxide. That is why, a systematic blends of low %OOC canola and high %OOC linseed epoxides were prepared and used them to prepare bioresins and biocomposites (Chapter-2). It was discovered that the bioresins and biocomposites prepared from an ELO/ECO epoxide blend in range of 80/20 to 60/40 shown the highest mechanical performances that were comparable with

the materials prepared from EHO. From this study, it can be concluded that the EHO can be replaced with the blend of ELO/ECO. Such blends of epoxides reduced the average %OOC to the level of EHO, and they can cure at slower rate resulting in a highly crosslinked polymer network. Both of these studies (Chapters 2 and 3) were conducted in presence of solvent: acetone, as the epoxides and curing agents are not miscible. It is an important and necessary requirement to have a one phase epoxide-curing agent mixture in order to crosslink these monomers with the curing agents.

Many synthetic epoxy systems are solvent free, but they are prepared from nonrenewable feedstocks that have higher carbon footprints. Plant oils and citric acid are fully biobased feedstocks that could be utilized to replace some of these synthetic epoxy resins. There are various multifunctional carboxylic acids that could be used as curing agents, but citric acid was used in this thesis because of the combination of the following features: 1. it is biobased; 2. it is multifunctional with the three carboxylic acids; 3. it is produced in large scale at low cost. However, plant oils and citric acid are not miscible, so they were modified through simple processes: transesterification of plant oil epoxides (Chapter 4) and monoesterification of citric acid (Chapter 5). Epoxidized linseed oil converted into linseed oil methyl esters becomes a low viscosity reactive diluent, capable of dissolving the curing agent at elevated temperatures (100 °C). Then, crosslinking occurs while dissolving the curing agent in linseed oil methyl esters, and this increases the mixtures viscosity. As a result, this system has a limited pot life, and so it may not be suitable for the majority of applications.

As an alternative, novel fully biobased curing agent mixtures were synthesized from citric acid via a simple process (Chapter 5), so that these would be compatible with the plant oil epoxides. This process produces a mixture that contains 4 possible components: unreacted citric acid, mono-

, di- and trialkyl citrates. Of these, the di- and trialkyl citrates do not participate in the crosslinking reaction, and they act as plasticizers and responsible for the low Tg and flexure strength materials. These components were therefore quantified via HPLC-ELSD so that these important criteria could be optimized in the reaction. The esterification reaction, that was aimed at maximizing the formation of mono-esters while the di- and trialkyl citrate formation are minimized or avoided. These was achieved by controlling the reaction temperature and time, and the citric acid to alcohol molar ratios. The optimum epoxy to carboxylic acid groups ratios were found to be in the range of 1.40 to 1.80 or epoxides to curing agent ratios were 1:0.4 (w/w). These ratios were important because they produced the strongest materials as demonstrated by measurements of their flexural modulus, yield strength, storage and loss modulus (Chapter-6). Utilizing these optimum ratios, bioresins and biocomposites with up to 100% biocontent were prepared via a solvent free manufacturing process (Chapter 6). The mechanical and thermomechanical performances suggests that they could be used to replace petrochemical resins in composites manufacturing. In addition, it could be used for other applications such as coatings for wood and other materials.

This thesis demonstrated the importance of miscibility between the plant oil epoxides and the curing agents developed in this thesis. This characteristic not only makes it possible to prepare bioresins and biocomposites via a solvent free process, but also making the production of high biocontent materials. Such a solvent-free manufacturing process and up to 100% biocontent materials could be produced with a low global warming potential impact. These high bio- and solid- content formulations could be used for woodworking and coating applications to replace synthetic resins.

The recyclability of products made from thermosetting resins is a big challenge. This is because if they are not recycled at the end of their service life, they slowly decompose in the land and water

releasing microplastics and other pollutants. There are not any efficient and cost effective solutions for this challenge, but one of the potential solution could be biodegradable materials. However, highly crosslinked thermoset resins may be difficult to depolymerize and biodegrade. Therefore, a future study of biodegradability behavior data of bioresins would be highly desirable.

In this thesis, an attempt has been made to reduce the overall carbon footprint of these materials by implementing many of the 12 green chemistry principals in manufacturing of bioresins and biocomposites.

1. Prevention

As described in sections 1.2 and 1.3, bioresins can be prepared from two components: epoxides and curing agents. Plant oil epoxidation process is not generating any hazardous waste except the acidic wash water that is used to remove the formic acid catalyst from the product.

The novel curing agent synthesized in this thesis is not generating any waste except a by-product of water.

2. Atom economy

By using the following atom economy formula, the atom economy to produce an epoxidized oil is about 75% and to produce novel biobased curing agent (ethyl citrates) is about 66%. The 25% lost atom efficiency in plant oil epoxidation process is due to the excess amount of hydrogen peroxide required for the reaction. Additionally, hydrogen peroxide decomposes to water and oxygen, so it produces harmless waste. In case of citric acid esterification, the atom efficiency of 66% calculated based on the consideration that the excess amount of ethanol not reused or

recycled. If the excess amount of ethanol is recycled then the atom efficiency of this reaction would be about 90%.

% Atom Economy = (MW of atoms utilised / MW of all reactants) * 100

For instance,

a. 1 mole canola oil, 6 moles of hydrogen peroxide and 1 mole of formic acid can produce 1 mole of epoxidized oil.

$$\text{Therefore, \% Atom economy} = \left[\frac{944}{933 + 34 + 6(46)}\right] \times 100$$

Where, MW of epoxidized canola oil = 944

MW of canola oil = 933

MW of hydrogen peroxide = 34

MW of formic acid = 46

b. 1 mole of citric acid and 2 moles of ethanol can produce 1 mole of novel biobased curing agent.

$$\text{Therefore, \% Atom economy} = \left[\frac{230}{192 + 2(78.4)}\right] \times 100$$

Where, MW of ethyl citrates = 230

MW of citric acid = 192

MW of ethanol = 78.4

3. Less hazardous chemical syntheses

The plant oil epoxides and biobased curing agents are produced without any hazardous chemicals.

4. Designing safer chemicals

Since we do not have performed any toxicity studies on these materials, but the feedstocks used are nontoxic and do not have any adverse human health effects.

5. Safer solvents and auxiliaries

The epoxidation of plant oils and esterification of citric acid processes are solvent free and do not generating any intermediate that are not safe. Ethanol….as solvent and reactant…

6. Design for energy efficiency

We do not have any data to claim the exact efficiency of these processes but both process parameters are mild: Epoxidation at 60 °C and esterification to make ethyl citrates at 90 °C.

7. Use of renewable feedstocks

Plant oils, citric acid, and ethanol are renewable feedstocks.

8. Reduce derivatives

Both processes (epoxidation of plant oils and esterification of citric acid) are single step process without any intermediate or derivatization to make the final product.

9. Catalysis

The epoxidation process is catalyzed by acidic catalyst (formic acid) that promote the reaction and that ultimately reduces reaction inputs without compromising the yield.

The citric acid esterification is self-catalyzing reaction means that the citric acid itself act as a catalyst to promote the reaction.

10. Design for degradation

This thesis has no data on degradation.

11. Real-time analysis for pollution prevention

This thesis has not looked into the real time data analysis.

12. Inherently safer chemistry for accident prevention

Neither of the synthetic steps produce any hazardous gas or byproduct during the process. The hydrogen peroxide needs to be handled with care to prevent explosion, but such procedures are widely practiced commercially.

7.2 Future work

This thesis has demonstrated some of the ways to prepare high biocontent thermoset materials, such as through the discovery of novel biobased curing agents. The novel feature of the CA-alkyl ester curing agents is their solubility in plant oil epoxides. The reason for such solubility could be due to the intrinsic surfactant effect of the mono- and di-alkyl citrates, and they could enhance the solubilizing citric acid to form a homogeneous mixture. Future work could confirm this hypothesis through a systematic study of the surfactant properties of mono-, di- and trialkyl citrates with citric acid. Additionally, it could make possible the synthesis of the lowest viscosity of CA-alkyl esters that contain the maximum amount of citric acid.

Many other potential new applications of fully biobased bioresins which could be explored. For example, wood and floor coatings require superior performance, such as high abrasion resistance. This. could be achieved if aromatic biobased curing agents were used to formulate partially biobased resins, so producing materials with the additional rigidity and mechanical performance required.

Thesis Bibliography

[1] "Resin | Chemical Compound." *Encyclopedia Britannica*,
https://www.britannica.com/science/resin. Accessed 27 May 2020.

[2] *How Plastics Are Made*. https://plastics.americanchemistry.com/How-Plastics-Are-Made/.
Accessed 27 May 2020.

[3] *Types of Resins and Their Uses and Applications*.
https://www.thomasnet.com/articles/plastics-rubber/types-of-resins. Accessed 27 May 2020.

[4] *Bioresins Suppliers*.
http://polymerdatabase.com/Polymer%20Brands/Bioplastic%20Suppliers.html. Accessed 29
May 2020.

[5] McKeon, Thomas, et al. *Industrial Oil Crops*. Elsevier, 2016.

[6] Zhang, Chaoqun, et al. "Recent Advances in Vegetable Oil-Based Polymers and Their
Composites." *Progress in Polymer Science*, vol. 71, Aug. 2017, pp. 91–143. *ScienceDirect*,
doi:10.1016/j.progpolymsci.2016.12.009.

[7] Miao, Shida, et al. "Vegetable-Oil-Based Polymers as Future Polymeric Biomaterials." *Acta
Biomaterialia*, vol. 10, no. 4, Apr. 2014, pp. 1692–704. *ScienceDirect*,
doi:10.1016/j.actbio.2013.08.040.

[8] Anderson, Dan, et al. "A Primer on Oils Processing Technology." *Bailey's Industrial Oil and
Fat Products*, American Cancer Society, 2020, pp. 1–47. *Wiley Online Library*,
https://onlinelibrary-wiley-
com.login.ezproxy.library.ualberta.ca/doi/abs/10.1002/047167849X.bio077.pub2.

[9] Wan, Peter J., and Phillip J. Wakelyn. *Technology and Solvents for Extracting Oilseeds and
Nonpetroleum Oils*. The American Oil Chemists Society, 1997.

[10] S. Omonov, Tolibjon, et al. "The Epoxidation of Canola Oil and Its Derivatives." *RSC
Advances*, vol. 6, no. 95, 2016, pp. 92874–86. *pubs-rsc-
org.login.ezproxy.library.ualberta.ca*, doi:10.1039/C6RA17732H.

[11] Ellis, B. "Introduction to the Chemistry, Synthesis, Manufacture and Characterization of Epoxy Resins." *Chemistry and Technology of Epoxy Resins*, edited by Bryan Ellis, Springer Netherlands, 1993, pp. 1–36. *Springer Link*, https://doi.org/10.1007/978-94-011-2932-9_1.

[12] Tayde Saurabh, Patnaik M., Bhagt S.L., Renge V.C. "Epoxidation of Vegetable Oils: A Review." *International Journal of Advanced Engineering Technology*, vol. II, no. IV, Dec. 2011, pp. 491–501.

[13] Mungroo, Rubeena, et al. "Epoxidation of Canola Oil with Hydrogen Peroxide Catalyzed by Acidic Ion Exchange Resin." *Journal of the American Oil Chemists' Society*, vol. 85, no. 9, 2008, pp. 887–96. *Wiley Online Library*, doi:10.1007/s11746-008-1277-z.

[14] Roy, Arindam Sinha, et al. "An Overview of Production, Properties, and Uses of Biodiesel from Vegetable Oil." *Green Fuels Technology: Biofuels*, edited by Carlos Ricardo Soccol et al., Springer International Publishing, 2016, pp. 83–105. *Springer Link*, https://doi.org/10.1007/978-3-319-30205-8_4.

[15] Turco, Rosa, et al. "Comparison of Different Possible Technologies for Epoxidation of Cynara Cardunculus Seed Oil." *European Journal of Lipid Science and Technology*, vol. 122, no. 1, 2020, p. 1900100. *Wiley Online Library*, doi:10.1002/ejlt.201900100.

[16] Goud, Vaibhav V., et al. "Epoxidation of Karanja (Pongamia Glabra) Oil Catalysed by Acidic Ion Exchange Resin." *European Journal of Lipid Science and Technology*, vol. 109, no. 6, June 2007, pp. 575–84. *onlinelibrary-wiley-com.login.ezproxy.library.ualberta.ca*, doi:10.1002/ejlt.200600298.

[17] La Scala, John, and Richard P. Wool. "Effect of FA Composition on Epoxidation Kinetics of TAG." *Journal of the American Oil Chemists' Society*, vol. 79, no. 4, Apr. 2002, pp. 373–78. *Springer Link*, doi:10.1007/s11746-002-0491-9.

[18] Ashcroft, W. R. "Curing Agents for Epoxy Resins." *Chemistry and Technology of Epoxy Resins*, edited by Bryan Ellis, Springer Netherlands, 1993, pp. 37–71. *Springer Link*, https://doi.org/10.1007/978-94-011-2932-9_2.

[19] Mikulcová, Veronika, et al. "Formulation, Characterization and Properties of Hemp Seed Oil and Its Emulsions." *Molecules : A Journal of Synthetic Chemistry and Natural Product Chemistry*, vol. 22, no. 5, Apr. 2017. *PubMed Central*, doi:10.3390/molecules22050700.

[20] Frischinger, Isabelle, and Stoil Dirlikov. "Toughening of Epoxy Resins by Epoxidized Soybean Oil." *Toughened Plastics I*, vol. 233, American Chemical Society, 1993, pp. 451–89. *ACS Publications*, https://doi.org/10.1021/ba-1993-0233.ch019.

[21] Niedermann, Péter, et al. "Effect of Epoxidized Soybean Oil on Curing, Rheological, Mechanical and Thermal Properties of Aromatic and Aliphatic Epoxy Resins." *Journal of Polymers and the Environment*, vol. 22, no. 4, Dec. 2014, pp. 525–36. *Springer Link*, doi:10.1007/s10924-014-0673-8.

[22] Kumar, Sudheer, et al. "Toughening of Petroleum Based (DGEBA) Epoxy Resins with Various Renewable Resources Based Flexible Chains for High Performance Applications: A Review." *Industrial & Engineering Chemistry Research*, vol. 57, no. 8, Feb. 2018, pp. 2711–26. *ACS Publications*, doi:10.1021/acs.iecr.7b04495.

[23] Mustapha, Rohani, et al. "Vegetable Oil-Based Epoxy Resins and Their Composites with Bio-Based Hardener: A Short Review." *Polymer-Plastics Technology and Materials*, vol. 58, no. 12, Aug. 2019, pp. 1311–26. *Taylor and Francis+NEJM*, doi:10.1080/25740881.2018.1563119.

[24] Ding, Cheng, and Avtar S. Matharu. "Recent Developments on Biobased Curing Agents: A Review of Their Preparation and Use." *ACS Sustainable Chemistry & Engineering*, vol. 2, no. 10, Oct. 2014, pp. 2217–36. *ACS Publications*, doi:10.1021/sc500478f.

[25] Baroncini, Elyse A., et al. "Recent Advances in Bio-Based Epoxy Resins and Bio-Based Epoxy Curing Agents." *Journal of Applied Polymer Science*, vol. 133, no. 45, 2016. *Wiley Online Library*, doi:10.1002/app.44103.

[26] Peng, Changgeng, et al. "The Hygroscopic Properties of Dicarboxylic and Multifunctional Acids: Measurements and UNIFAC Predictions." *Environmental Science & Technology*, vol. 35, no. 22, Nov. 2001, pp. 4495–501. *ACS Publications*, doi:10.1021/es0107531.

[27] Tsao, G. T., et al. "Production of Multifunctional Organic Acids from Renewable Resources." *Recent Progress in Bioconversion of Lignocellulosics*, edited by G. T. Tsao et al., Springer Berlin Heidelberg, 1999, pp. 243–80. *Springer Link*, https://doi.org/10.1007/3-540-49194-5_10.

[28] Ma, Songqi, and Dean C. Webster. "Naturally Occurring Acids as Cross-Linkers To Yield VOC-Free, High-Performance, Fully Bio-Based, Degradable Thermosets." *Macromolecules*, vol. 48, no. 19, Oct. 2015, pp. 7127–37. *ACS Publications*, doi:10.1021/acs.macromol.5b01923.

[29] Rizzi, George P., and Harry M. Taylor. "A Solvent-Free Synthesis of Sucrose Polyesters." *Journal of the American Oil Chemists' Society*, vol. 55, no. 4, 1978, pp. 398–401. *Wiley Online Library*, doi:10.1007/BF02911900.

[30] Monono, Ewumbua M., et al. "Pilot Scale (10kg) Production and Characterization of Epoxidized Sucrose Soyate." *Industrial Crops and Products*, vol. 74, Nov. 2015, pp. 987–97. *ScienceDirect*, doi:10.1016/j.indcrop.2015.06.035.

[31] *Sustainable Synthetic Approaches for the Preparation of Plant Oil-Based Thermosets | SpringerLink*. https://link-springer-com.login.ezproxy.library.ualberta.ca/article/10.1007/s11746-016-2932-4. Accessed 15 May 2020.

[32] Omonov, Tolibjon, and Jonathan Curtis. *Aldehyde Free Thermoset Bioresins and Biocomposites*. US20160215088A1, 28 July 2016, https://patents.google.com/patent/US20160215088A1/en.

[33] Li, Yantao, et al. "Synthesis and Characterization of Cast Resin Based on Different Saturation Epoxidized Soybean Oil." *European Journal of Lipid Science and Technology*, vol. 112, no. 4, Apr. 2010, pp. 511–16. *onlinelibrary-wiley-com.login.ezproxy.library.ualberta.ca*, doi:10.1002/ejlt.200900191.

[34] Fache, Maxence, et al. "Biobased Epoxy Thermosets from Vanillin-Derived Oligomers." *European Polymer Journal*, vol. 68, July 2015, pp. 526–35. *ScienceDirect*, doi:10.1016/j.eurpolymj.2015.03.048.

[35] Jian, Xin-Yi, et al. "All Plant Oil Derived Epoxy Thermosets with Excellent Comprehensive Properties." *Macromolecules*, vol. 50, no. 15, Aug. 2017, pp. 5729–38. *ACS Publications*, doi:10.1021/acs.macromol.7b01068.

[36] Pascault, Jean-Pierre, and Roberto J. J. Williams. *Epoxy Polymers: New Materials and Innovations*. John Wiley & Sons, 2009 pp. 215-230.

[37] Wool, Richard, et al. *High Modulus Polymers and Composites from Plant Oils*. US6121398A, 19 Sept. 2000, https://patents.google.com/patent/US6121398A/en.

[38] Lu, Yongshang, and Richard C. Larock. "Novel Polymeric Materials from Vegetable Oils and Vinyl Monomers: Preparation, Properties, and Applications." *ChemSusChem*, vol. 2, no. 2, Feb. 2009, pp. 136–47. *chemistry-europe-onlinelibrary-wiley-com.login.ezproxy.library.ualberta.ca (Atypon)*, doi:10.1002/cssc.200800241.

[39] Zhou, Yonghui, et al. "Interface and Bonding Mechanisms of Plant Fibre Composites: An Overview." *Composites Part B: Engineering*, vol. 101, Sept. 2016, pp. 31–45. *Crossref*, doi:10.1016/j.compositesb.2016.06.055.

[40] Sushanta K. Sahoo, Smita Mohanty, Sanjay K. Nayak. (2015). "Effect of lignocellulosic fibers on mechanical, thermomechanical and hydrophilic studies of epoxy modified with novel bioresin epoxy methyl ester derived from soybean oil." *Polymers Advanced Technologies*, 2015, 26 1619-1626.

[41] Rudi Dungani, Myrtha Karina, Subyakto, A. Sulaeman, Dede Hermawan and A. Hadiyane. "Agricultural Waste Fibers Towards Sustainability and Advanced Utilization: A Review." *Asian Journal of Plant Sciences*, vol. 15, no. 1–2, 2016, pp. 42–55.

[42] John, Maya Jacob, and Rajesh D. Anandjiwala. "Recent Developments in Chemical Modification and Characterization of Natural Fiber-Reinforced Composites." *Polymer Composites*, vol. 29, no. 2, 2008, pp. 187–207. *Wiley Online Library*, doi:10.1002/pc.20461.

[43] Célino, Amandine, et al. "Characterization and Modeling of the Moisture Diffusion Behavior of Natural Fibers." *Journal of Applied Polymer Science*, vol. 130, no. 1, 2013, pp. 297–306. *Wiley Online Library*, doi:10.1002/app.39148.

[44] Council, National Research, et al. *High Performance Synthetic Fibers for Composites*. National Academies Press, 1992.

[45] Monteiro, Sergio Neves, et al. "Natural-Fiber Polymer-Matrix Composites: Cheaper, Tougher, and Environmentally Friendly." *JOM*, vol. 61, no. 1, Jan. 2009, pp. 17–22. *Springer Link*, doi:10.1007/s11837-009-0004-z.

[46] Chen, Hongzhang. "Chemical Composition and Structure of Natural Lignocellulose." *Biotechnology of Lignocellulose: Theory and Practice*, edited by Hongzhang Chen, Springer Netherlands, 2014, pp. 25–71. *Springer Link*, https://doi.org/10.1007/978-94-007-6898-7_2.

[47] Fuqua, Michael A., et al. "Natural Fiber Reinforced Composites." *Polymer Reviews*, vol. 52, no. 3, July 2012, pp. 259–320. *Taylor and Francis+NEJM*, doi:10.1080/15583724.2012.705409.

[48] Savita Dixit, Ritesh Goel, Akash Dubey, Price Raj Shivhare, Tanmay Bhalavi. (2017). "Natural fiber reinforced polymer composite materials - A review" *Polymers from renewable resources*, Vol 8, No. 2, January 2017: 71-77.

[49] Maya Jacob John, Sabu Thomas. (2007)."Review: Biofibres and biocomposites" *Carbohydrate Polymers* 71 (2008) 343-364.

[50] A. Ticoalu, T. Aravinthan, F. Cardona. (2010). "A review of current development in natural fiber composites for structural and infrastructure applications." *Southern Region Engineering Conference*, 11-12 November 2010, Toowoomba, Australia.

[51] Alejandrina Campanella, Mingjiang Zhan, Paula Watt, Alexander T. Grous, Connie Shen, Richard P. Wool. (2015). "Triglyceride-based thermosetting resins with different reactive diluents and fiber reinforced composite applications." *Composites: Part A*, 72 (2015) 192-199.

[52] Marie-Alix Berthet, Claire Mayer-Laigle, Xavier Rouau, Nathalie Gontard, Helene Angellier-Coussy. 2017. "Sorting natural fibers: A way to better understand the role of fiber size polydispersity on the mechanical properties of biocomposites." *Composites Part A: Applied Science and Manufacturing*, 95 (2017): 12-21.

[53] George, Jayamol, et al. "A Review on Interface Modification and Characterization of Natural Fiber Reinforced Plastic Composites." *Polymer Engineering & Science*, vol. 41, no. 9, 2001, pp. 1471–85. *Wiley Online Library*, doi:10.1002/pen.10846.

[54] Wu, Yingji, et al. "Water-Resistant Hemp Fiber-Reinforced Composites: In-Situ Surface Protection by Polyethylene Film." *Industrial Crops and Products*, vol. 112, Feb. 2018, pp. 210–16. *ScienceDirect*, doi:10.1016/j.indcrop.2017.12.014.

[55] Ma, Songqi, et al. "Research Progress on Bio-Based Thermosetting Resins." *Polymer International*, vol. 65, no. 2, 2016, pp. 164–73. *Wiley Online Library*, doi:10.1002/pi.5027.

[56] Jin, Fan-Long, et al. "Synthesis and Application of Epoxy Resins: A Review." *Journal of Industrial and Engineering Chemistry*, vol. 29, Sept. 2015, pp. 1–11. *ScienceDirect*, doi:10.1016/j.jiec.2015.03.026.

[57] Paramarta, Adlina, and Dean C. Webster. "Bio-Based High Performance Epoxy-Anhydride Thermosets for Structural Composites: The Effect of Composition Variables." *Reactive and Functional Polymers*, vol. 105, Aug. 2016, pp. 140–49. *ScienceDirect*, doi:10.1016/j.reactfunctpolym.2016.06.008.

.[58] Chen, X. M., and B. Ellis. "Coatings and Other Applications of Epoxy Resins." *Chemistry and Technology of Epoxy Resins*, edited by Bryan Ellis, Springer Netherlands, 1993, pp. 303–25. *Springer Link*, https://doi.org/10.1007/978-94-011-2932-9_9.

[59] Shaw, S. J. "Epoxy Resin Adhesives." *Chemistry and Technology of Epoxy Resins*, edited by Bryan Ellis, Springer Netherlands, 1993, pp. 206–55. *Springer Link*, https://doi.org/10.1007/978-94-011-2932-9_7.

[60] *What Is Epoxy Paint? - Bright Hub Engineering*. https://www.brighthubengineering.com/building-construction-design/63632-characteristics-of-epoxy-paint-and-thinner/. Accessed 21 May 2020.

[61] Atul Tiwari, Anthony Galanis, and Mark D. Soucek. *Biobased and Environmental Benign Coatings*. 1st ed., John Wiley & Sons, Ltd, 2016. *Wiley Online Library*,

https://onlinelibrary-wiley-com.login.ezproxy.library.ualberta.ca/doi/10.1002/9781119185055. pp 121-140.

[62] Kovash Jr., Curtiss S., et al. "Thermoset Coatings from Epoxidized Sucrose Soyate and Blocked, Bio-Based Dicarboxylic Acids." *ChemSusChem*, vol. 7, no. 8, Aug. 2014, pp. 2289–94. *chemistry-europe-onlinelibrary-wiley-com.login.ezproxy.library.ualberta.ca (Atypon)*, doi:10.1002/cssc.201402091.

[63] Teaca, Carmen, Dan Roşu, Fănică Mustaţă, Teodora Rusu, Liliana Roşu, Irina Roşca, & Cristian-Dragoş Varganici. "Natural Bio-Based Products for Wood Coating and Protection against Degradation: A Review." *BioResources* [Online], 14.2 (2019): 4873-4901. Web. 22 May. 2020

[64] Edward M. Petrie. Handbook of Adhesives and Sealants, Second Edition. AN OVERVIEW OF ADHESIVES AND SEALANTS, Chapter (The McGraw-Hill Companies, Inc., 2007). https://www-accessengineeringlibrary-com.login.ezproxy.library.ualberta.ca/content/book/9780071479165/chapter/chapter1

[65] Magalhães, Solange, et al. "Brief Overview on Bio-Based Adhesives and Sealants." *Polymers*, vol. 11, no. 10, Oct. 2019, p. 1685. *www.mdpi.com*, doi:10.3390/polym11101685.

[66] Kong, Xiaohua, et al. "Characterization of Canola Oil Based Polyurethane Wood Adhesives." *International Journal of Adhesion and Adhesives*, vol. 31, no. 6, Sept. 2011, pp. 559–64. *ScienceDirect*, doi:10.1016/j.ijadhadh.2011.05.004.

[67] Maassen, Wiebke, et al. "Unique Adhesive Properties of Pressure Sensitive Adhesives from Plant Oils." *International Journal of Adhesion and Adhesives*, vol. 64, Jan. 2016, pp. 65–71. *ScienceDirect*, doi:10.1016/j.ijadhadh.2015.10.004.

[68] Panthapulakkal, Suhara, and Mohini Sain. "Agro-Residue Reinforced High-Density Polyethylene Composites: Fiber Characterization and Analysis of Composite Properties." *Composites Part A: Applied Science and Manufacturing*, vol. 38, no. 6, June 2007, pp. 1445–54. *ScienceDirect*, doi:10.1016/j.compositesa.2007.01.015.

[69] Rouison, David, et al. "Resin Transfer Molding of Hemp Fiber Composites: Optimization of the Process and Mechanical Properties of the Materials." *Composites Science and Technology*, vol. 66, no. 7, June 2006, pp. 895–906. *ScienceDirect*, doi:10.1016/j.compscitech.2005.07.040.

[70] Akampumuza, Obed, et al. "Review of the Applications of Biocomposites in the Automotive Industry." *Polymer Composites*, vol. 38, no. 11, 2017, pp. 2553–69. *Wiley Online Library*, doi:https://doi.org/10.1002/pc.23847.

[71] Birat, K. C., et al. "Hybrid Biocomposites with Enhanced Thermal and Mechanical Properties for Structural Applications." *Journal of Applied Polymer Science*, vol. 132, no. 34, 2015. *Wiley Online Library*, doi:https://doi.org/10.1002/app.42452.

[72] Khalfallah, M., et al. "Innovative Flax Tapes Reinforced Acrodur Biocomposites: A New Alternative for Automotive Applications." *Materials & Design*, vol. 64, Dec. 2014, pp. 116–26. *ScienceDirect*, doi:10.1016/j.matdes.2014.07.029.

[73] Ticoalu, A., et al. "A Review of Current Development in Natural Fiber Composites for Structural and Infrastructure Applications." *Proceedings of the Southern Region Engineering Conference (SREC 2010)*, edited by Steven C. Goh and Hao Wang, Engineers Australia, 2010, pp. 113–17. *eprints.usq.edu.au*, http://www.usq.edu.au/engsummit.

[74] Feng, Yechang, et al. "Biobased Thiol-Epoxy Shape Memory Networks from Gallic Acid and Vegetable Oils." *European Polymer Journal*, vol. 112, Mar. 2019, pp. 619–28. *ScienceDirect*, doi:10.1016/j.eurpolymj.2018.10.025.

[75] Baroncini, Elyse A., et al. "Recent Advances in Bio-Based Epoxy Resins and Bio-Based Epoxy Curing Agents." *Journal of Applied Polymer Science*, vol. 133, no. 45, 2016. *Wiley Online Library*, doi:https://doi.org/10.1002/app.44103.

[76] Patil, Deepak M., et al. "Design and Synthesis of Bio-Based Epoxidized Alkyd Resin for Anti-Corrosive Coating Application." *Iranian Polymer Journal*, vol. 27, no. 10, Oct. 2018, pp. 709–19. *Springer Link*, doi:10.1007/s13726-018-0646-1.

[77] *Types of Roofing Materials - Nationwide*. https://www.nationwide.com/lc/resources/home/articles/types-of-roofing. Accessed 21 May 2021.

[78] "12 Principles of Green Chemistry." *American Chemical Society*, https://www.acs.org/content/acs/en/greenchemistry/principles/12-principles-of-green-chemistry.html. Accessed 21 May 2021.

[79] R.P. Wool, X.S. Sun, *Bio-Based Polymers and Composites*, Elsevier Academic Press, Burlington, MA, (2005).

[80] W.D. Callister Jr., D.G. Rethwisch, *Materials Science and Engineering: An Introduction*, 9 ed., Wiley, Danvers, MA, (2014).

[81] K.L. Pickering, M.G.A. Efendy, T.M. Le, *Compos Part a-Appl S* **83** 98 (2016).

[82] L.W. McKeen, *Effect of Temperature and other Factors on Plastics and Elastomers*, William Andrew Inc., NY, USA, (2008).

[83] A. O'Donnell, M.A. Dweib, R.P. Wool, *Compos Sci Technol* **64**(9), 1135 (2004).

[84] D. Romanzini, A. Lavoratti, H.L. Ornaghi, S.C. Amico, A.J. Zattera, *Mater Design* **47** 9 (2013).

[85] L. Granda, Q. Tarres, F.X. Espinach, F. Julian, J.A. Mendez, M. Delgado-Aguilar, P. Mutje, *Cell Chem Technol* **50**(3-4), 417 (2016).

[86] M.S. Salit, M. Jawaid, N.B. Yusoff, M.E. Hoque, *Manufacturing of Natural Fibre Reinforced Polymer Composites*, Springer, Cham, Switzerland (2015).

[87] A.K. Mohanty, M. Misra, L.T. Drzal, *Natural Fibers, Biopolymers, and Biocomposites*, CRC Press Boca Raton. USA, (2005).

[88] K.O. Niska, M. Sain, *Wood-Polymer Composites*, Woodhead Publishing, Boca Raton, FL, (2008).

[89] R.D.S.G. Campilho, *Natural Fiber Composites*, CRC Press, Boca Raton, FL, (2016).

[90] A. Hodzic, R. Shanks, *Natural Fibre Composites. Materials, Processes and Properties*, Woodhead Publishing, Cambridge, UK, (2014).

[91] K.L. Pickering, *Properties and Performance of Natural-Fibre Composites*, Woodhead Publishing, Cambridge, UK, (2008).

[92] D.D. Stokke, Q. Wu, G. Han, *Introduction to Wood and Natural Fiber Composites*, John Wiley & Sons, West Sussex, UK, (2014).

[93] M.O. Seydibeyoglu, A.K. Mohanty, M. Misra, *Fiber Technology for Fiber-Reinforced Composites*, Woodhead Publishing, Cambridge, UK, (2017).

[94] S. Kalia, *Biodegradable Green Composites*, John Wiley & Sons, Hoboken, NJ, (2016).

[95] A. Rana, R.W. Evitts, *J Appl Polym Sci* **132**(15), 41807 (2015).

[96] A.K.-t. Lau, A.P.-Y. Hung, *Natural Fiber-Reinforced Biodegradable and Bioresorbable Polymer Composites*, Woodhead Publishing, Duxford, UK, (2017).

[97] T.S. Omonov, J.M. Curtis. *Aldehyde Free Thermoset Bioresins and Biocomposites*. (2016).

[98] A.K. Mohanty, M. Misra, L.T. Drzal, *Compos Interface* **8**(5), 313 (2001).

[99] M.R. Rahman, M.N. Islam, M.M. Huque, *J Polym Environ* **18**(3), 443 (2010).

[100] A. Ali, K. Shaker, Y. Nawab, M. Jabbar, T. Hussain, J. Militky, V. Baheti, *Journal of Industrial Textiles* **47**(8), 2153 (2018).

[101] ASTM-D1037-12, Standard Test Methods for Evaluating Properties of Wood-Base Fiber and Particle Panel Materials, ASTM, PA, USA, p. 32 (2012).

[102] ASTM-E1640-18, Standard Test Method for Assignment of the Glass Transition Temperature by Dynamic Mechanical Analysis, ASTM, PA, USA, p. 6 (2018).

[103] T.S. Omonov, E. Kharraz, J.M. Curtis, *Rsc Adv* **6**(95), 92874 (2016).

[104] T.S. Omonov, E. Kharraz, J.M. Curtis, *Ind Crop Prod* **107** 378 (2017).

[105] ASTM-D1652-11E1, Standard Test Method for Epoxy Content of Epoxy Resins, ASTM, PA, USA, p. 4 (2011).

[106] E. Crawford, A.J. Lesser, *J Polym Sci Pol Phys* **36**(8), 1371 (1998).

[107] J.M. Felix, P. Gatenholm, *J Appl Polym Sci* **42**(3), 609 (1991).

[108] R.X. Ou, Q.W. Wang, F.P. Yuan, B.Y. Liu, W.J. Yang, *Adv Mater Res-Switz* **221** 27 (2011).

[109] C. Ayranci, J. Carey, *Compos Struct* **85**(1), 43 (2008).

[110] M. Jawaid, M. Thariq, N. Saba, *Failure Analysis in Biocomposites, Fibre-Reinforced Composites and Hybrid Composites*, Woodhead Publishing, Duxford, UK, (2019).

[111] C.P. Dai, C.M. Yu, J.W. Jin, *Wood Fiber Sci* **40**(2), 146 (2008).

[112] N. Saba, M. Jawaid, O.Y. Alothman, M.T. Paridah, *Constr Build Mater* **106** 149 (2016).

[113] N. Boquillon, C. Fringant, *Polymer* **41**(24), 8603 (2000).

[114] Production of major vegetable oils worldwide, https://www.statista.com (Accessed March 1, 2019).

[115] Altuna, F. I., Pettarin, V., & Williams, R. J. J. (2013). Self-healable polymer networks based on the cross-linking of epoxidised soybean oil by an aqueous citric acid solution, *Green Chemistry*, **15**: 3360-66. https://doi.org/10.1039/c3gc41384e.

[116] Omonov, T. S., Kharraz, E., & Curtis, J. M. (2016). The epoxidation of canola oil and its derivatives, *RSC Advances*, **6**: 92874-86. https://doi.org/10.1039/c6ra17732h.

[117] Auvergne, R., Caillol, S., David, G., Boutevin, B., & Pascault, J. P. (2014). Biobased Thermosetting Epoxy: Present and Future, *Chemical Reviews*, **114**: 1082-115. https://doi.org/10.1021/cr3001274.

[118] Llevot, A. (2017). Sustainable Synthetic Approaches for the Preparation of Plant Oil-Based Thermosets, *Journal of the American Oil Chemists Society*, **94**: 169-86. https://doi.org/10.1007/s11746-016-2932-4.

[119] Omonov, T. S., Kharraz, E., & Curtis, J. M. (2017). Camelina (Camelina Sativa) oil polyols as an alternative to Castor oil, *Industrial Crops and Products*, **107**: 378-85. https://doi.org/10.1016/j.indcrop.2017.05.041.

[120] HealthCanada. (July 03, 2019). Statistics, Reports and Fact Sheets on Hemp, HealthCanada, https://www.canada.ca/en/health-canada/services/health-concerns/controlled-substances-precursor-chemicals/industrial-hemp/about-hemp-canada-hemp-industry/statistics-reports-fact-sheets-hemp.html.

[121] Omonov, T. S., & Curtis, J. M. (2016). 'Chapter 7. Plant Oil-Based Epoxy Intermediates for Polymers.' in Madbouly, S. A., Zhang, C. & Kessler, M. R. (eds.), *Bio-Based Plant Oil Polymers and Composites* (Elsevier Inc.: Oxford, UK). https://doi.org/10.1016/B978-0-323-35833-0.00007-4.

[122] Bai, J. (2013). *Advanced Fibre-Reinforced Polymer (FRP) Composites for Structural Applications* (Woodhead Publishing: Cambridge, UK). https://doi.org/10.1533/9780857098641.

[123] Madec, P. J., & Marechal, E. (1985). Kinetics and Mechanisms of Polyesterifications. 2. Reactions of Diacids with Diepoxides, *Advances in Polymer Science*, **71**: 153-228. https://doi.org/10.1007/3-540-15482-5_9.

[124] Shechter, L., & Wynstra, J. (1956). Glycidyl Ether Reactions with Alcohols, Phenols, Carboxylic Acids, and Acid Anhydrides, *Industrial and Engineering Chemistry*, **48**: 86-93. https://doi.org/10.1021/ie50553a028.

[125] Wang, R., & Schuman, T. (2015). 'Towards Green: A Review of Recent Developments in Bio-renewable Epoxy Resins from Vegetable Oils.' in Liu, Z. & Kraus, G. (eds.), *Green Materials from Plant Oils* (RSC: Cambridge, UK). https://doi.org/10.1039/9781782621850-00202.

[126] Shogren, R. L. (1999). Preparation and characterization of a biodegradable mulch: Paper coated with polymerized vegetable oils, *Journal of Applied Polymer Science*, **73**: 2159-67. https://doi.org/10.1002/(Sici)1097-4628(19990912)73:11<2159::Aid-App12>3.0.Co;2-Q.

[127] Coates, J. (2011). 'Interpretation of Infrared Spectra, A Practical Approach.' in Meyers, R. A. (ed.), *Encyclopedia of Analytical Chemistry* (John Wiley & Sons: Chichester, UK). https://doi.org/10.1002/9780470027318.a5606.

[128] Wang, Z., Cui, Y. T., Xu, Z. B., & Qu, J. (2008). Hot water-promoted ring-opening of epoxides and aziridines by water and other nucleopliles, *Journal of Organic Chemistry*, **73**: 2270-74. https://doi.org/10.1021/jo702401t.

[129] Ly, U. Q., Pham, M. P., Marks, M. J., & Truong, T. N. (2017). Density functional theory study of mechanism of epoxy-carboxylic acid curing reaction, *J Comput Chem*, **38**: 1093-102. https://doi.org/10.1002/jcc.24779.

[130] Sun, S. D., Li, P., Bi, Y. L., & Xiao, F. G. (2014). Enzymatic Epoxidation of Soybean Oil Using Ionic Liquid as Reaction Media, *Journal of Oleo Science*, **63**: 383-90. https://doi.org/10.5650/jos.ess13197.

[131] Johnson, D. S. (1983). Accelerator for anhydride-cured epoxy resins, U.S. Patent 4398013. Karak, N. (2012). *Vegetable oil-based polymers. Properties, processing and applications.* (Woodhead Publishing: Cambridge, UK). https://doi.org/10.1533/9780857097149.

[132] Petrie, E. M. (2006). *Epoxy adhesive formulations* (McGraw-Hill: New York, USA). https://doi.org/10.1036/0071455442.

[133] Omonov, T. S., & Curtis, J. M. (2014). Biobased Epoxy Resin from Canola Oil, *Journal of Applied Polymer Science*, **131**. https://doi.org/10.1002/app.40142.

[134] Shishikura, A., Takahashi, H., Hirohama, S., & Arai, K. (1992). Citric-Acid Purification Process Using Compressed Carbon-Dioxide, *Journal of Supercritical Fluids*, **5**: 303-12. https://doi.org/10.1016/0896-8446(92)90022-C.

[135] ASTM®. (American Society for Testing and Materials). (2019) ASTM D1652-11E1. Standard Test Method for Epoxy Content of Epoxy Resins, 4. https://doi.org/10.1520/D1652-11R19.

[136] Li, F. K., & Larock, R. C. (2000). Thermosetting polymers from cationic copolymerization of tung oil: Synthesis and characterization, *Journal of Applied Polymer Science*, **78**: 1044-56. https://doi.org/10.1002/1097-4628(20001031)78:5<1044::Aid-App130>3.0.Co;2-A.

[137] Pascault, J.-P., & Williams, R. J. J. (2010). *Epoxy Polymers: New Materials and Innovations* (Wiley-VCH: Germany). https://doi.org/10.1002/9783527628704.

[138] Fisch, W., Hofmann, W., & Koskikallio, J. (1956). The Curing Mechanism of Epoxy Resins, *Chemistry & Industry*: 756-57. https://doi.org/10.1002/jctb.5010061005.

[139] Steinmann, B. (1989). Investigations on the Curing of Epoxy-Resins with Hexahydrophthalic Anhydride, *Journal of Applied Polymer Science*, **37**: 1753-76. https://doi.org/10.1002/app.1989.070370702.

[140] Kolar, F., & Svitilova, J. (2007). Kinetics and mechanism of curing epoxy/anhydride systems, *Acta Geodynamica Et Geomaterialia*, **4**: 85-92.

[141] Barabanova, A. I., Lokshin, B. V., Kharitonova, E. P., Karandi, I. V., Afanasyev, E. S., Askadskii, A. A., & Philippova, O. E. (2019). Cycloaliphatic epoxy resin cured with anhydride in the absence of catalyst, *Colloid and Polymer Science*, **297**: 409-16. https://doi.org/10.1007/s00396-018-4430-8.

[142] Curtis, J. M., Liu, G., Omonov, T. S., & Kharraz, E. (2015). Polyol Synthesis from Fatty Acids and Oils., U.S. Patent 9,216,940 B2.

[143] Alvarez-Builla, J., Vaquero, J. J., & Barluenga, J. (2011). *Modern Heterocyclic Chemistry* (Wiley-VCH Verlag: Weinheim, Germany). https://doi.org/10.1002/9783527637737.

[144] Bhattacharyya, L., & Rohrer, J. S. (2012). *Applications of Ion Chromatography for Pharmaceutical and Biological Products* (Wiley: New Jersey, USA). https://doi.org/10.1002/9781118147009.

[145] Carey, F. A., & Giuliano, R. M. (2017). 'Carboxylic Acid Derivatives: Nucleophilic Acyl Substitution.' in Carey, F. A. & Giuliano, R. M. (eds.), *Organic Chemistry* (McGraw-Hill: Boston, USA).

[146] Chen, M., Ding, W., Kong, Y., & Diao, G. (2008). Conversion of the surface property of oleic acid stabilized silver nanoparticles from hydrophobic to hydrophilic based on host-guest binding interaction, *Langmuir*, **24**: 3471-78. https://doi.org/10.1021/La704020j.

[147] Miller, D. R., & Macosko, C. W. (1988). Network Parameters for Crosslinking of Chains with Length and Site Distribution, *Journal of Polymer Science Part B-Polymer Physics*, **26**: 1-54. https://doi.org/10.1002/polb.1988.090260101.

[148] Lee, D. H., & Condrate, R. A. (1999). FTIR spectral characterization of thin film coatings of oleic acid on glasses: I. Coatings on glasses from ethyl alcohol, *Journal of Materials Science*, 34: 139-46. https://doi.org/10.1023/A:1004494331895.

[149] Mahendran, A. R., Aust, N., Wuzella, G., & Kandelbauer, A. (2012). Synthesis and Characterization of a Bio-Based Resin from Linseed Oil, *Macromolecular Symposia*, **311**: 18-27. https://doi.org/10.1002/masy.201000134.

[150] Vlachos, N., Skopelitis, Y., Psaroudaki, M., Konstantinidou, V., Chatzilazarou, A., & Tegou, E. (2006). Applications of Fourier transform-infrared spectroscopy to edible oils, *Analytica Chimica Acta*, **573**: 459-65. https://doi.org/10.1016/j.aca.2006.05.034.

[151] Wu, N. Q., Fu, L., Su, M., Aslam, M., Wong, K. C., & Dravid, V. P. (2004). Interaction of fatty acid monolayers with cobalt nanoparticles, *Nano Letters*, **4**: 383-86. https://doi.org/10.1021/Nl1035139x.

[152] Park, C.-M., & Sheehan, R. J. (2000). 'Phthalic acids and other benzenepolycarboxylic acids.' in Kroschwitz, J. I. & Howe-Grant, M. (eds.), *Kirk-Othmer Encyclopedia of Chemical Technology* (Wiley-Interscience: New Jersey, USA). https://doi.org/10.1002/0471238961.1608200816011811.a01.

[153] Theophanides, T. (2012). *Infrared Spectroscopy. Materials Science, Engineering and Technology* (InTech Open: Rijeka, Croatia). https://doi.org/10.5772/2055.

[154] Vlcek, T., & Petrovic, Z. S. (2006). Optimization of the Chemoenzymatic Epoxidation of Soybean Oil, *Journal of the American Oil Chemists Society*, **73**: 247-52. https://doi.org/10.1007/s11746-006-1200-4.

[155] Vo-Dinh, T. (2015). *Biomedical Photonics Handbook. Volume 1. Fundamentals, Devices, and Techniques* (CRC Press: Boca Raton,FL). https://doi.org/10.1201/b17290.

[156] Arjunan, V., Raj, A., Subramanian, S., & Mohan, S. (2013). Vibrational, electronic and quantum chemical studies of 1,2,4-benzenetricarboxylic-1,2-anhydride, *Spectrochimica Acta Part A - Molecular and Biomolecular Spectroscopy*, **110**: 141-50. https://doi.org/10.1016/j.saa.2013.02.031.

[157] Matejka, L., Pokorny, S., & Dusek, K. (1982). Network Formation Involving Epoxide and Carboxyl Groups - Course of the Model Reaction Monoepoxide-Monocarbonic Acid, *Polymer Bulletin*, **7**: 123-28. https://doi.org/10.1007/BF00265462.

[158] Zhou, Y., Chen, G. F., Wang, W., Wei, L. H., Zhang, Q. J., Song, L. P., & Fang, X. Z. (2015). Synthesis and characterization of transparent polyimides derived from ester-containing dianhydrides with different electron affinities, *Rsc Advances*, **5**: 79207-15.

[159] Campanella, A., & Baltanas, M. A. (2006). Degradation of the oxirane ring of epoxidized vegetable oils in liquid-liquid heterogeneous reaction systems, *Chemical Engineering Journal*, **118**: 141-52. https://doi.org/10.1016/j.cej.2006.01.010.

[160] Menard, K. P., & Menard, N. R. (2014). 'Dynamic Mechanical Analysis in the Analysis of Polymers and Rubbers.' in Mark, H. F. (ed.), *Encyclopedia of Polymer Science and Technology* (John Wiley & Sons: Hoboken, NJ). https://doi.org/10.1002/0471440264.pst102.pub2.

[161] Hill, L. W. (1997). Calculation of crosslink density in short chain networks, *Progress in Organic Coatings*, **31**: 235-43. https://doi.org/10.1016/S0300-9440(97)00081-7.

[162] Last, D. J., Najera, J. J., Percival, C. J., & Horn, A. B. (2009). A comparison of infrared spectroscopic methods for the study of heterogeneous reactions occurring on atmospheric aerosol proxies, *Physical Chemistry Chemical Physics*, **11**: 8214-25. https://doi.org/10.1039/B901815h.

[163] Hill, L. W. (2012). 'Dynamic Mechanical and Tensile Properties.' in Koleske, J. V. (ed.), *Paint and Coating Testing Manual: 15th. Edition of the Gardner-Sward Handbook* (ASTM International: West Conshohocken, PA, USA). https://doi.org/10.1520/MNL12229M.

[164] Gerbase, A. E., Petzhold, C. L., & Costa, A. P. O. (2002). Dynamic mechanical and thermal behavior of epoxy resins based on soybean oil, *Journal of the American Oil Chemists Society*, **79**: 797-802. https://doi.org/10.1007/s11746-002-0561-z.

[165] Crawford, E., & Lesser, A. J. (1998). The effect of network architecture on the thermal and mechanical behavior of epoxy resins, *Journal of Polymer Science Part B-Polymer Physics*, **36**: 1371-82. https://doi.org/10.1002/(SICI)1099-0488(199806)36:8<1371::AID-POLB11>3.0.CO;2-4.

[166] Barbooti, M. M., & Alsammerrai, D. A. (1986). Thermal-Decomposition of Citric-Acid, *Thermochimica Acta*, **98**: 119-26. https://doi.org/10.1016/0040-6031(86)87081-2.

[167] Umemura, K., Ueda, T., & Kawai, S. (2012). Characterization of wood-based molding bonded with citric acid, *Journal of Wood Science*, **58**: 38-45. https://doi.org/10.1007/s10086-011-1214-x.

[168] Wyrzykowski, D., Hebanowska, E., Nowak-Wiczk, G., Makowski, M., & Chmurzynski, L. (2011). Thermal behaviour of citric acid and isomeric aconitic acids, *Journal of Thermal Analysis and Calorimetry*, **104**: 731-35. https://doi.org/10.1007/s10973-010-1015-2.

[169] Li, F., Marks, D. W., Larock, R. C., & Otaigbe, J. U. (2000). Fish oil thermosetting polymers: synthesis, structure, properties and their relationships, *Polymer*, **41**: 7925-39. https://doi.org/10.1016/S0032-3861(00)00030-6.

[170] Wool, R., & Sun, X. S. (2005). *Bio-Based Polymers and Composites* (Elsevier Academic Press: Waltham, MA, USA). https://doi.org/10.1016/B978-0-12-763952-9.X5000-X.

[171] ASTM D1475-13. Standard Test Method for Density of Liquid Coatings, Inks, and Related Products. https://doi.org/10.1520/D1475-13.

[172] ASTM D1652-11. (Reapproved 2019). Standard Test Method for Epoxy Content of Epoxy Resins. https://doi.org/10.1520/D1652-11R19.

[173] ASTM E1640-18. Standard Test Method for Assignment of the Glass Transition Temperature by Dynamic Mechanical Analysis. https://doi.org/10.1520/E1640-18.

[174] Bandzierz, K., Reuvekamp, L., Dryzek, J., Dierkes, W., Blume, A., & Bielinski, D., 2016. Influence of Network Structure on Glass Transition Temperature of Elastomers, Materials, 9: 607. https://doi.org/10.3390/ma9070607.

[175] Belgacem, M.N., & Gandini, A., 2008. Monomers, Polymers and Composites from Renewable Resources, Elsevier: Oxford, UK. https://doi.org/10.1016/B978-0-08-045316-3.X0001-4.

[176] Borugadda, V.B., & Goud, V.V., 2019. Hydroxylation and hexanoylation of epoxidized waste cooking oil and epoxidized waste cooking oil methyl esters: Process optimization and

physico-chemical characterization, Ind Crop Prod, 133: 151-159. https://doi.org/10.1016/j.indcrop.2019.01.069.

[177] Curtis, J.M., Omonov, T.S., Kharraz, E., Kong, X., & Tavassoli-Kafrani, M.H., 2019. Method for Polyol Synthesis from Triacylglyceride Oils, U.S. Patent 10,189,761 B2.

[178] Di Pietro, M.E., Mannu, A., & Mele, A., 2020. NMR Determination of Free Fatty Acids in Vegetable Oils, Processes, 8: 410-425. https://doi.org/10.3390/pr8040410.

[179] Dotan, A., 2014. Biobased Thermosets, in: Dodiuk, H. & Goodman, S. (Eds.), Handbook of Thermoset Plastics, Elsevier: Amsterdam, pp. 577-622. https://doi.org/10.1016/B978-1-4557-3107-7.00015-4.

[180] Espinoza-Perez, J.D., Nerenz, B.A., Haagenson, D.M., Chen, Z.G., Ulven, C.A., & Wiesenborn, D.P., 2011. Comparison of Curing Agents for Epoxidized Vegetable Oils Applied to Composites, Polym Composite, 32: 1806-1816. https://doi.org/10.1002/pc.21213.

[181] Gerbase, A.E., Petzhold, C.L., & Costa, A.P.O., 2002. Dynamic mechanical and thermal behavior of epoxy resins based on soybean oil, J Am Oil Chem Soc, 79: 797-802. https://doi.org/10.1007/s11746-002-0561-z.

[182] Hayes, D.G., Kitamoto, D., Solaiman, D.K.Y., & Ashby, R.D., 2009. Biobased Surfactants and Detergents. Synthesis, Properties, and Applications, AOCS Press: Urbana, USA.

[183] Hild, G., 1998. Model networks based on 'endlinking' processes: Synthesis, structure and properties, Prog Polym Sci, 23: 1019-1149. https://doi.org/10.1016/S0079-6700(97)00055-5.

[184] Hill, L.W., 1997. Calculation of crosslink density in short chain networks, Prog Org Coat, 31: 235-243. https://doi.org/10.1016/S0300-9440(97)00081-7.

[185] Hill, L.W., 2012. Dynamic Mechanical and Tensile Properties, in: Koleske, J.V. (Ed.), Paint and Coating Testing Manual, ASTM International, pp. 624. https://doi.org/10.1520/MNL12229M.

[186] Holser, R.A., 2008. Transesterification of epoxidized soybean oil to prepare epoxy methyl esters, Ind Crop Prod, 27: 130-132. https://doi.org/10.1016/j.indcrop.2007.06.001.

[187] Honary, L.A.T., & Richter, E., 2011. Biobased Lubricants and Greases. Technology and Products, John Wiley & Sons: Chichester, UK. https://doi.org/10.1002/9780470971956.

[188] Huang, X.J., Yang, X.X., Liu, H., Shang, S.B., Cai, Z.S., & Wu, K., 2019. Bio-based thermosetting epoxy foams from epoxidized soybean oil and rosin with enhanced properties, Ind Crop Prod, 139: 111540. https://doi.org/10.1016/j.indcrop.2019.111540.

[189] Kabasci, S., 2014. Bio-based plastics. Materials and Applications, John Wiley & Sons: Chichester, UK. https://doi.org/10.1002/9781118676646.

[190] Khundamri, N., Aouf, C., Fulcrand, H., Dubreucq, E., & Tanrattanakul, V., 2019. Bio-based flexible epoxy foam synthesized from epoxidized soybean oil and epoxidized mangosteen tannin, Ind Crop Prod, 128: 556-565. https://doi.org/10.1016/j.indcrop.2018.11.062.

[191] Kim, J.R., & Sharma, S., 2012. The development and comparison of bio-thermoset plastics from epoxidized plant oils, Ind Crop Prod, 36: 485-499. https://doi.org/10.1016/j.indcrop.2011.10.036.

[192] Kirpluks, M., Kalnbunde, D., Benes, H., & Cabulis, U., 2018. Natural oil based highly functional polyols as feedstock for rigid polyurethane foam thermal insulation, Ind Crop Prod, 122: 627-636. https://doi.org/10.1016/j.indcrop.2018.06.040.

[193] Lee, C.S., Ooi, T.L., Chuah, C.H., & Ahmad, S., 2007. Synthesis of palm oil-based diethanolamides, J Am Oil Chem Soc, 84: 945-952. https://doi.org/10.1007/s11746-007-1123-8.

[194] Li, F., Marks, D.W., Larock, R.C., & Otaigbe, J.U., 2000. Fish oil thermosetting polymers: synthesis, structure, properties and their relationships, Polymer, 41: 7925-7939. https://doi.org/10.1016/S0032-3861(00)00030-6.

[195] Li, F.K., & Larock, R.C., 2000. Thermosetting polymers from cationic copolymerization of tung oil: Synthesis and characterization, J Appl Polym Sci, 78: 1044-1056. https://doi.org/10.1002/1097-4628(20001031)78:5<1044::Aid-App130>3.0.Co;2-A.

[196] Li, Y., Luo, X., & Hu, S., 2015. Bio-based Polyols and Polyurethanes, Springer: London, UK. https://doi.org/10.1007/978-3-319-21539-6.

[197] Liang, B., Zhao, J., Li, G., Huang, Y.K., Yang, Z.H., & Yuan, T., 2019. Facile synthesis and characterization of novel multi-functional bio-based acrylate prepolymers derived from tung oil and its application in UV-curable coatings, Ind Crop Prod, 138: 111585. https://doi.org/10.1016/j.indcrop.2019.111585.

[198] Madbouly, S., Zhang, C., & Kessler, M.R., 2016. Bio-Based Plant Oil Polymers and Composites, Elsevier: Oxford, UK. https://doi.org/10.1016/C2014-0-02157-0.

[199] McKenna, G.B., 1989. Glass Formation and Glassy Behavior, in: Allen, G. & Bevington, J.C. (Eds.), Comprehensive Polymer Science and Supplements, Pergamon Press: UK, pp. 311-362. https://doi.org/10.1016/B978-0-08-096701-1.00047-1.

[200] Menard, K.P., 2008. Dynamic Mechanical Analysis: A Practical Introduction, CRC Press: Boca Raton, FL. https://doi.org/10.1201/9781420053135.

[201] Menard, K.P., & Menard, N.R., 2014. Dynamic Mechanical Analysis in the Analysis of Polymers and Rubbers, in: Mark, H.F. (Ed.), Encyclopedia of Polymer Science and Technology, John Wiley & Sons: USA, pp. 12344 https://doi.org/10.1002/0471440264.pst102.pub2.

[202] Miller, D.R., & Macosko, C.W., 1988. Network Parameters for Crosslinking of Chains with Length and Site Distribution, J Polym Sci Pol Phys, 26: 1-54. https://doi.org/10.1002/polb.1988.090260101.

[203] Moawia, R.M., Nasef, M.M., Mohamed, N.H., Ripin, A., & Farag, H., 2019. Production of Biodiesel from Cottonseed Oil over Aminated Flax Fibres Catalyst: Kinetic and Thermodynamic Behaviour and Biodiesel Properties, Advances in Chemical Engineering and Science, 9: 281-298. https://doi.org/10.4236/aces.2019.94021.

[204] Mohanty, A.K., Misra, M., & Drzal, L.T., 2005. Natural Fibers, Biopolymers, and Biocomposites, CRC Press Boca Raton. USA. https://doi.org/10.1201/9780203508206.

[205] Omonov, T.S., & Curtis, J.M., 2014. Biobased Epoxy Resin from Canola Oil, J Appl Polym Sci, 131: 40142. https://doi.org/10.1002/app.40142.

[206] Omonov, T.S., & Curtis, J.M., 2016. Plant Oil-Based Epoxy Intermediates for Polymers, in: Madbouly, S.A., Zhang, C. & Kessler, M.R. (Eds.), Bio-Based Plant Oil Polymers and Composites, Elsevier: Oxford, UK, pp. 99-125. https://doi.org/10.1016/B978-0-323-35833-0.00007-4.

[207] Omonov, T.S., Kharraz, E., & Curtis, J.M., 2016. The epoxidation of canola oil and its derivatives, RSC Adv, 6: 92874-92886. https://doi.org/10.1039/c6ra17732h.

[208] Omonov, T.S., Kharraz, E., & Curtis, J.M., 2017. Camelina (Camelina Sativa) oil polyols as an alternative to Castor oil, Ind Crop Prod, 107: 378-385. https://doi.org/10.1016/j.indcrop.2017.05.041.

[209] Omonov, T.S., Patel, V., & Curtis, J.M., 2019. The Development of Epoxidized Hemp Oil Prepolymers for the Preparation of Thermoset Networks, J Am Oil Chem Soc, 96: 1389-1403. https://doi.org/10.1002/aocs.12290.

[210] Omonov, T.S., Patel, V.R., & Curtis, J.M., 2018. "Epoxidized Hemp Oil: Synthesis, Cure Kinetics and Properties of Polymers." In *15th International Symposium on Bioplastics, Biocomposites and Biorefining*. Guelph, ON, Canada

[211] Pascault, J.-P., & Williams, R.J.J., 2010. Epoxy Polymers: New Materials and Innovations, Wiley-VCH: Germany. https://doi.org/10.1002/9783527628704.

[212] Perera, M.C.S., 2001. Development of formulations based on acrylate monomers for optical cable applications, J Appl Polym Sci, 82: 3001-3012. https://doi.org/10.1002/app.2155.abs.

[213] Rashid, U., & Anwar, F., 2008. Production of biodiesel through base-catalyzed transesterification of safflower oil using an optimized protocol, Energ Fuel, 22: 1306-1312. https://doi.org/10.1021/ef700548s.

[214] Ray, D., 2017. Biocomposites for High-Performance Applications. Current Barriers and Future Needs Towards Industrial Development, Woodhead Publishing: Duxford, UK. https://doi.org/10.1016/C2015-0-04020-5.

[215] Roudsari, G.M., Misra, M., & Mohanty, A.K., 2017. A study of mechanical properties of biobased epoxy network: Effect of addition of epoxidized soybean oil and poly(furfuryl alcohol), J Appl Polym Sci, 134: 44352. https://doi.org/10.1002/app.44352.

[216] Shaw, M.T., & MacKnight, W.J., 2005. Introduction to Polymer Viscoelasticity, John Wiley & Sons: New Jersey. https://doi.org/10.1002/0471741833.

[217] Sindt, O., Perez, J., & Gerard, J.F., 1996. Molecular architecture mechanical behaviour relationships in epoxy networks, Polymer, 37: 2989-2997. https://doi.org/10.1016/0032-3861(96)89396-7.

[218] Smith, P.B., & Gross, R.A., 2012. Biobased Monomers, Polymers, and Materials, American Chemical Society: Washington, USA. https://doi.org/10.1021/bk-2012-1105.

[219] Smitthipong, W., Chollakup, R., & Nardin, M., 2014. Bio-Based Composites for High-Performance Materials: From Strategy to Industrial Application, CRC Press: Boca Raton, USA. https://doi.org/10.1201/b17601.

[220] Snyder, S.W., 2016. Commercializing Biobased Products. Opportunities, Challenges, Benefits, and Risks, Royal Society of Chemistry: Cambridge, UK. https://doi.org/10.1039/9781782622444.

[221] Steinmann, B., 1989. Investigations on the Curing of Epoxy-Resins with Hexahydrophthalic Anhydride, J Appl Polym Sci, 37: 1753-1776. https://doi.org/10.1002/app.1989.070370702.

[222] Thakur, V.K., Thakur, M.K., & Kessler, M.R., 2017. Soy-based Bioplastics, Smithers Rapra: Shawbury, UK.

[223] Wang, R., & Schuman, T.P., 2013. Vegetable oil-derived epoxy monomers and polymer blends: A comparative study with review, Express Polym Lett, 7: 272-292. https://doi.org/10.3144/expresspolymlett.2013.25.

[224] Wool, R., & Sun, X.S., 2005. Bio-Based Polymers and Composites, Elsevier: Burlington, USA. https://doi.org/10.1016/B978-0-12-763952-9.X5000-X.

[225] Zheng, S., Patel, P.G., Vedage, G.A., Tijsma, E.J., & Lal, G.S., 2018. Epoxy liquid curing agent compositions, U.S. Patent US 9,862,798 B2.

[226] S. Omonov, Tolibjon, et al. "The Epoxidation of Canola Oil and Its Derivatives." RSC Advances, vol. 6, no. 95, 2016, pp. 92874–86.

[227] Omonov, Tolibjon S., et al. "The Development of Epoxidized Hemp Oil Prepolymers for the Preparation of Thermoset Networks." *Journal of the American Oil Chemists' Society*, vol. 96, no. 12, 2019, pp. 1389–403.

[228] Ashcroft, W. R. "Curing Agents for Epoxy Resins." *Chemistry and Technology of Epoxy Resins*, edited by Bryan Ellis, Springer Netherlands, 1993, pp. 37–71

[229] Tan, S. G., and W. S. Chow. "Biobased Epoxidized Vegetable Oils and Its Greener Epoxy Blends: A Review." *Polymer-Plastics Technology and Engineering*, vol. 49, no. 15, Nov. 2010, pp. 1581–90.

[230] Sahoo, Sushanta K., et al. "Development of Toughened Bio-Based Epoxy with Epoxidized Linseed Oil as Reactive Diluent and Cured with Bio-Renewable Crosslinker." *Polymers for Advanced Technologies*, vol. 29, no. 1, 2018, pp. 565–74.

[231] Bourne, L. B., et al. "Health Problems of Epoxy Resins and Amine-Curing Agents." *Occupational and Environmental Medicine*, vol. 16, no. 2, Apr. 1959, pp. 81–97.

[232] Suaza, Andrea, et al. "Dibutyl Citrate Synthesis, Physicochemical Characterization, and Px Data in Mixtures with Butanol." *Journal of Chemical & Engineering Data*, vol. 63, no. 6, June 2018, pp. 1946–54. *ACS Publications*, doi:10.1021/acs.jced.7b01064.

[233] Wang, Junqi, et al. "Techno-Economic Analysis and Environmental Impact Assessment of Citric Acid Production through Different Recovery Methods." *Journal of Cleaner Production*, vol. 249, Mar. 2020, p. 119315. *ScienceDirect*, doi:10.1016/j.jclepro.2019.119315.

[234] Kakasaheb Y. Nandiwale, Vijay V. Bokade. "Sustainable Catalytic Process for Synthesis of Triethyl Citrate Plasticizer over Phosphonated USY Zeolite." *Bulletin of Chemical Reaction Engineering and Catalysis*, vol. 11, no. 3, 2016, pp. 292–98.

[235] BCC market report. *BCC Library - Report View - CHM088A*. https://academic-bccresearch-com.login.ezproxy.library.ualberta.ca/market-research/chemicals/carboxylic-acids-applications-and-global-markets.html. Accessed 10 Apr. 2021.

[236] Hongqin Yang, Haiyan Song, Han Zhang, Ping Chen, Zhixi Zhao. "Esterification of Citric Acid with N-Butanol over Zirconium Sulfate Supported on Molecular Sieves." *Journal of Molecular Catalysis A: Chemical*, vol. 381, 2014, pp. 54–60.

[237] X.U. Junming, Jiang Jianchun, Zuo Zhiyue, Li Jing. "Synthesis of Tributyl Citrate Using Acid Ionic Liquid as Catalyst." *Process Safety and Environmental Protection*, vol. 88, 2010, pp. 28–30.

[238] Pratibha Singh, Sanjay P. Kable, Prakash V. Chavan. "Kinetics of Esterification of Citric Acid with Butanol Using Sulphuric Acid." *Int. J. Chem. Sci.*, vol. 12, no. 3, 2014, pp. 915–20.

[239] Yun Lu, Shengxian Xu, and Feng Zhao. "Synthesis of Tributyl Citrate Using Preyssler Acid as Catalyst." *AIP Conference Proceedings*, 2017, https://aip.scitation.org/doi/abs/10.1063/1.4971953.

[240] Michael P. Kotick, Elkhart, Ind. *Regioselective Synthesis of Mono-Alkyl Citric Acid Esters*. 5,049,699.

[241] G.S. Grigoryan, Z.G. Grigoryan, A.Ts. Malkhasyan. *Obtaining Esters of Citric Acid with High Aliphatic Alcohols*. Proceedings of the Yerevan State University, Chemistry and Biology, 51(2), p. 88-91 2017.

[242] Kuhns, Roger James, and George H. Shaw. "Peak Oil and Petroleum Energy Resources." *Navigating the Energy Maze: The Transition to a Sustainable Future*, edited by Roger James Kuhns and George H. Shaw, Springer International Publishing, 2018, pp. 53–63. *Springer Link*, https://doi.org/10.1007/978-3-319-22783-2_7.

[243] Yildizhan, Fatih Selim. "A Technical and Industrial Analysis of Global Plastics Market, Trade, Financing, and Operations." *ScienceOpen Preprints*, Jan. 2021. *www.scienceopen.com*, doi:10.14293/S2199-1006.1.SOR-.PPDUNRN.v1.

[244] Pham, Ha Q., and Maurice J. Marks. "Epoxy Resins." *Ullmann's Encyclopedia of Industrial Chemistry*, American Cancer Society, 2005. *Wiley Online Library*, https://onlinelibrary-wiley-com.login.ezproxy.library.ualberta.ca/doi/abs/10.1002/14356007.a09_547.pub2.

[245] Jin, Fan-Long, et al. "Synthesis and Application of Epoxy Resins: A Review." *Journal of Industrial and Engineering Chemistry*, vol. 29, Sept. 2015, pp. 1–11. *ScienceDirect*, doi:10.1016/j.jiec.2015.03.026.

[246] Vom Saal, Frederick S., and Laura N. Vandenberg. "Update on the Health Effects of Bisphenol A: Overwhelming Evidence of Harm." *Endocrinology*, vol. 162, no. 3, Mar. 2021. *academic.oup.com*, doi:10.1210/endocr/bqaa171.

[247] Galankis, Charis M. *Biobased Products and Industries*. Elsevier, 2020. University of Alberta Internet Internet Access, *EBSCOhost*, https://login.ezproxy.library.ualberta.ca/login?url=https://search.ebscohost.com/login.aspx?direct=true&db=cat03710a&AN=alb.8927031&site=eds-live&scope=site.

[248] Reddy, Gopal, et al. "Amylolytic Bacterial Lactic Acid Fermentation — A Review." *Biotechnology Advances*, vol. 26, no. 1, Jan. 2008, pp. 22–34. *ScienceDirect*, doi:10.1016/j.biotechadv.2007.07.004.

[249] Babu, Ramesh P., et al. "Current Progress on Bio-Based Polymers and Their Future Trends." *Progress in Biomaterials*, vol. 2, no. 1, Mar. 2013, p. 8. *Springer Link*, doi:10.1186/2194-0517-2-8.

[250] S. Omonov, Tolibjon, et al. "The Epoxidation of Canola Oil and Its Derivatives." *RSC Advances*, vol. 6, no. 95, 2016, pp. 92874–86. *pubs-rsc-org.login.ezproxy.library.ualberta.ca*, doi:10.1039/C6RA17732H.

[251] Baroncini, Elyse A., et al. "Recent Advances in Bio-Based Epoxy Resins and Bio-Based Epoxy Curing Agents." *Journal of Applied Polymer Science*, vol. 133, no. 45, 2016. *Wiley Online Library*, doi:https://doi.org/10.1002/app.44103.

[252] Omonov, Tolibjon S., et al. "The Development of Epoxidized Hemp Oil Prepolymers for the Preparation of Thermoset Networks." *Journal of the American Oil Chemists' Society*, vol. 96, no. 12, 2019, pp. 1389–403. *Wiley Online Library*, doi:https://doi.org/10.1002/aocs.12290.

[253] Ljungberg, Nadia, and Bengt Wesslén. "Tributyl Citrate Oligomers as Plasticizers for Poly (Lactic Acid): Thermo-Mechanical Film Properties and Aging." *Polymer*, vol. 44, no. 25, Dec. 2003, pp. 7679–88. *ScienceDirect*, doi:10.1016/j.polymer.2003.09.055.

[254] "Entropy Resins | Biobased Epoxy Resins | Learn More." *Entropy Resins*, https://entropyresins.com/. Accessed 31 May 2021.

[255] D. Ray, S. Sain. "Thermosetting Bioresins as Matrix for Biocomposites." *Biocomposites for High-Performance Applications*, Jan. 2017, pp. 57–80. *www-sciencedirect-com.login.ezproxy.library.ualberta.ca*, doi:10.1016/B978-0-08-100793-8.00003-X.

[256] Maffezzoli, Alfonso, et al. "Cardanol Based Matrix Biocomposites Reinforced with Natural Fibres." *Composites Science and Technology*, vol. 64, no. 6, May 2004, pp. 839–45. *ScienceDirect*, doi:10.1016/j.compscitech.2003.09.010.

[257] Babu, Ramesh P., et al. "Current Progress on Bio-Based Polymers and Their Future Trends." Progress in Biomaterials, vol. 2, no. 1, Mar. 2013, p. 8. Springer Link, https://doi.org/10.1186/2194-0517-2-8.

[258] Stephan Kabasci. Biobased Plastics: Materials and Applications. First edition, vol. 1, John Wiley & Sons, Ltd. Accessed 22 Aug. 2021. http://medien.ubitweb.de/pdfzentrale/978/111/999/Leseprobe_1_9781119994008.pdf

[259] Curran, Mary Ann. "Biobased Materials." Kirk-Othmer Encyclopedia of Chemical Technology, American Cancer Society, 2010, pp. 1–19. Wiley Online Library, https://onlinelibrary-wiley-com.login.ezproxy.library.ualberta.ca/doi/abs/10.1002/0471238961.biobcurr.a01.

[260] Finlay, Mark R. "Old Efforts at New Uses: A Brief History of Chemurgy and the American Search for Biobased Materials." Journal of Industrial Ecology, vol. 7, no. 3–4, 2003, pp. 33–46. Wiley Online Library, https://doi.org/https://doi.org/10.1162/108819803323059389.

[261] Biswas, E., et al. "Recent Advances and Technologies of Biobased Composites." Biobased Composites, John Wiley & Sons, Ltd, 2021, pp. 107–21. Wiley Online Library, https://onlinelibrary-wiley-com.login.ezproxy.library.ualberta.ca/doi/abs/10.1002/9781119641803.ch8.

[262] Kumar, Sudheer, et al. "Recent Development of Biobased Epoxy Resins: A Review." Polymer-Plastics Technology and Engineering, vol. 57, no. 3, Feb. 2018, pp. 133–55. Taylor and Francis+NEJM, https://doi.org/10.1080/03602559.2016.1253742.

[263] Ding, Cheng, and Avtar S. Matharu. "Recent Developments on Biobased Curing Agents: A Review of Their Preparation and Use." ACS Sustainable Chemistry & Engineering, vol. 2, no. 10, Oct. 2014, pp. 2217–36. ACS Publications, https://doi.org/10.1021/sc500478f.

[264] De Nograro, F.Fdez, et al. "Dynamic and Mechanical Properties of Epoxy Networks Obtained with PPO Based amines/mPDA Mixed Curing Agents." Polymer, vol. 37, no. 9, Apr. 1996, pp. 1589–600. ScienceDirect, https://doi.org/10.1016/0032-3861(96)83707-4.

[265] Maity, T., et al. "Curing Study of Epoxy Resin by New Aromatic Amine Functional Curing Agents along with Mechanical and Thermal Evaluation." Materials Science and Engineering: A, vol. 464, no. 1, Aug. 2007, pp. 38–46. ScienceDirect, https://doi.org/10.1016/j.msea.2007.01.128.

[266] Froidevaux, Vincent, et al. "Biobased Amines: From Synthesis to Polymers; Present and Future." Chemical Reviews, vol. 116, no. 22, Nov. 2016, pp. 14181–224. ACS Publications, https://doi.org/10.1021/acs.chemrev.6b00486.

[267] La Scala, John, and Richard P. Wool. "Effect of FA Composition on Epoxidation Kinetics of TAG." Journal of the American Oil Chemists' Society, vol. 79, no. 4, Apr. 2002, pp. 373–78. Springer Link, https://doi.org/10.1007/s11746-002-0491-9.

[268] Kim, Joo Ran, and Suraj Sharma. "The Development and Comparison of Bio-Thermoset Plastics from Epoxidized Plant Oils." Industrial Crops and Products, vol. 36, no. 1, Mar. 2012, pp. 485–99. ScienceDirect, https://doi.org/10.1016/j.indcrop.2011.10.036.

[269] Unnikrishnan, K. P., and Eby Thomas Thachil. "Synthesis and Characterization of Cardanol-Based Epoxy Systems." Designed Monomers and Polymers, vol. 11, no. 6, Jan. 2008, pp. 593–607. Taylor and Francis+NEJM, https://doi.org/10.1163/156855508X363870.

[270] Kanehashi, Shinji, et al. "Preparation and Characterization of Cardanol-Based Epoxy Resin for Coating at Room Temperature Curing." Journal of Applied Polymer Science, vol. 130, no. 4, 2013, pp. 2468–78. Wiley Online Library, https://doi.org/https://doi.org/10.1002/app.39382.

[271] Hu, Fengshuo, et al. "Preparation and Characterization of Fully Furan-Based Renewable Thermosetting Epoxy-Amine Systems." Macromolecular Chemistry and Physics, vol. 216, no. 13, 2015, pp. 1441–46. Wiley Online Library, https://doi.org/https://doi.org/10.1002/macp.201500142.

[272] Eid, Nadim, et al. "Synthesis and Properties of Furan Derivatives for Epoxy Resins." ACS Sustainable Chemistry & Engineering, vol. 9, no. 24, June 2021, pp. 8018–31. ACS Publications, https://doi.org/10.1021/acssuschemeng.0c09313.

[273] Zhang, Haibo, et al. "Synthesis and Characterization of Bio-Based Epoxy Thermosets Using Rosin-Based Epoxy Monomer." Iranian Polymer Journal, vol. 30, no. 7, July 2021, pp. 643–54. Springer Link, https://doi.org/10.1007/s13726-021-00918-9.

[274] Vevere, Laima, et al. "A Review of Wood Biomass-Based Fatty Acids and Rosin Acids Use in Polymeric Materials." Polymers, vol. 12, no. 11, Nov. 2020, p. 2706. www.mdpi.com, https://doi.org/10.3390/polym12112706.

[275] Xu, Chunbao, and Fatemeh Ferdosian. "Lignin-Based Epoxy Resins." Conversion of Lignin into Bio-Based Chemicals and Materials, edited by Chunbao Xu and Fatemeh Ferdosian, Springer Berlin Heidelberg, 2017, pp. 111–31. Springer Link, https://doi.org/10.1007/978-3-662-54959-9_7.

[276] Lu, Xinyu, et al. "Pyrolysis Mechanism and Kinetics of High-Performance Modified Lignin-Based Epoxy Resins." Journal of Analytical and Applied Pyrolysis, vol. 154, Mar. 2021, p. 105013. ScienceDirect, https://doi.org/10.1016/j.jaap.2020.105013.

[277] Jahandideh, Arash, et al. "Synthesis and Characterization of Novel Star-Shaped Itaconic Acid Based Thermosetting Resins." Journal of Polymers and the Environment, vol. 26, no. 5, May 2018, pp. 2072–85. Springer Link, https://doi.org/10.1007/s10924-017-1112-4.

[278] Li, Peng, et al. "Itaconic Acid as a Green Alternative to Acrylic Acid for Producing a Soybean Oil-Based Thermoset: Synthesis and Properties." ACS Sustainable Chemistry & Engineering, vol. 5, no. 1, Jan. 2017, pp. 1228–36. ACS Publications, https://doi.org/10.1021/acssuschemeng.6b02654.

[279] Patil, Deepak M., et al. "Synthesis of Bio-Based Epoxy Resin from Gallic Acid with Various Epoxy Equivalent Weights and Its Effects on Coating Properties." Journal of Coatings Technology and Research, vol. 14, no. 2, Mar. 2017, pp. 355–65. Springer Link, https://doi.org/10.1007/s11998-016-9853-x.

[280] Tarzia, Antonella, et al. "Synthesis, Curing, and Properties of an Epoxy Resin Derived from Gallic Acid." BioResources, vol. 13, no. 1, 2018, pp. 632–45.

[281] Yuan, Wangchao, et al. Research Progress on Vanillin-Based Thermosets. 2018, https://www-ingentaconnect-com.login.ezproxy.library.ualberta.ca/contentone/ben/cgc/2018/00000005/00000003/art00004.

[282] Mogheiseh, Mohsen, et al. "Vanillin-Derived Epoxy Monomer for Synthesis of Bio-Based Epoxy Thermosets: Effect of Functionality on Thermal, Mechanical, Chemical and Structural Properties." Chemical Papers, vol. 74, no. 10, Oct. 2020, pp. 3347–58. Springer Link, https://doi.org/10.1007/s11696-020-01164-8.

[283] Saxon, Derek J., et al. "Next-Generation Polymers: Isosorbide as a Renewable Alternative." Progress in Polymer Science, vol. 101, Feb. 2020, p. 101196. ScienceDirect, https://doi.org/10.1016/j.progpolymsci.2019.101196.

[284] Yum, Sugil, et al. "Synthesis and Characterization of Isosorbide Based Polycarbonates." Polymer, vol. 179, Sept. 2019, p. 121685. ScienceDirect, https://doi.org/10.1016/j.polymer.2019.121685.

[285] Bang, Hyun Bae, et al. "High-Level Production of Trans-Cinnamic Acid by Fed-Batch Cultivation of Escherichia Coli." Process Biochemistry, vol. 68, May 2018, pp. 30–36. ScienceDirect, https://doi.org/10.1016/j.procbio.2018.01.026.

[286] Xin, Junna, et al. "Study of Green Epoxy Resins Derived from Renewable Cinnamic Acid and Dipentene: Synthesis, Curing and Properties." RSC Advances, vol. 4, no. 17, 2014, pp. 8525–32. pubs-rsc-org.login.ezproxy.library.ualberta.ca, https://doi.org/10.1039/C3RA47927G.

[287] Caillol, Sylvain, et al. "Eugenol, a Developing Asset in Biobased Epoxy Resins." Polymer, vol. 223, May 2021, p. 123663. ScienceDirect, https://doi.org/10.1016/j.polymer.2021.123663.

[288] Chen, Chien-Han, et al. "A Facile Strategy to Achieve Fully Bio-Based Epoxy Thermosets from Eugenol." Green Chemistry, vol. 21, no. 16, 2019, pp. 4475–88. pubs-rsc-org.login.ezproxy.library.ualberta.ca, https://doi.org/10.1039/C9GC01184F.